

Technical Report Documentation Page

1. REPORT No.

CA-DOT-TL-2115-9-74-37

2. GOVERNMENT ACCESSION No.**3. RECIPIENT'S CATALOG No.****4. TITLE AND SUBTITLE**

Earthwork Reinforcement Techniques

5. REPORT DATE

November 1974

6. PERFORMING ORGANIZATION

19202-762503-632115

7. AUTHOR(S)

Chang, Jerry C.

8. PERFORMING ORGANIZATION REPORT No.

CA-DOT-TL-2115-9-74-37

9. PERFORMING ORGANIZATION NAME AND ADDRESS

Transportation Laboratory
5900 Folsom Boulevard
Sacramento, California 95819

10. WORK UNIT No.**11. CONTRACT OR GRANT No.**

D-4-93

12. SPONSORING AGENCY NAME AND ADDRESS

Department of Transportation
Division of Highways
Sacramento, California 95807

13. TYPE OF REPORT & PERIOD COVERED

Final

14. SPONSORING AGENCY CODE**15. SUPPLEMENTARY NOTES**

This study was conducted in cooperation with the U.S. Department of Transportation, Federal Highway Administration for the research project "Earthwork Reinforcement Techniques".

16. ABSTRACT

This report represents the basic theory, design, construction, instrumentation and field data for the reinforced earth fill constructed on California State Highway 39, Los Angeles County. Design equations for designing the reinforcing strip and the skin plate were developed. The calculated stresses based on the design equations agree reasonably well with the field data. Theoretical analysis by the finite element method based on composite elastic properties of the soil and the reinforcement was conducted. The distribution patterns of the analyzed steel stresses generally agree with the measured data but with some discrepancies in magnitude. Also presented are corrosion studies and cost comparisons between the reinforced earth wall and three other types of retaining wall. Presented in the Appendix are the derivation of equations for designing in the skin plate; the analysis of the composite material properties of reinforced earth; the User's Manual and list of the finite element computer programs.

17. KEYWORDS

Reinforced earth, reinforcing strip, skin plate, stress, strains, movement, stability, corrosion, cost, pull test, peak, yield residual, finite element analysis, composite material

18. No. OF PAGES:

301

19. DRI WEBSITE LINK

<http://www.dot.ca.gov/hq/research/researchreports/1974-1975/74-37.pdf>

20. FILE NAME

74-37.pdf

CALIFORNIA DIVISION OF HIGHWAYS
TRANSPORTATION LABORATORY
RESEARCH REPORT

Earthwork Reinforcement
Techniques

74-37

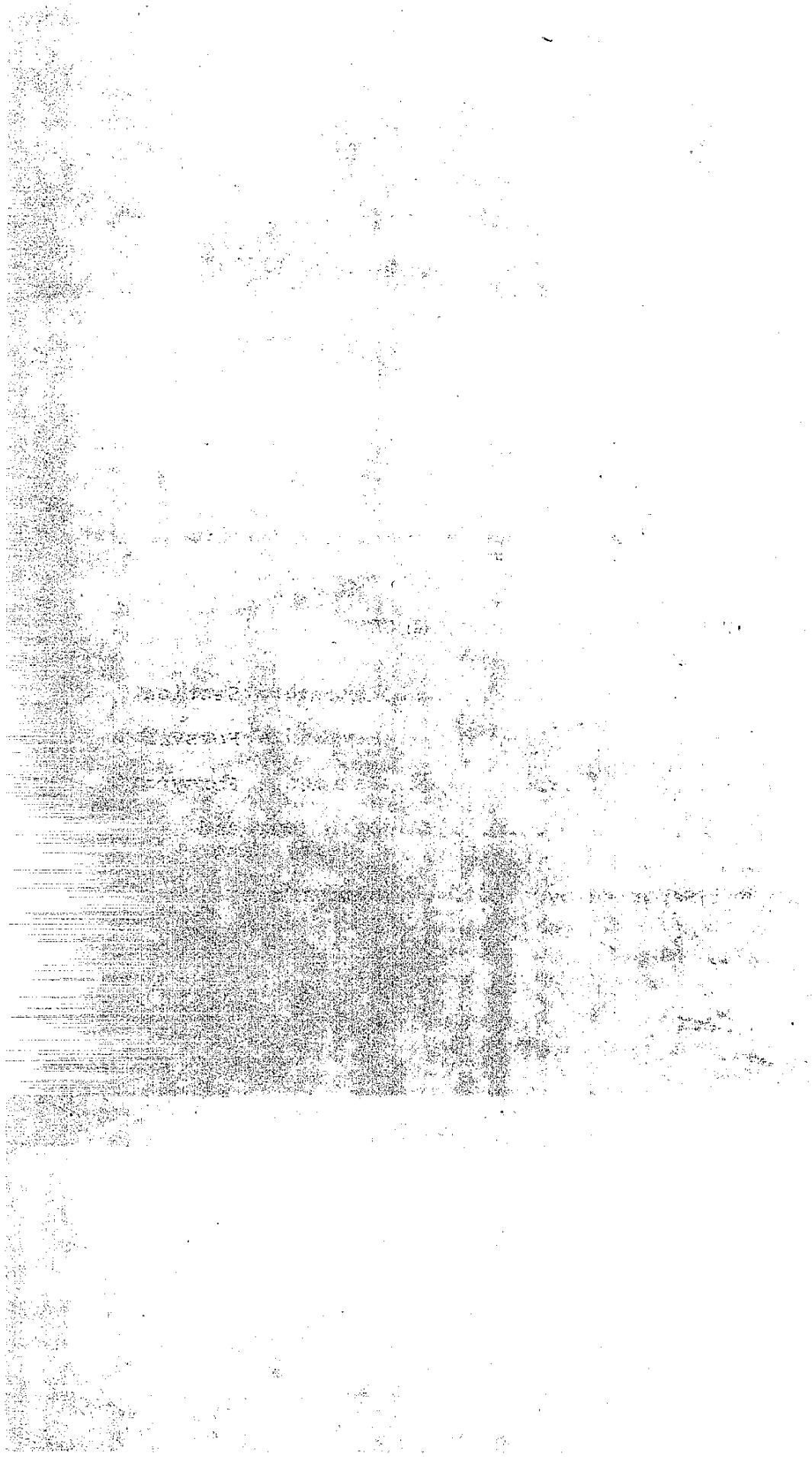
FINAL REPORT
CA-DOT-TL-2115-9-74-37
OCTOBER 1974

Prepared in Cooperation with the U.S. Department of Transportation,
Federal Highway Administration



1. REPORT NO.		2. GOVERNMENT ACCESSION NO.		3. RECIPIENT'S CATALOG NO.	
4. TITLE AND SUBTITLE Earthwork Reinforcement Techniques				5. REPORT DATE November 1974	
				6. PERFORMING ORGANIZATION CODE 19202-762503-632115	
7. AUTHOR(S) Chang, Jerry C.				8. PERFORMING ORGANIZATION REPORT NO. CA-DOT-TL-2115-9-74-37	
9. PERFORMING ORGANIZATION NAME AND ADDRESS Transportation Laboratory 5900 Folsom Boulevard Sacramento, California 95819				10. WORK UNIT NO.	
				11. CONTRACT OR GRANT NO. D-4-93	
12. SPONSORING AGENCY NAME AND ADDRESS Department of Transportation Division of Highways Sacramento, California 95807				13. TYPE OF REPORT & PERIOD COVERED Final	
				14. SPONSORING AGENCY CODE	
15. SUPPLEMENTARY NOTES This study was conducted in cooperation with the U.S. Department of Transportation, Federal Highway Administration for the research project "Earthwork Reinforcement Techniques".					
16. ABSTRACT This report represents the basic theory, design, construction, instrumentation and field data for the reinforced earth fill constructed on California State Highway 39, Los Angeles County. Design equations for designing the reinforcing strip and the skin plate were developed. The calculated stresses based on the design equations agree reasonably well with the field data. Theoretical analysis by the finite element method based on composite elastic properties of the soil and the steel reinforcement was conducted. The distribution patterns of the analyzed steel stresses generally agree with the measured data but with some discrepancies in magnitude. Also presented are corrosion studies and cost comparisons between the reinforced earth wall and three other types of retaining wall. Presented in the Appendix are the derivation of equations for designing the skin plate; the analysis of the composite material properties of reinforced earth; the User's Manual and list of the finite element computer programs.					
17. KEY WORDS reinforced earth, reinforcing strip, skin plate, stress, strains, movement, stability, corrosion, cost, pull test, peak, yield residual, finite element analysis, composite material.			18. DISTRIBUTION STATEMENT Unlimited		
19. SECURITY CLASSIF. (OF THIS REPORT) Unclassified		20. SECURITY CLASSIF. (OF THIS PAGE) Unclassified		21. NO. OF PAGES 301	22. PRICE





(

●

●

●

ACKNOWLEDGEMENTS

The researchers wish to express their appreciation to the personnel of Transportation District 07 for their assistance in this project. Special acknowledgement and thanks are extended to the following persons for their valuable assistance: Gary Bork and John Kenan who were in charge of overall design of the Route 39 project; Robert F. Britton, the Resident Engineer during construction, Ronald Gierloff, the Survey Party Chief.

Special appreciation is extended to Professors L. R. Herrmann, K. M. Romstad, and C. K. Shen of U. C. Davis who developed the finite element computer program using the composite material property approach and voluntarily devoted a great amount of their time to assist in performing the finite element analysis, interpreting and analyzing the results.

Ralph E. Haverkamp and George G. Fung of the Office of Structures are the coordinators for implementation of this research project. Their assistance in various respects is appreciated.

Transportation Laboratory personnel who were involved in developing, installing and reading the instrumentation are as follows:

Foundation Section: Rich Freeman, Barry McGee, Ron Thompson, Frank Champion, and Joe Egan

Electrical Section: Don Larsen, Sam Muraki, Del Gans, Vic VanMatre, and Al Sequeira

Machine Shop: George Oki, Ervin Eisenbraun and Floyd Martin

Personnel who were involved in data analysis for this project are:

F. J. Sage, Bert Van Voris, Ellsworth L. Chan, and David R. Castanon

The contents of this report reflect the views of the Transportation Laboratory which is responsible for the facts and the accuracy of the data presented herein. The contents do not necessarily reflect the official view or policies of the State of California or the Federal Highway Administration. This report does not constitute a standard, specification, or regulation.

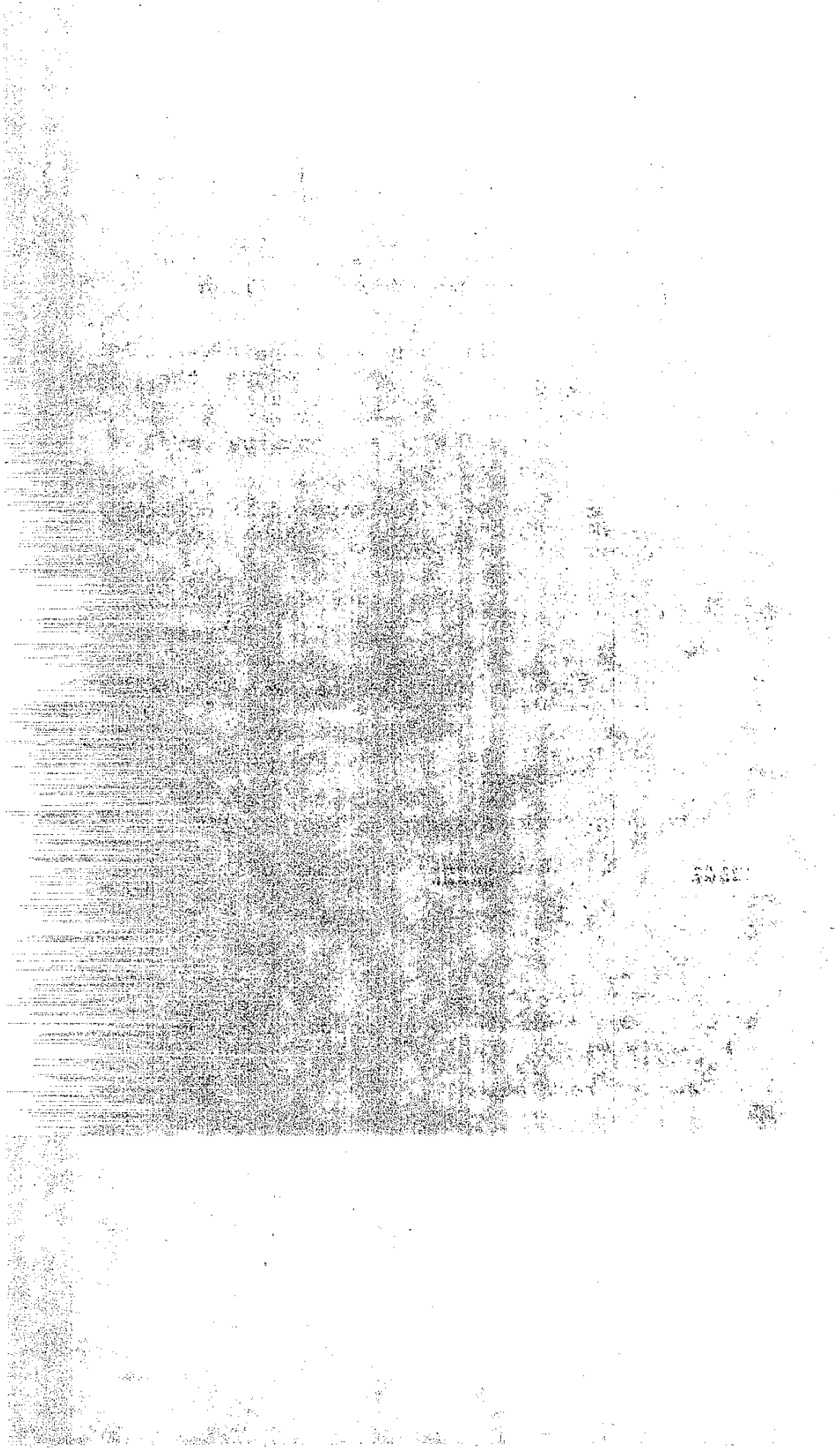


TABLE OF CONTENTS

	<u>Page</u>
ACKNOWLEDGEMENTS	i
LIST OF TABLES	iv
LIST OF PHOTOS	v
LIST OF FIGURES	vi
<u>CHAPTER</u>	
I. INTRODUCTION	1
II. CONCLUSIONS	3
A. Field Behavior	3
B. Design Methods	4
C. Theoretical Analysis	4
D. Cost	5
III. RECOMMENDATION	6
A. Continual Field Studies	6
B. Improving the Finite Analysis Computer Program	6
C. Earthquake Resistance Studies	7
1. Theoretical Analysis by the Finite Element Method	7
2. Field Dynamic Test on Prototype Structure	7
IV. DISCUSSION	8
A. Basic Theory	8
B. Design of Reinforcement	9
C. Design of Skin Plates	10
D. Stability	11
E. Corrosion	12
F. Demonstration Project	12
1. Soil Testing	13
2. Skin Plates and Steel Reinforcement	13
3. Construction Operation	14
4. Construction Equipment and Labor Work	15
5. Construction Cost	15
6. Instrumentation	16
7. Field Data	16

[The page contains extremely faint and illegible text, likely a scan of a document with very low contrast or significant noise. The text is mostly concentrated in the left and center portions of the page.]



TABLE OF CONTENTS (Con't.)

	<u>Page</u>
a. Internal Movement of Embankment	17
b. Movements of the Reinforced Earth Fill	17
c. Settlement of Reinforced Earth Fill	18
d. Soil Stresses in Reinforced Earth Fill	18
e. Stresses in Steel Strips	19
f. Strain in Steel and Soil	20
g. Horizontal Soil Stresses and Converted Steel Stresses	20
h. Axial Force in Dummy Strips	21
i. Stress in Skin Element	21
j. Field Behavior of Steel Skin Plate	22
8. Field Pulling Tests	22
G. Theoretical Analysis by the Finite Element Method	25
1. Elastic Property of Fill Material	26
2. Finite Element Analysis	28
3. Analyzed Results and Comparison with Field Data	29
a. Vertical Soil Stresses	29
b. Horizontal Soil Stresses	29
c. Shear Stresses	30
d. Theoretical Steel Strip Forces	30
e. Stresses in the Skin Plate	30
f. Settlement in the Reinforced Earth Fill	31
g. Horizontal Movement of Berm and Face Wall	31
h. Horizontal Movement in Embankment	31
4. Discussion of the Finite Element Results	32
REFERENCES	33
TABLES	
PHOTOS	
FIGURES	
APPENDIX A - Derivation of Equation for Analysis of Stress in Skin Plate	
APPENDIX B - Composite Material Properties of Reinforced Earth	
APPENDIX C - User's Manual for the Plane Strain Incremental Construction Program	
APPENDIX D - List of the Finite Element Computer Program and Example of Input and Output Data	

CONFIDENTIAL

...the ... of ...
...the ... of ...
...the ... of ...

...the ... of ...
...the ... of ...

...the ... of ...

...the ... of ...
...the ... of ...

...the ... of ...
...the ... of ...
...the ... of ...
...the ... of ...

...the ... of ...

...the ... of ...

...the ... of ...

...the ... of ...

...the ... of ...

...the ... of ...

...the ... of ...



LIST OF TABLES

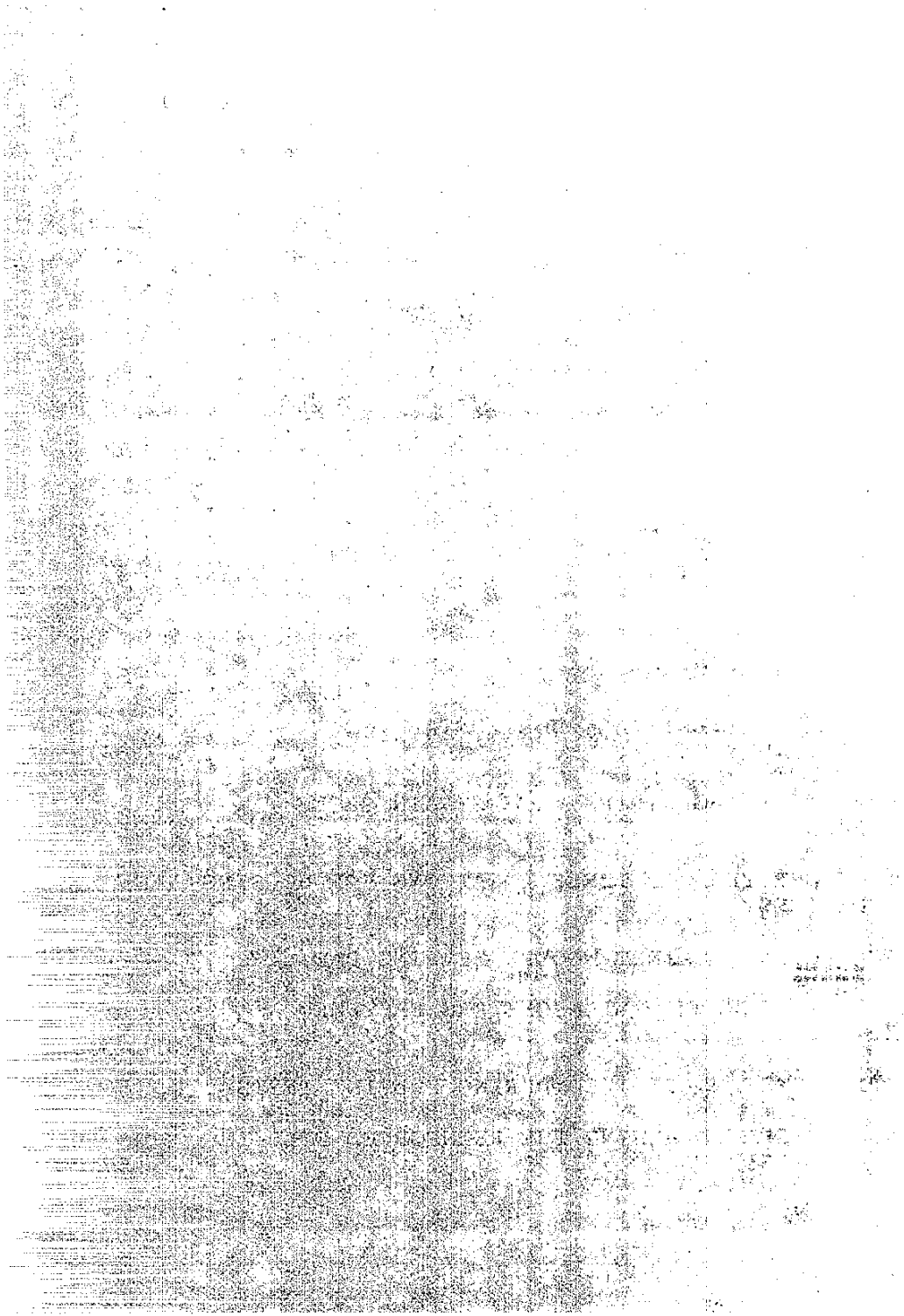
<u>Table No.</u>	<u>Title</u>	<u>Page</u>
1.	LABORATORY SOIL TEST RESULTS	36
2.	FIELD NUCLEAR GAGE DENSITY READINGS.	37
3.	CONSTRUCTION EQUIPMENT AND RENTAL RATE	38
4.	CONSTRUCTION LABOR DESCRIPTION AND HOURLY RATE	39
5.	AVERAGE UNIT QUANTITIES AND COSTS.	40
6.	COST COMPARISON BETWEEN FOUR TYPES OF WALLS	41
7.	INSTRUMENTATION INSTALLATION DATA - LEVEL "A"	42
8.	INSTRUMENTATION INSTALLATION DATA - LEVEL "B"	43
9.	INSTRUMENTATION INSTALLATION DATA - LEVEL "C"	44
10.	SLOPE INDICATOR INSTALLATION DATA	45
11.	IDENTIFICATION OF SOIL SAMPLES	46
12.	SHEAR STRENGTH PARAMETERS	47
13.	TANGENT MODULUS VALUES	48
14.	TANGENT POISSON'S RATIO PARAMETERS	49
15.	TANGENT POISSON'S RATIO VALUES	50

[The page contains extremely faint and illegible text, likely a scan of a document with very low contrast or significant noise. The text is organized into several paragraphs, but the individual words and sentences are not discernible.]



LIST OF PHOTOS

<u>Photo No.</u>	<u>Title</u>	<u>Page</u>
1.	COMPLETED VIEW OF THE REINFORCED EARTH EMBANKMENT	51
2.	BATTER BOARDS AND INSTRUMENTED SKIN ELEMENT	51
3.	PLACING REINFORCING STRIPS.	52
4.	COMPLETED WALL FACE WITH WOODEN WEDGES BETWEEN SKIN ELEMENTS AND INSTRUMENTATION SHELTERS ON BERM	52
5.	COMPACTION OPERATION.	53
6.	INSTRUMENTATION TRENCH WITH SETTLEMENT PLATFORM IN PLACE	53
7.	EXTENSOMETER INSTALLED	54
8-a	INSTALLATION OF SOIL PRESSURE CELL	54
8-b	SOIL PRESSURE CELL ON VERTICAL, HORIZONTAL AND INCLINED PLANES	54
9.	INSTRUMENTED REINFORCING STRIPS WITH STRAIN GAGES PROTECTED BY SAND	55
10.	INSTRUMENTATION SHELTERS AT THREE LOCATIONS FOR HOUSING THE READ OUT DEVICES.	55
11.	HYDRAULIC JACK ACTING AGAINST WOODEN BEARING PAD.	56
12.	DUMMY STEEL STRIP WITH TWO EXTENSOMETERS FASTENED AT EACH SIDE.	56
13.	DATA ACQUISITION SYSTEM UTILIZED DURING PULLING TESTS	56
14.	PAVEMENT CRACKS OBSERVED BEHIND THE REINFORCED FILL IN APRIL 1973 STATION 552+90 TO 553+75	57



LIST OF FIGURES

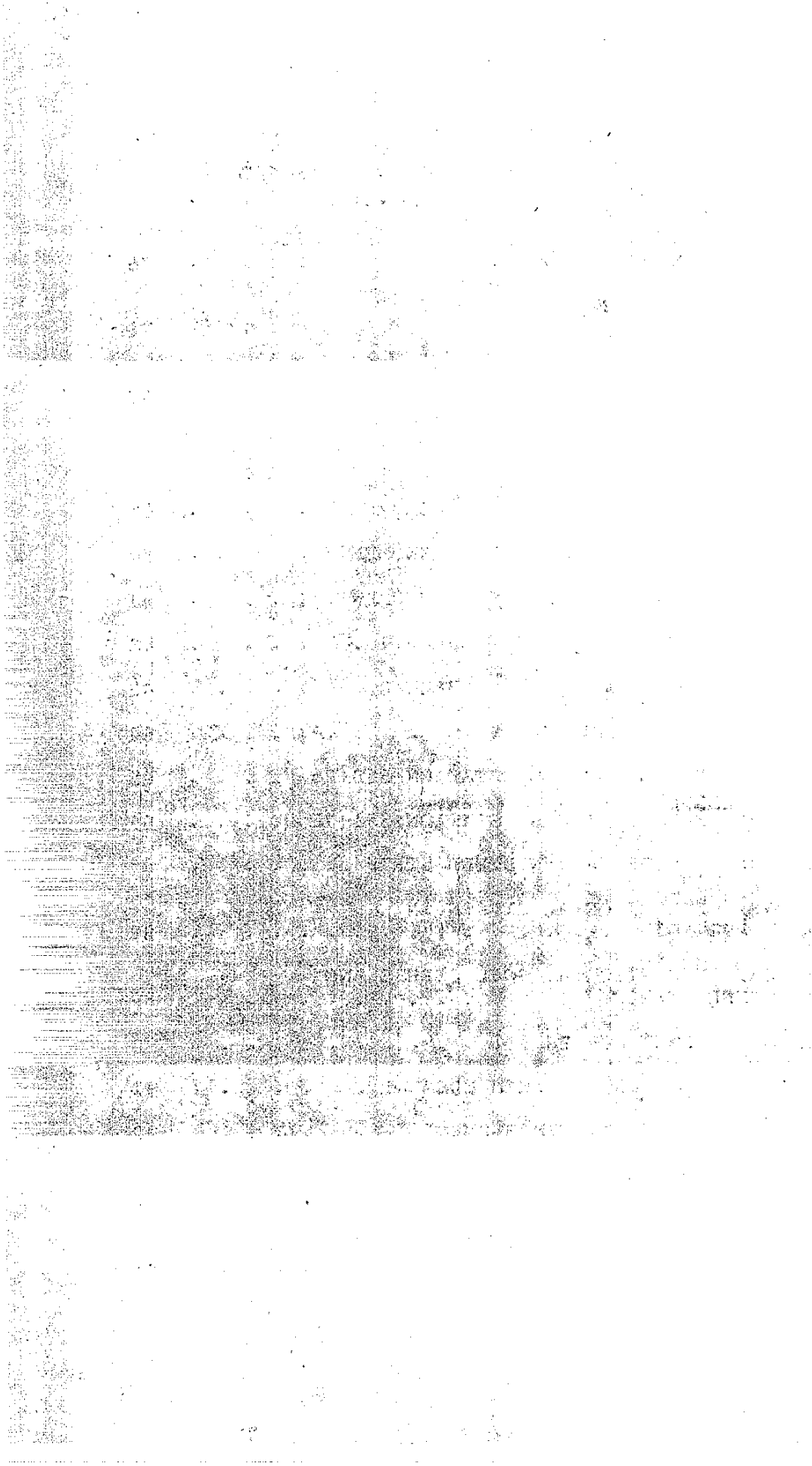
<u>Figure Number</u>	<u>Title</u>	<u>Page</u>
1.	SCHEMATIC OF REINFORCED EARTH FILL	58
2.	SAND CUBE ($\sigma_1 = \sigma_3$)	58
3.	SAND CUBE ($\sigma_1 > \sigma_3$)	58
4.	MOHR CIRCLE (AT IMMINENT FAILURE)	58
5.	REINFORCED SOIL ELEMENT	58
6.	MOHR CIRCLE (WITHOUT IMMINENT FAILURE)	59
7.	SCHEMATIC OF REINFORCED EARTH BLOCK	59
8.	LOADING DIAGRAM ON SKIN PLATE	59
9.	STABILITY REQUIREMENTS - RULE OF THUMB	60
10.	CHART FOR ESTIMATING CORROSION RATE OF STEEL PIPE	61
11.	PLAN AND SECTION	62
12.	STRESS-DEFORMATION CURVE FROM LABORATORY PULLING TESTS	63
13.	SKIN FRICTION ENVELOPE LINE	64
14.	DAILY RECORD OF HEIGHT DURING EMBANKMENT CONSTRUCTION	65
15.	DAILY RECORD OF CONSTRUCTION QUANTITIES	66
16.	WEEKLY RECORD OF CONSTRUCTION COSTS	67
17.	COST COMPARISON BETWEEN FOUR TYPES OF WALLS	68
18.	INSTRUMENTATION SECTIONS	69
19.	HORIZONTAL MOVEMENT IN THE E-W DIRECTION MEASURED BY SLOPE INDICATOR SI-1	70
20.	HORIZONTAL MOVEMENT IN THE N-S DIRECTION MEASURED BY SLOPE INDICATOR SI-1	71
21.	HORIZONTAL MOVEMENT IN THE E-W DIRECTION MEASURED BY SLOPE INDICATOR SI-2	72
22.	HORIZONTAL MOVEMENT IN THE N-S DIRECTION MEASURED BY SLOPE INDICATOR SI-2	73

[The page contains a large area of extremely faint, illegible text, likely due to heavy noise or low resolution in the scan. The text is organized into several columns and paragraphs, but the characters are not discernible.]



LIST OF FIGURES (con't.)

<u>Figure Number</u>	<u>Title</u>	<u>Page</u>
23.	HORIZONTAL MOVEMENT IN THE E-W DIRECTION MEASURED BY SLOPE INDICATOR SI-3	74
24.	HORIZONTAL MOVEMENT IN THE N-S DIRECTION MEASURED BY SLOPE INDICATOR SI-3	75
25.	EMBANKMENT SETTLEMENT MEASURED BY SLOPE INDICATOR SI-1	76
26.	EMBANKMENT SETTLEMENT MEASURED BY SLOPE INDICATOR SI-2	77
27.	EMBANKMENT SETTLEMENT MEASURED BY SLOPE INDICATOR SI-3	78
28.	HORIZONTAL MOVEMENTS - SERIES "A" MONUMENTS	79
29.	HORIZONTAL MOVEMENTS - SERIES "B" MONUMENTS	80
30.	HORIZONTAL MOVEMENTS - SERIES "C" MONUMENTS	81
31.	DISPLACEMENTS ALONG WALL FACE - SHEET 1	82
32.	DISPLACEMENTS ALONG WALL FACE - SHEET 2	83
33.	DAILY HISTORY OF SETTLEMENT	84
34.	DAILY HISTORY OF SOIL STRESS, STATION 550+25	85
35.	DAILY HISTORY OF SOIL STRESS, STATION 551+75	86
36.	DAILY HISTORY OF STRESSES IN STEEL STRIP	87
37.	DAILY HISTORY OF HORIZONTAL STRAIN IN STEEL STRIP AND SOIL	88
38.	DAILY HISTORY OF HORIZONTAL SOIL STRESS AND CONVERTED STEEL STRESS	89
39.	AXIAL FORCE IN DUMMY STRIPS	90
40.	DAILY HISTORY OF STRESS IN SKIN ELEMENT	91
41.	FIELD BEHAVIOR OF STEEL SKIN ELEMENT	92
42.	LOAD DEFORMATION CURVE FROM FIELD PULLING TESTS - SHEET 1	93
43.	LOAD DEFORMATION CURVE FROM FIELD PULLING TESTS - SHEET 2	94



LIST OF FIGURES (con't.)

<u>Figure Number</u>	<u>Title</u>	<u>Page</u>
44.	FIELD PULLING TEST RESULTS	95
45.	RELATIONSHIP BETWEEN PULL LOAD AND SKIN FRICTION FORCE	96
46.	TYPICAL STRESS-STRAIN CURVES OF SOIL SAMPLES	97
47.	TYPICAL TRANSFORMED HYPERBOLIC STRESS-STRAIN CURVES	98
48.	TYPICAL MOHR CIRCLES	99
49.	VARIATION OF INITIAL TANGENT MODULUS WITH CONFINING PRESSURE	100
50.	POISSON'S RATIO VS RADIAL STRAIN CURVES	101
51.	POISSON'S RATIO VS DEVIATOR STRESS	102
52.	TYPICAL SECTION FOR FINITE ELEMENT ANALYSIS AT STATION 551+75	103
53.	CONTOURS OF THEORETICAL VERTICAL SOIL STRESS	104
54.	COMPRESSIVE VERTICAL SOIL STRESS DISTRIBUTION STATION 551+75	105
55.	CONTOURS OF THEORETICAL HORIZONTAL SOIL STRESS	106
56.	COMPRESSIVE HORIZONTAL SOIL STRESS DISTRIBUTION STATION 551+75	107
57.	CONTOURS OF THEORETICAL STRESS RATIO, $k = \sigma_x/\sigma_y$	108
58.	CONTOURS OF THEORETICAL SHEAR STRESS	109
59.	CONTOURS OF THEORETICAL FACTOR OF SAFETY	110
60.	CONTOURS OF THEORETICAL STEEL STRIP FORCES	111
61.	DISTRIBUTION OF STEEL STRIP STRESS, STATION 551+75	112
62.	COMPARISON OF THEORETICAL AND FIELD STRESS IN SKIN PLATE	113
63.	SETTLEMENT WITH RESPECT TO BERM READOUT POINT, STATION 551+75	114

[The text in this section is extremely faint and illegible due to heavy noise and low contrast. It appears to be a dense block of text, possibly a list or a series of entries, but no specific words or structures can be discerned.]



I. INTRODUCTION

Reinforced earth is a soil mass composed of soil and reinforcing elements (Figure 1). The reinforcing elements provide tensile strength to the soil mass.

The concept of strengthening soil by adding reinforcing elements is not new. Some animals and birds have used straw and branches mixed with soil to build their habitations. Straw has also been used since biblical time to strengthen adobe bricks (1). Alternating layers of earth and logs were used by the Gauls to build fortifications (2). In China, mattresses made of wood branches have been placed in soil to form dikes and revetments along the Yellow River for more than a thousand years. Bundles of brushwood called faggots were used in stabilizing the bank of the Mississippi River in the 1880's (3). In England, faggots were used extensively for erosion control of levees and repairing landslides (4,5). In Taiwan, China, bamboo or steel wire mesh has been used for a long time to enclose stone or gravel in a cylindrical form called wire-stone sausage for building spur dikes and revetments (6). The California Division of Highways utilized redwood logs as reinforcing elements to build highway embankments in the 1930's (7) by laying 20-foot long wood logs in rows and covered with earth to form the embankment section. The concept of using wooden beams as reinforcement for constructing vertical retaining walls was patented in 1930 (8). The strengthening of the downstream slope of earth dams by layers of metal reinforcements along with metal grids or concrete panels for facing elements was proposed early in 1904 (9). Using this concept, several dams were constructed in Mexico in the 1930's and 1940's (10). Similar types of construction have been used in Africa (11), Australia (12, 13, 14) and New Guinea (15).

The California Division of Highways used wire mesh in the 1940's to stabilize embankment slopes against erosion and to prevent slumping (16). Wire mesh fence of 5 feet in width were laid horizontally in the outer edge of the embankment at 10 to 15 foot intervals.

In the 1960's a French engineer, Henri Vidal, developed a disciplined approach based upon a rational design procedure for the use of reinforced earth for application to important engineering structures (17, 18, 19).

Most recently, Harrison and Gerrard (20) used the concept of composite elastic properties of reinforced media proposed by Westergaard (21) to develop mathematical expressions of the elastic constants of reinforced earth. Model testing has been conducted by Yamanouchi (22, 23) to study the improvement of bearing capacity of soft ground by layers of resinous net.

Lee et. al., (24,25) conducted laboratory model tests to study the failure mode of a small-scale reinforced earth wall model and the stresses developed in the reinforcements and soil due to static and horizontal sinusoidal seismic loading.

In July 1970, a research work plan entitled "Earthwork Reinforcement Techniques" was initiated by the Transportation Laboratory, California Department of Transportation, to develop a design method based on established principles of soil mechanics. A field performance study was proposed to study the engineering behavior of a prototype reinforced earth fill on California State Highway 39 near Crystal Lake, Los Angeles County. A comprehensive instrumentation was then installed in the embankment and the reinforced earth fill. Observation of field data was conducted during construction and extended for one year after completion of construction. Laboratory tests were performed to investigate the pulling resistance for different type of reinforcements. Design equations were developed for designing the reinforcement and the skin plate enclosed at the front face of reinforced earth fill. Finite element analyses were conducted to predict the field behavior.

A movie film was also developed to present the basic theory, design method, field data, construction cost, and all aspects of soil investigation, construction, instrumentation and reading instruments.

II. CONCLUSIONS

The study substantiates the following conclusions.

A. Field Behavior

1. The settlement of the reinforced earth embankment is primarily attributable to the densification and the associated slight horizontal movements of the deep foundation slide debris. These large foundation settlements and the associated horizontal movement are probably the main cause of continuing change in stresses of the steel and soil after completion of the fill.

The differential settlements between the center portion and each end of the reinforced earth embankment are the primary causes of the axial tensile stresses in the skin plates. It has been proven that the continuous steel skin elements are very effective in linking the reinforced earth embankment into a monolithic soil mass. This monolithic action helps the redistribution of the horizontal movement along the alignment of the reinforced earth embankment.
2. The measured vertical soil stresses generally agree with the calculated, theoretical vertical earth pressures. The stress ratios, K , between the horizontal and vertical soil stresses were their highest during construction and then decreased after completion of the fill with large variations from point to point.
3. The measured stresses in the steel strips near the wall face were generally smaller than, but approached the calculated theoretical stresses, σ_a , based on Rankine's active state-of-stress theory. The highest steel stresses developed in the inner middle portion of the reinforced earth section. The steel stresses may increase to the value corresponding to the theoretical "at rest" earth pressure.
4. The strains measured in the steel strips and soil generally agreed with each other. The converted steel stresses, however, were generally smaller than the horizontal soil stresses. This phenomenon is probably attributable to the soil arching action.
5. The structural behavior of the skin plates was as expected in the design assumptions in deformed shape

and stress values. The vertical deformation of the skin plate, which is a measurement of settlement within each skin element, is proportional to the overburden height.

6. Field pulling test results indicate that the load-deformation curves resembled the stress-strain curves obtained from laboratory triaxial compression tests on dense sands. When the strips were pulled loose, the yielding, peak, and residual load points are all clearly defined. The frictional forces developed on the steel strips were proportional to the overburden load for each overburden height. The field measured skin friction angle agreed well with the laboratory test results under equal overburden height.

B. Design Methods

1. Equation 4 presented in this paper for the design of reinforcing strips has been verified. The use of the active earth pressure coefficient, K_a , for calculating the steel stress is applicable for the end portion of the reinforcements. For the middle portion of the reinforcement, the coefficient of "at rest" earth pressure, K_0 , should be used in the design.
2. The relationships between overburden height, strip length, and the factor of safety against slippage shown in Figure 21-g can be used for determining the minimum length of reinforcement, providing the requirement for stability is met.
3. Design Equation 7, developed in this paper for design of the steel skin plate, accurately predicted the stresses developed in the skin plate. Use of the vertical deformation, δ_v , of the skin plate for one of the major design functions has proven to be a satisfactory approach. The assumption of a semi-circular shape simplified the calculation of the stresses in the skin plate and accurately predicted the measured stresses.

C. Theoretical Analysis

The theoretically analyzed results of soil stresses and horizontal movement by the finite element method in general compare favorably with the measured values. The distribution patterns of calculated steel stresses generally agree with the measured data but magnitude are different. The calculated stresses in the skin plate are

all smaller than the measured values. The difference is probably because the finite element program calculated the hoop tension only without consideration of bending. The field data indicates that the predominant stresses developed in the skin plate are due to bending.

The discrepancies between the calculated and measured results are thought to be attributable to the following factors:

1. Two dimensional analysis - The finite element mesh model assumes a two-dimensional structure. The prototype embankment, however, is a three-dimensional structure. The alignment of the reinforced earth fill follows three chords of a horizontal arc, and the embankment was placed in cone shape canyon.
2. Time function - The measured data shows significant changes in steel stress with time because of the continued settlement of the embankment foundation. The finite element program does not include time function of foundation settlement in the analysis.
3. Construction increments - The number of construction increments assumed in the analysis may have a significant effect on the stresses computed in the reinforcing strips. For moderately large increments, the top layer of strips initially have compressive stresses (much like the compression steel in concrete beams). As subsequent layers are added the initial compression is overcome by the expected tensile forces. The actual construction process is almost continuous.
4. Edge effect - The skin plate is curved in shape. The soil may not be in continuous contact with the skin plate. A void may exist between the skin plate and the compacted soil mass at some points. This "edge effect" was not accounted for in the composite element representation of soil-strip behavior.

D. Cost

Even though this demonstration project of the reinforced earth embankment was the first of its kind in the United States and was located in a relatively remote mountainous area with very limited work space, it was found that the reinforced earth embankment was still more economical than all three other types of retaining walls (metal crib wall, reinforced concrete crib wall, and reinforced concrete retaining wall).

III. RECOMMENDATION

The basic concept of reinforced earth design using conventional soil mechanics theory for determining the stress developed in the reinforcement has been verified from the research project. The field data indicates, however, a wide range of variation, depending on boundry geometry and foundation conditions of the site. Additional research is necessary to further define the factors which influence behavior of soil-reinforcement interaction. In addition, one of the major unknowns is the possible effect of an earthquake on the stability of reinforced earth fill. Following are the specific recommendations for further studies.

A. Continual Field Studies

The Transportation District 2 of the California Department of Transportation is constructing a reinforced earth fill on Interstate Highway 5, near Dunsmuir, Siskiyou County. Another one near Lakehead, Shasta County will be constructed in 1975. Both of these will be constructed on relative rigid foundations using steel strips for reinforcement and concrete panels for facing. These sites offer the ideal location for theoretical analyses by the finite element method. It is proposed to install instrumentation on these projects to further study reinforced earth field behavior. A research work plan was submitted to the Federal Highway Administration for approval on January 31, 1974.

B. Improving the Finite Element Analysis Computer Program

It is proposed to improve the finite element analysis computer program by taking into consideration the following:

1. Accounting for possible movement of reinforcement relative to the soil
2. Consideration of including elasto-plastic behavior of soil and reinforcement
3. Consideration of the "edge effects" on using skin plate and concrete facing
4. Improving procedure for handling the overburden dependent and time dependent effects on the elastic properties of the composite material.

C. Earthquake Resistance Studies

The objective of the earthquake resistance studies are necessary to develop a method for evaluating the dynamic response, and the stability of reinforced earth fill under earthquake loading. This study will involve two phases.

1. Theoretical Analysis by the Finite Element Method

In cooperation with University of California at Davis a computer program similar to the QUAD4 program (26) will be developed by considering the following factors.

- a. The stress-strain behavior of the steel-soil composite material
- b. The damping behavior of the steel-soil composite material
- c. The Poisson's ratio of the steel-soil composite material

2. Field Dynamic Test on Prototype Structure

Instruments for measuring dynamic response of stress and strains under seismic loading will be installed in the field prototype structure. A steady-state-vibration and a controlled dynamic blasting to produce earthquake-like seismic excitation will be conducted in the field. The dynamic response will be measured by the installed instrumentation. The field test data will then be compared with the analytical results by the finite element method.

IV. DISCUSSION

A. Basic Theory

The basic mechanism of a reinforced earth embankment can be explained by Rankine's State-of-Stress theory. Assuming that an element of cohesionless soil mass in a fill is acted on by vertical and lateral stresses, the element of soil mass will be compressed (Figure 2). If the lateral stresses are smaller than the vertical stresses, lateral expansion and vertical compression will occur (Figure 3). When the lateral strain reaches a critical value, the element of soil mass will fail by shearing along a failure plane. A triaxial compression test indicates the same mechanism as described above. The state-of-stress at an imminent failure condition can be described by a Mohr diagram (Figure 4) in which Point A represents the state-of-stress shown by Figure 2 where σ_1 equals σ_3 . In order to hold the soil element without failure the lateral stress (σ_3) must be increased. By providing reinforcement in a soil element (Figure 5), the skin friction of the reinforcement will supply additional lateral strain. This additional lateral resistance acts as an imaginary plate fixed at each end of the soil element to prevent failure. The state-of-stress at a stable condition is shown by Figure 6.

The state-of-stress developed in a reinforced earth embankment may vary from an "at rest" state in the inner portion of the embankment to the "active" state near the outer face of the embankment. However, the maximum frictional force required to prevent the soil mass from failure can be assumed to be equal to the active earth pressure as shown in Figure 4. The frictional force developed along the surface of the reinforcement is then resisted by its tensile strength.

Referring to Figures 1 and 7, the frictional forces along the surfaces of the reinforcing strips will create a soil arching action in the vertical plane which, in effect, causes the soil particles to link together to form a series of vertical counterfort walls or reinforcing wedges which provide internal stability of the soil mass in a reinforced earth fill.

The determination of the maximum allowable vertical and horizontal spacing of the reinforcements is still uncertain. However, it can be assumed that the reinforcements must be closely spaced so that an arch action within the soil mass can be developed between reinforcements. This arch action, which causes the soil particles to link together

without separation, may depend upon the size of soil particles, the skin friction between the soil and reinforcements, the internal frictional angle of the soil, and the stress developed within the soil mass. Because it is difficult to determine the influence of these unknown factors, the only rational way to select the maximum reinforcement spacing is through large-scale model tests and field performance studies. However, experience has shown that rather small size reinforcements at relatively close spacing (5-foot horizontally and 1-foot vertically) are satisfactory.

B. Design of Reinforcement

Based on the theory and principle discussed in the previous paragraph, the basic equations for designing the reinforcement are presented as follows:

Referring to Figures 4 and 7, following are the notations to be used in developing the basic design equations:

- p = active earth pressure in pounds per square foot
- f_s = steel tensile stress, in psi
- K_a = Rankine active earth pressure coefficient
- b = steel strip width, in inches
- t = steel strip thickness, in inches
- γ = soil density, in pounds per cubic foot
- H = overburden height, in feet
- d = horizontal steel strip spacing, in feet
- Δh = vertical steel strip spacing, in feet
- T = tensile force in steel strip, in pounds
- F = frictional resistance, in pounds
- L = length of steel strip, in feet
- δ = friction angle between steel and soil

It is believed that the wall face may rotate slightly outward after compaction. A Rankine's active earth pressure may develop on the inner face of the skin plate, as

$$p = \sigma_3 = K_a \gamma H \quad (1)$$

The total earth pressure acting on the inner face of the skin plate will tend to either pull out or break the steel strips. The pull force, T, developed in each steel strip will be then

$$T = K_a \gamma H d \Delta h, \quad (2)$$

$$\text{and } T = f_s b t, \quad (3)$$

$$\text{or } f_s = \frac{K_a \gamma_H d \Delta h}{bt} \quad (4)$$

The friction force developed on each face of the reinforcing plate will be then

$$F = \frac{\gamma_H b L \tan \delta}{12} \quad (5)$$

Therefore, the factor of safety against slippage can be expressed as

$$F.S. = \frac{2F}{T} = \frac{2 \gamma_H b L \tan \delta}{12 K_a \gamma_H d \Delta h} = \frac{b L \tan \delta}{6 K_a d \Delta h} \quad (6)$$

Equations 4 and 6 are the basic equations developed by the Transportation Laboratory for evaluating the reinforcement design provided by the Reinforced Earth Company.

C. Design of Skin Plates

The skin plate which provides restraint for the soil between individual rows of reinforcing strips must be rigid enough to resist anticipated impact or shocks and flexible enough to tolerate a certain degree of deformation to conform with the settlement of the soil mass upon loading. The standard shape of the skin plate used by the Reinforced Earth Company consists of semi-elliptical element of 10 to 13 inches high with a thickness of about 1/8" (3mm).

For simplicity in stress analysis, a semicircular section of skin plate with the assumed soil pressure and deformation configuration is shown in Figure 8. The vertical load, P, which represents the resulting force transferred from a uniform vertical pressure acting along an effective length of reinforcing strip will cause a vertical deformation, δ_v , on the skin plate. This vertical deformation is assumed to have the same magnitude as the settlement of the soil mass caused by a uniform vertical soil pressure acting on the top and bottom row of reinforcement. Using strain energy principles (27), the equations for computing the vertical load, P, and end moment, M_a , are developed (see Appendix A) as follows:

For hinged end conditions at A and B (Figure 8),

$$P = \frac{4EI\delta_v}{R^3\pi} - \frac{4K_a\gamma HR}{3\pi} - \frac{\gamma HR}{24\pi} (3\pi - 32); \quad (7)$$

and for fixed end conditions at A and B (Figure 8),

$$P = \frac{\delta_v EI}{\pi R^3} \left(4 - \frac{32}{8-\pi^2}\right) + \gamma HR \left(\frac{4-4K_a}{3\pi} - \frac{1}{8}\right) - \frac{8\gamma HR}{8-\pi^2} \left(\frac{4-4K_a}{3\pi} - \frac{(1+\pi - \pi K_a)}{8} + \frac{1}{9}\right); \quad (8)$$

and

$$M_a = \frac{8\delta_v EI}{R^2(8-\pi^2)} + \frac{2\pi\gamma HR^2}{(8-\pi^2)} \left(\frac{4-4K_a}{3\pi} - \frac{(1+\pi - \pi K_a)}{8} + \frac{1}{9}\right) \quad (9)$$

In Equations 7 and 8, magnitude of P depends upon the restraint conditions at the ends A and B and the value of vertical settlement, δ_v . In Equation 9, the value of M_a also depends upon the value of δ_v which can be measured or estimated for settlements of embankment based on field observed data or previous experience.

Once the load, P, and the end moment, M_a , are known, the calculation of the stresses in the skin plate becomes a statically determinate problem. These stresses can be readily computed. Equations 7 and 9 can be verified by measuring strain and thus, stresses at selected points on the skin plate and the vertical deformations, δ_v , in field performance studies on prototype structure or laboratory scale model tests.

D. Stability

The overall stability of a reinforced earth embankment under all expected loading conditions was analyzed by considering the reinforced earth mass as a solid block or a gravity type of concrete retaining wall. Sliding instability and earth pressure developed within the backfill behind the reinforced earth mass, and the potential sliding or bearing failure of the foundation was investigated in the same manner as is ordinarily done for design of embankments and retaining walls.

As a rule of thumb suggested by the Reinforced Earth Company, for stability considerations, the ratio of depth to clear height of a reinforced earth embankment is suggested to be at least 0.8. It is also suggested that the footing of the reinforced earth embankment be embedded in an excavated or backfilled berm to one-fifth of the clear height of the reinforced earth embankment; the width of the berm should be at least 5 feet and the outer slope of the berm should be not steeper than 1.5 feet horizontal on 1 foot vertical (Figure 9).

E. Corrosion

The durability of the steel reinforcement and skin plate is one of the major concerns in the design of reinforced earth structures. According to Herbert Uhlig (28), the major factors that govern corrosivity of a given soil are porosity (aeration), electrical conductivity, content of dissolved salts including depolarizers or inhibitors, moisture content, and acidity or alkalinity. In general, life expectancy of steel strips is governed by the rate of metal loss due to corrosion. Havilard, Bellair and Morrell (29) reported the results of ten studies concerning the durability of galvanized steel culverts. It was found that the rate of metal loss for uncoated steel culvert varies from 0.0001 to 0.0056 inch per year.

The California Transportation Laboratory developed a method for estimating relative soil corrosivity by combining the relative influences of the hydrogen-ion concentration (pH) and the minimum resistivity of the soil (30). Figure 10 is a chart developed for estimating underground corrosion rate of steel pipe. This chart shows the relationship between corrosion rate, minimum soil resistivity (ohm/cm^3) and pH values for acid soils and alkaline soils. A thorough investigation of soil samples and corrosive environment for a given construction site is recommended. Laboratory and field soil tests should be conducted to determine various factors which affect corrosion.

Figure 10 can be used for estimating the rate of metal loss, and to establish the required thickness (corrosion allowance) of steel reinforcement for the design life. In excessively corrosive soils, cathodic protection (31) may be employed to prevent reinforcement deterioration.

F. Demonstration Project

A reinforced earth fill, the first in the United States, was constructed between August 1 and October 18, 1972.

This project is located on Route 39, near Crystal Lake, in the San Gabriel Mountains, Los Angeles County. The reinforced earth fill is constructed on top of a random fill embankment founded over slide debris. At the bottom of the slide debris a toe buttress was built to act as a stabilizing fill embankment. The overall height of the system is approximately 360 feet. The reinforced earth fill has a maximum height of 55 feet and a length of 528 feet. A drainage system consisting of surface and subsurface drain pipes were installed to remove surface water and seepage. The detailed design and stability analysis of the Route 39 embankment was reported in Highway Focus, January, 1972, published by the U.S. Department of Transportation (32). Figure 11 shows a plan view and a sectional view. Photo 1 shows the completed view of the project. Several important features pertaining to the demonstration project are discussed as follows:

1. Soil Testing

Soil material for the embankment and reinforced earth fill consists primarily of decomposed granite obtained from two sources; (1) slide debris at construction site and (2) borrow material from a borrow site located approximately 1.5 miles northwest of the construction site on California State Highway 2. Soil samples were taken from these two sources for laboratory tests. A summary of testing results of the borrow material is shown in Table 1. The coefficient of earth pressure at rest, K_0 , was computed based on J. Jaky's (33) expression, $K_0 = 1 - \sin \phi$. Laboratory pulling tests to determine the skin friction were conducted using a specially designed small shear box (32). The stress-deformation curve obtained from the laboratory pulling test is shown in Figure 12. Based on the residual shear stress as indicated in Figure 12, the envelope line shown in Figure 13 indicates a skin friction angle of 31 degrees between the galvanized reinforcing steel strip and the decomposed granite borrow material.

Corrosion tests were also conducted for the borrow material. It was found that the borrow material is an alkaline soil with a pH value of 7.7 and an average resistivity of 13,000 ohms per cubic centimeter. The rate of metal loss is less than 1 mil per year based on Figure 10. A life of more than 50 years can be expected for the galvanized steel strip.

2. Skin Plates and Steel Reinforcement

The galvanized reinforcing steel and the skin plate were all purchased from the Reinforced Earth Company and imported from France at \$750 per ton. The dimensions of the steel

reinforcing strips are as follows:

Thickness: 0.118 inches (3 mm)
Width: 2.362 inches (60 mm)
Length: 22.79 to 46.0 feet (7 to 14 m)

A standard tension test was conducted at the structural material laboratory of the Transportation Laboratory. Testing results are as follows:

Yielding strength: $F_y = 37,000$ pounds per square inch
Ultimate strength: $F_u = 50,000$ " " " "
Young's Modulus: $E = 28.5 \times 10^6$ " " " "
Poisson's ratio: = 0.28

The skin plates are semi-elliptical in shape, 10 inches high along the major axis, and 3.7 inches deep along the minor axis. The skin plate has a thickness of 0.118 inches (3 mm) and length varying from 6.56 feet (2 meters) to 39.37 feet (12 meters).

3. Construction Operation

The construction of the embankment was started on March 14, 1972 and completed to Elevation 6353, the footing of the reinforced earth fill, on July 31, 1972. Figure 14 shows the daily history of the fill height.

The construction of the reinforced earth was begun August 1, 1972. The fill area was leveled with an approximately 1% downward slope back from the face of the wall. Batter boards (Photo 2) were erected at approximately 10-foot spacing to provide the initial horizontal and vertical control for placing the skin elements which are laid against the batter boards and brought to a precise level. The reinforcing strips were laid perpendicular to the alignment of the skin element on the compacted fill (Photo 3). Each strip was then bolted to the skin element. Wooden wedges were driven between the skin elements to tilt the elements inward towards the fill (Photo 4). As the fill was placed and compacted against the upper edge of the skin plate (Photo 5), the skin element was forced outward to a plumb position. The correct amount of inward cant determined by trial and error to be approximately one-half inch. At each end of the skin element an expansion gap of one inch was provided. Connection plates were placed over the gap at each end of the skin elements to prevent local soil sloughing. Three skin elements were erected prior to placing and compacting the first 10-inch lift of fill.

The purpose of maintaining three skin elements above the last compacted lift of fill throughout the wall construction is to provide a sufficient resistance to the outward force during compaction of the fill and to serve as a safety barrier at the wall face. Compaction control of the fill was maintained using a nuclear gage. The field measured densities are shown in Table 2.

4. Construction Equipment and Labor Work

The construction of the reinforced earth fill requires only ordinary highway construction equipment and the usual labor force. Tables 3 and 4 show, respectively, the equipment and labor work with hourly rates used in construction of the California Highway 39 reinforced earth project.

5. Construction Cost

The construction cost of the reinforced earth fill consists primarily of the following three parts described below:

- a. The galvanized steel skin elements and reinforcing strips were imported from the Reinforced Earth Company of France. The price of steel was \$750 per ton, delivered from France to the job site, which include patent rights, transportation, packing, custom duty, and required service in design and supervision of construction.
- b. The borrow material is a contract item. The bid price was \$1.80 per cubic yard, which includes excavation, grading, and transportation of the fill material from the borrow site to the job site.
- c. The erection of the skin element, placing and compaction of fill material were paid by force account. The hours of rent for each piece of construction equipment and labor work hours were recorded daily by the Resident Engineer's Staff. The hourly rate was based on the values listed in Tables 3 and 4. Figure 15 shows the daily record of construction quantities. The cost spent each week for rent of the construction equipment and labor service, together with the unit cost are shown in Figure 16. It is seen that at the time when the equipment and labor were mobilized at the highest peak, the unit cost of compacted fill and the total unit cost including equipment, labor, steel and fill material became the minimum at \$3.50 and \$7.40 per cubic yard of fill, respectively. Average unit

quantities and costs are shown in Table 5. It should be pointed out that this project was the first of its kind in the United States and was located in relatively remote mountain area with very limited working space. Thus, the cost data may not be representative of present-day construction in a more accessible site.

Based on the unit price of \$750 per ton for the steel and \$5.00 per cubic yard for placing and compaction of the fill material, the unit cost of reinforced earth fill versus height is plotted in Figure 17 and tabulated in Table 6. For comparison purposes, the unit cost for reinforced concrete crib wall, metal crib wall, and Type 1 reinforced concrete retaining wall (spread footing), which are indicated in California Division of Highways' 1973 "Standard Plans" pages 35, 37, 87, respectively, are also plotted in Figure 17 based on current contract bid prices furnished by the Office of Structures of the California Department of Transportation. The structural backfill is estimated to be \$8.00 per cubic yard for the crib walls and the reinforced concrete wall. It is seen that the reinforced earth fill is lower in cost than the three types of retaining walls.

6. Instrumentation

In order to monitor the behavior of the completed structure, a comprehensive instrumentation program was planned and implemented. These instruments included (1) slope indicators to measure the internal movement of the embankment and the slide debris, (2) settlement platforms (Photo 6) to measure the vertical settlements, (3) extensometers (Photo 7) to measure the soil strains (4) soil pressure cells (Photo 8) to measure soil stresses, (5) strain gages to measure the stresses developed in the reinforcing strips (Photo 9) and skin elements (Photo 2), (6) gage points to measure the deformations of the skin plates and the wall face, (7) monuments to measure the displacements on the wall face, top of fill, and top of the berm. Locations of the instruments are shown in Figures 11 and 18. Photo 10 shows three instrumentation shelters for reading the instruments. Installation details of instruments are shown in Table 7, 8 and 9. The detailed data of slope indicator holes and its installation are shown in Table 10.

7. Field Data

All instruments in the reinforced earth fill were read periodically during construction and after completion of construction for approximately one year. The slope

indicators installed in the embankment were read periodically since March 28, 1972. The various field data are discussed separately as follows:

a. Internal Movement of Embankment

The internal movements in the embankment were measured by slope indicators. A total of 10 slope indicators was originally planned for the embankment and the reinforced earth fill. Due to the difficulty of drilling through the talus and the considerable expense involved, only three slope indicators were installed. The locations of the three slope indicators are shown by Figure 11.

Horizontal movements measured by slope indicators SI-1 through SI-3 are shown in Figures 19 through 24. Slope indicator SI-1 initially deflected about 1.5 inches westward during construction and almost recovered to the vertical position at 15 feet deep about one year later. In the southward direction, the top of SI-1, deflected continuously to more than 3 inches but recovered almost to the vertical position at about 15 feet deep. The slope indicator SI-2, deflected continuously westward and northward for 0.9 inch at 10 to 20 feet deep. The slope indicator SI-3 deflected about 3.9 inches westward but only 0.5 inch northward. The pattern of the plotted data shown in Figures 23 and 24 indicate that the slope indicator casing is not locally deflected but the whole section of embankment was moving in the down slope direction. This movement is probably the cause of the cracking of the roadway pavement directly above and behind the reinforced earth fill (Photo 14) between Station 552+95 and Station 553+75 observed in April 1974.

The settlements of the embankment were also measured by slope indicators SI-1, SI-2, and SI-3 and shown in Figures 25 through 27. The maximum settlements are 0.55 foot, 0.73 foot, and 0.95 foot measured by SI-1, SI-2, and SI-3, respectively.

b. Movements of the Reinforced Earth Fill

The horizontal movements of the reinforced earth fill were measured by three series of survey monuments located on the embankment berm (Series "A", Figure 28), on the wall face (Series "B", Figure 29), and on top of the wall (Series "C", Figure 30). Appreciable horizontal movements were observed along the left wing of the reinforced earth fill (wall Station 13+04 to 14+75). The horizontal movements vary from 0.3 foot to 0.45 foot

on the berm (Figure 28), 0.1 foot to 0.55 foot on the wall face (Figure 29), and 0.1 foot to 0.65 foot on top of the wall (Figure 30). The largest horizontal movement occurred between wall Station 13+25 and Station 14+50 where the crack was observed in April 1973 (Photo 14). This horizontal movement is consistent with the movement measured by slope indicator SI-3. These cracks were patched by District 07 Maintenance Department personnel in the summer of 1973. The data shown in Figures 28 through 30 indicate that movement diminished considerably after June 1973. Figures 31 and 32 show the displacements of the wall face. An appreciable rotation of the wall face was observed at Stations 12+75, and 14+00.

c. Settlement of Reinforced Earth Fill

A daily history of settlements and fill heights of the reinforced earth fill are shown in Figure 33. At Station 551+75, approximately at the middle of the wall alignment, the measured settlements were proportional to the increases in fill height and continued to increase at a reduced rate after completion of fill. The settlements at Levels B and C were comparable. Much larger settlements occurred at Level A. The readings on June 20, 1973 indicate an average settlement of 1.3 feet at Levels B and C and 3.5 feet at Level A. The average difference in settlement between Level A and the average of Levels B and C from Section I through Section IV is about 1.2 feet which is believed to be primarily attributable to densification of the slide debris below the embankment.

At Station 550+25, much smaller settlements were observed, due to the lower wall height (36 feet as compared to 53 feet at Station 551+75) and lesser thickness of slide debris in the foundation. The readings on June 20 indicate the average settlements are 0.75, 0.68 and 0.50 feet at Levels A, B, C respectively, from Section I through IV. The average difference in settlement is only 0.07 foot between Levels B and C. The rate of settlement after completion of fill at Station 550+25 was much smaller than that at Station 551+75.

d. Soil Stresses in the Reinforced Earth Fill

Figures 34 and 35 show the soil stresses measured at Station 550+25 and Station 551+75, respectively.

The ratio, K , between the horizontal stress and vertical stress is also plotted on these two figures. The γH lines represent the theoretical vertical soil stresses in pounds per sq. in. computed from the unit weight, γ , 143 pounds per cubic foot and the depth of fill, H , over each instrument level. The K values varied irregularly during and immediately after construction. The values of the vertical and horizontal stresses were close in magnitude in the beginning which is believed to be due to the equal influence of the compaction operation. As the fill height increased over the instrumentation level, the influence of the compaction operation diminished. After completion of the fill, the K values still varied slightly in the range of 0.11 to 0.41 at Station 550+25. The calculated Rankine's coefficient of active earth pressure, K_a , is 0.22 and the coefficient of earth at rest, K_0 , is 0.36, based on an internal friction angle of 40° obtained from laboratory triaxial compression tests on the borrow material (Table I).

At Station 551+75, the K values range from 0.20 to 0.90. The K values at this station are much greater than K_a and K_0 except at Section I, Level C where some bulging has been observed on the skin plates.

e. Stresses in Steel Strips

The daily history of stresses in the steel strips is shown in Figure 36. The steel stresses are computed from products of the average values of strains recorded on tops and bottoms of the strips and the modulus of elasticity (28.5×10^6 psi) obtained from laboratory tests of the steel strip. For comparison, the steel stresses for the active earth pressure case and "at rest" case were computed and are shown on Figure 36 using Equation 4 based on data as shown.

At Station 550+25, on Level A tensile steel stresses were observed at one foot from the wall face. After completion of the fill, the stresses near the wall face decreased with time and eventually became compressive on Level A. This phenomenon was probably due to the restraint provided by the berm. At 15 and 25 feet from the wall face, the tensile steel stresses increased with time and finally reached σ_a , the calculated active earth pressure. At Level B, the tensile steel stresses at 15 feet from the wall face decreased with time to values much lower than σ_a , while the stresses

at 25 feet from wall face increased with time and approached the calculated earth pressure at rest, σ_0 . At Level C, the magnitude of tensile steel stresses at 15 and 25 feet from wall face decreased with time, and approached σ_a . The steel stress at one foot from wall face decreased to below σ_a but approached σ_a at a later time.

At Station 551+75, all strips on Level A were in compression with the maximum stresses developed near the wall face. This phenomenon is undoubtedly due to the restraint provided by the berm, since Level A is about 10 feet below the top of the berm. At Level B, all strips were stressed in tension with the magnitude much less than σ_a near the wall face and at 30 feet from the wall face, while the strip at 15 feet from the wall face was stressed to approach σ_a . At Level C, all steel stresses increased with time. The reading on June 20, 1973 shows that the stress approached σ_a near the wall face, and becomes greater than σ_a at 15 and 30 feet away from the wall face.

f. Strain in Steel and Soil

Daily history of horizontal strains in the steel strips and soil are compared in Figure 37. The strains in the steel strip were measured by strain gages glued one each on bottom and top face of the strip at each planned location. The strains in the soil were measured by an extensometer and read out electronically. The strains measured in both the steel strip and soil were reasonably consistent with each other and approach the same magnitude with increasing time after completion of the fill, except for those measured at Section II, Level C, at Station 551+75.

The constant discrepancy in strains measured by strain gages C-15 and 16 on the steel strip and by Extensometer 78 for the soil on Level C, Section II, at Station 551+75, may indicate that slippage of the steel strips occurred since bulging out of the skin plate occurred at this level. This may explain the high steel stresses, with magnitudes greater than σ_0 , (Figure 36, Gages C-15, 16, 17 and 18) and the horizontal soil stress approaching σ_a (Figure 35, PC 135).

g. Horizontal Soil Stresses and Converted Steel Stresses

The daily histories of horizontal soil stress and converted steel stress are compared in Figure 38. The

converted steel stresses, representing the equivalent soil stress, are computed using Equation 4 with measured steel strain data and the elastic modulus of steel equal to 28.5×10^6 psi. All the converted steel stresses are smaller than the comparable soil stresses. This difference is probably due to the soil arching action. This would cause the soil near the steel strip to be strained less than that at the center of the interval between two steel strips.

h. Axial Force in Dummy Strips

Addition instrumented steel strips were installed in the fill for pulling tests. Strain gages were installed at each 5 feet spacing for measuring the strains along the steel strips before and during pulling tests. The case histories of the axial forces developed in two of the instrumented dummy strips are shown by dotted lines in Figures 39-a and 39-b for the 23-foot and 46-foot strip, respectively. The maximum stresses are all developed at about 10 feet from the wall face for the 46-foot strip. In the 23-foot strip, it is believed that the maximum stresses developed between 10 and 15 feet from the wall face. Figure 39-c shows the relationship between overburden loads and the maximum axial force observed at gage Point 10 for the 46-foot strip and the extrapolated maximum axial force between gage Points 10 and 15 for the 23-foot strip. The axial forces developed during construction are all lower than the calculated tensile force, T_a , from Equation 4, based on the Rankine's active earth pressure case. However, after the fill was completed the axial force continued to increase and the maximum axial force reached T_a , in the 23-foot strip. In the 46-foot strip the maximum axial force finally reached T_o , the calculated tensile force from Equation 4 based on the "at rest" earth pressure case. The continuous increase in tensile force after completion of the fill was probably due to the continuing settlement developed in the fill as shown in Figure 33. It has also been observed that the face of the wall has been continuously moving horizontally downslope since completion of the fill (Figures 28 through 32).

The solid line shown in Figures 39-a and 39-b are the axial forces observed during field pulling tests to be discussed later.

i. Stress in Skin Element

Figure 40 shows the daily history of stresses in the skin elements. The locations and the identification numbers of the strain gages are shown on the upper right of the

figure. Gages 1, 5 and 9 measure strains on the front face in the axial direction; Gages 3, 7 and 11, measure strains on the inner face in the axial direction; Gages 2, 6 and 10, measure the circumferential strain on the front face; and Gages 4, 8 and 12, measure the circumferential strain on the inner face. The actual deformation of the skin elements closely approximated the deformation assumed in developing Equations 7, 8 and 9 for designing the skin plates. Tensile circumferential stresses developed on the front face and compressive circumferential stresses on the inner face. The axial stresses were in tension except for skin element 8 which is embedded in the embankment berm. The tensile axial stresses are believed to be attributable to the greatest settlement occurring at the middle of the reinforced earth fill. Because the largest settlement occurred at the middle of the fill, all skin plates were being pulled toward the middle where end to end buckling has been observed for many of the skin elements.

j. Field Behavior of Steel Skin Plate

Deformation of the skin elements were measured at 5 separate gage points on the faces of the skin plates with a specially designed vernier-micrometer caliper capable of accurately measuring to one-thousandth of an inch.

The deformation of skin element No. 20 (on Elevation 6368.92, near Station 551+75), which is a typical case, is shown in Figure 41. The relationship between the magnitude of deformation and fill height is also shown. These deformations agree very well with the assumptions made in developing the design Equations 7, 8 and 9. Based on the vertical deformations observed in the field, the stresses in the skin plates were calculated using these equations, for both hinged and fixed end conditions. A comparison of the measured and computed stresses is shown in Figure 41. The calculated Stresses based on hinged end assumption (Equation 7) agree reasonably well with the measured data, while the calculated stresses using Equations 8 and 9 (fixed end condition) are almost three times larger than those measured.

8. Field Pulling Tests

Additional dummy steel strips were installed in the fill at 5 levels for field pulling tests. Three strips, 5, 10, and 15 feet in length, were embedded at each of three levels under overburden heights of 7.5, 12.4 and 18.2 feet. Three

23-foot strips were embedded at a depth of 18 feet and three 46-foot strips were embedded at a depth of 38 feet. One each of the 23-foot and 46-foot strips was instrumented with strain gages on both top and bottom at 5-foot intervals.

Pulling loads were applied using a hydraulic jack acting against wooden blocks for bearing pads (Photo 11). The pulling loads were measured with a load cell. Deformation or extension of the steel strips was measured with two extensometers fastened on each side of the steel strip (Photo 12). A Hewlett-Packard 2010A Data Acquisition System (Photo 13) was used to record electronically the pulling loads and strains of the steel strips.

Load deformation curves obtained from field pulling tests are shown in Figure 42 for the 5-, 10- and 15-foot strips and Figure 43 for the 23- and 46-foot strips. Three pulling loads were selected for analysis and are indicated on the curves. These three loads are (1) yield load representing the proportional limit of the load-deformation relationship; (2) peak load representing the maximum pulling load observed; (3) the residual load representing the pulling load when deformation increased appreciably without changing in the pulling load.

One of the 23-foot strips was broken at a pulling load of 14,000 pounds. Three of the 46-foot strips were broken at pulling loads of 13,460; 14,200 and 14,450 pounds. The rest of the strips failed by slipping at the residual loads shown in Figures 42 and 43.

The yielding loads represent the elastic properties of the steel. When the strip is long enough and the overburden load is high enough, i.e., when the frictional grip is large enough, the yield load will reach the yield capacity of the steel (about 10,300 pounds). If the frictional grip is not sufficient at the front end of the strip, the soil will start to strain before reaching the yield strength of the steel. Therefore, it appears that the yield load represents the yield capacity of the steel or the maximum possible frictional grip of the compacted soil without the introduction of strain of the soil. The peak load represents the maximum mobile pulling resistance of the composite material of the reinforcement and soil. After the peak load, the strip becomes partially loose and progressively, the whole length of the strip starts sliding when the pulling loads drop to the residual level. If the strips break there will be no peak load or residual load. Figures 44-a, 44-b and 44-c show the relationship between the three types of pulling loads and the overburden height and strip length. The skin-friction angles, ϕ_u , decrease with increasing overburden height as shown in Figure 44-c. This phenomenon cannot be explained theoretically.

It is interesting to note that under a constant overburden height, the yield, peak and residual loads are all proportional to the overburden loads which are the products of the overburden height, H , the unit weight, γ , the width of steel strip, b and the length of the steel strip, L . Since γ , b and H are constant under a constant overburden height, the yield, peak and residual loads are all proportional to the strip length. A field soil unit weight of 143 pounds per cubic foot was used in calculating the overburden loads. When the length of strip is constant, the relationships between the yield load and peak load with the overburden load are nearly linear. This is not the case, however, with respect to the relationship between the residual and overburden load. This phenomenon is probably attributable to the fact that the residual loads are not well defined on the pulling test curves as shown on Figures 42 and 43. Some of the pull tests were not continued long enough to establish the flat portion of the load-deformation curve. Because the peak load represents the maximum mobilized friction grip, the factors of safety were evaluated using the peak loads as failure loads and the designed tensile loads were calculated using Equation 2. The relationships between overburden height, H , strip length, L and the factor of safety (F.S.) are shown in Figure 44-d.

Because the residual load, representing a complete slippage failure, is much lower than the peak load, a conservative factor of safety of 4 is recommended for design purposes to select the minimum length of strip at different overburden heights. According to Figure 44-d, for a factor of safety of 4 and under a fill height of 10 feet, the minimum strip length required is about 9 feet.

Referring to Figures 39-a and 39-b, during pulling tests, the externally applied pulling force strained the 46-foot strip only up to Gage Point 10. There was no increase in axial stress in the 46-foot strip beyond Gage Point 10. The 46-foot strips were all broken at the external extended portion. It appears that the frictional grip was so great along the 46-foot strip that the strip was acting as though fixed at Gage Point 10, so that there was no change in stress occurring beyond this point due to the externally applied pulling load. In the 23-foot strip, only a slight increase in stresses were observed beyond Gage Point 15 due to the externally applied pulling load.

Figure 45 shows the relationship between peak pull load and the calculated skin friction force. It is interesting to note that the peak pull loads exceed the skin friction force as the strip length exceeds 10 feet. It may be concluded that strip length should be at least 10 feet.

G. Theoretical Analysis by the Finite Element Method

A finite element computer program was developed by Professors L. R. Herrmann and K. M. Romstad of the University of California, Davis, under a special service contract. A detailed description of the formulation of the material properties of reinforced earth are given in Appendix B with the user's manual for the computer program in Appendix C.

In the theoretical analysis, the reinforced earth is assumed to be a composite material, and that if the pattern of the reinforcement is repeated a sufficiently large number of times, the composite material can be considered homogeneous at the phenomenological level. Each strip of reinforcement bounded by the centerline of both the vertical and horizontal spacing can be viewed as a "unit cell" which, when it is repeated in all directions, results in the configuration at the phenomenological level of a composite material.

The "unit cell" of the reinforced earth mass shown in Figure B-2 (Appendix B), consists of a soil with thin steel strips parallel to each other at chosen spacings and extend deep into the soil mass. In formulating the composite stress-strain relationship it is assumed that the composite stress-strain state in the 2 and 3 directions equals the stress-strain state of soil, and the displacements of all points in any 2-3 plane are equal for both soil and strip, therefore, the composite material exhibits an isotropic behavior with perfect bond at the soil-strip contact. The mathematical expression of the composite stress-strain state is given in Appendix B.

Although this program was specifically designed for the analysis of reinforced earth embankments, it can be applied to a wide range of problems such as the calculation of stresses and deformations in embankments and foundations; computation of rebound in slope and foundation excavations; and determination of stresses and strains developed in embedded conduit in a large soil mass. The program calculates the composite stresses and strains of the composite material in the "unit cell". Using the composite stresses and strains the corresponding stresses and strains in the soil and axial forces and moments developed in the reinforcing strips are then determined. Several special provisions contained in this program are as follows:

1. The incremental construction sequence
2. Overburden dependent material properties

3. Orthotropic material behavior
4. Reinforced earth construction
5. Bending members

The details of using this program to solve various problems relating to the above provisions are referred to in Appendix C.

1. Elastic Property of Fill Material

For evaluating the elastic property of the fill material, three soil samples as identified in Table 11 were taken during construction. These soil samples were subjected to triaxial compression tests for determining the shear strength parameters (Table 12), which are required for evaluating the elastic constants. To arrive at the shear strength parameters, three failure criteria as suggested by Chang, et. al., (34) were investigated.

1. The peak or the maximum deviator stress represents the "failure stress" of the specimen.
2. When the deviator stress and the axial strain increase continuously during the test and there is no well defined peak on the stress-strain curve, the deviator stress at 15 percent axial strain is considered the "failure stress".
3. The ultimate deviator stress, represented by the deviator stress at the asymptote of an idealized hyperbolic fit of the stress-strain curve, is to be considered as the "failure stress".

According to Chang, et. al., (35) the equation for computing the tangent modulus, E_t , of soil is

$$E_t = E_i \left[1 - \frac{\gamma H \sin\phi (1 - \sin\phi)}{2C \cos\phi + 2q \sin\phi} \right]^2 \quad (10)$$

where

$$\begin{aligned} E_i &= A+B(1-\sin\phi)\gamma H = \text{initial tangent modulus in} \\ &\quad \text{pounds per square foot,} \\ c, \phi &= \text{shear strength parameters determined from} \\ &\quad \text{ultimate strength criterion (c is expressed} \\ &\quad \text{with unit in pounds per square foot),} \\ \gamma &= \text{density of soil in pounds per cubic foot,} \\ H &= \text{height of embankment overburden in feet,} \\ N_\phi &= \tan^2 (45 \text{ deg } + \frac{\phi}{2}), \text{ and} \\ q &= \frac{\gamma H}{N_\phi} - \frac{2c}{(N_\phi)^{1/2}} \end{aligned}$$

A and B are constants to be determined from the arithmetic plots of the initial tangent modulus, E_i , and the confining pressure, σ_3 , obtained from the triaxial compression stress-strain curve.

The calculated tangent modulus values are shown in Table 13. Figure 46 shows typical stress-strain curves obtained from triaxial compression test on Sample No. RE-7. Figure 47 is a plot of the stress-strain data in a transformed hyperbolic form from which the ultimate deviator stress and the initial tangent modulus, E_i , was determined (34). Figure 48 shows the typical Mohr Circles on which the ultimate friction angle for Sample No. RE-7 was determined based on the ultimate deviator stress obtained from Figure 47. The variation of the initial modulus with confining pressure is shown in Figure 49 from which the A and B constants was then obtained.

Poisson's ratio of the fill material was also evaluated using the method and equations developed by Kulhawy, Duncan and Seed (36). The computed results of Poisson's ratio are shown in Figures 50 and 51. Tables 14 and 15 show respectively, the values of the calculated parameters and Poisson's ratio based on the equations suggested by Kulhawy, et. al(36). The Poisson's ratio ranges from 0.13 to 0.78 for the fill material. Based on previous experience for the finite element analysis of the stresses and strains in the Jail Gulch embankment (34), a Poisson's ratio of 0.3 was chosen in this study.

2. Finite Element Analysis

In the finite element method, the cross-section of a continuous body is idealized as a set of small, but finite elements connected at their joints or nodal points. The finite element mesh or assemblage of elements for this study is shown in Figure 52, which represents a section at Station 551+75 of the reinforced earth fill. The assumed boundary condition construction sequence and representative materials samples are also shown in Figure 52.

The boundary on foundation rock is considered to be fixed assuming no deformation. The right side vertical boundary is considered to be a free surface assuming that a crack is developed in the slide debris area behind the reinforced earth fill (crack lines were observed in that area in the field). Several roller joints were assumed along the rock foundation immediately below the right side vertical boundary to allow the downward movement of the slide debris upon loading. The vertical boundary at the left side is considered to be on rollers to allow downward movement due to settlement of the embankment.

The material of the model consists of foundation rock, original overburden, slide debris, and borrow material. Each material was represented by the elastic property of the selected soil samples as indicated in Figure 52. Soil Sample No. RE-8 which was taken from the borrow material represents the soil material for the original overburden, the embankment, the berm, and the backfill. The slide debris is represented by Soil Sample No. 1384-85 which was obtained from the slide debris material. The reinforced earth fill is represented by Soil Sample No. RE-7, which was obtained from the borrow material during construction of the reinforced earth fill. Composite elastic properties were evaluated by considering the elastic property of the reinforcing strip and the soil. Due to variations of spacing of the reinforcing strip at three different elevations, the composite material is represented by three fictitious sub-grouped soil samples, RE-7-A through RE-7-C, representing the composite material in the reinforced earth fill as shown in Figure 52. The elastic property of the composite material was automatically computed by the computer with the special provisions in the finite element program.

The construction sequence is divided in 12 sequential stages as shown in Figure 52 by circled numbers.

3. Analyzed Results and Comparison With Field Data

The theoretically analyzed results by the finite element method are all compared with the field data obtained at Station 551+75 on November 1, 1973, which is about two weeks after completion of the reinforced earth fill coinciding with the date of completion of the embankment berm and the roadway pavement. Most of the field data at Station 551+75 has continued to change. It appears that the field data obtained on November 1, 1972 in general compared more favorably to the theoretically analyzed results.

a. Vertical Soil Stresses

The theoretical vertical soil stresses are shown by contours in Figure 53. Field data are also shown in parentheses. The contours of the theoretical vertical soil stress indicate two particularly interesting characteristics:

1. Stress concentration at the toe of the reinforced earth fill which is also substantiated by the field data. This phenomenon may be due to the combination effect of the overturning moment from the backfill earth pressure and the lateral restraint of the berm;
2. A substantial reduction in vertical soil stress occurs along the boundary line (the inclined dashed line - Fig. 53) between the slide debris and the backfill and embankment (Figure 52). This characteristic is obviously due to the sudden change in rigidity of the soil from a high value of tangent modulus in the embankment and backfill to the low tangent modulus in the slide debris.

Figure 54 shows a comparison of vertical soil stress distribution between the theoretical results and field data. It is seen that a relatively good agreement exists between the theoretical results and field data.

b. Horizontal Soil Stresses

The contours of the theoretical horizontal soil stress are shown in Figure 55. It is interesting to note that the backfill behind the reinforced fill is almost completely in tension which obviously cannot be sustained by the soil. Field observation indicated numerous seam cracks in the backfill area (Photo 16). The observed substantial

settlement and horizontal movement of the wall face of the reinforced earth fill could be the evidence that a slight slide movement occurred along the boundary line of the slide debris due to considerable densification of the slide debris material. Figure 55 shows an extremely large buildup of horizontal stress at the toe of the wall corresponding to the concentration of the vertical soil stress shown in Figure 53.

The comparison of the distribution of the horizontal soil stress between the field data and the analytical results are shown in Figure 56. It also indicates moderately good agreement.

Figure 57 shows the contours of the theoretical stress ratio, $K (\sigma_x/\sigma_y)$, which is in poor agreement with the field data (Figure 35).

c. Shear Stresses

Figure 58 shows the contours of the theoretical shear stress. It shows additional evidence of the stress concentration at the toe of the reinforced earth fill. The calculated maximum shear stress of 1600 pounds per square foot is well below the available shear strength of the soil at that location. Contours of zero shear stress developed at the upper part, the back part of the reinforced earth fill, and also the berm of the embankment. This indicates changes in direction of shear stresses occurred along the zero contours.

Figure 59 shows contours of factor of safety based on the ratio of the available shear strength and the theoretical maximum shear stress.

d. Theoretical Steel Strip Forces

The contours of the forces developed in the reinforcing steel strip are shown in Figure 60. All the theoretical strip forces are in tension with force concentrations at Level B and at back side on Level A. The field data are much smaller than the theoretical results at Levels B and C. At Level A, the field data indicates compression forces developed in the steel strip at the toe of the reinforced earth fill. Therefore, the comparison between the analytical and field data shows rather poor quantitative agreement but similar patterns of stress distribution (Figure 61).

e. Stresses in the Skin Plate

A comparison of the theoretical and observed stresses in the skin plate is shown in Figure 62. The theoretical

stresses are generally smaller than those measured. This discrepancy is due to the assumption that the skin plate is treated as a hoop tension member in the finite element program and no bending stress is considered. In the field data the predominant stresses are due to bending.

f. Settlement in the Reinforced Earth Fill

A relative comparison of the theoretical and field settlements is shown in Figure 63. These settlement data are with respect to the reference point at the berm by assuming zero settlement at the berm reference point. The actual settlement should be the sum of the actual settlement at the berm reference point and the data shown in Figure 63.

The theoretical settlements are smaller than those of the field data at Levels A and C, but larger at Level B. The agreement between the theoretical and field data is rather poor in magnitude.

g. Horizontal Movement of Berm and Wall Face

The results of finite element analysis for the horizontal movement at three different levels along the wall face are compared with field data in Figures 28 through 31. It is seen that the theoretical results agree well with the field data observed in March through May 1973 for all three levels of measurement.

The theoretical results of wall face displacement agree well with the field data at the lower part of the wall face, however, they are much smaller than the field data near the top of the wall (Figure 31).

h. Horizontal Movement in Embankment

The theoretical horizontal movements in the embankment are also plotted in Figures 21 and 23 for comparison with the field data measured by slope indicators. The results of finite element analysis agree well with the field data measured by slope indicator SI-1 in November 1972 through April 1973 (Figure 21). However, in Figure 23 only part of the theoretical results agree with the field data observed by slope indicator SI-3 in April 1973. Within a 10 to 30 feet depth, the theoretical results are much smaller than the field data (Figure 23).

4. Discussion of Finite Element Results

The results of the finite element study were very encouraging, in consideration of the complexity of the geometry and of the materials. The analyses show that:

- a. The use of the "composite material property" in the analysis is a satisfactory approach.
- b. The general trend of stress and deformation patterns agree reasonably well with the field data.
- c. Further improvements of the finite element analysis program are needed which take into consideration the factors such as the edge effect by the skin plate, the number and size of construction increments, the linearity of the Poisson's ratio of the soil, the time effects, and three dimensional nature of field behavior.

REFERENCES

1. Old Testament, Exodus, Chapter 5, vs 6-9.
2. Caesar, Vol. 1, Translated by William Duncan, Harper and Brothers, Publishers, 329 and 331 Pear Street, Franklin Square, New York, 1855, p. 201.
3. Haas, Raymond H., and Weller, Harvill, E., "Bank Stabilization by Revetments and Dikes," Transaction, ASCE, Vol. 118, Paper No. 2564, pp. 849-860.
4. Doran, W. E., "Stabilization of River Banks," Proceedings of the 2nd International Conference on Soil Mechanics and Foundation Engineering, Vol. II, 1948, pp. 60-63.
5. Earth Retaining Structures, Civil Engineering Code of Practice No. 2 (1951), The Institution of Structural Engineers, 11 Upper Belgrave Street, London, S. W. 1.
6. Design Manual, Taiwan Provincial Water Conservancy Bureau.
7. Amesbury, H. Clyde, Final Report for the Construction of a Portion of Primary State Highway in Del Norte County, between Last Chance Slide and Flannigans, Road I-DN-1-B Contract 61TCl, February 1935, Division of Highways, State of California.
8. Munster, Andreas, United States Patent No. 1,762,343, June 10, 1930.
9. Reed, Frederick H., United States Patent No. 776,799, December 6, 1904.
10. Weiss, Andrew, Construction Technique of Passing Floods Over Earth Dams," Transaction, ASCE, Vol. 116, 1951, pp. 1158-1173 (also Vol. 76, No. 40, Oct. 1950).
11. Pells, H. N. F., "Reinforcement of Rockfill Dams in South Africa," 7th International Conference on Soil Mechanics and Foundation Engineering Vol. II, Mexico City, 1969, pp. 345-348.
12. Australian National Committee on Large Dams, "Large Dams in Australia, General Paper for period 1962/1965. (Also ninth International Congress on Large Dams, Vol. IV, Istanbul, Turkey 1967, pp. 545-584.

13. Parkins, Alan K., Trollope, David H., and Lawson, John D., "Rockfill Structures Subject to Water Flow," Journal of the Soil Mechanics and Foundations Division, ASCE, Vol. 92, No. SM6, Proc. Paper 4973, November, 1966, pp. 135-151.
14. Fraser, J. B., "A Steel-Faced Rockfill Dam for Papua," Transactions, Institute of Engineers, Australia, Vol. CE4, No. 2, 1962, p. 35.
15. "Steel-Faced Rockfill Dam Proves as Easy to Heighten as to Build," Engineering News Record, April 2, 1970, pp. 29-30.
16. Erosion Control on California State Highways, Division of Highways, State of California, (circa 1950) pp. 44-48.
17. Vidal, Henri, "The Principle of Reinforced Earth," Highway Research Record, No. 282, pp. 1-16, Washington, D.C. 1969.
18. Vidal, Henri, "Reinforced Earth, Recent Application," English translation of the text entitled "La Terre Armee" as published in the Annales de l'Institute Technique du Batiment et des Travaux Publics, Series - Material (38) - No. 259-260 July/August 1969.
19. Vidal, H., "Reinforced Earth - Steel Retaining Wall," Civil Engineering, ASCE, February 1970, pp. 70-73.
20. Harrison, W. Jill, and Gerrard, Charles M., "Elastic Theory Applied to Reinforced Earth," Journal of the Soil Mechanics and Foundations Division, ASCE, Vol. 98, No. SM12, Proc. Paper 9417, December 1972, pp. 1325-1345.
21. Westergaard, H. M., "A Problem of Elasticity Suggested by a Problem in Soil Mechanics," Mechanics of Solids, Timoshenko 60th Anniversary Volume, Macmillan and Co., New York, 1938.
22. Yamanouchi, T., "Structural Effect of a Restraint Layer on a Subgrade of Low Bearing Capacity," Proc., 2nd Int. Conf. on Structural Design of Asphalt Pavements, Ann Arbor, Michigan, 1967, pp. 381-389.
23. Yamanouchi, T., "Experiment Study on the Improvement of the Bearing Capacity of Soft Ground by Laying a Resinous Net," Proceedings of the Symposium Foundations on Interbedded Sands, Commonwealth Scientific and Industrial Research Organization, Division of Applied Geomechanics, 1970, pp. 144-150.
24. Lee, Kenneth L., Adams, Bobby Dean, Vagneron, Jean-Marie J., "Reinforced Earth Retaining Walls," Journal of the Soil Mechanics and Foundations Division, ASCE, Vol. 99, No. SM10, October 1973, pp. 745-764.

25. Lee, Kenneth L., and Richardson, Gregory N., "Seismic Design of Reinforced Earth Walls," presented at ASCE National Meeting on Water Resource Engineering at Los Angeles, January 25, 1974.
26. Idriss, I. M., Lysmer, J., Wang, R. and Seed, H. B., "QUAD-4, A Computer Program for Evaluating the Seismic Response of Soil Structures by Viable Damping," Report No. EERC 73-16, July 1973.
27. Seely, F. B., and Smith, J. O., "Advanced Mechanics of Materials," John Wiley and Sons, Inc., New York, July 1962, pp. 421-437.
28. Uhlig, Herbert H., "Corrosion and Corrosion Control," John Wiley and Sons, Inc., New York, 1964, pp. 150-153.
29. Haviland, John E., Bellair, Peter J., and Morrell, Vicent D., "Durability of Corrugated Metal Culverts," Highway Research Record Number 242, pp. 41-55. Washington, D.C. 1968.
30. Stratfull, R. F., "A New Test for Estimating Soil Corrosivity Based on Investigation of Metal Highway Culverts," Corrosion, National Association of Corrosion Engineers, April, 1961, pp. 115-118.
31. Morgan, J. H., "Cathodic Protection," Leonard Hill (Books) Limited, London, 1959.
32. Chang, Jerry; Forsyth, Raymond; and Smith, Travis, "Reinforced Earth Highway Embankment - Road 39," Highway Focus, Volume 4, Number 1, January 1972, Federal Highway Administration, U.S. Department of Transportation.
33. Jaky, J., "Pressure in Silos," Proc. 1st Conf. on Soil Mechanics and Foundation Engineering (Rotterdam) 1948.
34. Chang, J. C., Forsyth, R. A., Shirley, E. C., and Smith, T. W., "Stresses and Deformation in Jail Gulch Embankments," Interim Report, M&R No. 632509-2, Transportation Laboratory, California Department of Transportation, February 1972, p. 15.
35. Chang, J. C., and Forsyth, R. A., "Stress and Deformation in Jail Gulch Embankment," Highway Research Record, Number 457, December, 1973, pp. 51-59.
36. Kulhawy, F. H., Duncan, J. M., and Seed, H. B., "Finite Element Analysis of Stresses and Movement in Embankments During Construction," Department of Civil Engineering, University of California, Berkeley, 1969, pp. 55-62.

TABLE 1 - LABORATORY SOIL TEST RESULTS

Soil Property	Slide Debris		Borrow Material		
	1384-85	1617	RE-2	RE-7	RE-8
	May 1970	June 1971	June 1971	April 1972	August 1972
Frictional Angle, ϕ	35.5°	44°	37°	38.5°	40°
Cohesion C (psi)	2.5	0	4.2	5.6	4.2
Max. Dry Density, (pcf)	141	141	141	143	139
$K_a = \frac{1-\sin\phi}{1+\sin\phi}$	0.27	0.18	0.25	0.23	0.22
$K_o = 1-\sin\phi$	0.42	0.31	0.40	0.38	0.36
Grading	Percent Passing by Weight				
3"	100	93	100	98	99
2½"	100	87	99	96	98
2"	99	79	98	94	97
1½"	97	71	89	90	92
1"	92	59	83	83	84
¾"	86	48	77	78	77
½"	79	35	66	-	68
3/8"	75	30	59	66	62
#4	66	23	46	54	49
#8	55	19	35	50	41
#16	48	14	24	36	30
#30	40	10	17	25	23
#50	32	8	11	17	16
#100	21	5	8	12	12
#200	13	4	6	9	9

TABLE 2 - FIELD NUCLEAR GAGE DENSITY READINGS

Date	Location	Elevation	Density Reading (PCF)			Average Density
3-23-72	Embankment	6136.	131.2			131.2
4-21-72	"	6225.	124.8	127.8		126.3
4-26-72	"	6246.	125.6	127.0	127.0	126.5
4-28-72	"	6260.	125.0	126.2	126.1	125.8
5-16-72	"	6312.	131.0			131.0
8-3-72	"	6357.4	143.6	144.0	140.5	142.7
8-9-72	"	6361.5	147.0	142.0	144.5	144.5
8-14-72	Instrument Trench	6362.7	132.5	139.0	135.5	135.7
8-31-72	Reinforced Earth Fill	6373.8	142.0	145.0	142.0	143.0
9-8-72	Instrument Trench	6378.3	136.2	135.0		135.6
9-13-72	Reinforced Earth Fill	6382.0	142.0	142.0	139.0	141.0
10-2-72	Instrument Trench	6400.0	139.5	130.5		135.0
10-10-72	Reinforced Earth Fill	6406.6	142.0	142.5	144.0	142.8

TABLE 3: Construction Equipment and Rental Rate

<u>Item</u>	<u>Type or Model</u>	<u>Rental Rate</u>	<u>Function</u>
Crawler Tractor	Cat. D-8	\$28.50/hr	Spreading of fill material
Crawler Tractor	John Deer JD-450	\$5.35/hr	Towing vibratory roller
Vibratory Roller	Essick V72S	\$7.75/hr	Compaction of fill material
Road Grader	Cat	\$7.50/hr	Leveling of fill material
Front End Loader	Cat 966 B & C	\$17.00/hr	Spreading of fill material
Water Truck		\$11.00/hr	Moisture conditioning fill material
Water Monitor		\$2.00/day	Adding moisture to fill material
Generator	10 KW	\$1.80/hr	Provide electrical power as necessary for small tools, etc.
Acetylene Torch		\$2.00/day	Cutting skin and strip
Surveying Equipment	State supplied		Transit & level for alignment & elevations
Water pump		\$4.50/day	High pressure supply to water monitor

TABLE 4: Construction Labor Description and Hourly Rate

<u>Item</u>	<u>Description</u>	<u>No. of Laborers</u>	<u>Hourly Rate</u>
Carpenter	Set batter boards and erect skin elements	2	\$9.50/hr
Equipment Operator	Operate construction equipment such as hauling, spreading, compacting of fill material & handling of steel strips & skin elements	4	\$9.69/hr
Common Laborer	Erection of skin element & steel strips, hand shoveling & hand compacting fill material near the wall face	3	\$7.54/hr
Grade Setter	Insure the proper thickness & grade of fill material	1	\$10.18/hr

TABLE 5 - AVERAGE UNIT QUANTITIES AND COSTS

<u>ITEM DESCRIPTION</u>	<u>QUANTITY OR COST</u>
STEEL PER SQUARE FOOT OF WALL FACE	9.876 x 10 ⁻³ TONS
STEEL PER CUBIC YARD OF FILL	0.164 TONS
BORROW MATERIAL COST PER CUBIC YARD	\$1.80
STEEL COST PER SQ. FT. OF WALL FACE	\$7.40
FILL COST " " " " " "	<u>8.15</u>
TOTAL COST " " " " " "	15.55
STEEL COST PER CU. YD. OF WALL FILL	\$4.55
FILL COST PER CU. YD. " " "	<u>5.00</u>
TOTAL COST " " " " " "	9.55

TABLE 6 - COST COMPARISON BETWEEN FOUR
TYPES OF WALLS
(Cost in Dollars per Sq. Ft. of Wall Face)

Type of Wall	Description	Height of Wall (ft)					
		10	20	30	36	40	50
Reinforced Earth Wall	Cost of Wall Members	\$3.70	\$4.30	\$5.20	\$6.00	\$6.60	\$8.40
	Cost of Backfill	2.40	3.50	4.50	5.10	5.60	6.00
	Total	6.10	7.80	9.70	11.10	12.20	14.40
Metal Crib Wall	Cost of Wall Members	8.50	9.35	12.00	15.00	-	-
	Cost of Backfill	1.50	2.80	4.10	4.80	-	-
	Total	10.00	12.15	16.10	19.80	-	-
Reinforced Concrete Crib Wall	Cost of Wall Members	9.50	10.50	13.00	15.60	17.30	22.30
	Cost of Backfill	3.10	4.50	5.90	6.80	7.40	8.00
	Total	12.60	15.00	18.90	22.40	24.70	30.30
Reinforced Concrete Retaining Wall Type I	Cost of Wall Members	10.50	13.75	20.80	26.10	-	-
	Cost of Backfill	1.20	2.05	3.05	3.60	-	-
	Total	11.70	15.80	23.85	29.70	-	-

TABLE 7 - INSTRUMENTATION INSTALLATION DATA

LEVEL "A"

Item	Station 550+25			Station 551+75		
	Designation No.	Elevation (ft)	Distance From Wall Face (ft)	Designation No.	Elevation (ft)	Distance From Wall Face (ft)
Settlement Platform	SP-13	6391.96	36.5	SP-1	6359.55	46
	SP-14	6392.07	24.8	SP-2	6358.83	31
	SP-15	6392.12	16.1	SP-3	6358.57	16
	SP-16	6392.14	5.6	SP-4	6358.40	2
Soil Pressure Cell	137 H	6391.6	37.5	101 V	6359.0	44
	138 V	6391.6	39.6	102 H	6359.1	46
	139 H	6391.8	24.2	*103 I	6358.8	42
	140 V	6391.9	27.8	104 V	6358.4	32.3
	142 H	6392.0	16.6	105 H	6358.7	34.3
	141 V	6391.9	19.2	*106 I	6358.6	30.5
	144 H	6391.8	4.3	107 V	6358.4	17.0
143 V	6391.9	6.6	108 H	6358.5	18.6	
Extensometer	75	6392.2	33.2	*109 I	6358.5	15.3
	76	6392.2	28.3	110 V	6358.2	5.0
	83	6392.4	8.1	111 H	6358.3	6.5
	84	6392.4	12.9	*112 I	6358.5	3.0
Strain Gage on Reinforcing Strips	17-18	6393.8	25.1	69	6359.90	46.5
	15-16	6393.6	15.1	68	6359.70	41.8
	13-14	6393.5	1.2	88	6359.38	31.5
				87	6359.33	26.5
				86	6359.00	11.5
				85	6359.00	6.8
				17-18	6358.5	30.2
				15-16	6358.5	15.2
				13-14	6358.5	1.1

NOTE: The soil pressure cell designation numbers with the asterisk (*) are Geotran cells, the rest are Glotzel cells. V, H, & I indicate vertical, horizontal, or 45° inclinations.

TABLE 8 - INSTRUMENTATION INSTALLATION DATA

LEVEL "B"

Item	Station 550+25			Station 551+75		
	Designation No.	Elevation (ft)	Distance from Wall Face (ft)	Designation No.	Elevation (ft)	Distance From Wall Face (ft)
Settlement Platform	SP-17	6399.52	39.7	SP-5	6372.04	44.7
	SP-18	6399.44	29.5	SP-6	6371.99	29.8
	SP-19	6399.40	17.2	SP-7	6371.77	14.9
	SP-20	6399.14	5.5	SP-8	6371.56	5.2
Soil Pressure Cell	145	6399.5	40.5	113	6371.6	45.4
	146	6399.3	38.7	114	6371.6	44.0
	147	6399.4	30.2	*115	6371.7	42.4
	148	6399.2	28.3	116	6371.8	32.2
	149	6399.2	18.2	117	6371.6	30.7
	150	6398.9	16.1	*118	6371.5	29.2
	151	6399.0	8.2	119	6371.4	17.0
	152	6398.9	6.2	120	6371.3	15.0
Extensometer	89	6399.5	7.9	121	6371.2	13.5
	90	6399.5	12.7	122	6371.3	7.3
	80	6399.7	28.2	123	6371.2	6.0
	79	6399.7	33.05	*124	6371.1	4.5
				73	6372.3	11.9
				74	6372.4	16.7
				67	6372.8	27.4
Strain Gage on Reinforcing Strips	13-14	6400.8	1.5	70	6372.9	32.2
	15-16	6401.0	15.6	93	6373.1	41.8
	17-18	6401.0	25.6	94	6373.1	46.8
				13-14	6371.4	1.5
			15-16	6371.6	15.0	
			17-18	6371.9	30.0	

NOTE: The soil pressure cell designation numbers with the asterisk (*) are Gentran cells, the rest are Glotzel cells. V, H, & I indicate vertical, horizontal, or 45° inclinations.

TABLE 9 - INSTRUMENTATION INSTALLATION DATA
LEVEL "C"

Item	Station 550+25			Station 551+75		
	Designation No.	Elevation (ft)	Distance From Wall Face (ft)	Designation No.	Elevation (ft)	Distance From Wall Face (ft)
Settlement Platform	SP-21	6407.06	34.5	SP-9	6387.16	44.5
	SP-22	6407.31	24.5	SP-10	6387.09	28.7
	SP-23	6407.37	14.2	SP-11	6387.18	14.9
	SP-24	6407.22	5.4	SP-12	6387.14	4.0
Soil Pressure Cell	153	6406.61	36.7	125	6386.9	47.6
	154	6406.60	34.4	126	6386.9	45.7
	155	6407.18	26.8	*127	6386.7	43.7
	156	6407.06	24.8	128	6386.7	31.8
	157	6407.43	16.8	129	6386.8	29.5
	158	6407.14	14.4	*130	6386.8	27.5
	159	6407.21	7.0	131	6386.9	17.7
Extensometer	160	6407.00	4.5	132	6387.1	15.9
	71	6407.3	7.55	*133	6387.1	14.2
	72	6407.3	12.8	134	6387.0	6.5
	91	6407.2	28.05	135	6387.0	4.7
	92	6407.0	32.9	*136	6387.0	2.9
				77	6388.2	7.2
Strain Gages on Reinforcing Strips	13-14	6408.79	1.05	78	6388.2	12.1
	15-16	6408.81	15.10	81	6388.1	26.6
	17-18	6408.58	25.20	82	6388.0	31.5
			95	6388.0	42.2	
			96	6388.0	47.1	
			13-14	6387.1	1.2	
			15-16	6387.3	15.0	
			17-18	6387.0	30.0	

NOTE: The soil pressure cell designation numbers with the asterisk (*) are Gentrans cells, the rest are Glotzel cells. V, H, & I indicate vertical, horizontal, or 45° inclinations.

TABLE 10 - SLOPE INDICATOR INSTALLATION DATA

a. SLOPE INDICATOR HOLE ELEVATIONS

Description	SI No. 1	SI No. 2	SI No. 3
Surface of slide debris	6122.0	6156.0	6249.0
Top of bedrock	6097.0	6140.5	6192.0
Bottom of hole	6092.0	6136	6188.0

b. INSTALLATION DATA OF SLOPE INDICATOR CASING

Description	SI No. 1	SI No. 2	SI No. 3
Installation date of casing No. 1	12-17-71	3-13-72	3-25-72
Coordinates at top of casing surveyed on 3-29-72	N4238750.01 E4332717.86	N4238784.07 E4332829.48	N4238811.29 E4333024.98
	Casing No. 12	Casing No. 6	Casing No. 12
Elevation at top of casing	6156.86	6167.65	6254.63
Bottom of casing	El. 6094.89	El. 6136.44	El. 6189.32

TABLE 11 - IDENTIFICATION OF SOIL SAMPLES

<u>Sample No.</u>	<u>Material</u>	<u>Elevation</u>	<u>Description</u>
1384-85	Slide Debris	6150-6410	Loose granular combination of cobbles and sand. Located immediately below embankment material.
RE-8	Embankment	6150-6356	Weathered Gneiss embankment compacted above slide debris. Forms R.E. wall foundation.
RE-7	R.E. Backfill	6356-6400	Weathered Gneiss backfill used in R.E. wall construction. 10" maximum material.

TABLE 12 - SHEAR STRENGTH PARAMETERS

Sample Number	Percent Compaction	Peak Value Criteria		15% Strain Criteria		Ultimate Deviator Stress Criteria		Triaxial Test
		ϕ Degrees	c (PSF)	ϕ Degrees	c (PSF)	ϕ Degrees	c (PSF)	
1384-85	90	35.5	400	39	200	40	0	CD
	90	34	400	34	400	30	0	CU ^e
RE-7	95	38.5	800	39	800	39.5	1000	CD
RE-8	95	40	600	40	600	40	900	CD

TABLE 13 - TANGENT MODULUS VALUES

Sample No.	Fill Height	Initial Modulus, E_i (PSF)	Tangent Modulus, E_T (PSF)
1384-85	5	5.97×10^5	1.92×10^4
	10	6.40×10^5	2.05×10^4
	15	6.82×10^5	2.18×10^4
	20	7.24×10^5	2.31×10^4
	25	7.67×10^5	2.45×10^4
	50	9.78×10^5	3.12×10^4
	100	1.40×10^6	4.47×10^4
	200	2.25×10^6	7.17×10^4
	300	3.09×10^6	9.87×10^4
RE-7	5	1.53×10^6	7.41×10^5
	10	1.61×10^6	5.02×10^5
	15	1.70×10^6	3.88×10^5
	20	1.79×10^6	3.24×10^5
	25	1.88×10^6	2.84×10^5
	50	2.31×10^6	2.09×10^5
	75	2.75×10^6	1.93×10^5
RE-8	5	1.19×10^6	5.36×10^5
	10	1.38×10^6	3.88×10^5
	15	1.56×10^6	3.20×10^5
	20	1.75×10^6	2.84×10^5
	25	1.94×10^6	2.63×10^5
	50	2.88×10^6	2.35×10^5
	100	4.76×10^6	2.65×10^5
	150	6.65×10^6	3.15×10^5
	200	8.53×10^6	3.70×10^5
	300	1.23×10^7	4.85×10^5

TABLE 14 - TANGENT POISSON'S RATIO PARAMETERS

Sample Number	Percent Compaction	Confining Pressure (PSI)	f	d	v_i	G	F	d
1384-85	90	6.94	.554	.418	.55	0.44	0.36	1.63
		14.0	.432	1.04	.43			
		28.1	.384	1.40	.38			
		56.1	.211	3.67	.21			
RE-7	95	6.94	.526	.218	.53	0.42	0.34	1.80
		15.0	.423	1.12	.42			
		30.0	.271	2.75	.27			
		60.0	.238	3.13	.24			
RE-8	95	8.06	.408	1.77	.41	0.39	0.24	2.64
		15.0	.466	.751	.47			
		30.0	.297	2.69	.30			
		60.0	.219	5.37	.22			

TABLE 15 - TANGENT POISSON'S RATIO VALUES

Fill Height (Ft)	Confining Pressure (TSF)	Initial Poisson's Ratio, ν_i			Tangent Poisson's Ratio, ν_T		
		#1384-85	#RE-7	#RE-8	#1384-85	#RE-7	#RE-8
5	.13	.773	.726	.611	.784	.727	.613
10	.26	.664	.624	.538	.682	.626	.541
15	.38	.601	.564	.495	.624	.568	.500
20	.51	.556	.522	.464	.582	.527	.471
25	.64	.521	.489	.441	.551	.495	.448
50	1.28	.413	.388	.367	.450	.397	.378
75	1.92	.349	.328	.324	.389	.340	.337
100	2.55	.304	.286	.294	.344	.298	.307
150	3.83	.241	.226	.251	.278	.239	.264
200	5.11	.196	.184	.220	.229	.196	.233
250	6.39	.161	.151	.197	.189	.162	.208
300	7.66	.133	.125	.177	.157	.134	.188

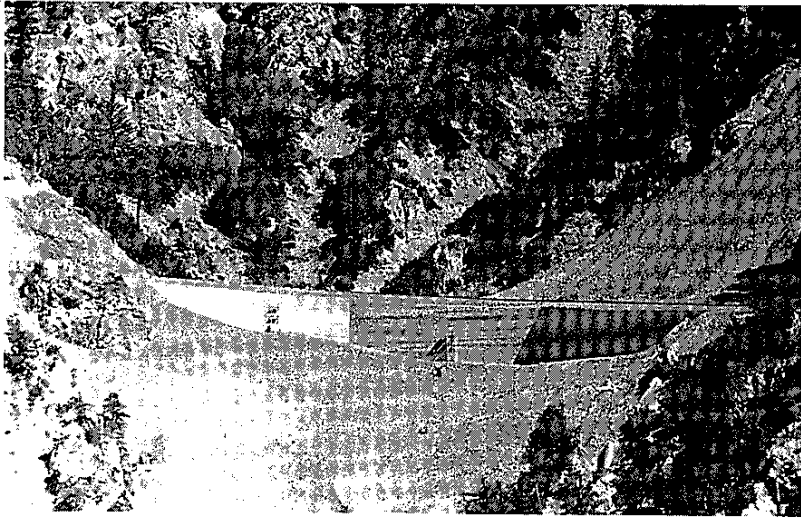


Photo 1 - Completed view of the reinforced earth embankment



Photo 2 - Batter boards and instrumented skin element

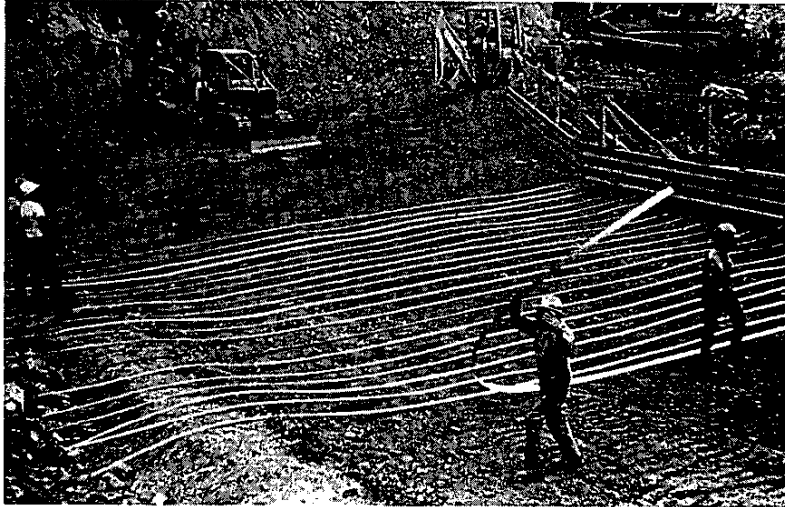


Photo 3 - Placing reinforcing strips

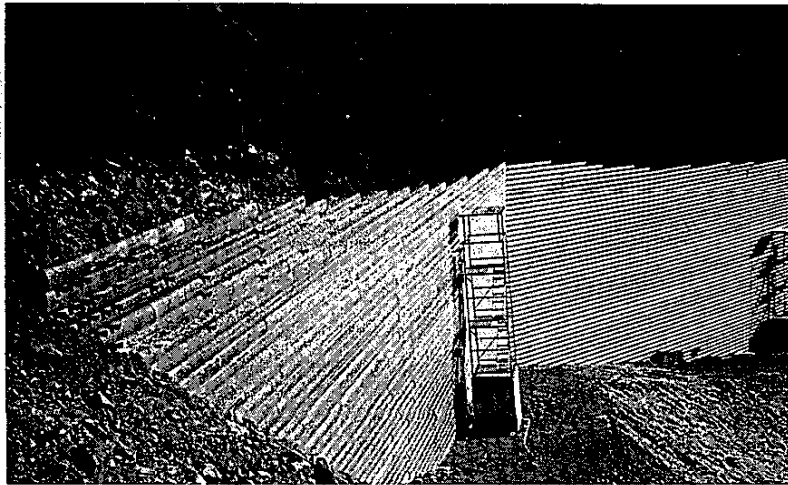


Photo 4 - Completed wall face with wooden wedges between skin elements and instrumentation shelters on berm

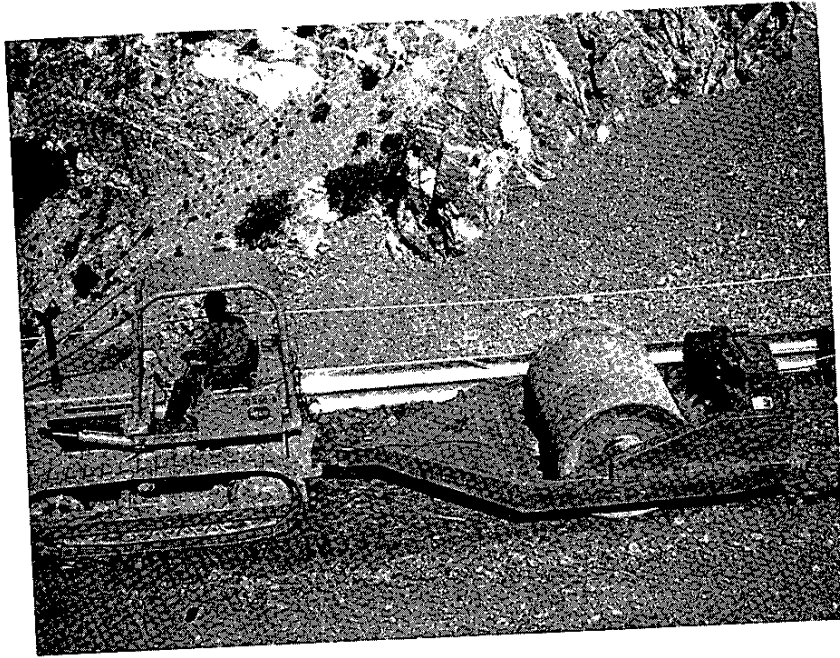


Photo 5 - Compaction operation

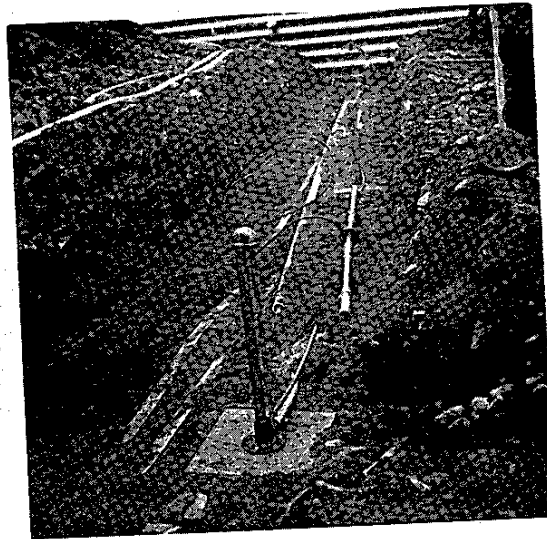


Photo 6 - Instrumentation Trench with settlement platform in place

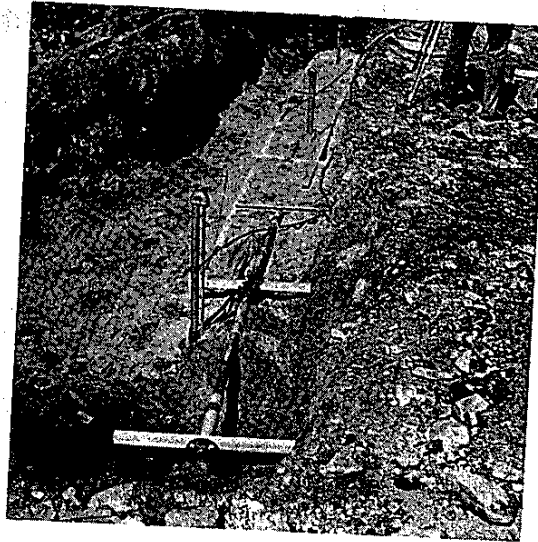


Photo 7 - Extensometer installed

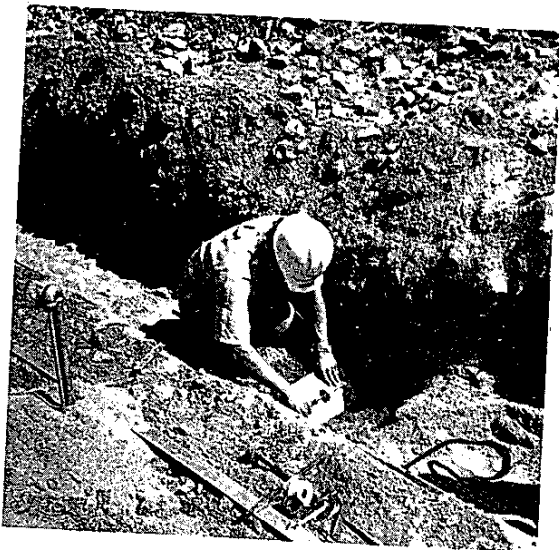


Photo 8

a. Installation of soil pressure cell

b. Soil pressure cell on vertical, horizontal and inclined planes

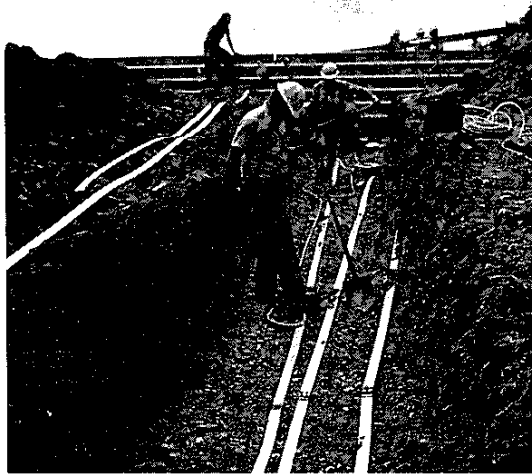


Photo 9 - Instrumented reinforcing strips
with strain gages protected by sand

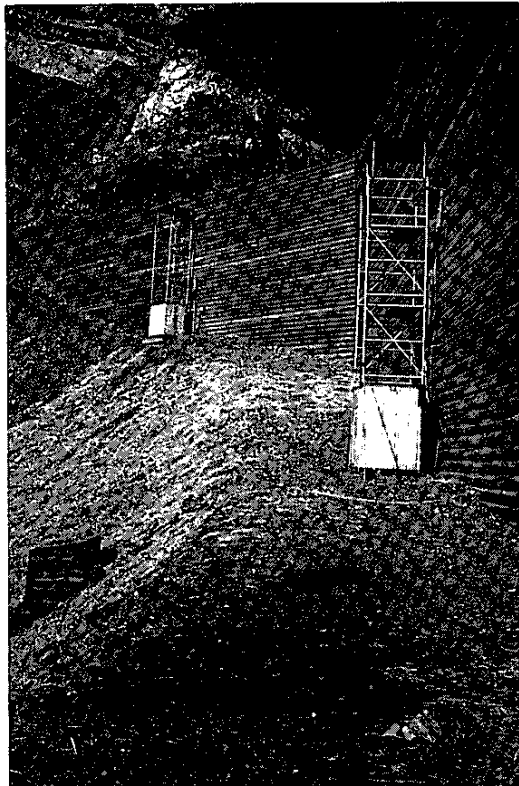


Photo 10 - Instrumentation shelters at
three locations for housing
the readout devices

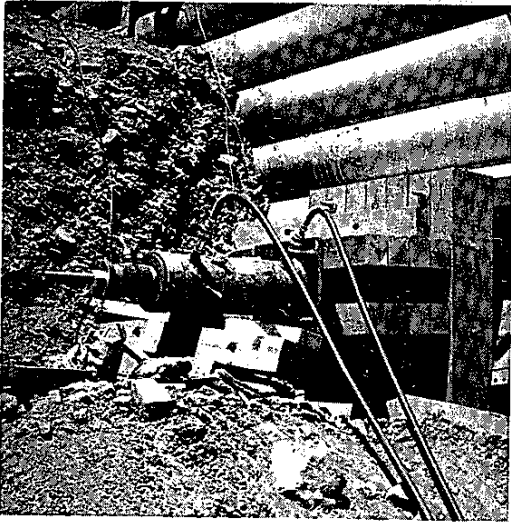


Photo 11 - Hydraulic jack acting against wooden bearing pad

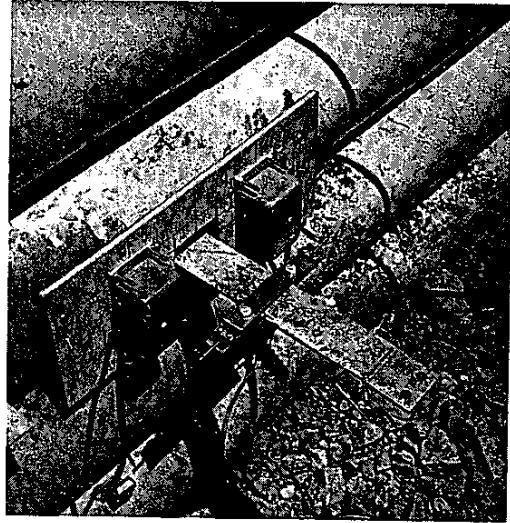


Photo 12 - Dummy steel strip with two extendometers fastened at each side

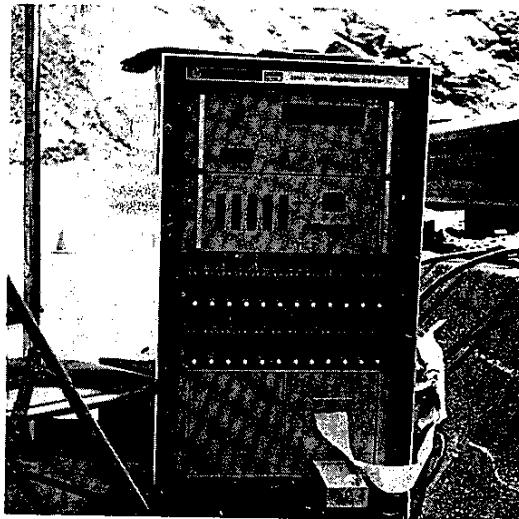


Photo 13 - Data acquisition system utilized during pulling tests

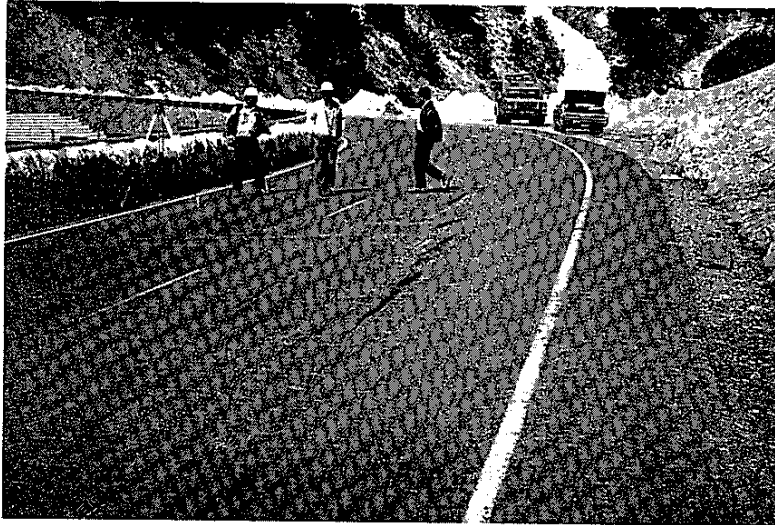


Photo 14 - Pavement cracks observed behind the
reinforced earth fill in April 1973
Station 552+90 - 553+75

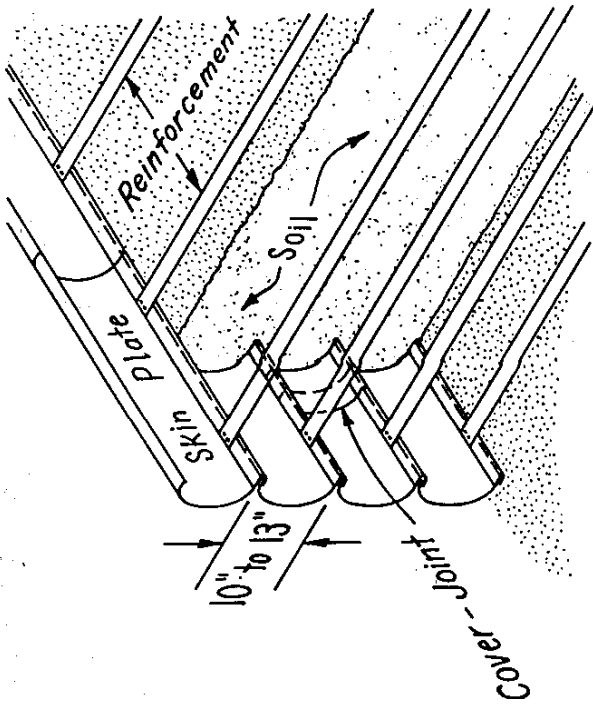


Figure 1 SCHEMATIC OF REINFORCED EARTH FILL

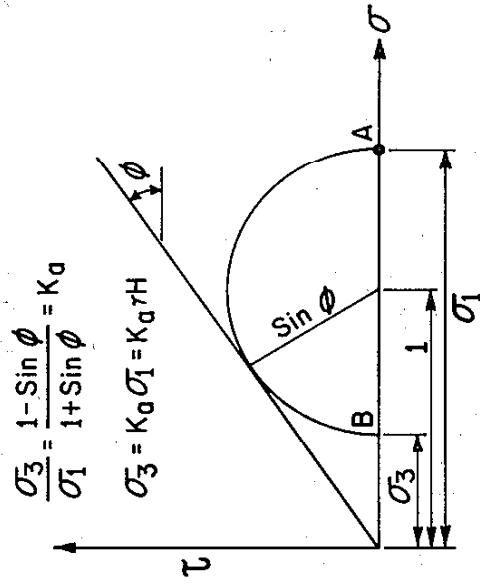


Figure 4 MOHR CIRCLE
(AT IMMINENT FAILURE)

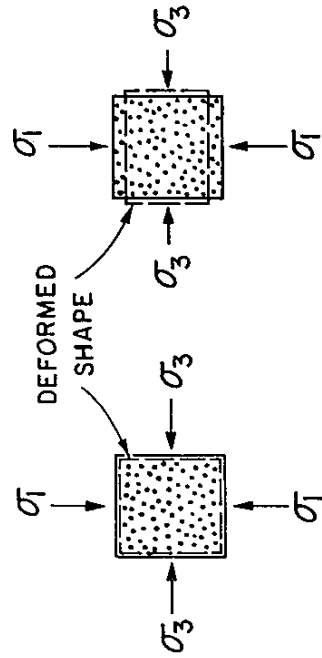


Figure 2 SAND CUBE $(\sigma_1 = \sigma_3)$
Figure 3 SAND CUBE $(\sigma_1 > \sigma_3)$

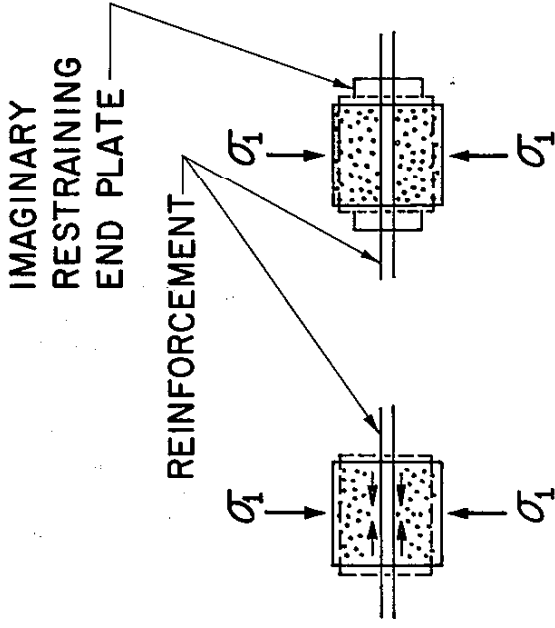
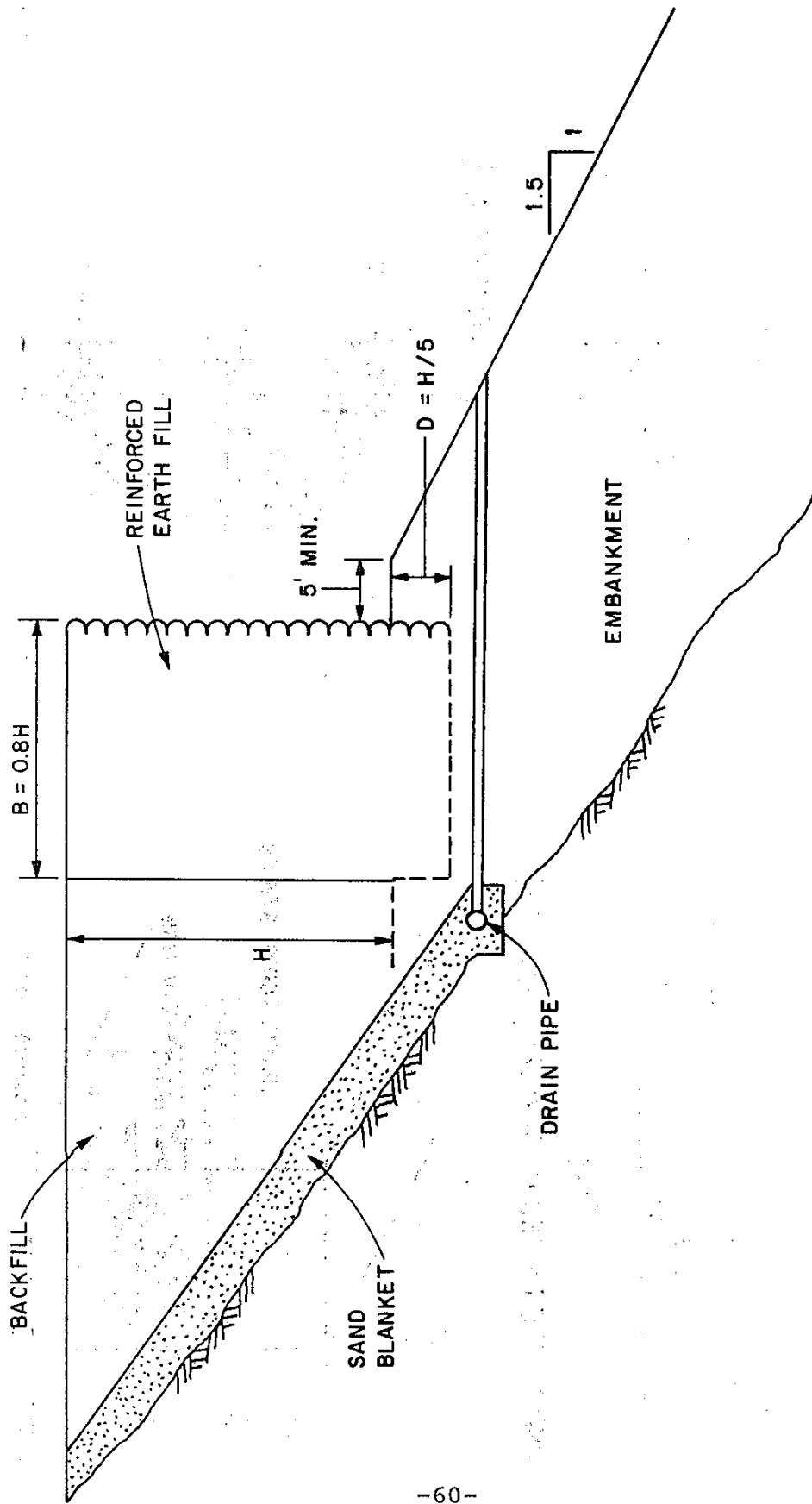


Figure 5 REINFORCED SOIL ELEMENT



**STABILITY REQUIREMENTS
 (RULE OF THUMB)**

Figure 9

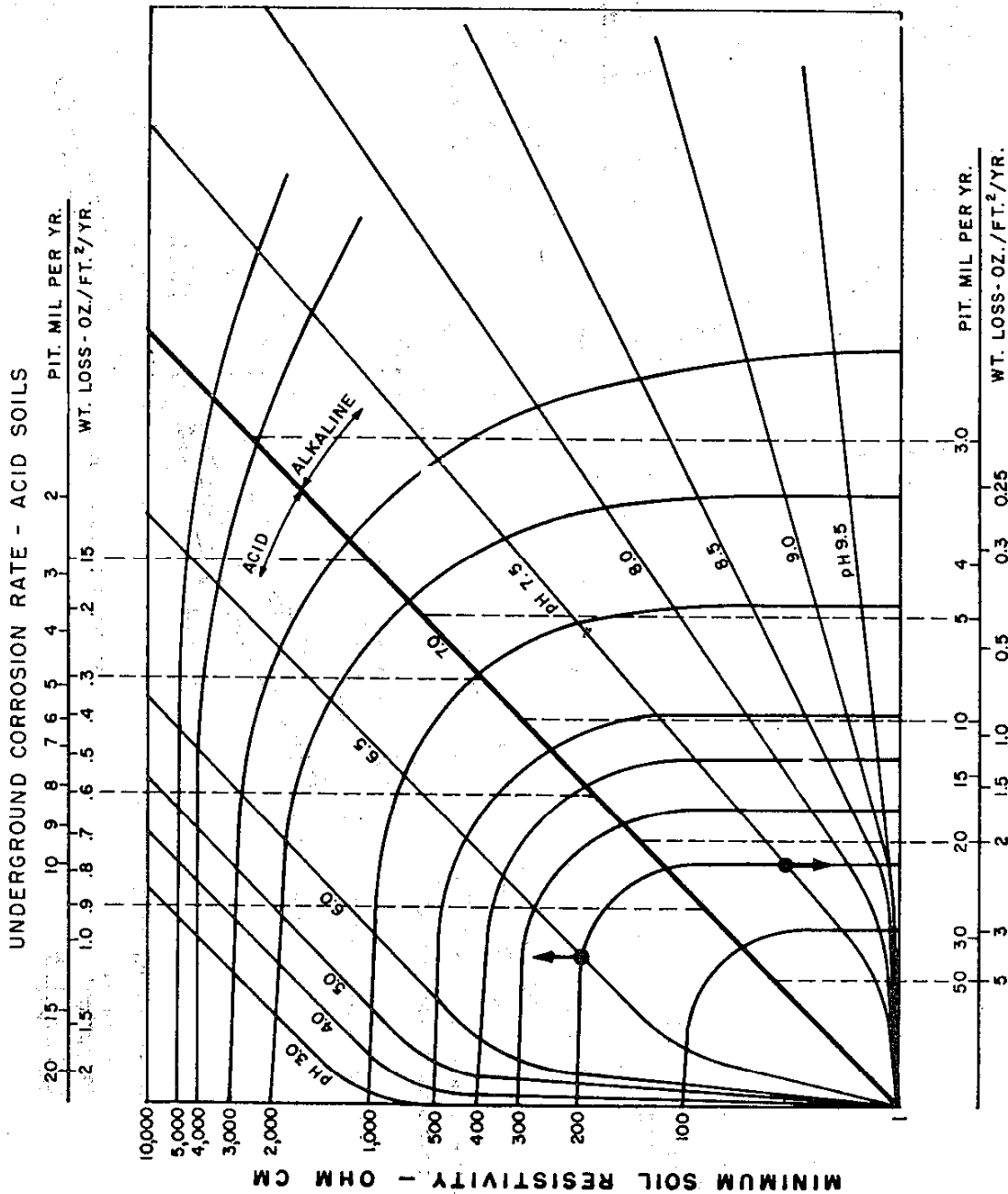
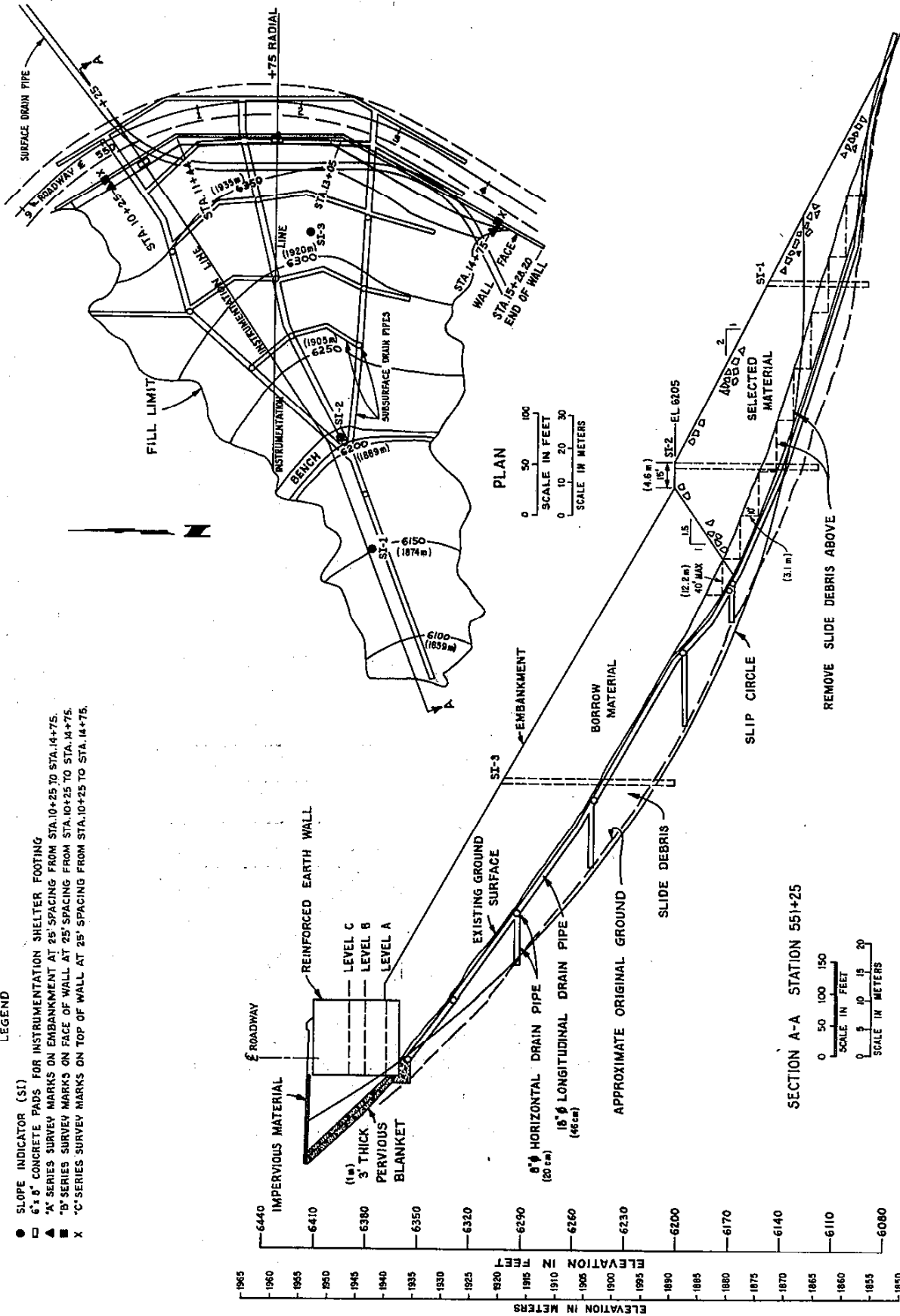


Figure 10—Chart for estimating corrosion rate of steel pipe. Example 1: with pH of 6.5 and resistivity of 200 ohm cm, the underground pipe loss is about 1.0 oz/sq ft/yr and the pitting rate about 0.013 ipy. Example 2: with pH of 7.5 and resistivity of 200 ohm cm, the underground pipe loss is about 2.2 oz; sq ft/yr and the pitting rate is about 0.022 ipy.

LEGEND

- SLOPE INDICATOR (SI)
- 6" x 6" CONCRETE PADS FOR INSTRUMENTATION SHELTER FOOTING
- ▲ 'A' SERIES SURVEY MARKS ON EMBANKMENT AT 25' SPACING FROM STA. 10+25 TO STA. 14+75.
- 'B' SERIES SURVEY MARKS ON FACE OF WALL AT 25' SPACING FROM STA. 10+25 TO STA. 14+75.
- X 'C' SERIES SURVEY MARKS ON TOP OF WALL AT 25' SPACING FROM STA. 10+25 TO STA. 14+75.



PLAN AND SECTION

FIGURE 11

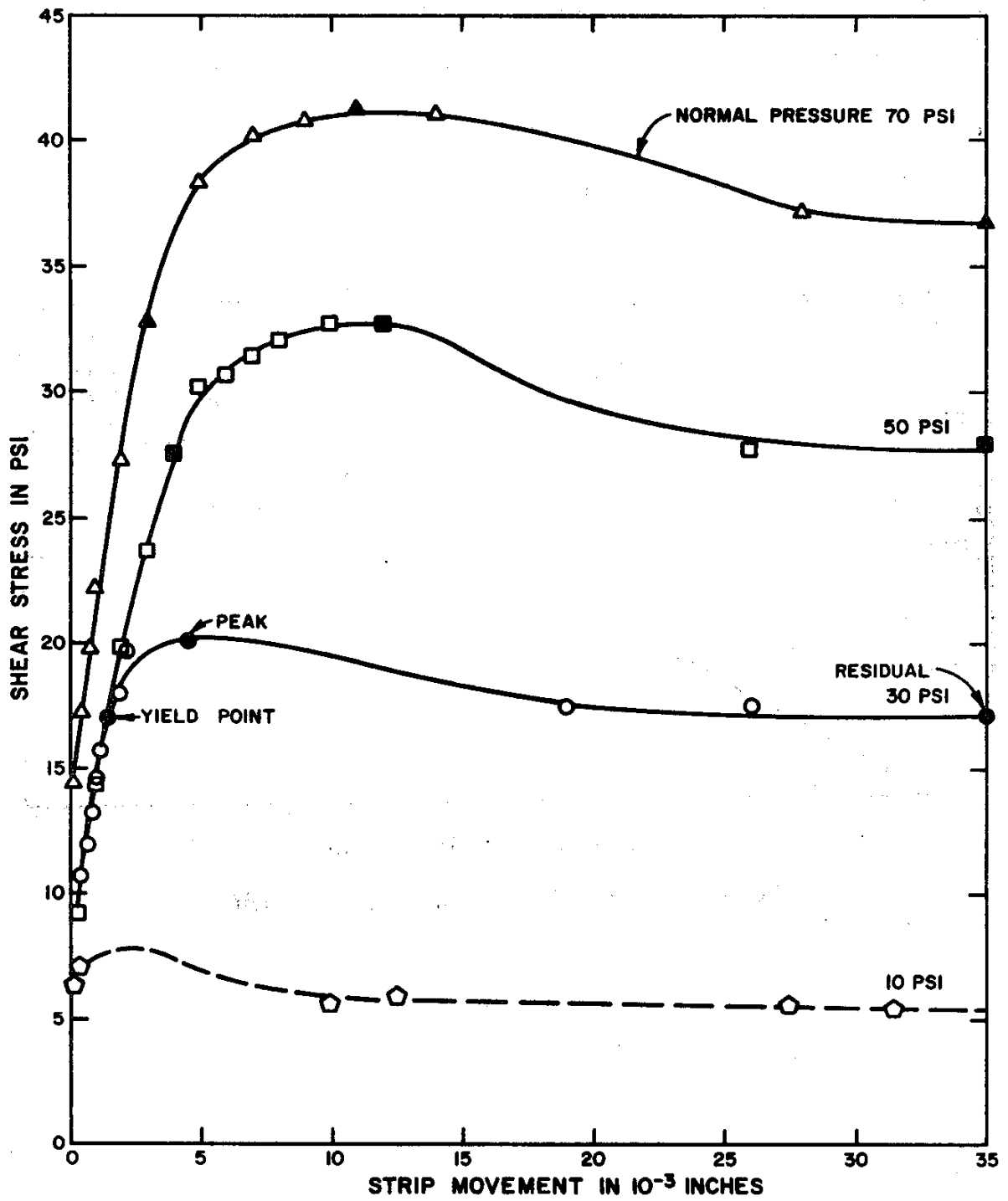


Figure 12: STRESS-DEFORMATION CURVE FROM LABORATORY PULLING TESTS

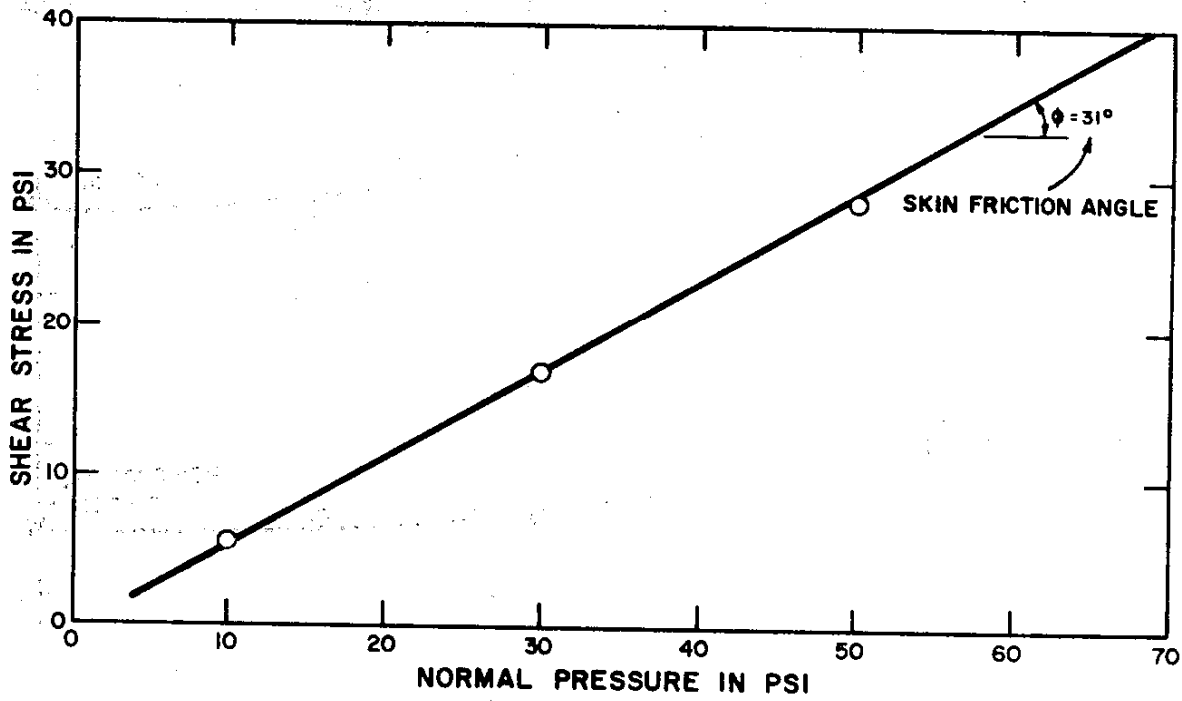


Figure 13: SKIN FRICTION ENVELOPE LINE

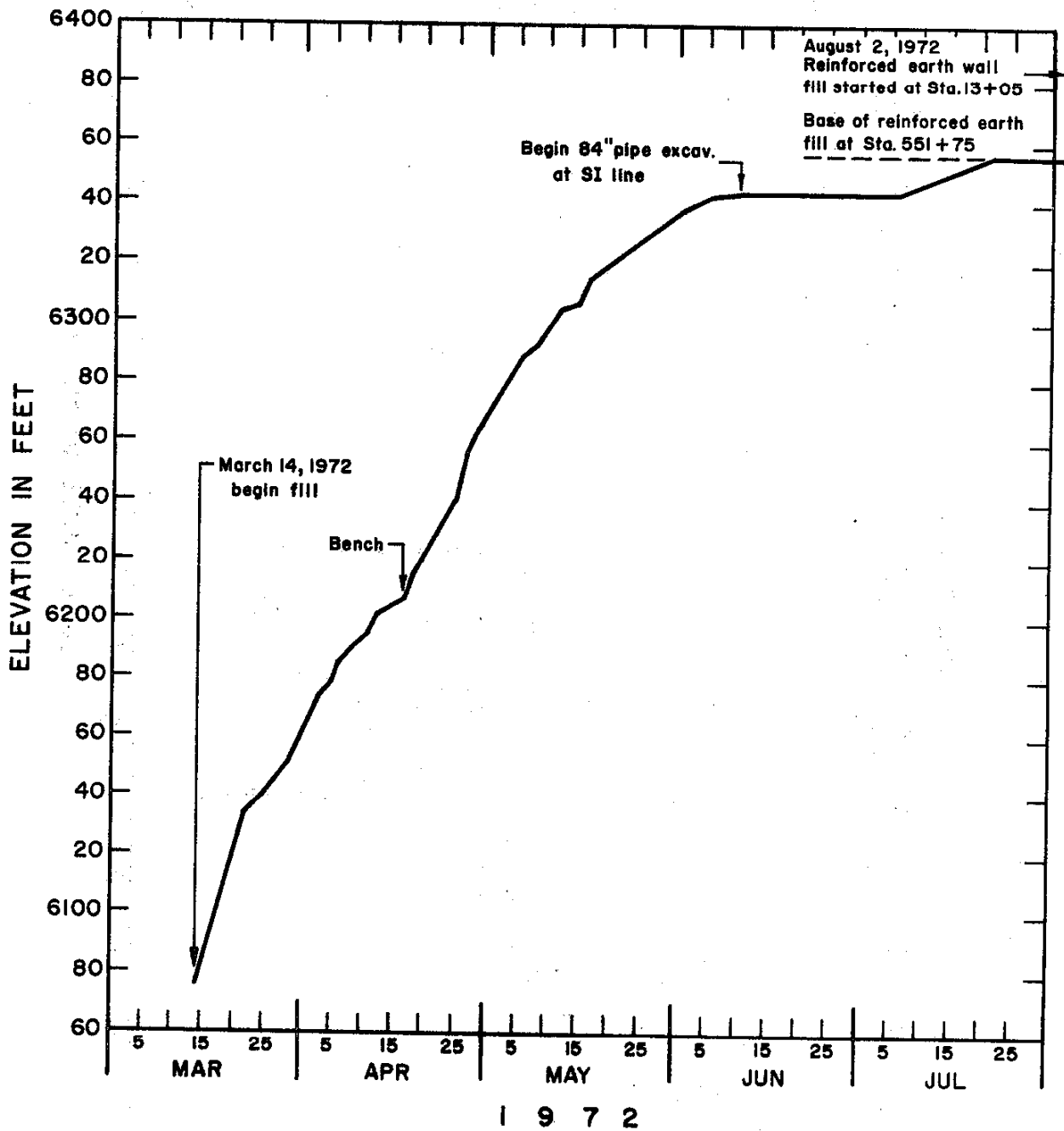
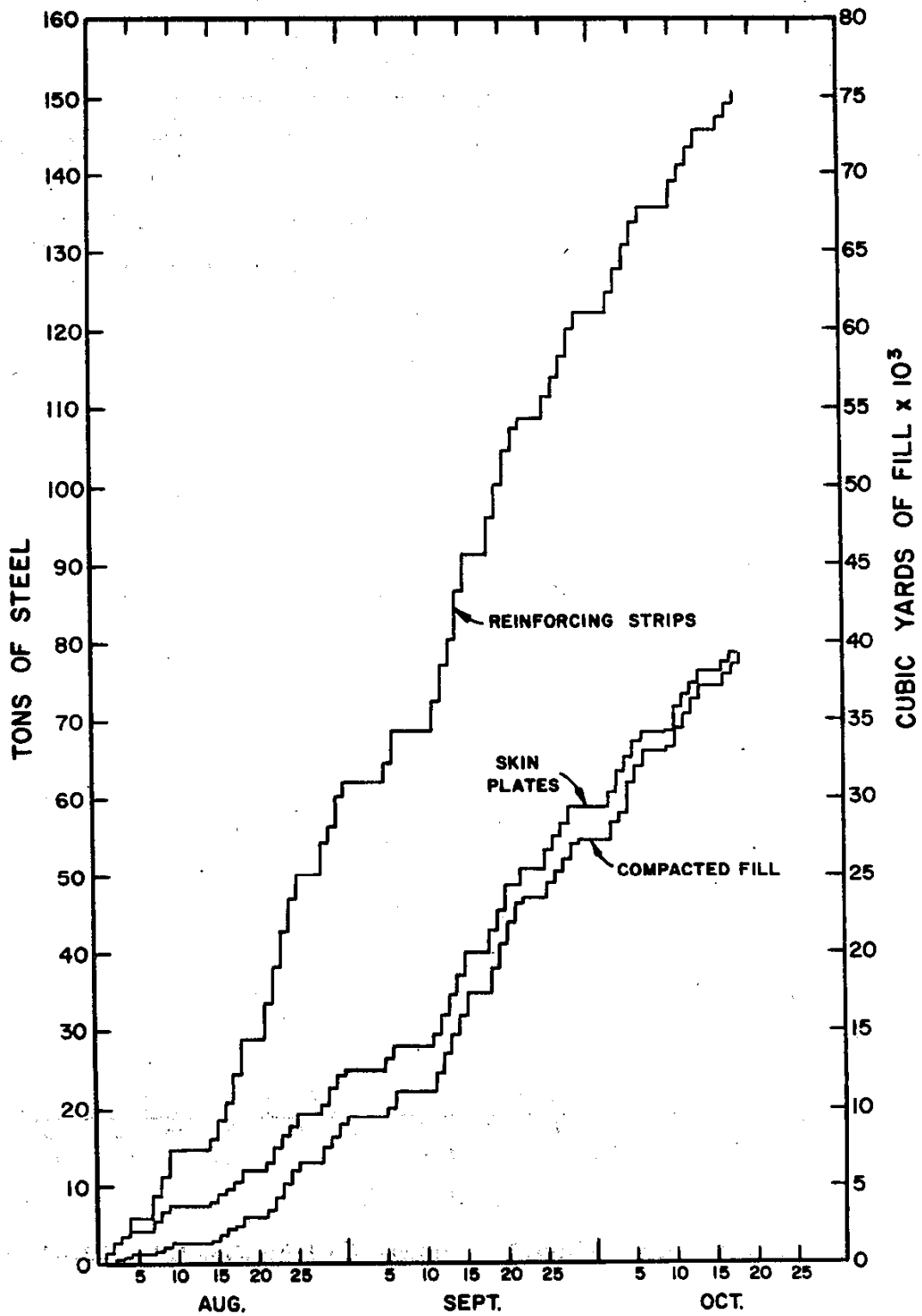


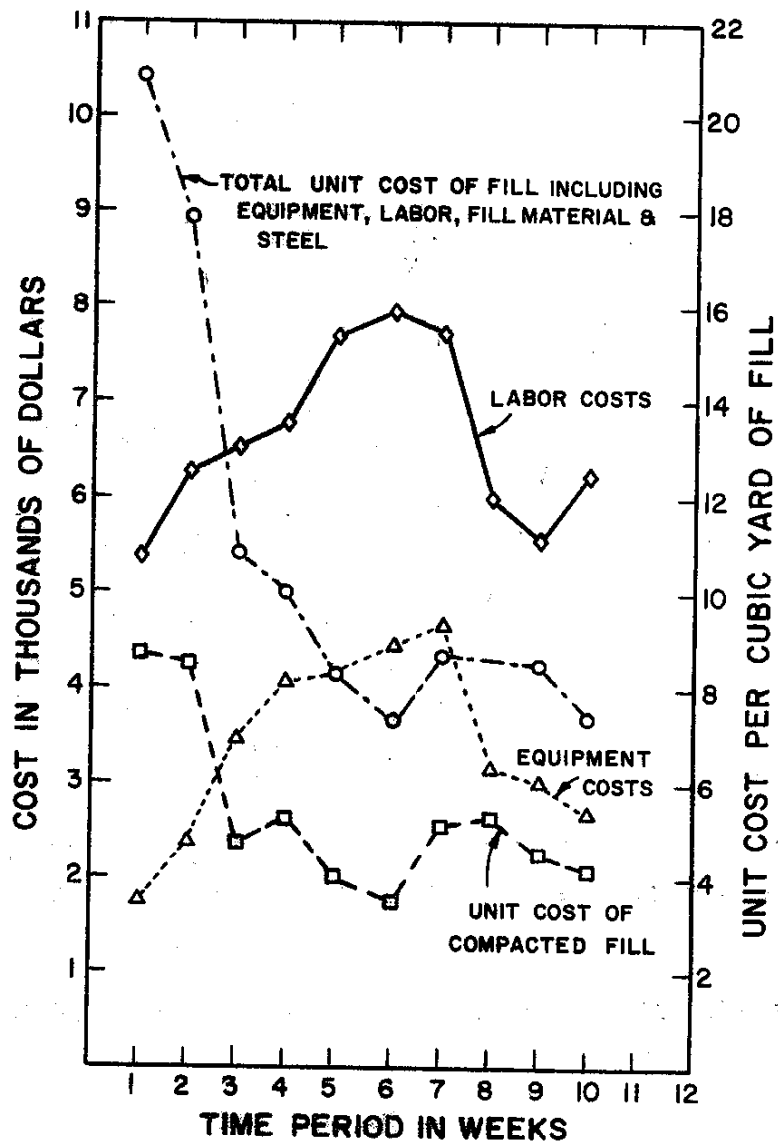
Figure 14: DAILY RECORD OF HEIGHT DURING EMBANKMENT CONSTRUCTION



DAILY RECORD OF CONSTRUCTION QUANTITIES

Figure 15

- NOTE (1) EACH WEEK IS COMPOSED OF FIVE WORK DAYS.
 (2) ALL COSTS PLOTTED ARE THE TOTAL COSTS IN EACH WEEK.
 (3) UNIT COSTS PLOTTED ARE THE AVERAGE UNIT COSTS WITHIN EACH WEEK.



WEEKLY RECORD OF CONSTRUCTION COSTS

Figure 16

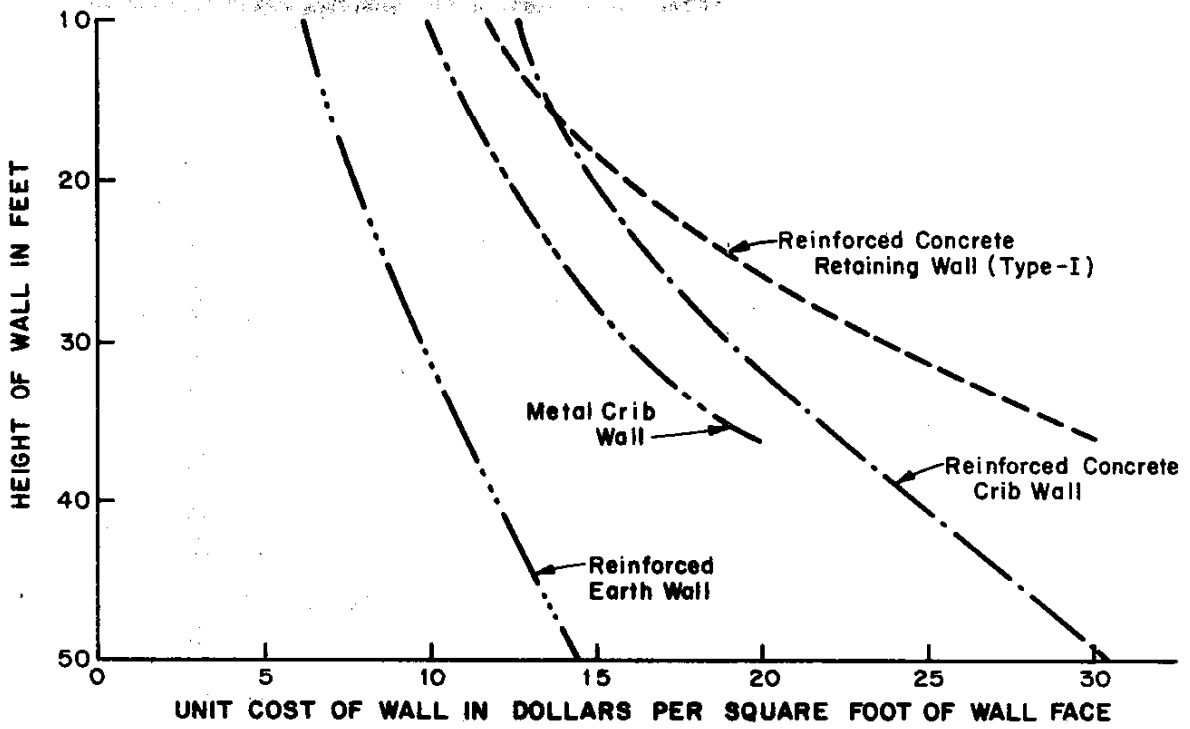
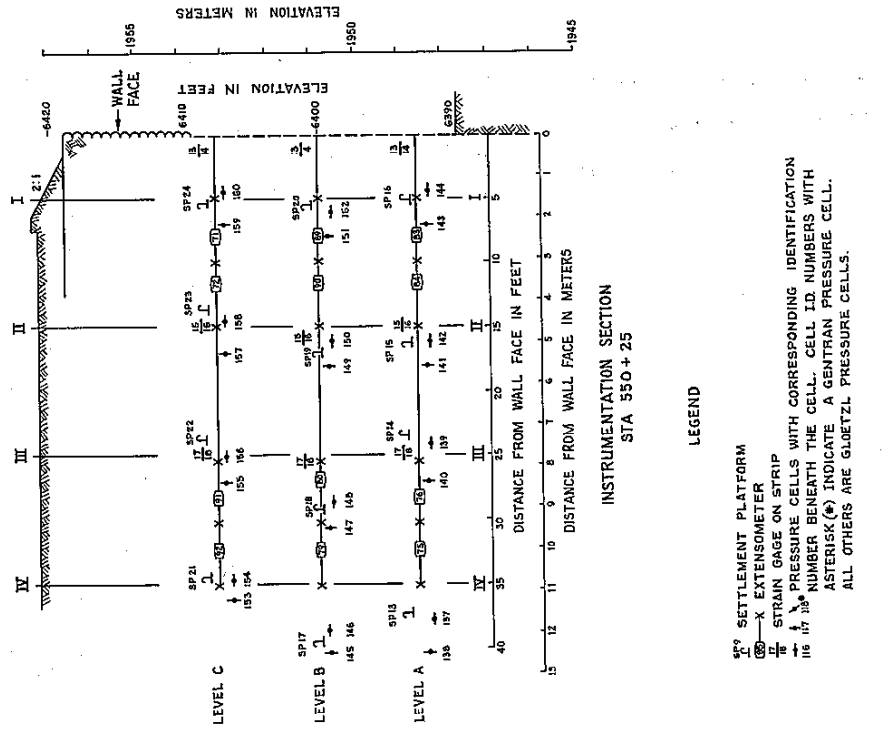
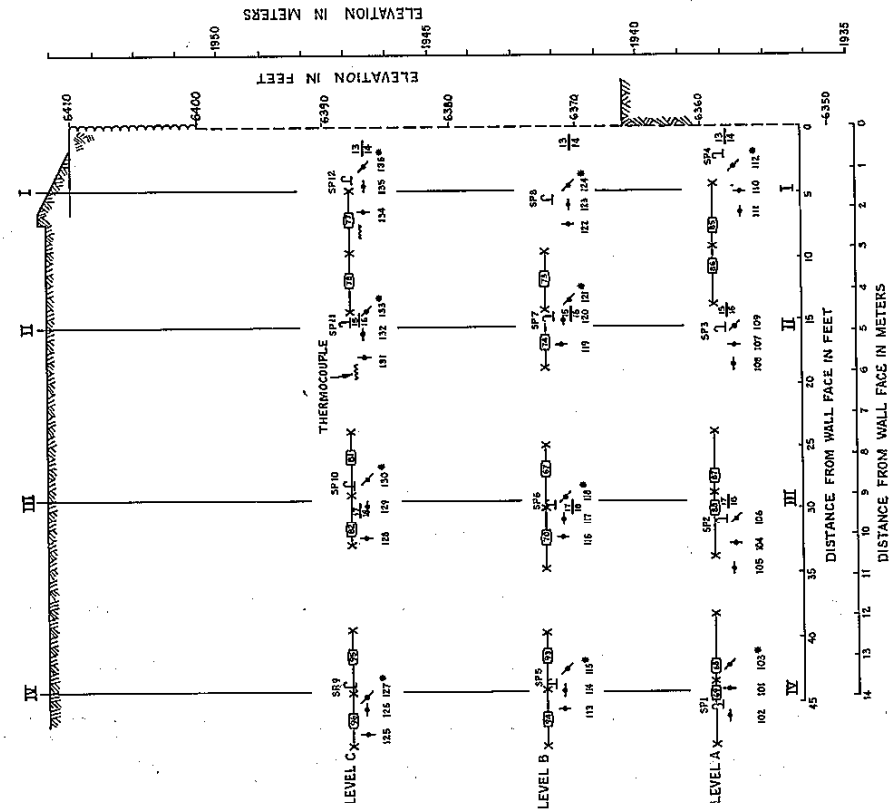


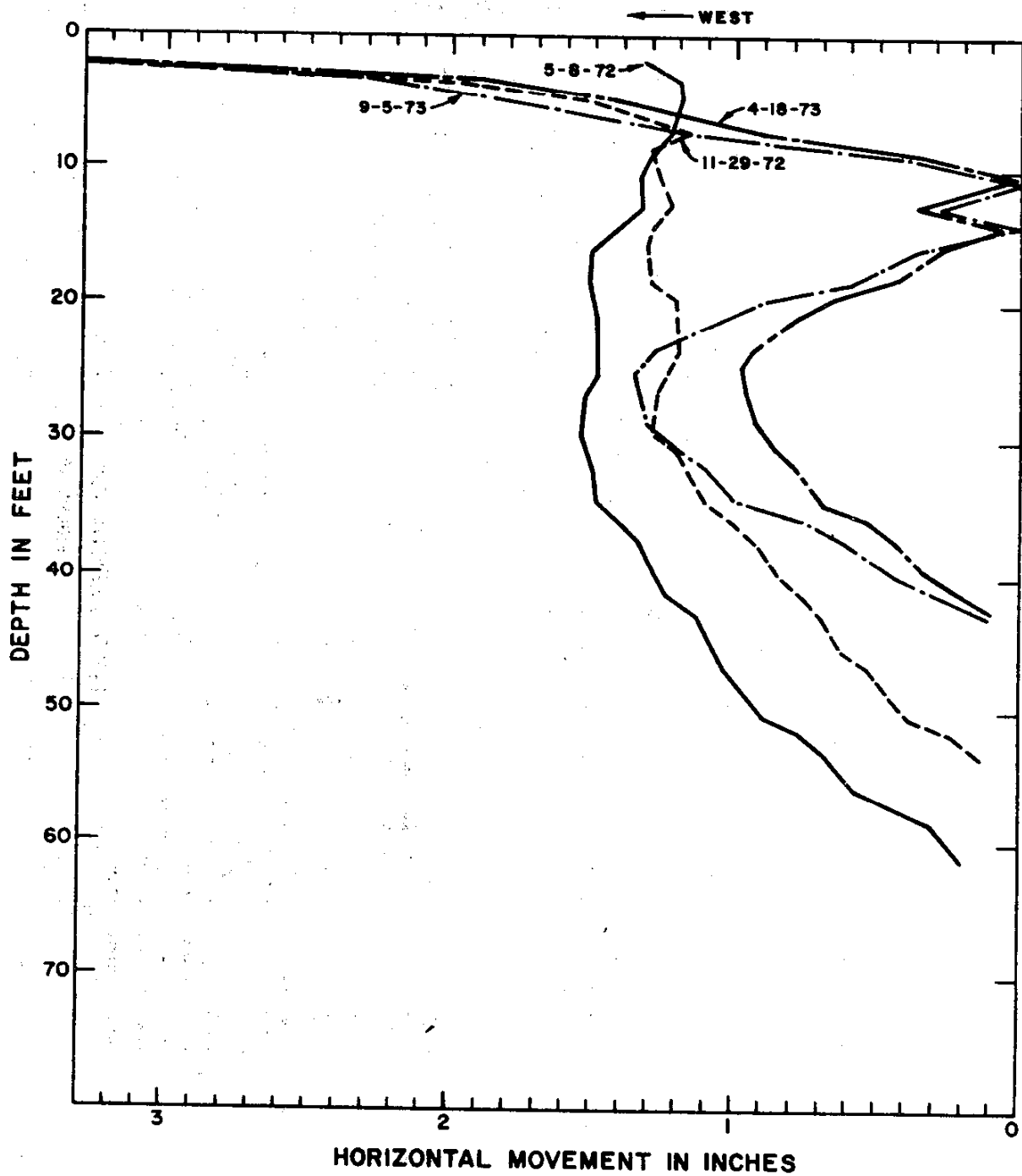
Figure 17: COST COMPARISON BETWEEN FOUR TYPES OF WALLS



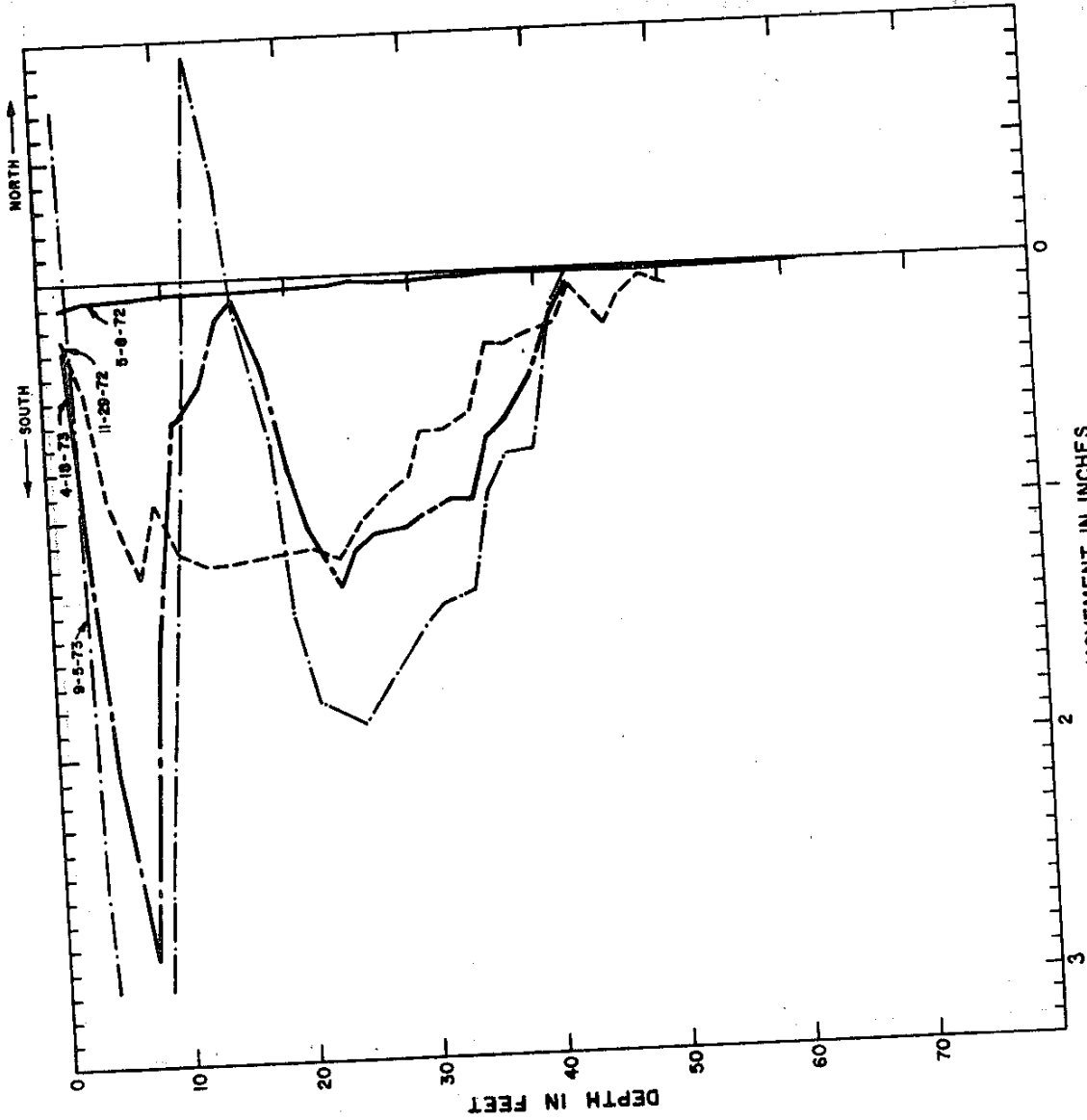
INSTRUMENTATION SECTIONS

FIGURE 18





**Figure 19: HORIZONTAL MOVEMENT IN THE E-W DIRECTION
MEASURED BY SLOPE INDICATOR SI-1**



HORIZONTAL MOVEMENT IN INCHES
 HORIZONTAL MOVEMENT IN THE N-S DIRECTION MEASURED BY
 SLOPE INDICATOR SI-1

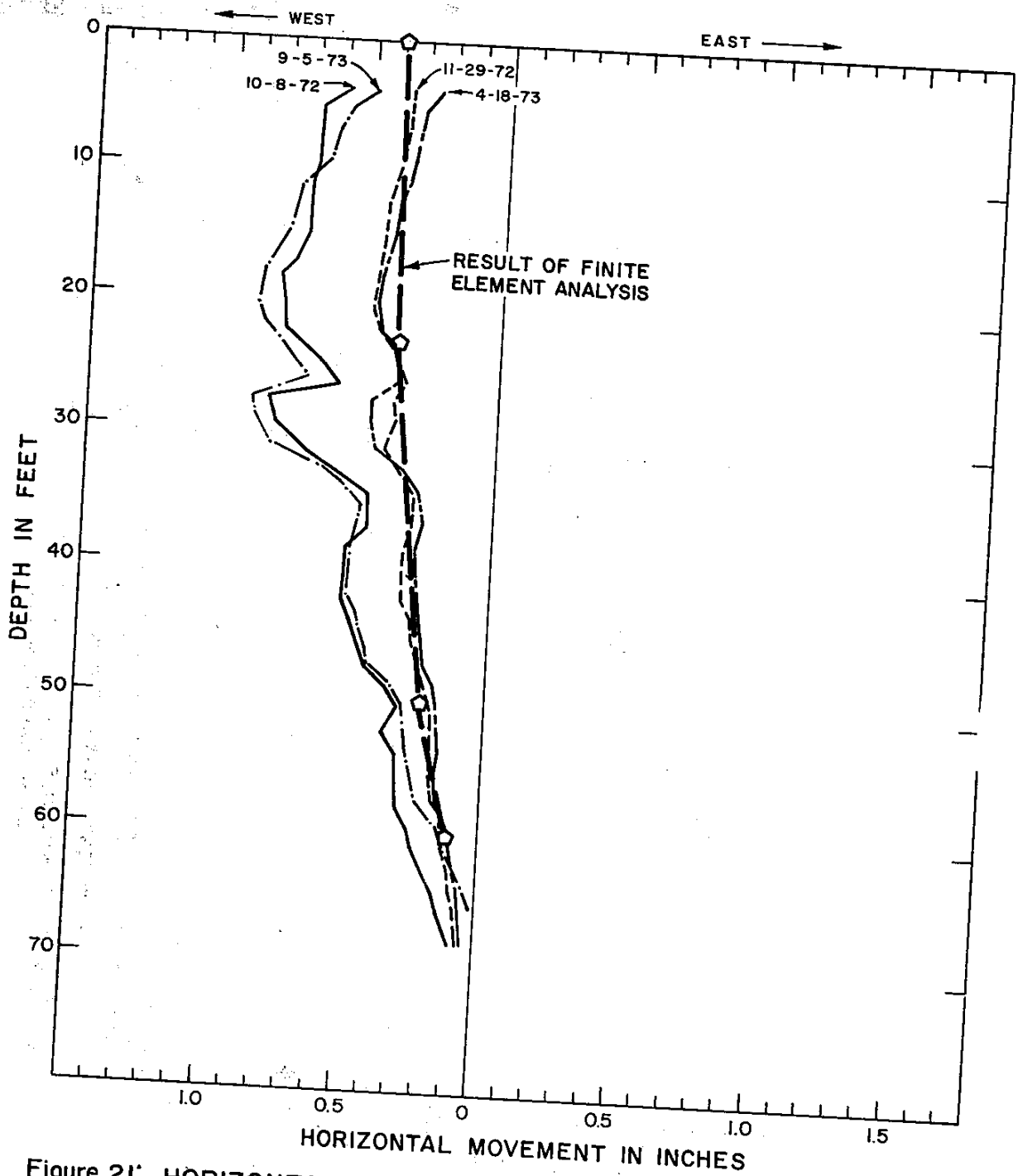


Figure 21: HORIZONTAL MOVEMENT IN THE E-W DIRECTION
MEASURED BY SLOPE INDICATOR SI-2

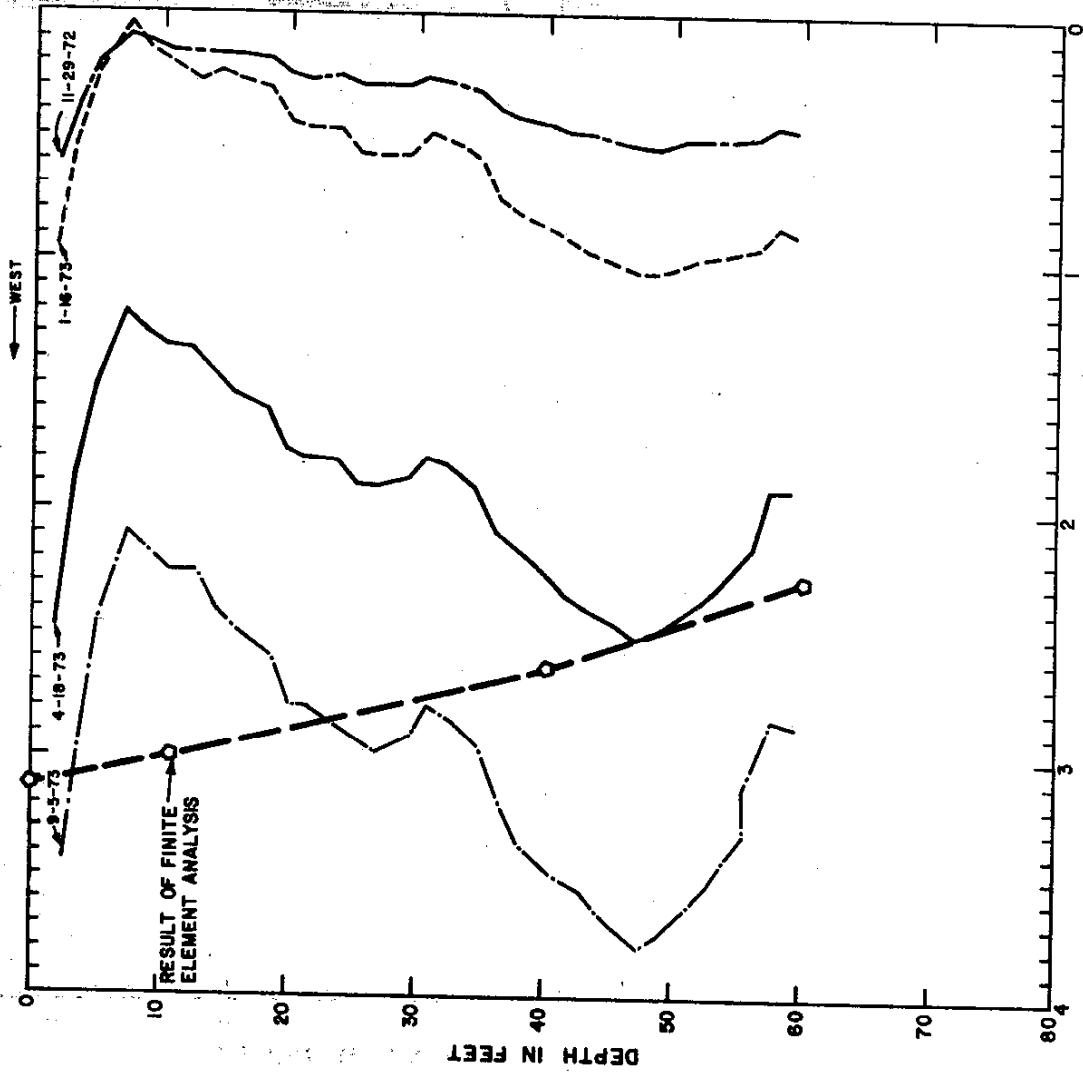


Figure 23: HORIZONTAL MOVEMENT IN THE E-W DIRECTION MEASURED BY SLOPE INDICATOR SI-3

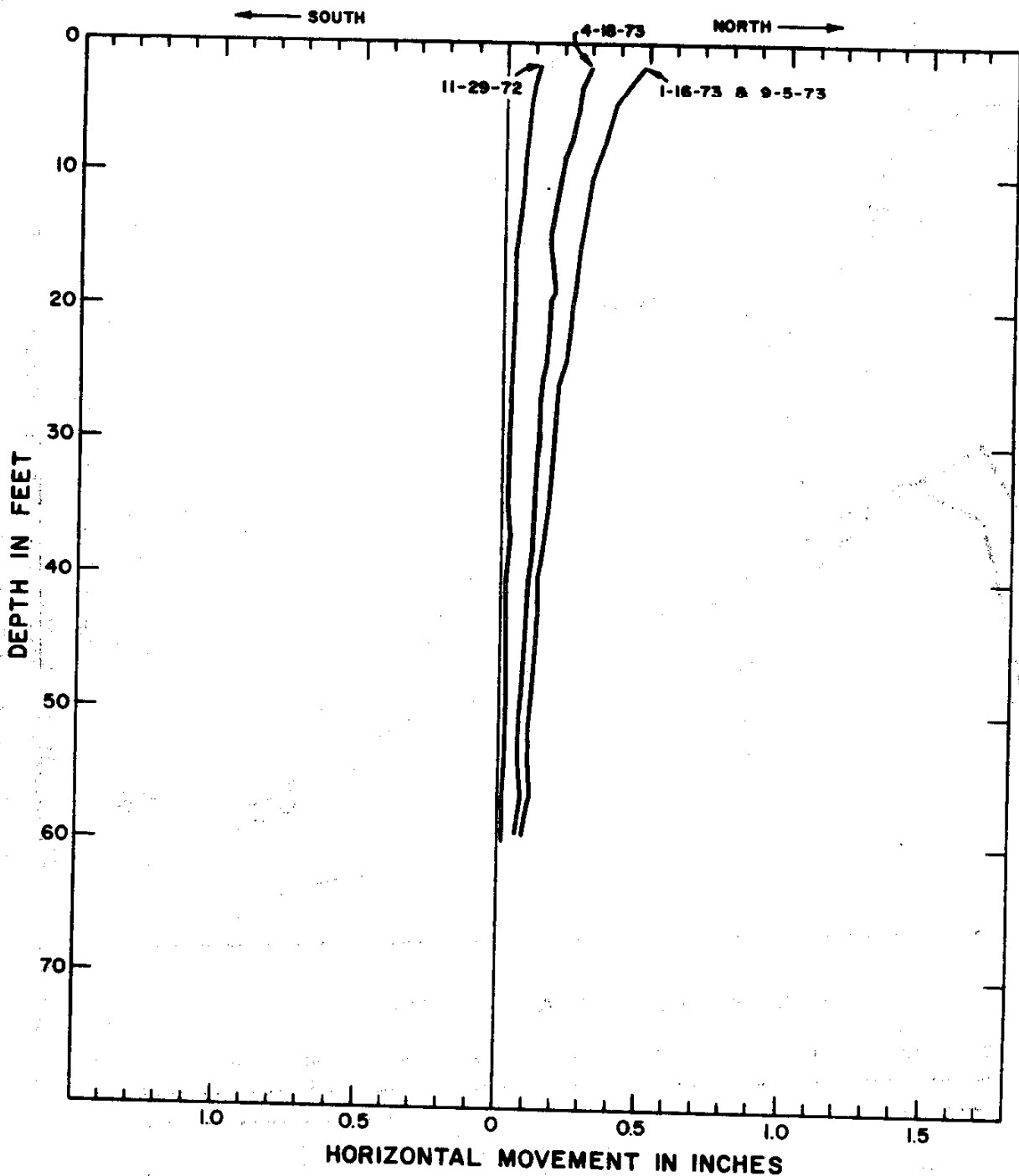


Figure 24: HORIZONTAL MOVEMENT IN THE N-S DIRECTION MEASURED BY SLOPE INDICATOR SI-3

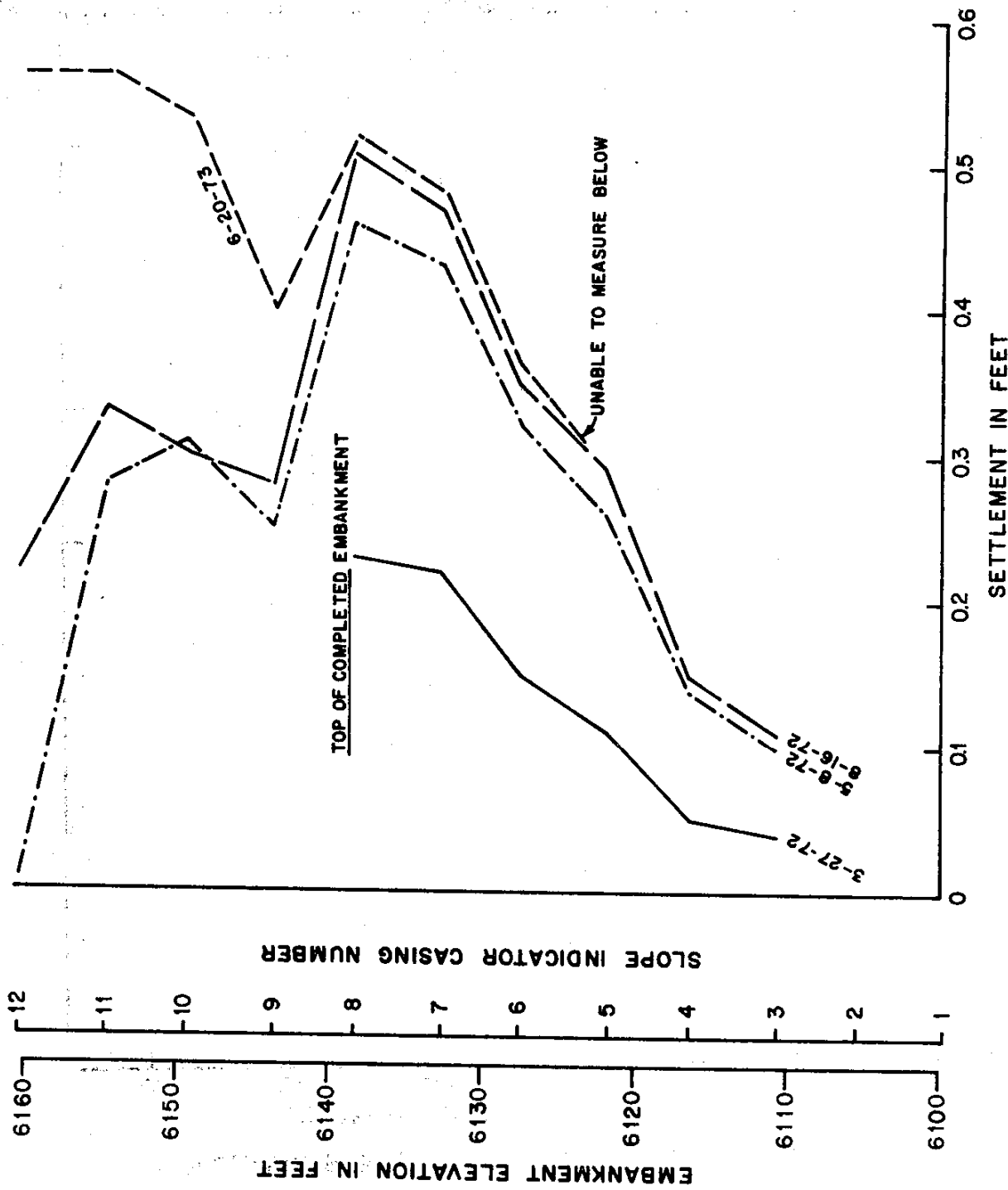


Figure 25: EMBANKMENT SETTLEMENT MEASURED BY SLOPE INDICATOR SI-1

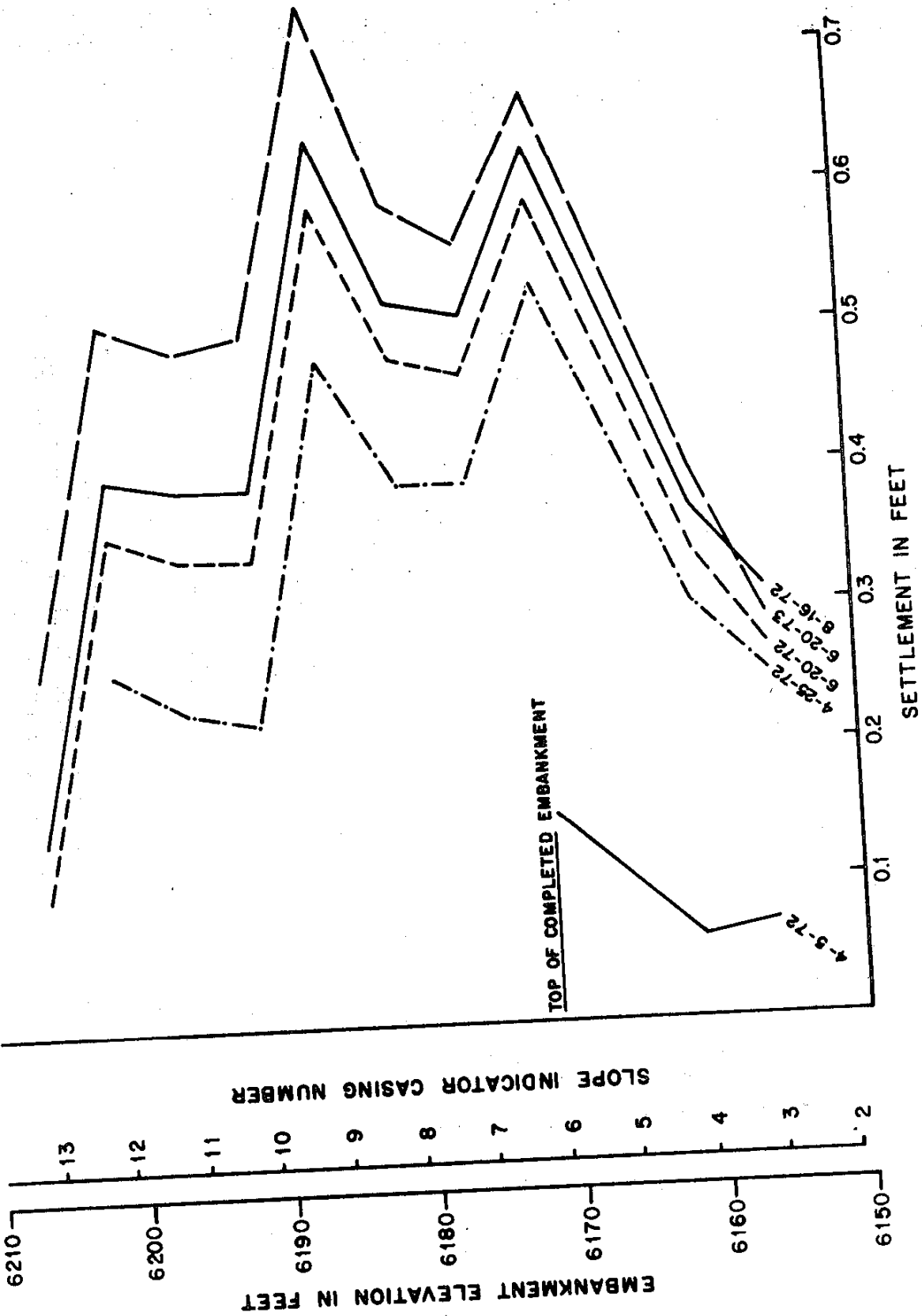


Figure 26: EMBANKMENT SETTLEMENT MEASURED BY SLOPE INDICATOR SI-2

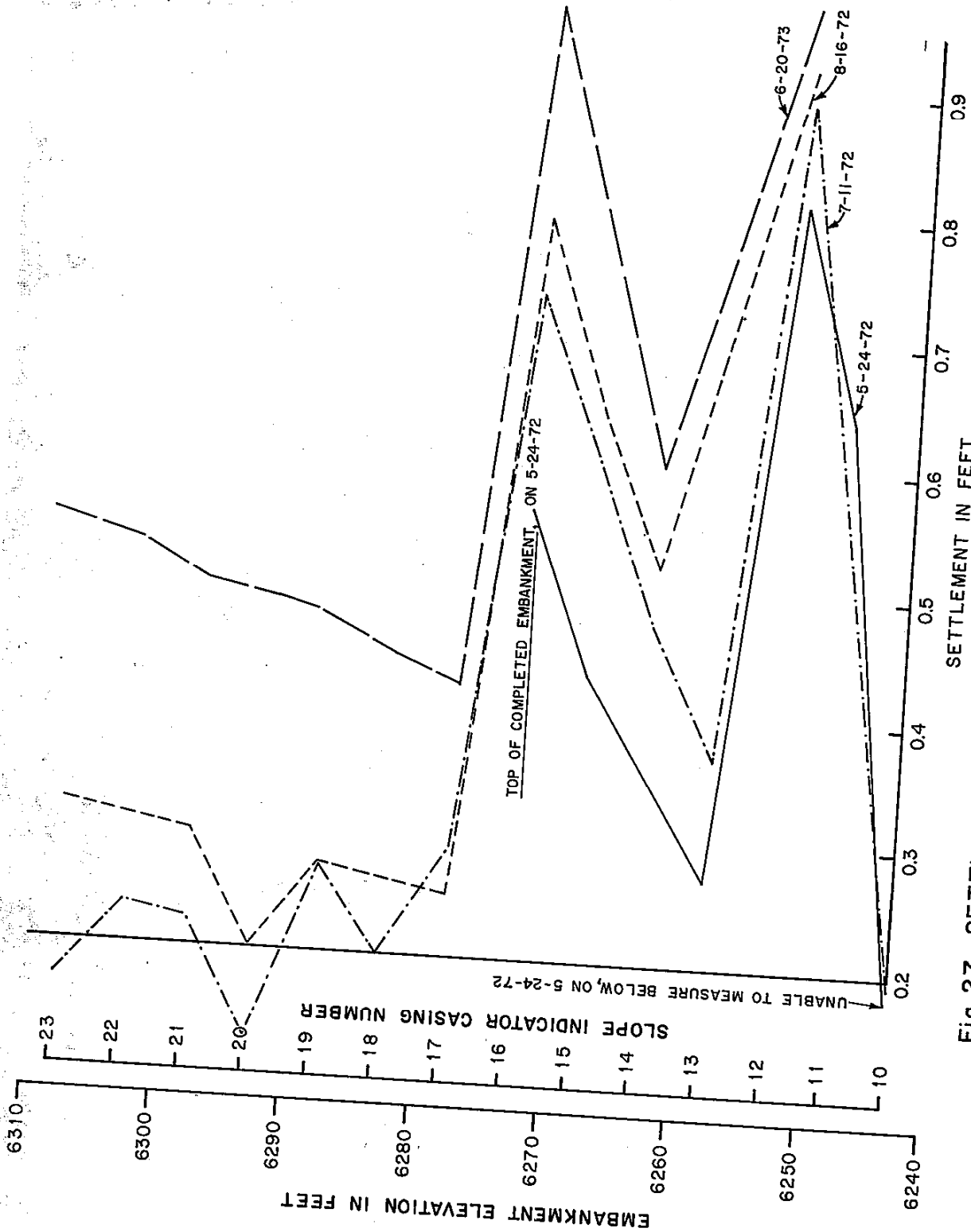
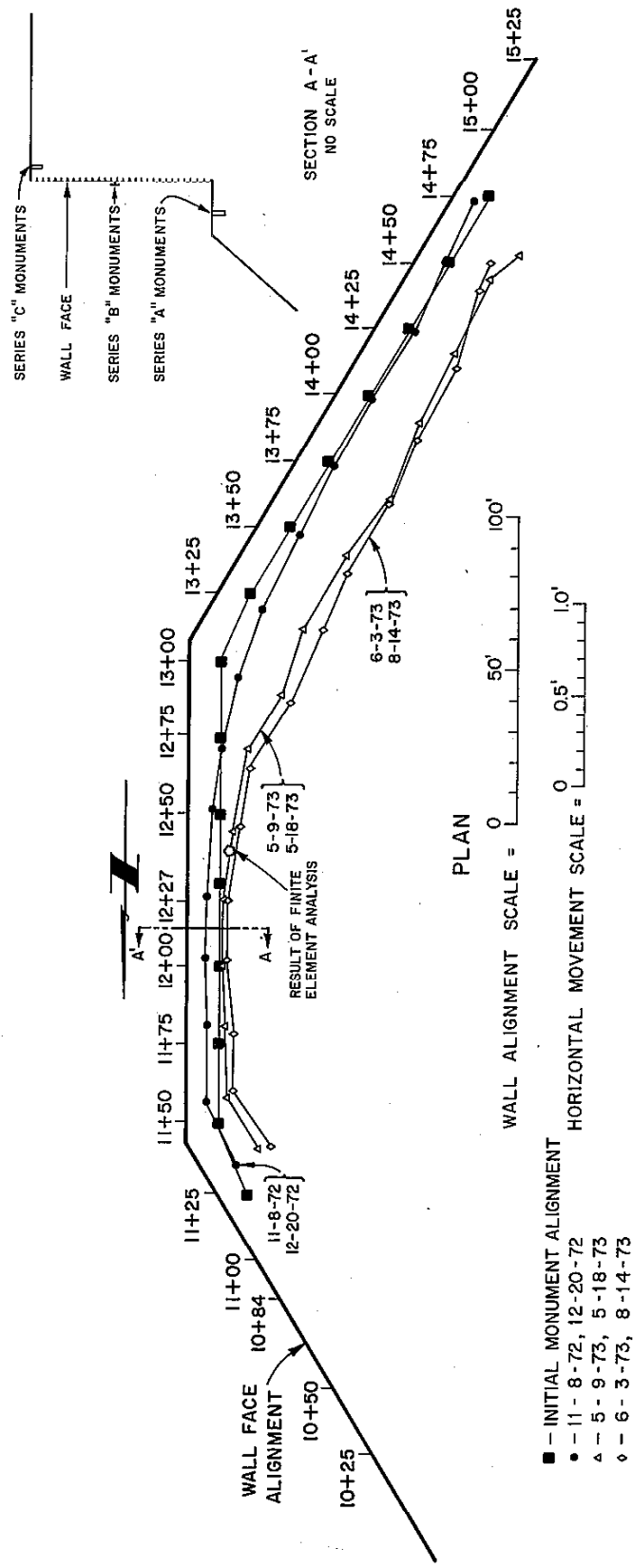
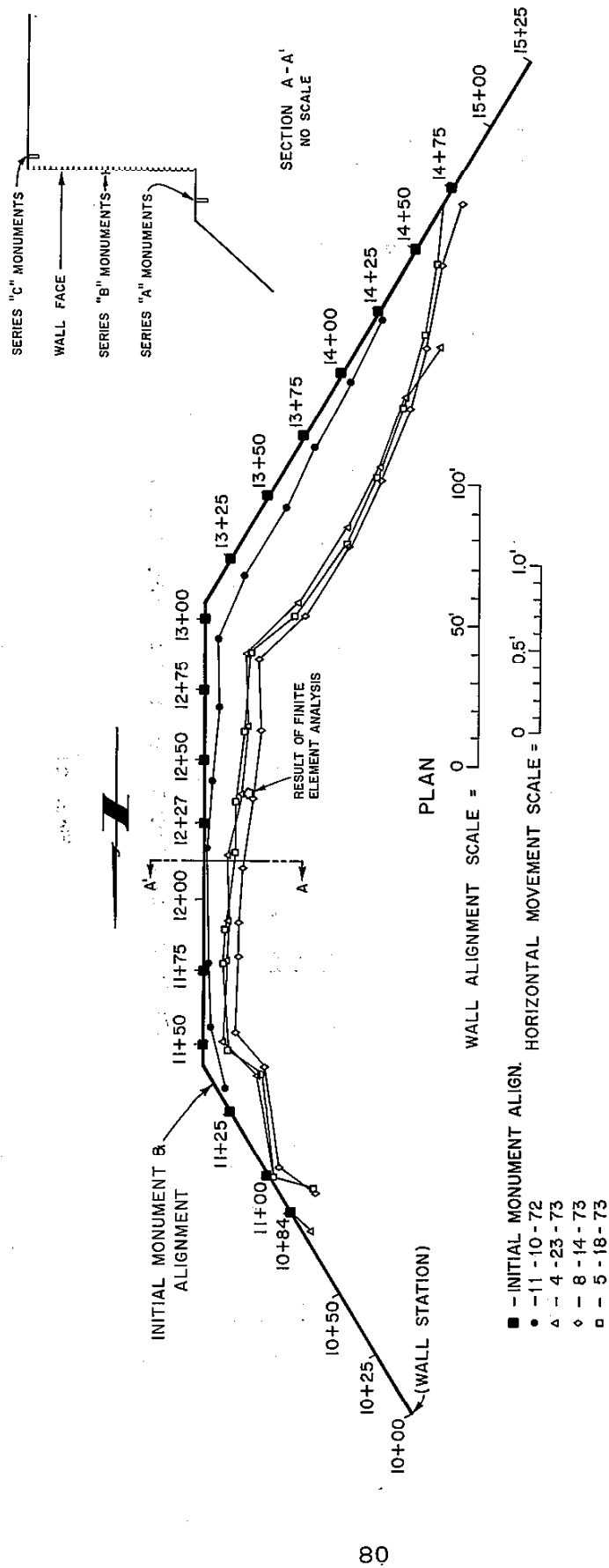


Fig. 27 SETTLEMENT OF EMBANKMENT MEASURED BY SLOPE INDICATOR, SI-3



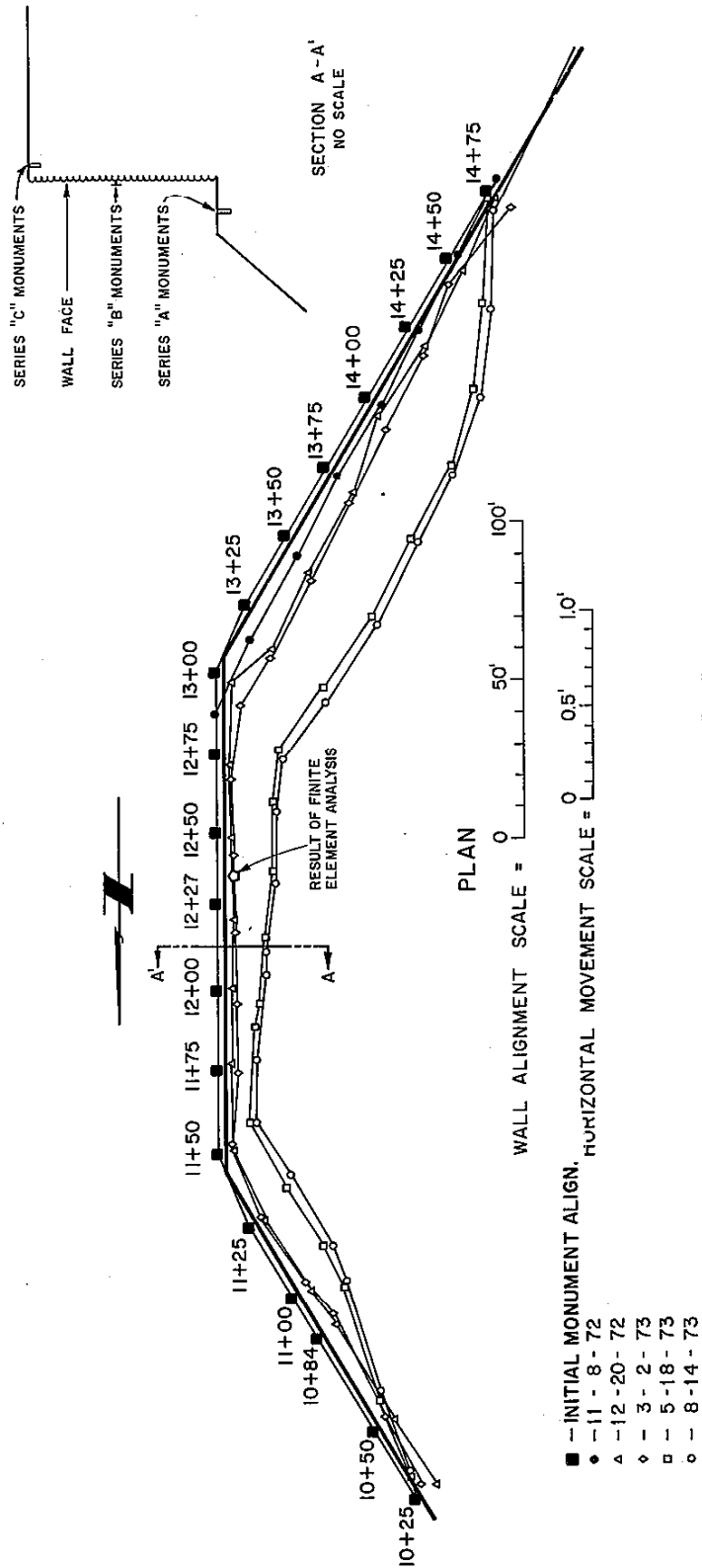
HORIZONTAL MOVEMENT - SERIES "A" MONUMENTS

Figure: 28



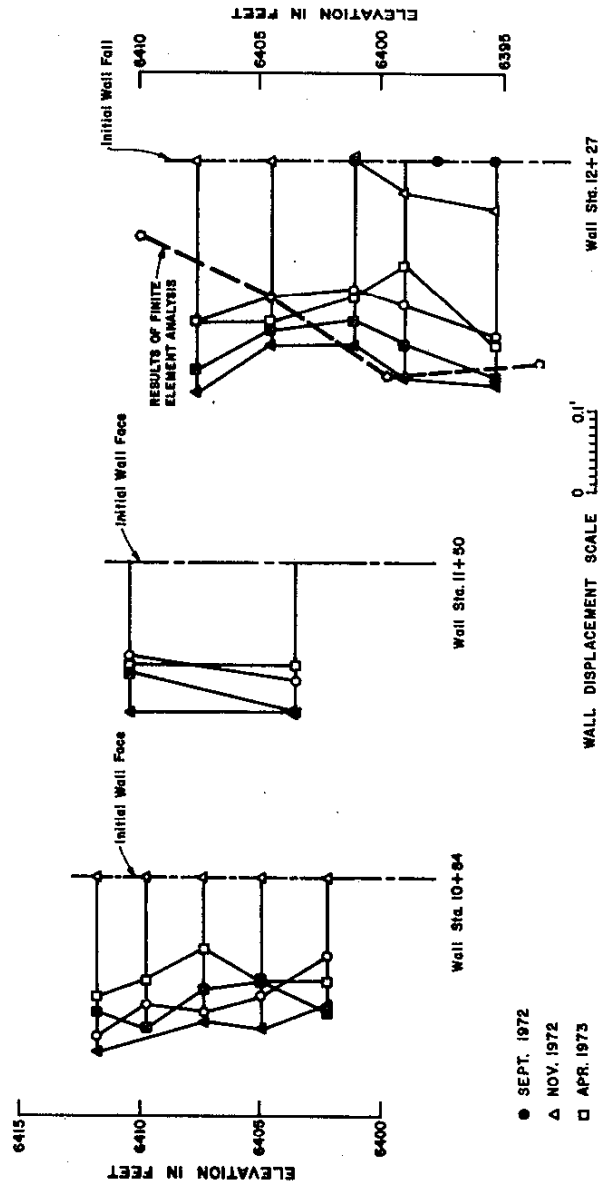
HORIZONTAL MOVEMENT - SERIES "B" MONUMENTS

Figure: 29



HORIZONTAL MOVEMENT - SERIES "C" MONUMENTS

Figure: 30

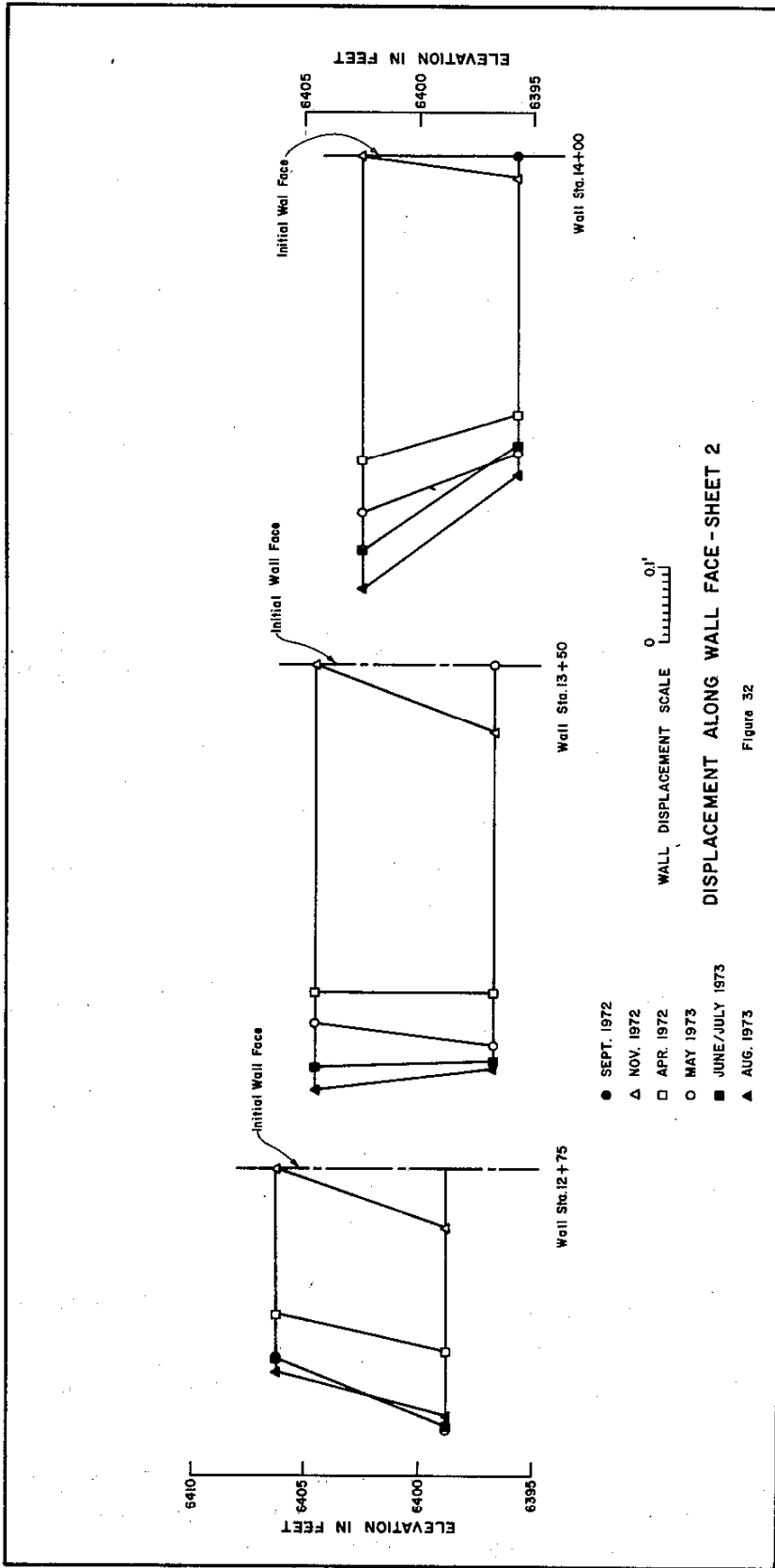


- SEPT. 1972
- ▲ NOV. 1972
- APR. 1973
- MAY 1973
- JUNE/JULY 1973
- ▲ AUG. 1973

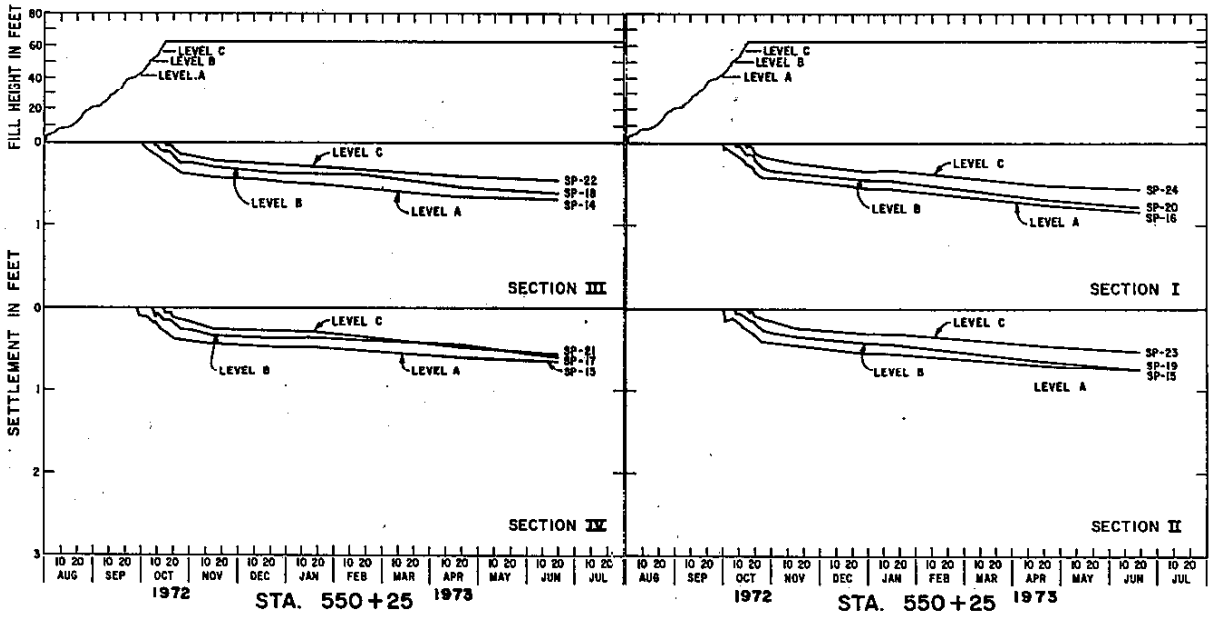
WALL DISPLACEMENT SCALE 0 0.1'

DISPLACEMENT ALONG WALL FACE - SHEET I

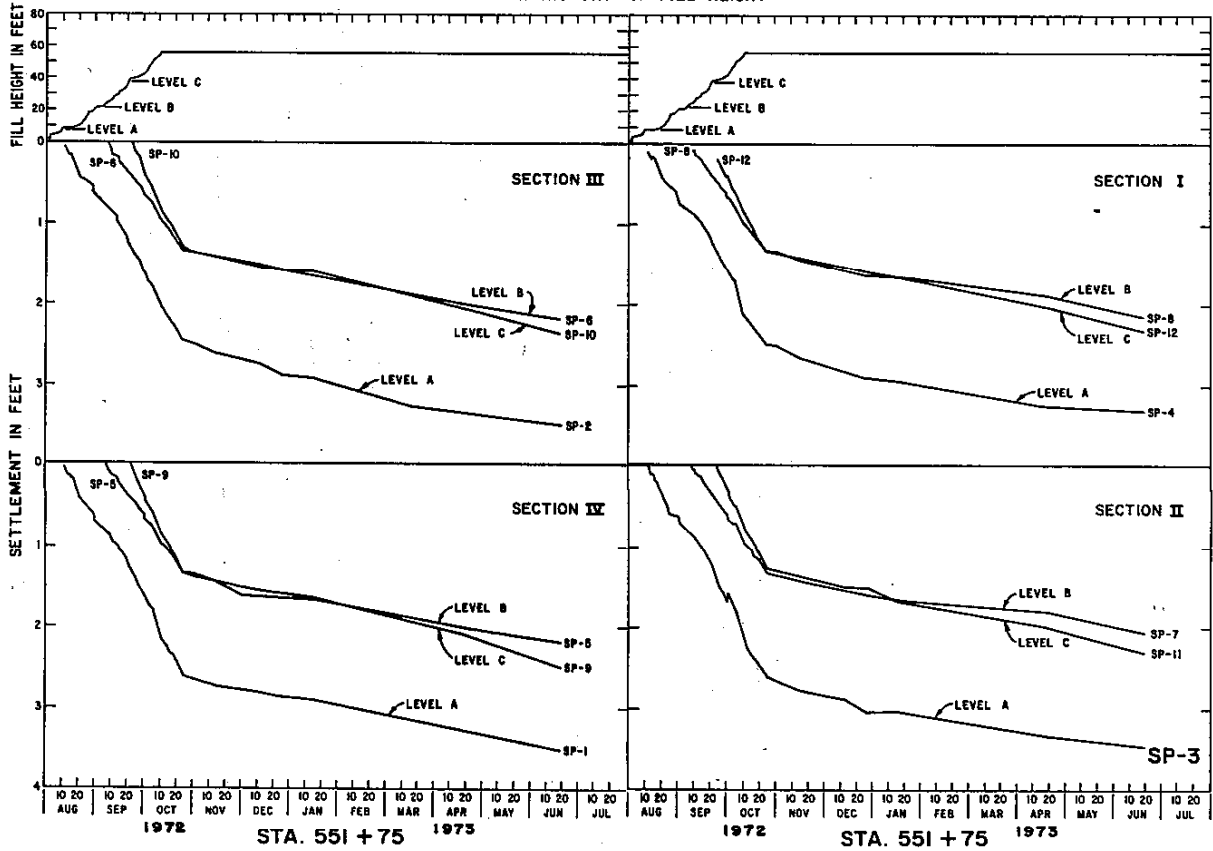
Figure 31



DAILY HISTORY OF FILL HEIGHT



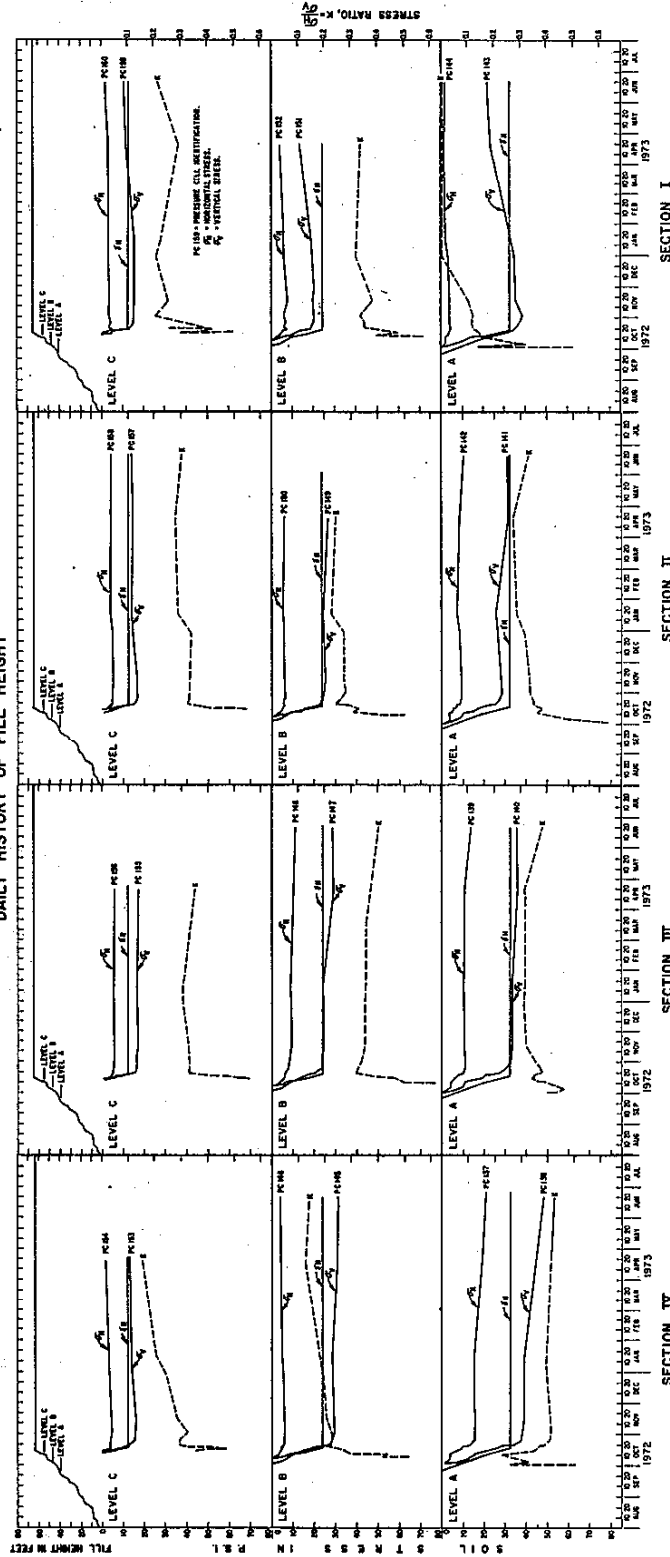
DAILY HISTORY OF FILL HEIGHT



DAILY HISTORY OF SETTLEMENT

Figure 33

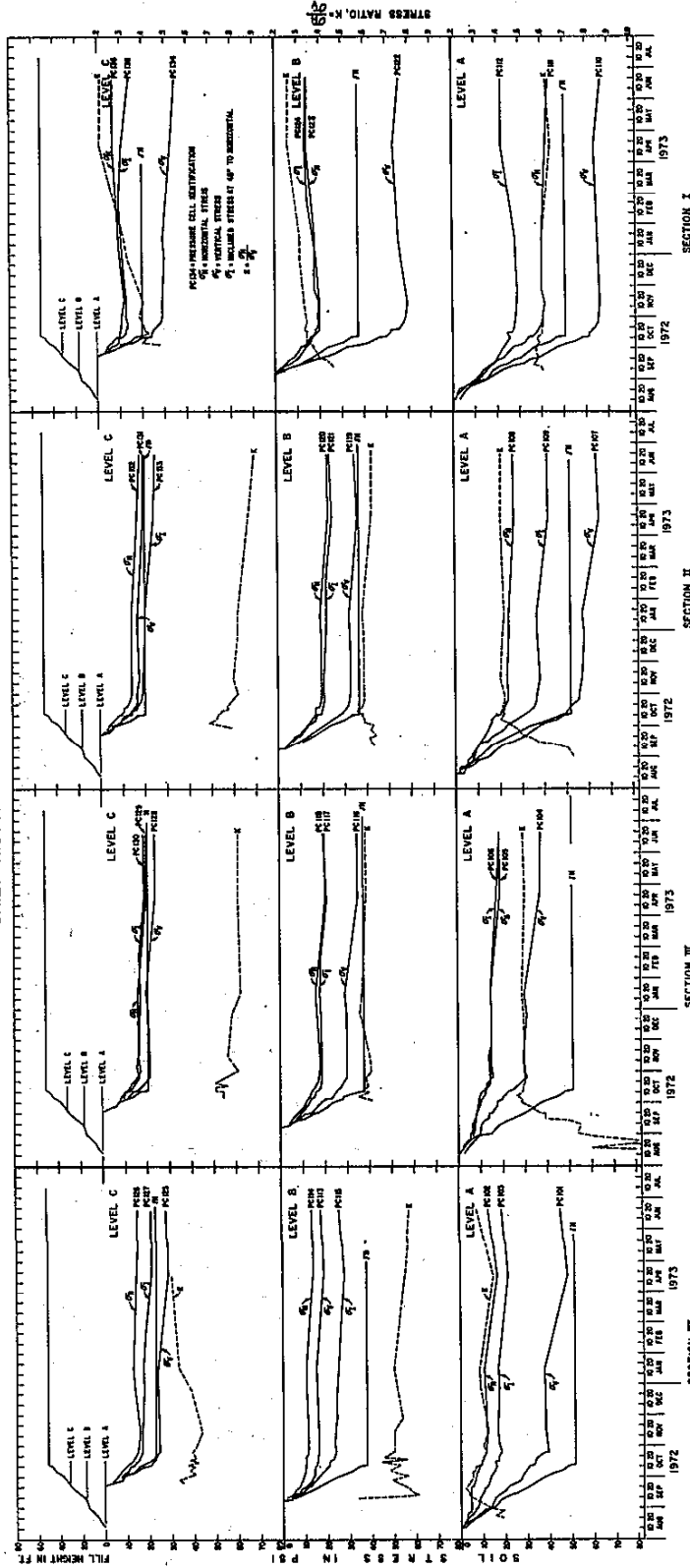
DAILY HISTORY OF FILL HEIGHT



STATION 550+25
DAILY HISTORY OF SOIL STRESS

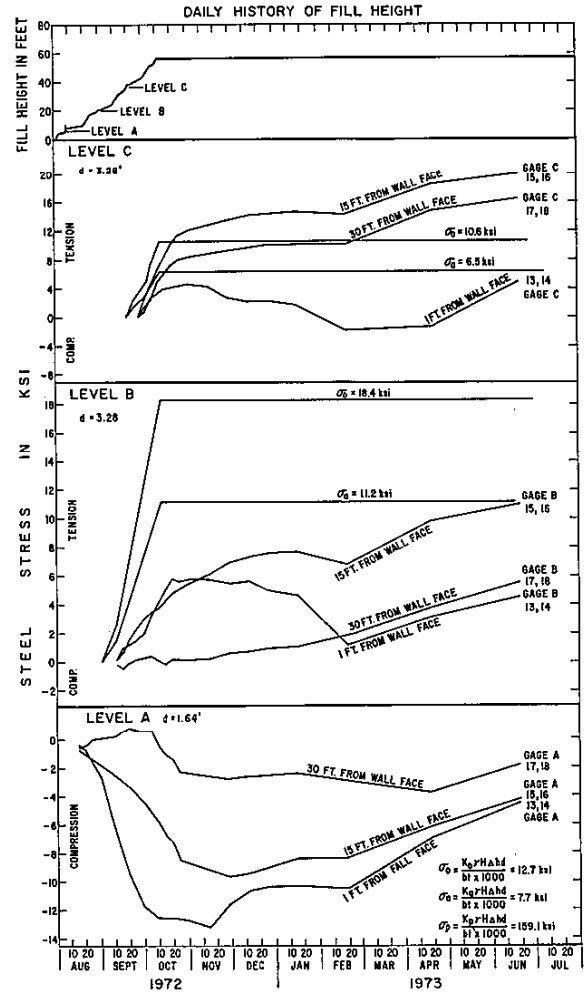
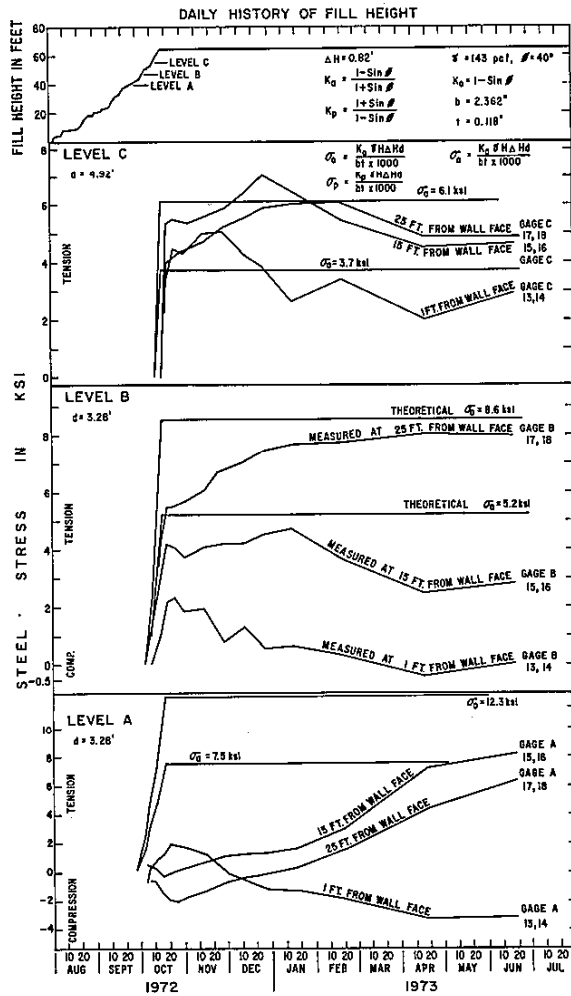
Figure 34

DAILY HISTORY OF FILL HEIGHT



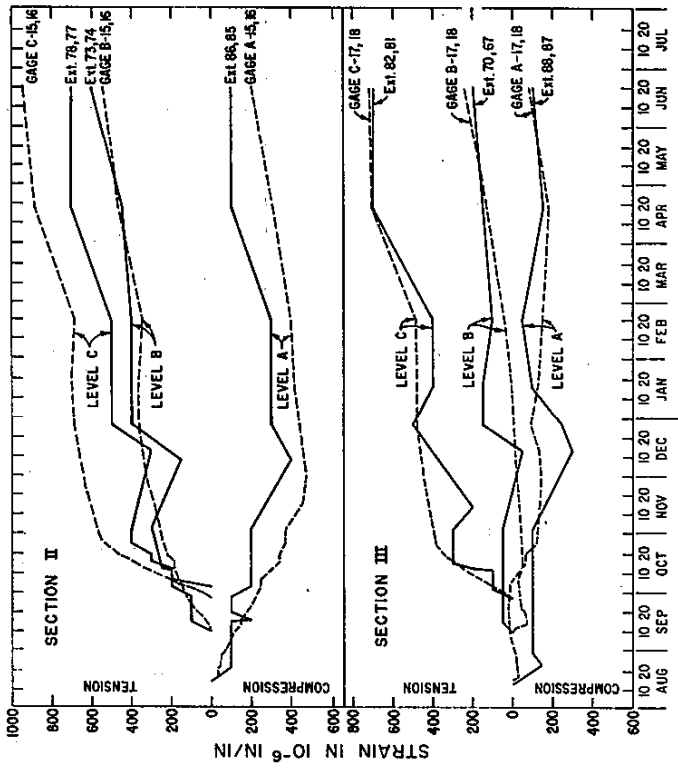
STATION 551+75
DAILY HISTORY OF SOIL STRESS

Figure 35



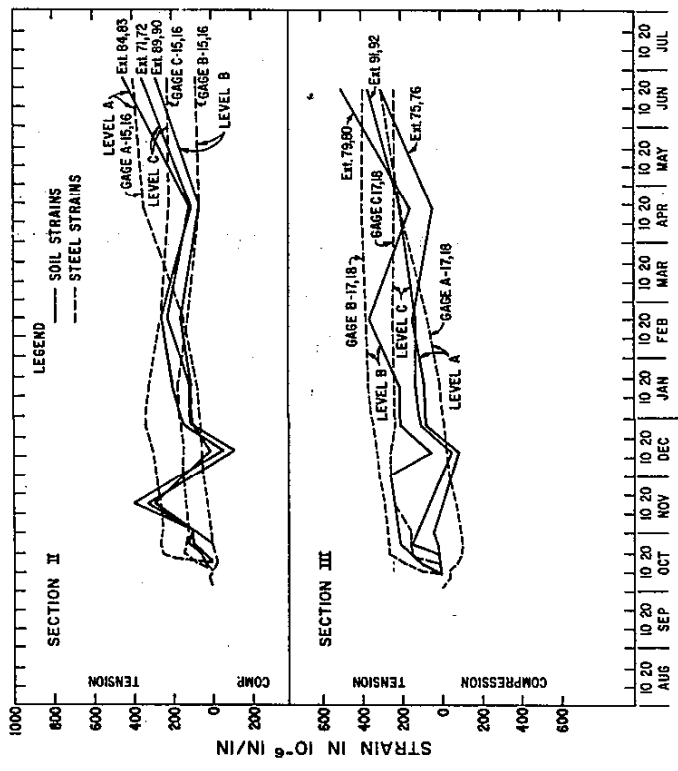
DAILY HISTORY OF STRESSES IN STEEL STRIP

Figure 36



STATION 551+75 SECTIONS II & III

DAILY HISTORY OF HORIZONTAL STRAIN IN STEEL STRIP AND SOIL
FIGURE 37



STATION 550+25 SECTIONS II & III

DAILY HISTORY OF HORIZONTAL STRAIN IN STEEL STRIP AND SOIL
FIGURE 37

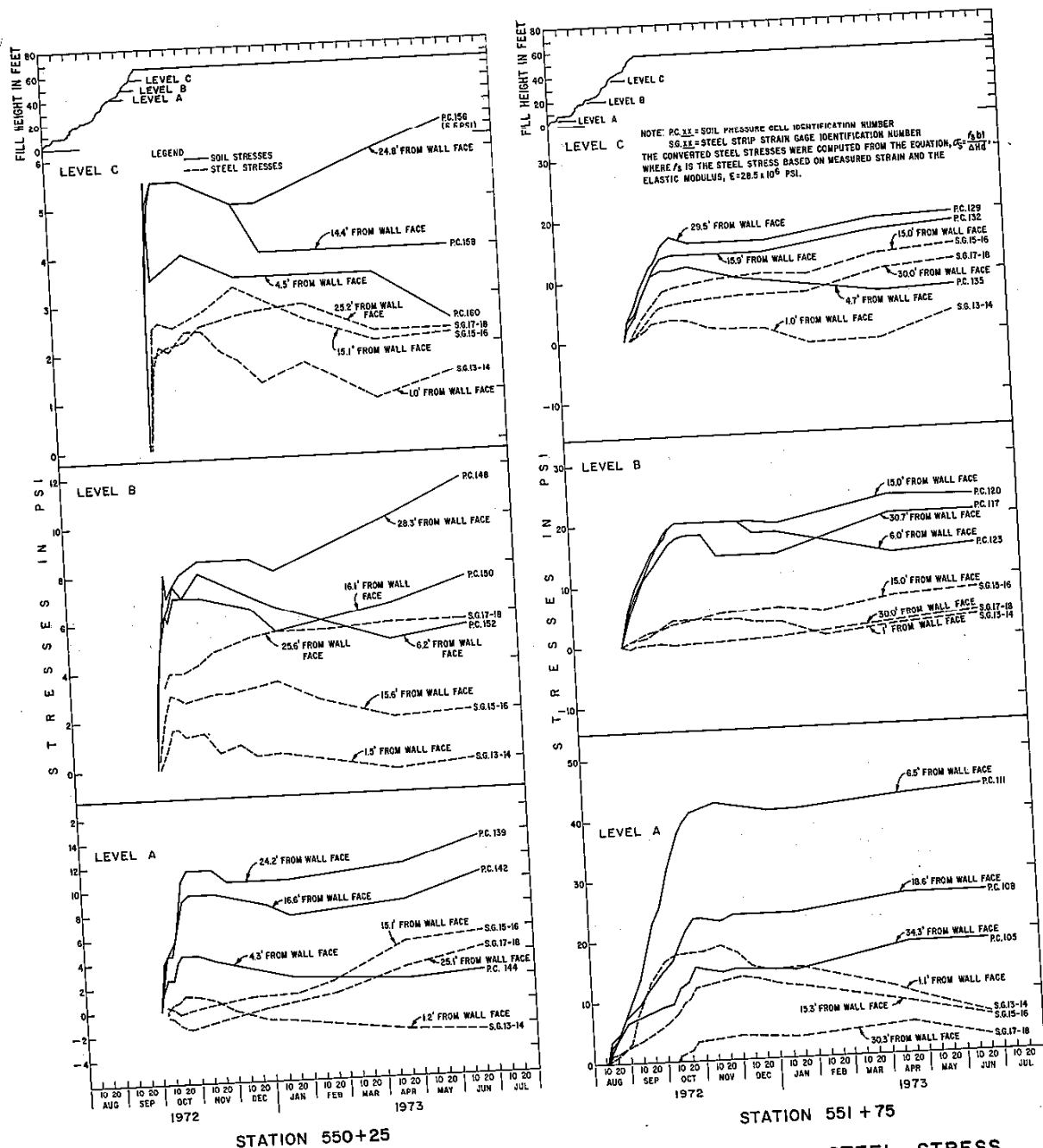
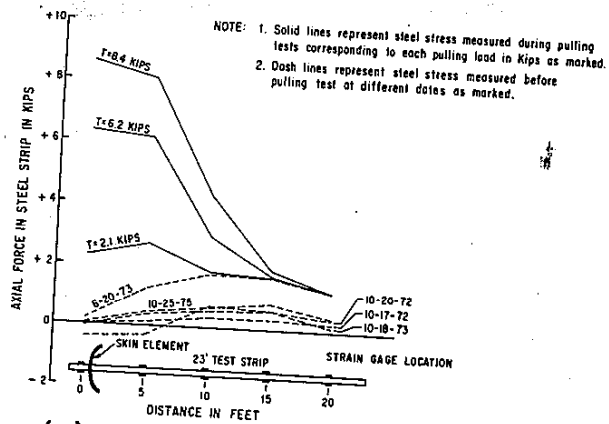
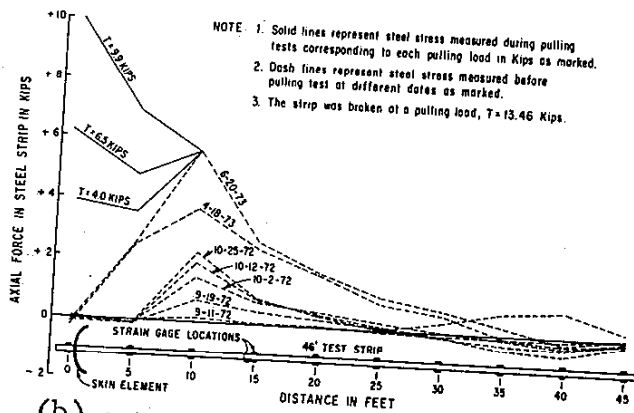


Figure 38



(a) CASE HISTORY OF AXIAL FORCE IN STEEL STRIP



(b) CASE HISTORY OF AXIAL FORCE IN STEEL STRIP

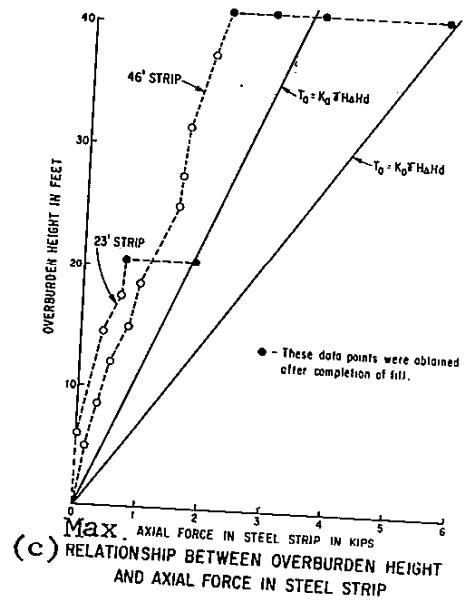
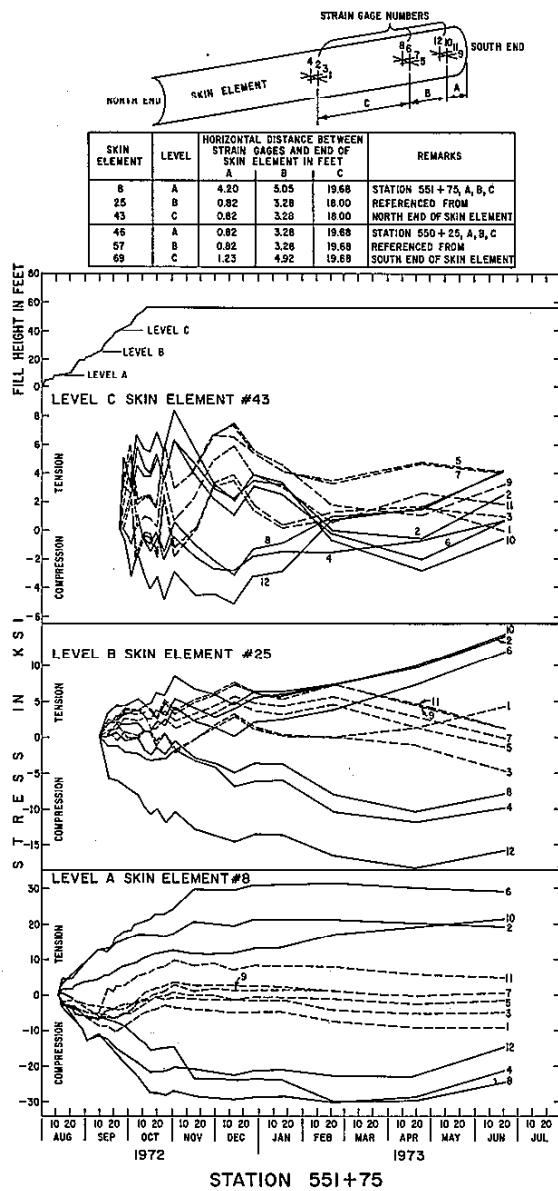
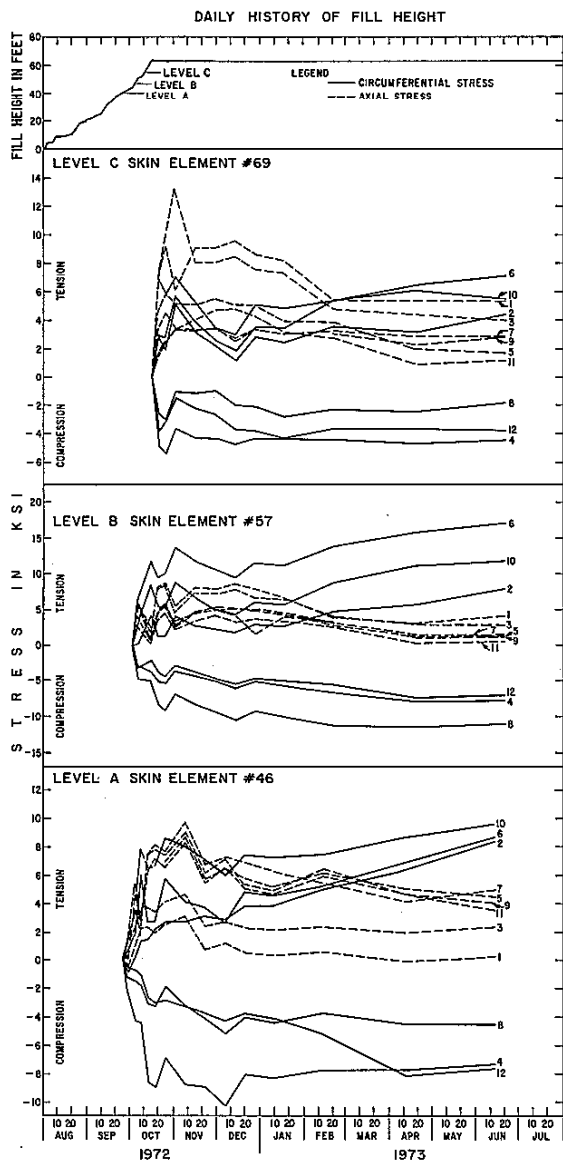


Figure 39: AXIAL FORCE IN DUMMY STRIPS

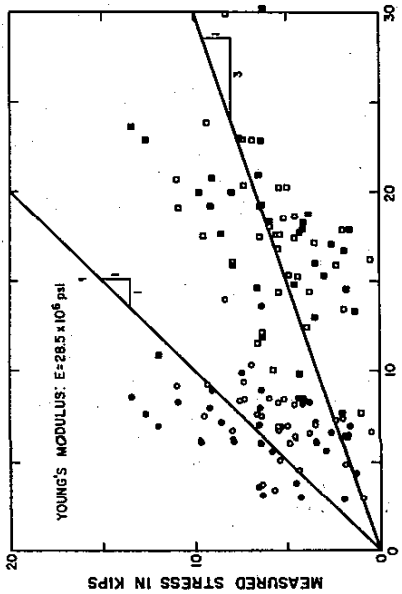


STRAIN GAGE NUMBERS

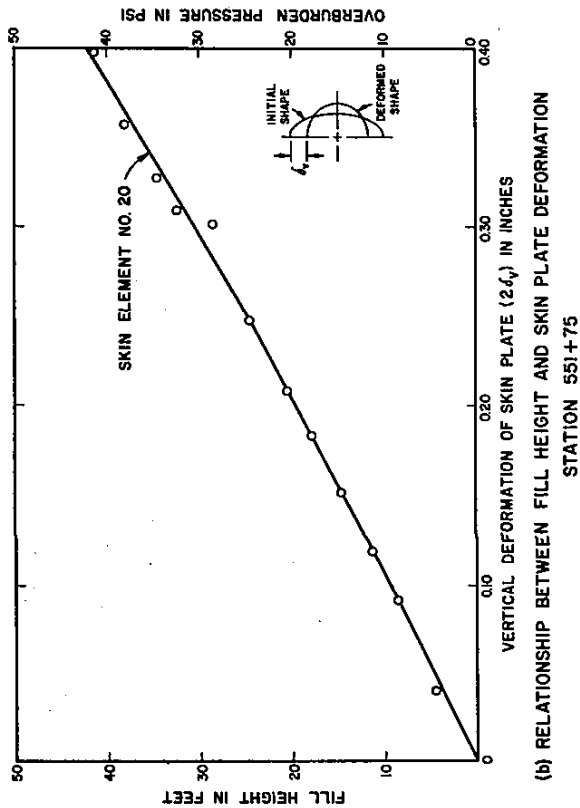
SKIN ELEMENT	LEVEL	HORIZONTAL DISTANCE BETWEEN STRAIN GAGES AND END OF SKIN ELEMENT IN FEET			REMARKS
		A	B	C	
8	A	4.20	3.05	19.68	STATION 551+75, A, B, C REFERENCED FROM NORTH END OF SKIN ELEMENT
25	B	0.82	3.28	18.00	
43	C	0.82	3.28	18.00	
46	A	0.82	3.28	19.68	STATION 550+25, A, B, C REFERENCED FROM SOUTH END OF SKIN ELEMENT
57	B	0.82	3.28	19.68	
69	C	1.23	4.92	19.68	

DAILY HISTORY OF STRESS IN SKIN ELEMENT
Figure 40

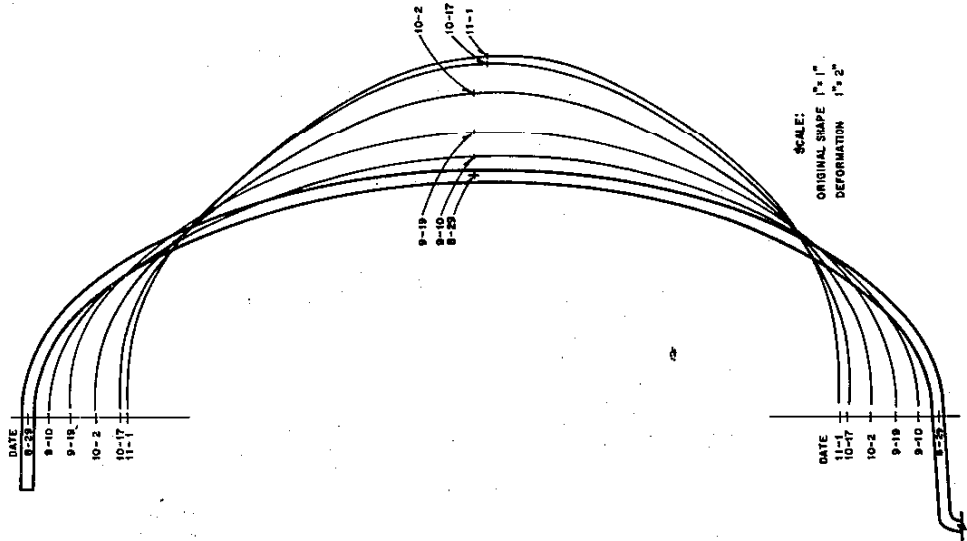
EQ 7	EQB89
HINGED END	FIXED END
OUTSIDE FACE	INSIDE FACE
○	□
○	□



(a) COMPARISON OF MEASURED AND CALCULATED CIRCUMFERENTIAL STRESS AT SPRING LINE OF SKIN PLATE

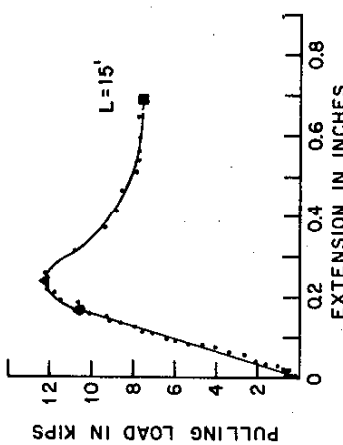
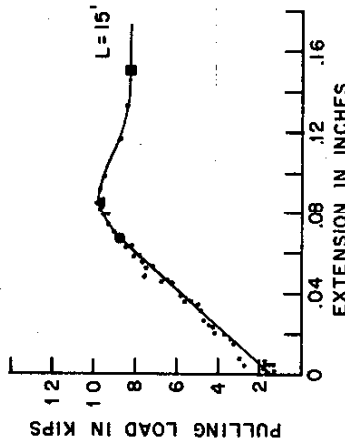
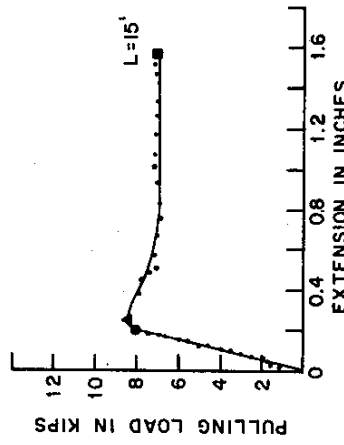
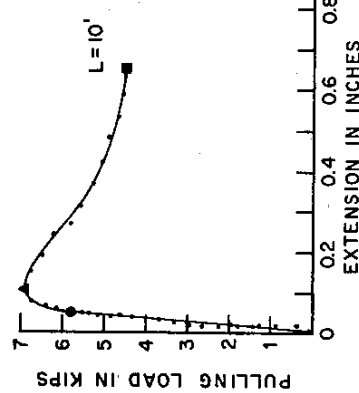
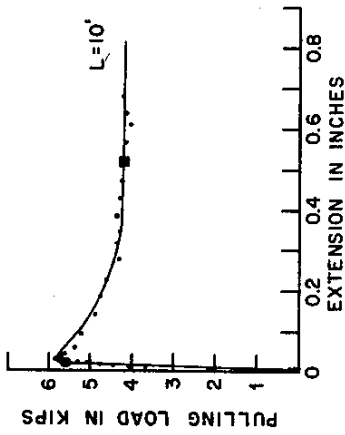
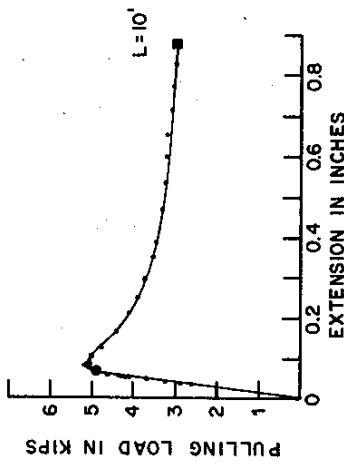
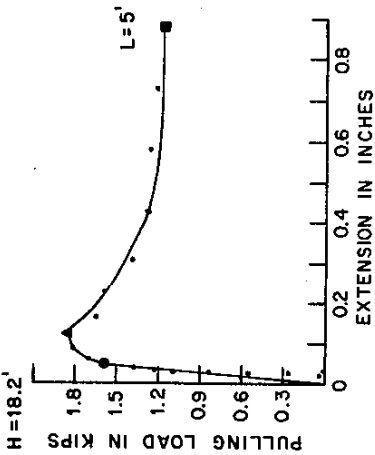
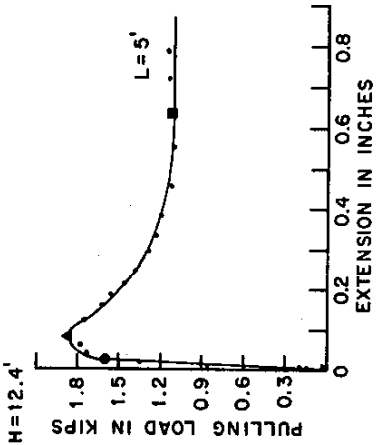
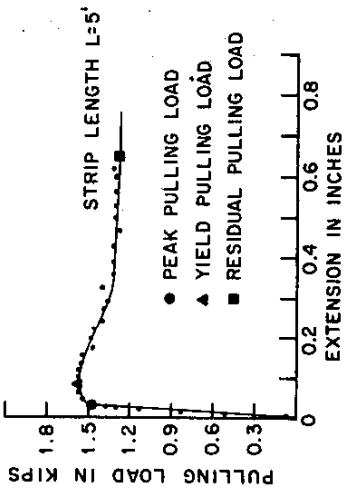


(b) RELATIONSHIP BETWEEN FILL HEIGHT AND SKIN PLATE DEFORMATION
STATION 551+75

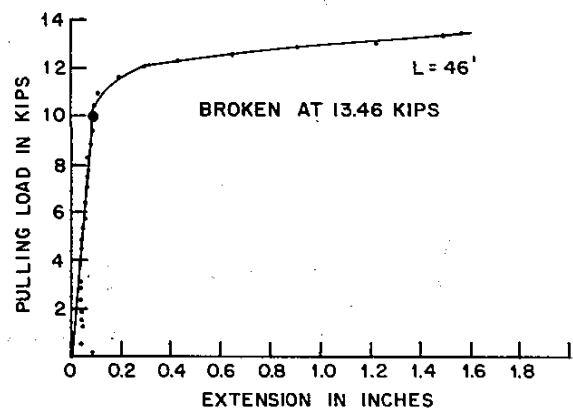
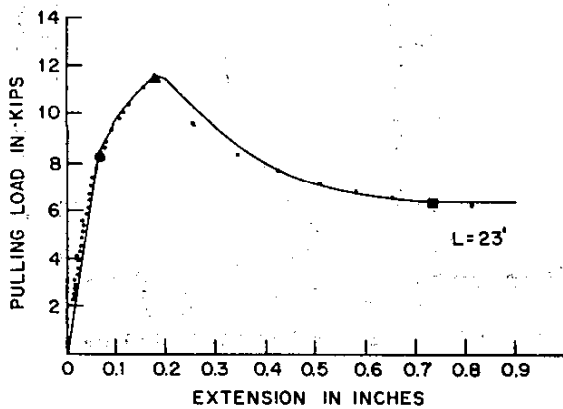
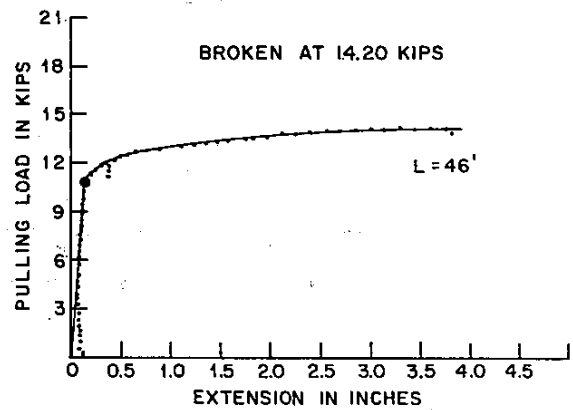
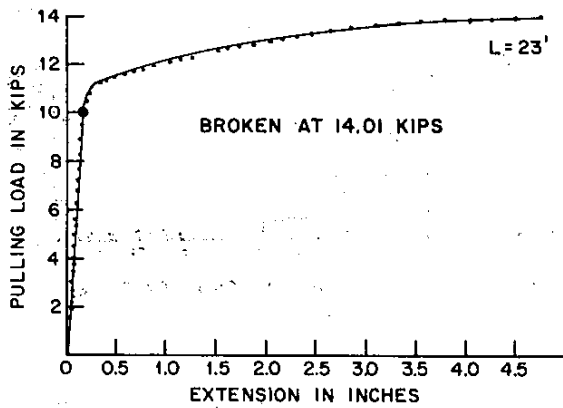
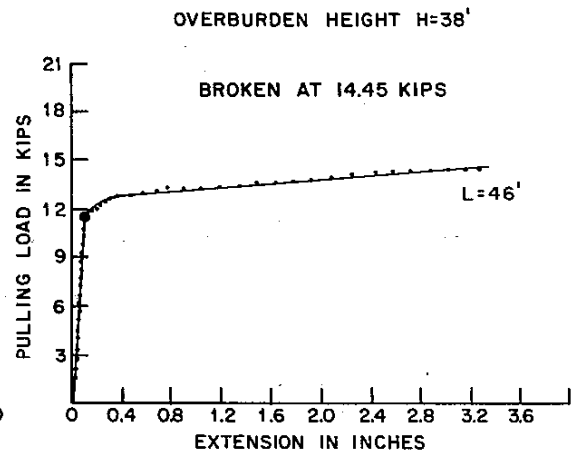
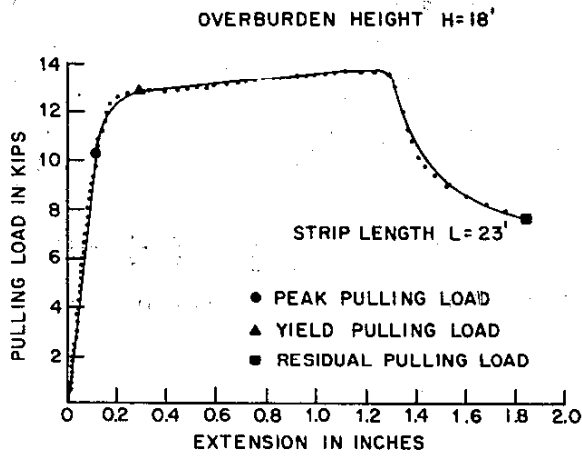


STATION 551+75, LEVEL A, SKIN ELEMENT NO. 20
(c) CASE HISTORY OF DEFORMATION OF SKIN PLATE

OVERBURDEN
HEIGHT H=7.5'

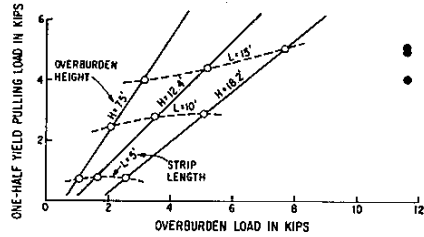


LOAD DEFORMATION CURVE FROM FIELD PULLING TESTS--SHEET I
Figure 42

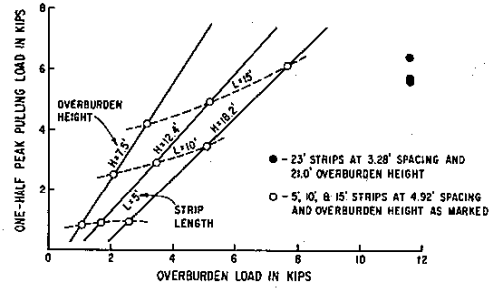


LOAD DEFORMATION CURVE FROM FIELD PULLING TESTS-SHEET 2

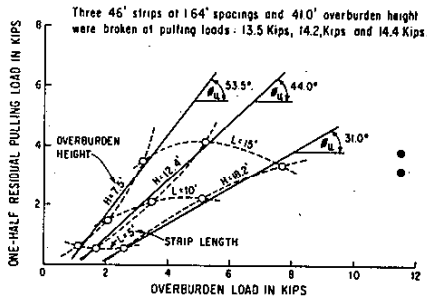
Figure 43



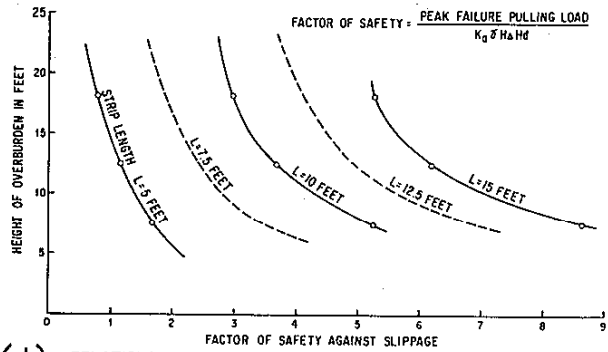
(a.) RELATIONSHIP BETWEEN YIELD PULLING LOAD, OVERBURDEN LOAD, OVERBURDEN HEIGHT AND STRIP LENGTH



(b.) RELATIONSHIP BETWEEN PEAK PULLING LOAD, OVERBURDEN LOAD, OVERBURDEN HEIGHT, AND STRIP LENGTH



(c.) RELATIONSHIP BETWEEN RESIDUAL PULLING LOAD, OVERBURDEN LOAD, OVERBURDEN HEIGHT AND STRIP LENGTH



(d.) RELATIONSHIP BETWEEN OVERBURDEN HEIGHT, STRIP LENGTH, AND SLIPPING FACTOR OF SAFETY

FIELD PULLING TEST RESULTS

Figure 44

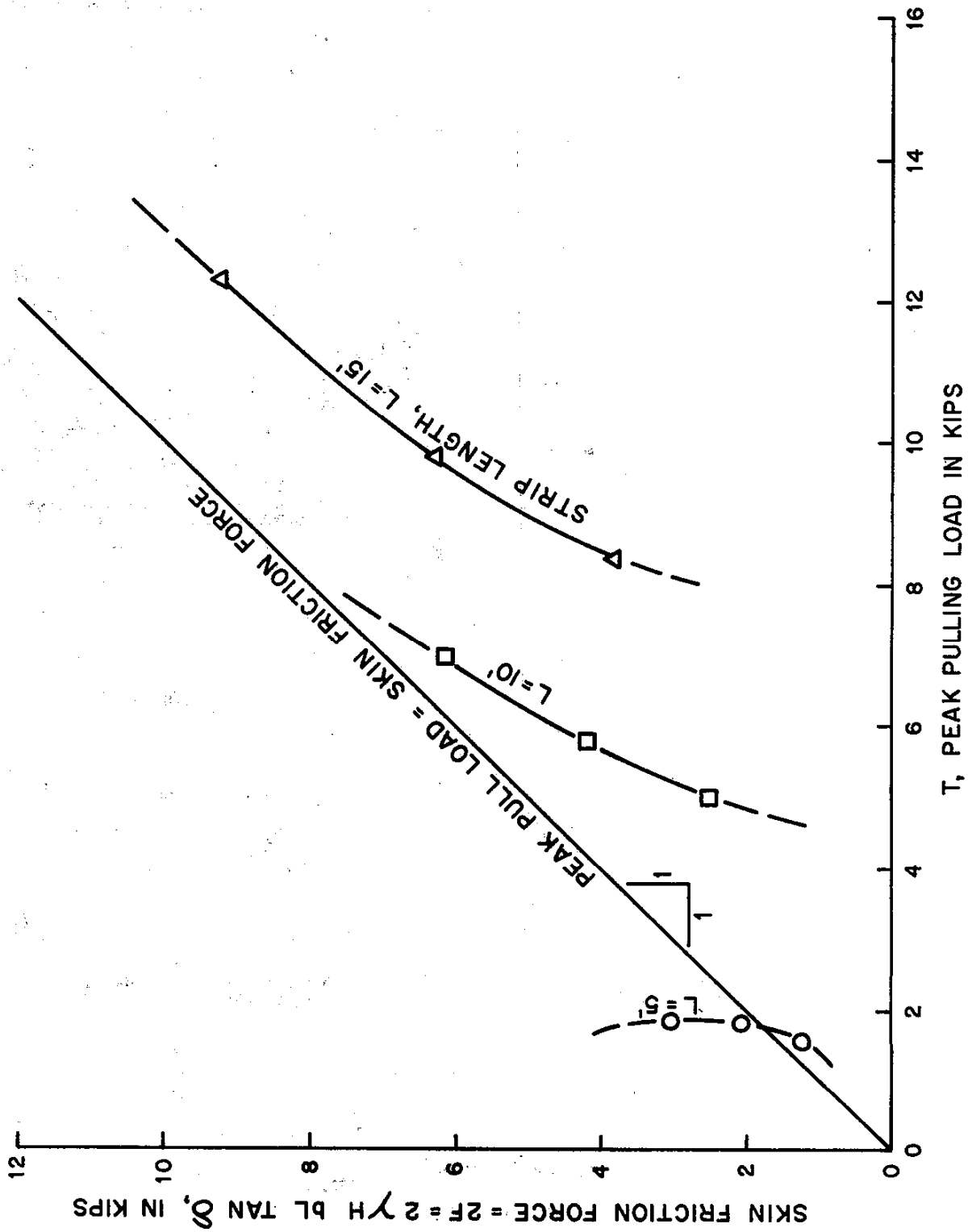


Figure 45: RELATIONSHIP BETWEEN PULL LOAD AND SKIN FRICTION FORCE

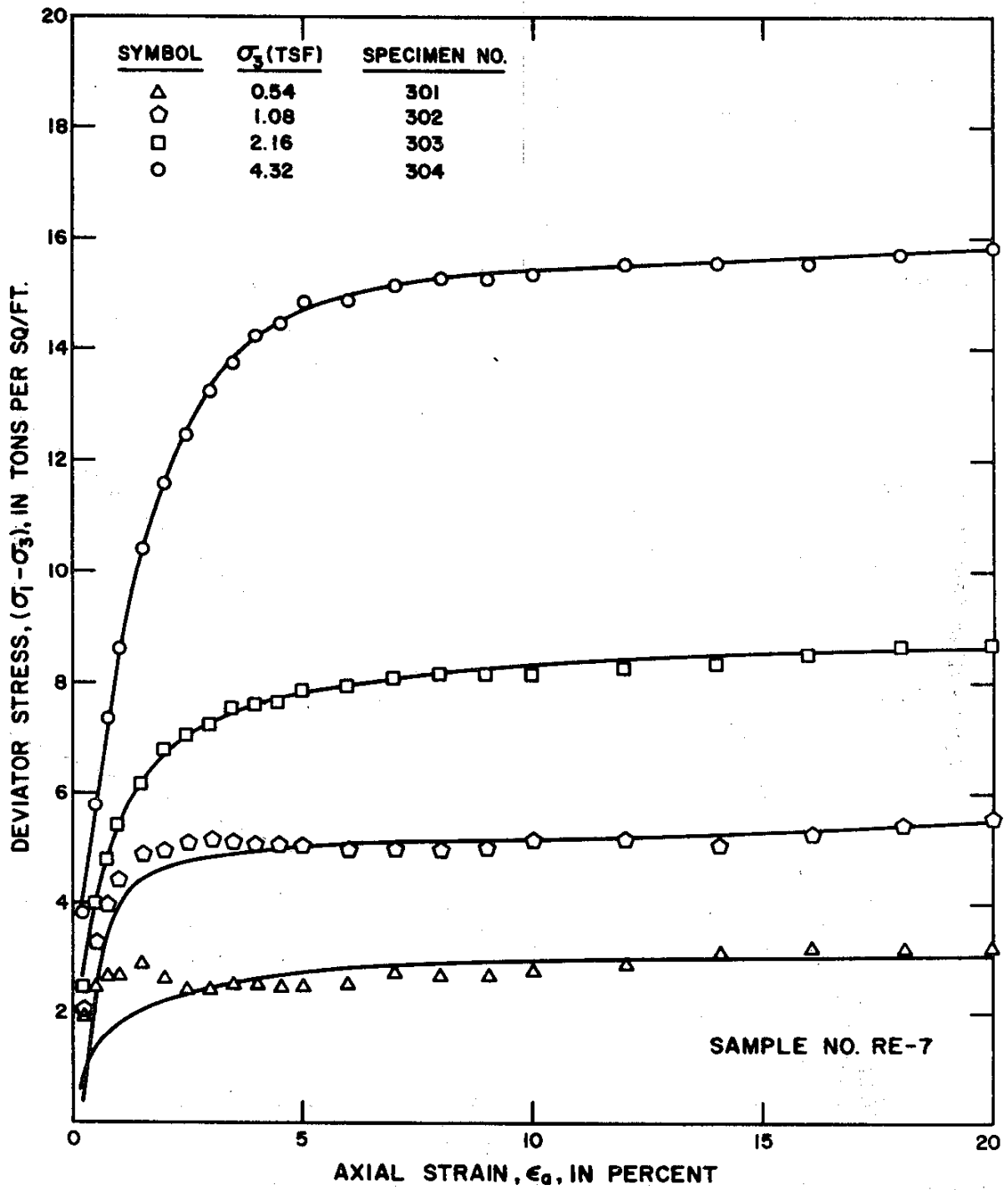


Figure 46: TYPICAL STRESS - STRAIN CURVE OF SOIL SAMPLE

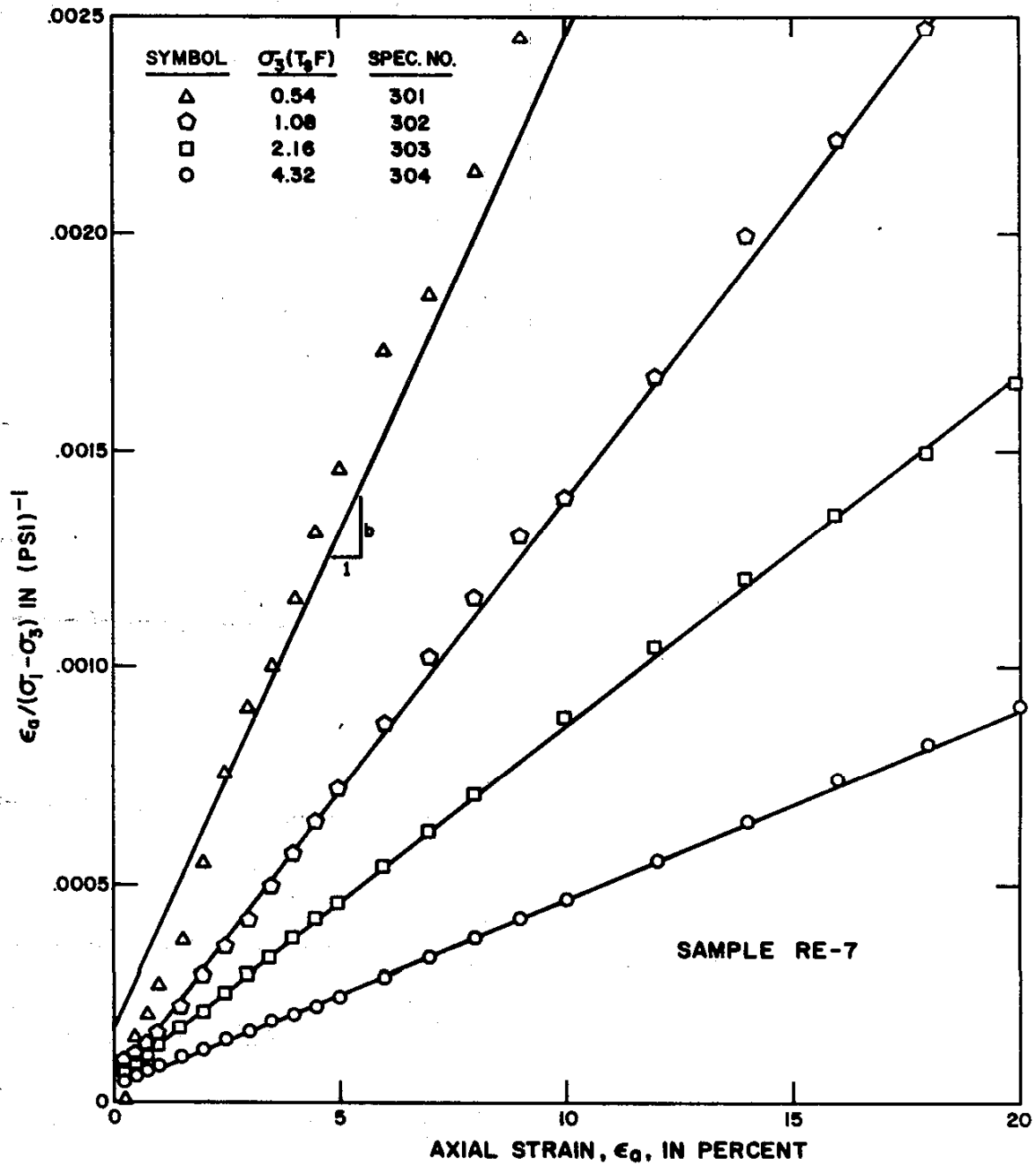


Figure 47: TYPICAL TRANSFORMED HYPERBOLIC STRESS-STRAIN CURVES

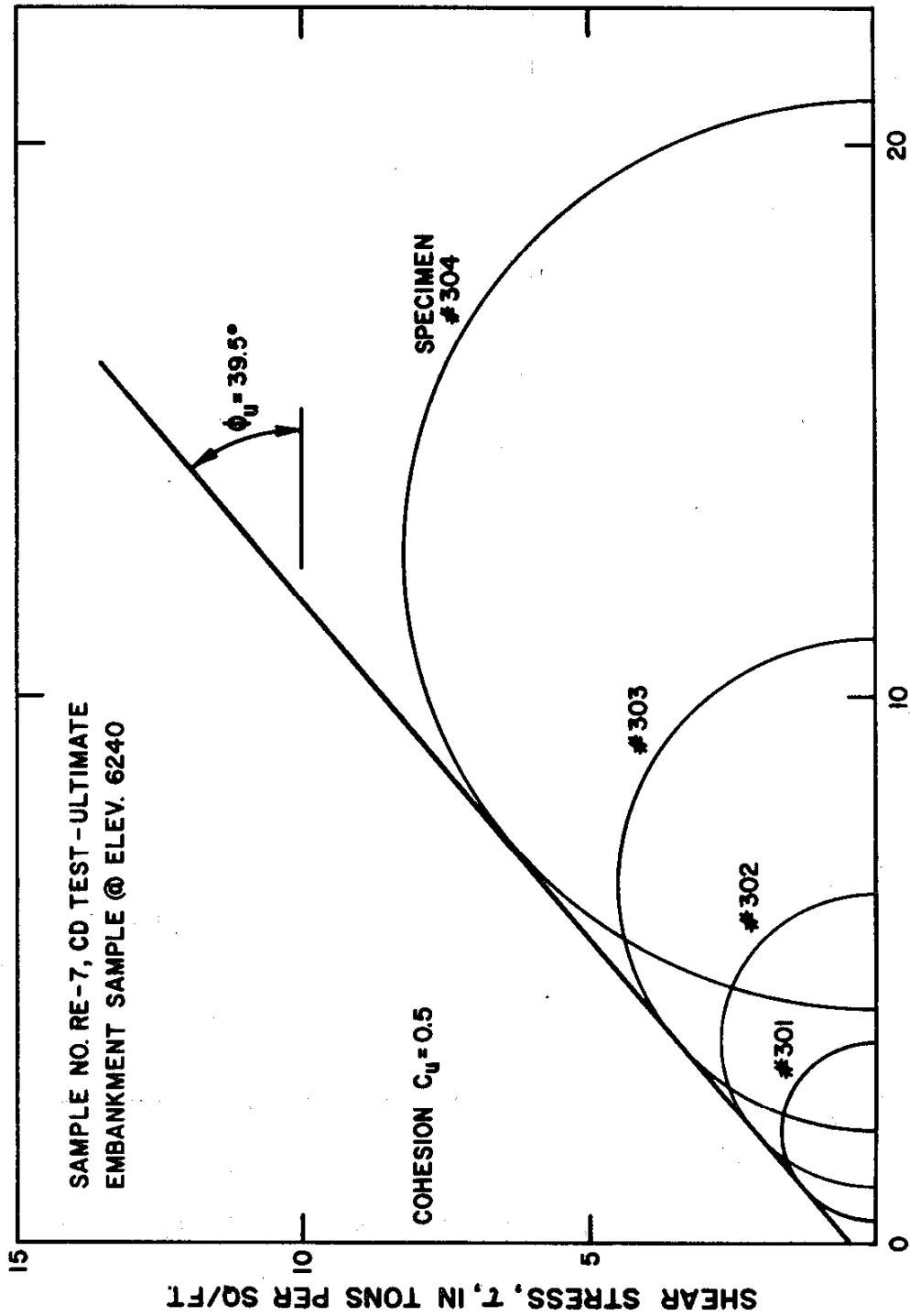


Figure 48: TYPICAL MOHR CIRCLES

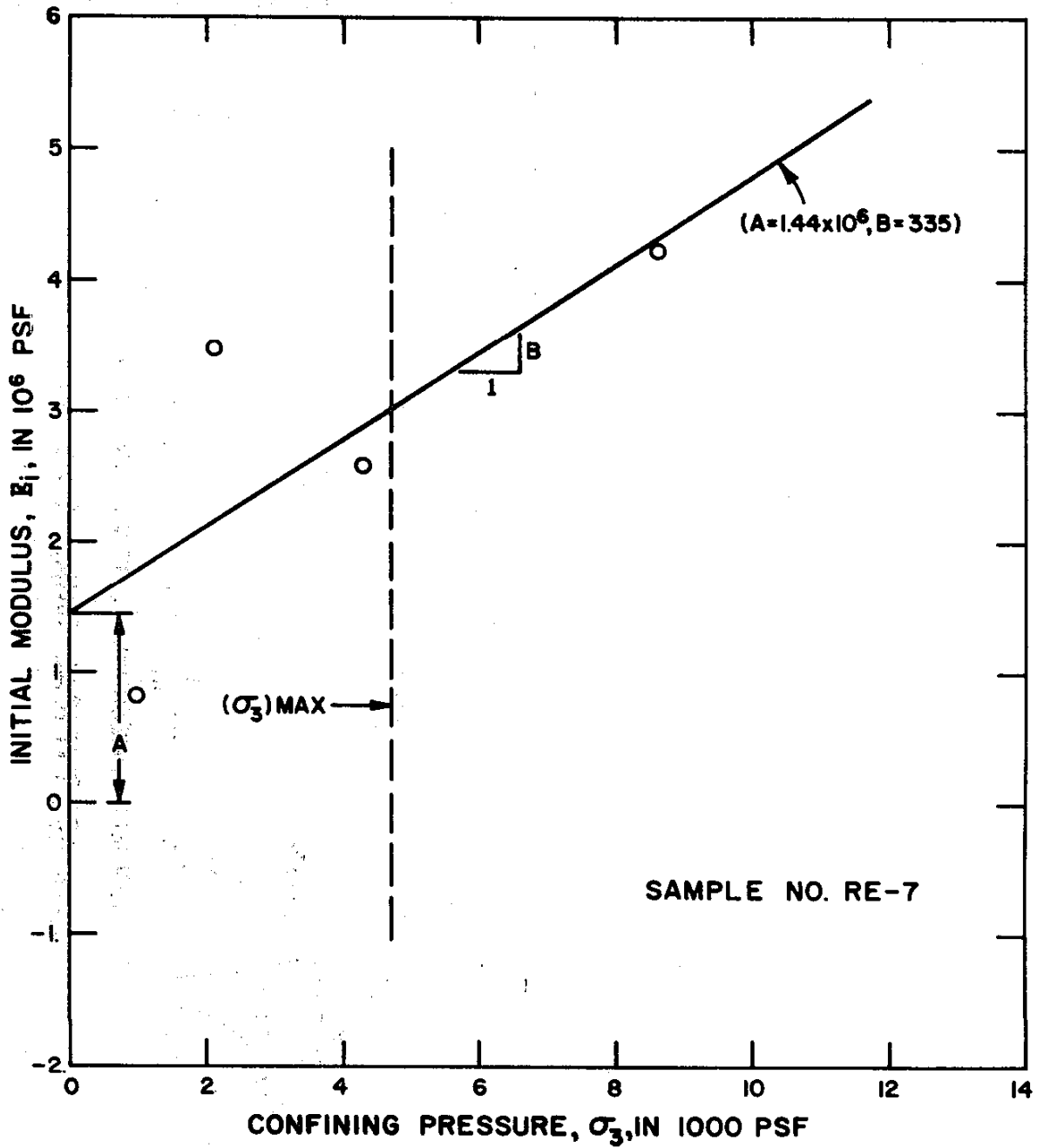


Figure 49: VARIATION OF INITIAL TANGENT MODULUS WITH CONFINING PRESSURE

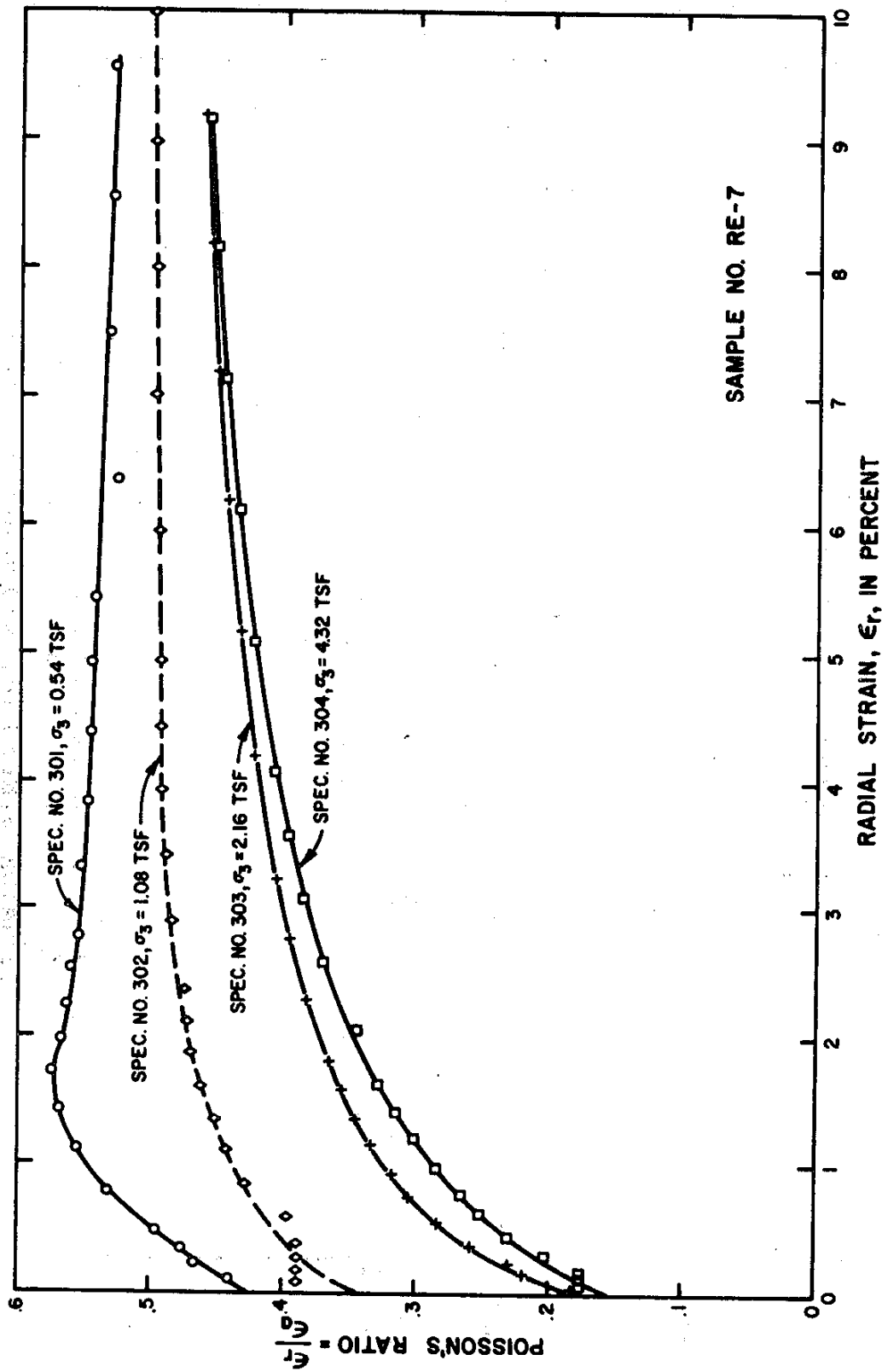


Figure 50: POISSON'S RATIO VS RADIAL STRAIN CURVES

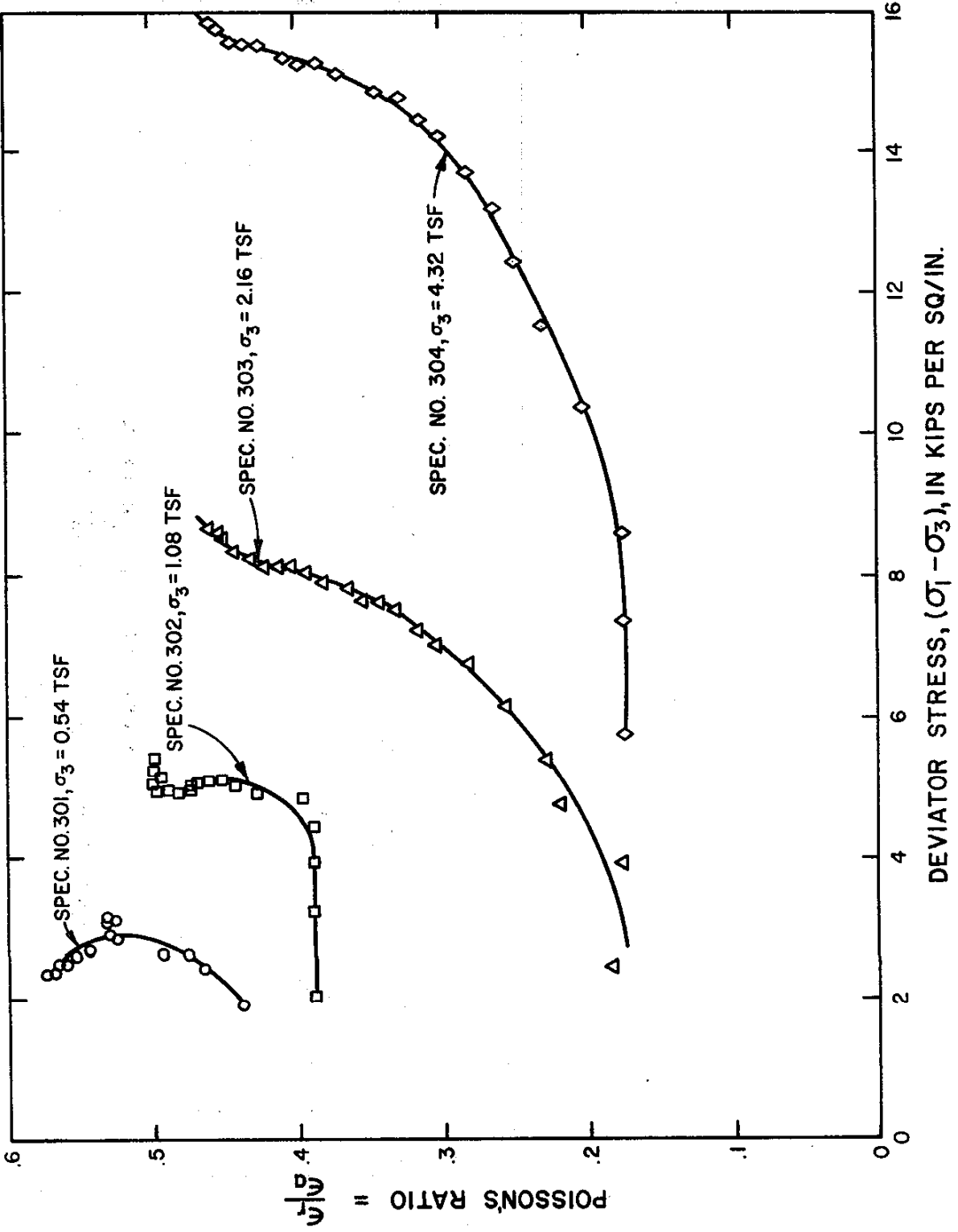


Figure 51: POISSON'S RATIO VS DEVIATOR STRESS

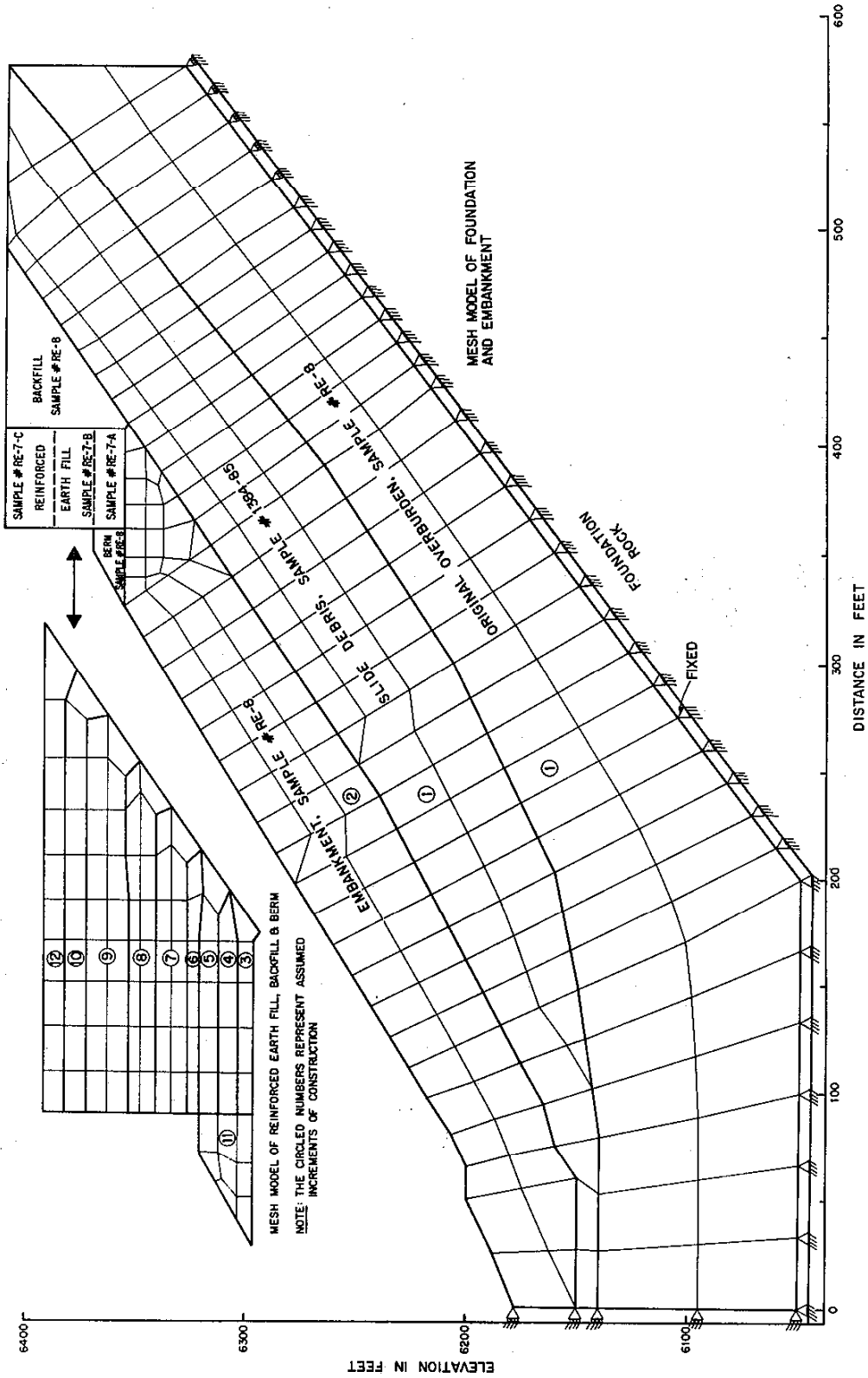
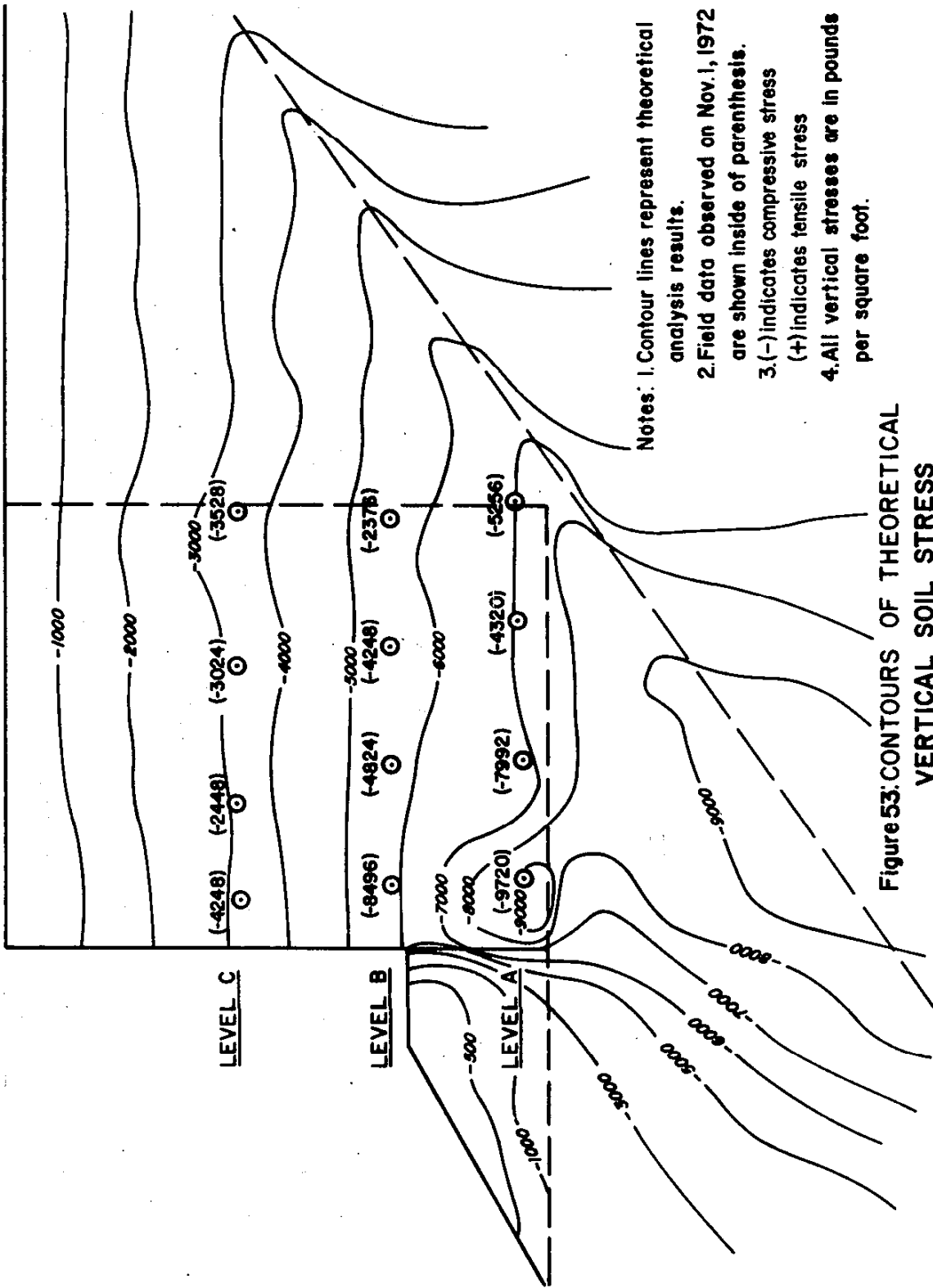


FIGURE 52: TYPICAL SECTION FOR FINITE ELEMENT ANALYSIS, STATION 551+75



- Notes:
1. Contour lines represent theoretical analysis results.
 2. Field data observed on Nov. 1, 1972 are shown inside of parenthesis.
 3. (-) indicates compressive stress (+) indicates tensile stress
 4. All vertical stresses are in pounds per square foot.

Figure 53: CONTOURS OF THEORETICAL VERTICAL SOIL STRESS

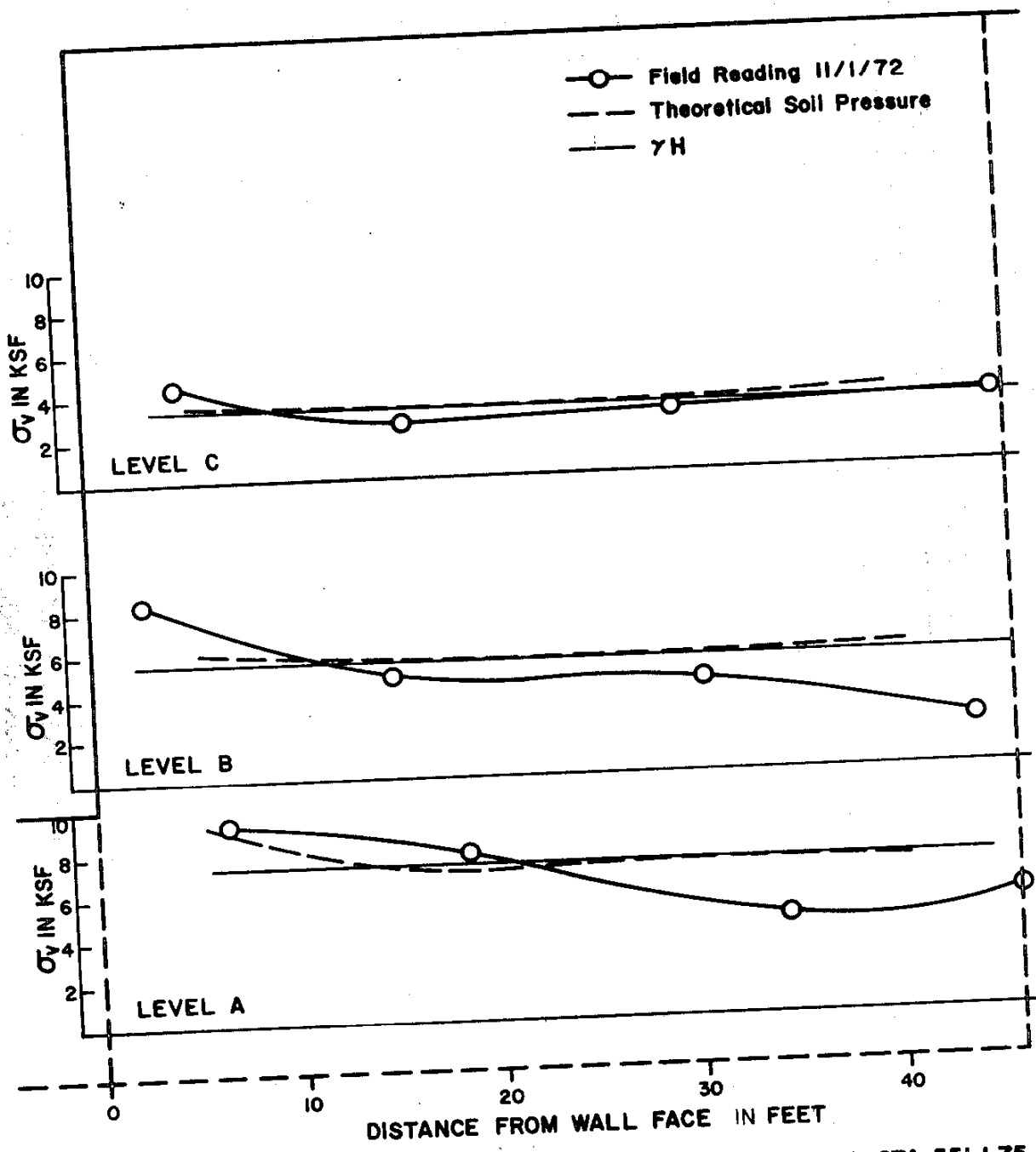
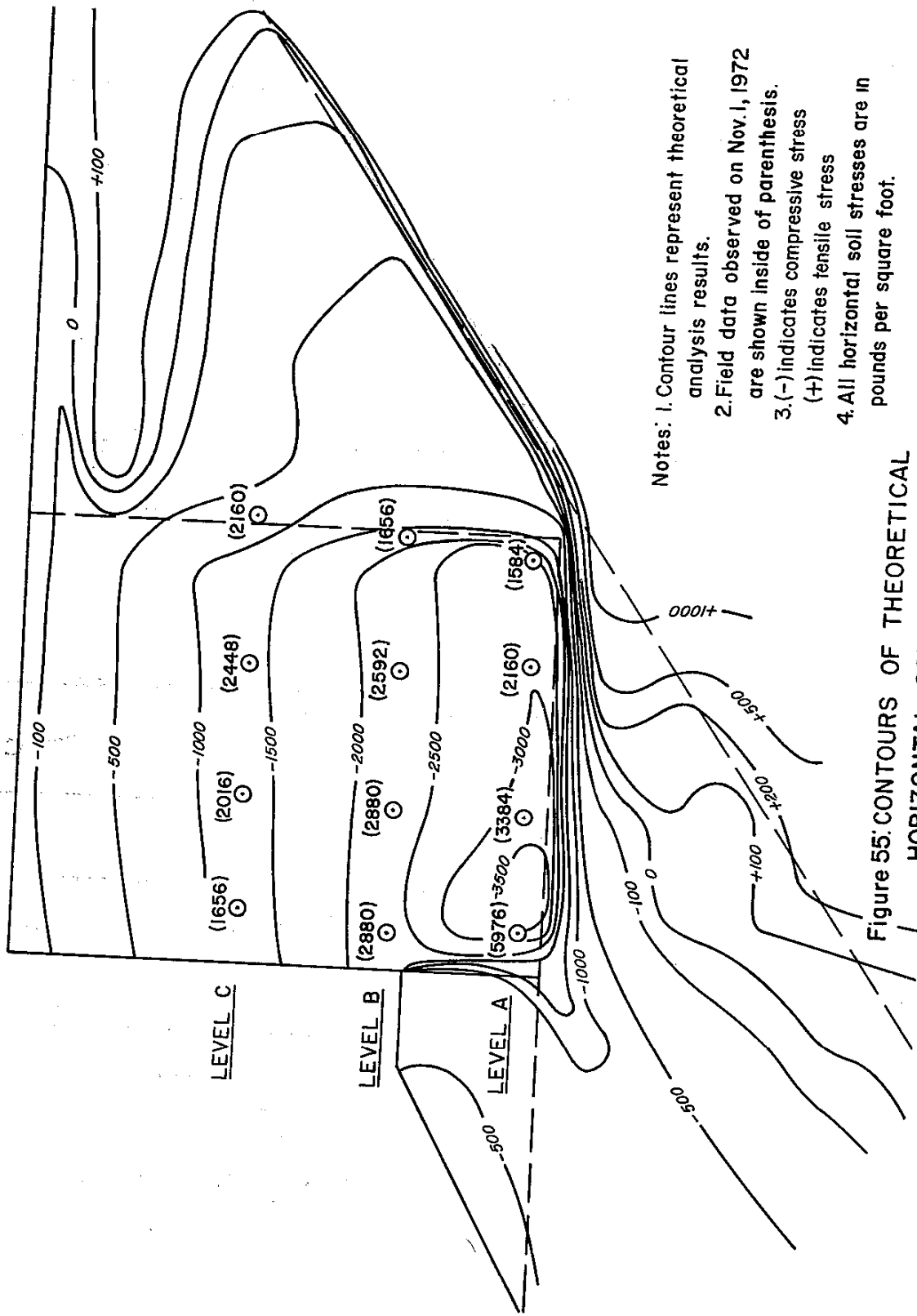


Figure 54: COMPRESSIVE VERTICAL SOIL STRESS DISTRIBUTION, STA. 551+75



- Notes:
1. Contour lines represent theoretical analysis results.
 2. Field data observed on Nov. 1, 1972 are shown inside of parenthesis.
 3. (-) indicates compressive stress (+) indicates tensile stress
 4. All horizontal soil stresses are in pounds per square foot.

Figure 55: CONTOURS OF THEORETICAL HORIZONTAL SOIL STRESS

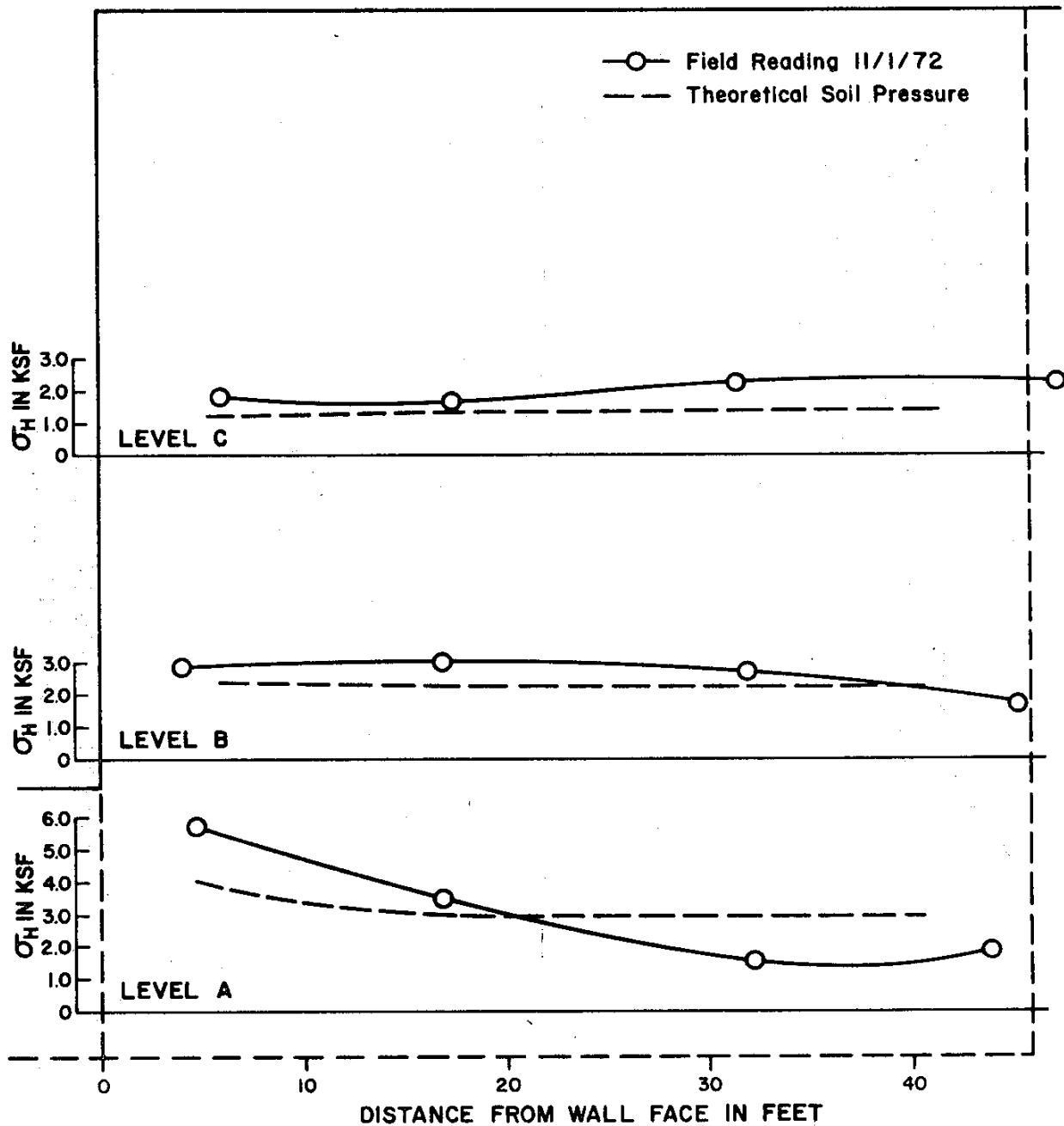
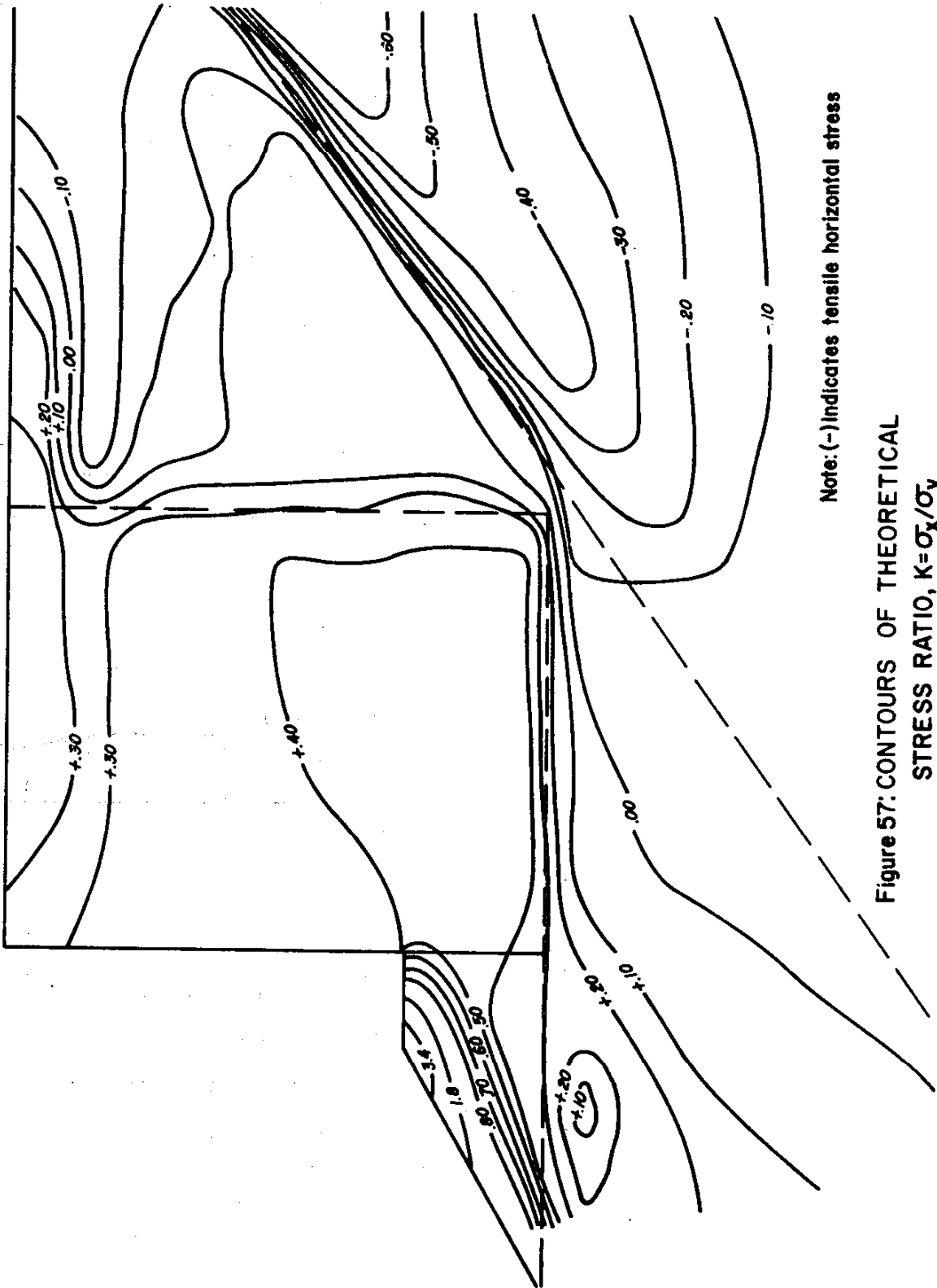
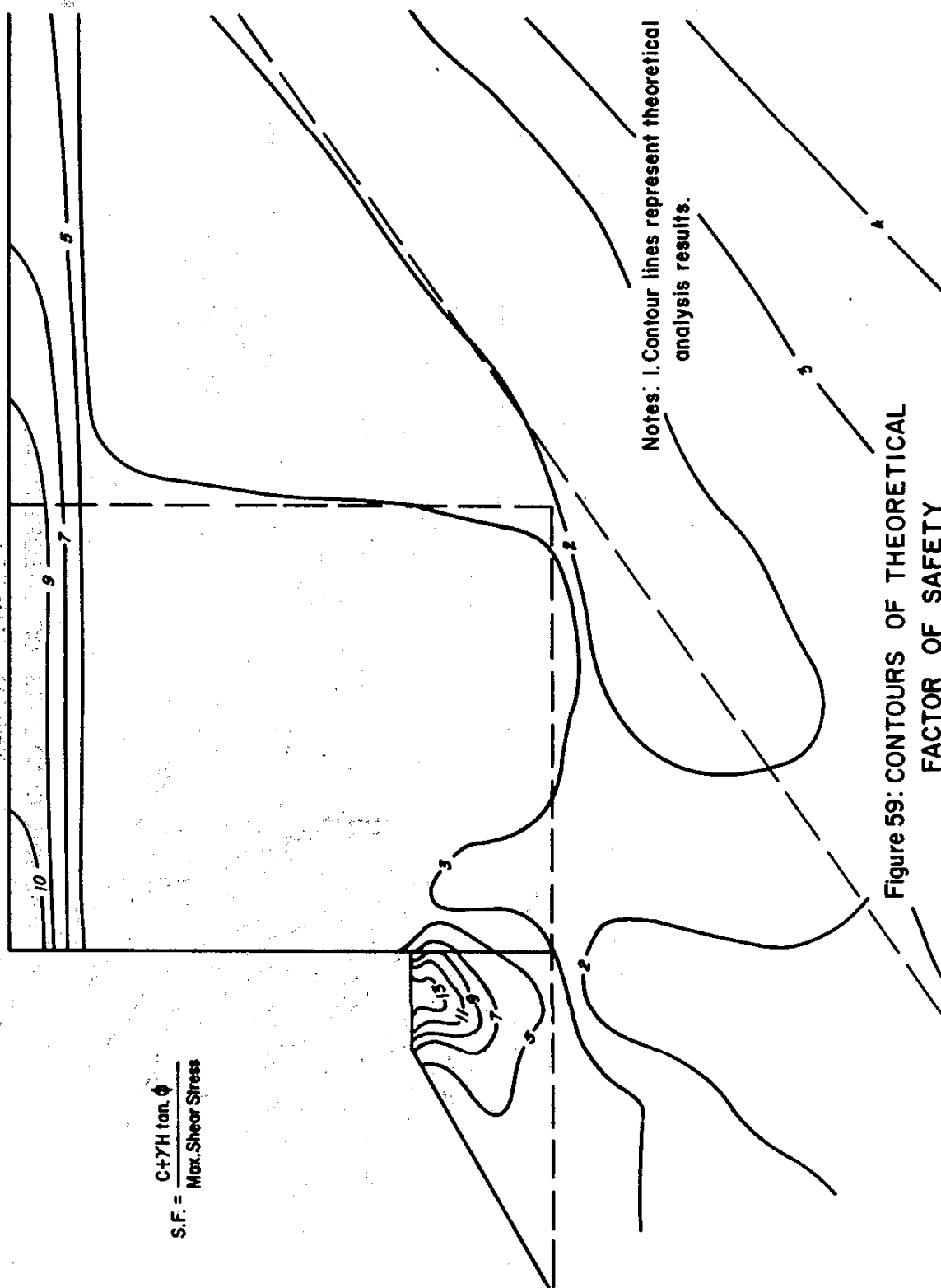


Figure 56 COMPRESSIVE HORIZONTAL SOIL STRESS DISTRIBUTION, STATION 551+75



Note: (-) indicates tensile horizontal stress

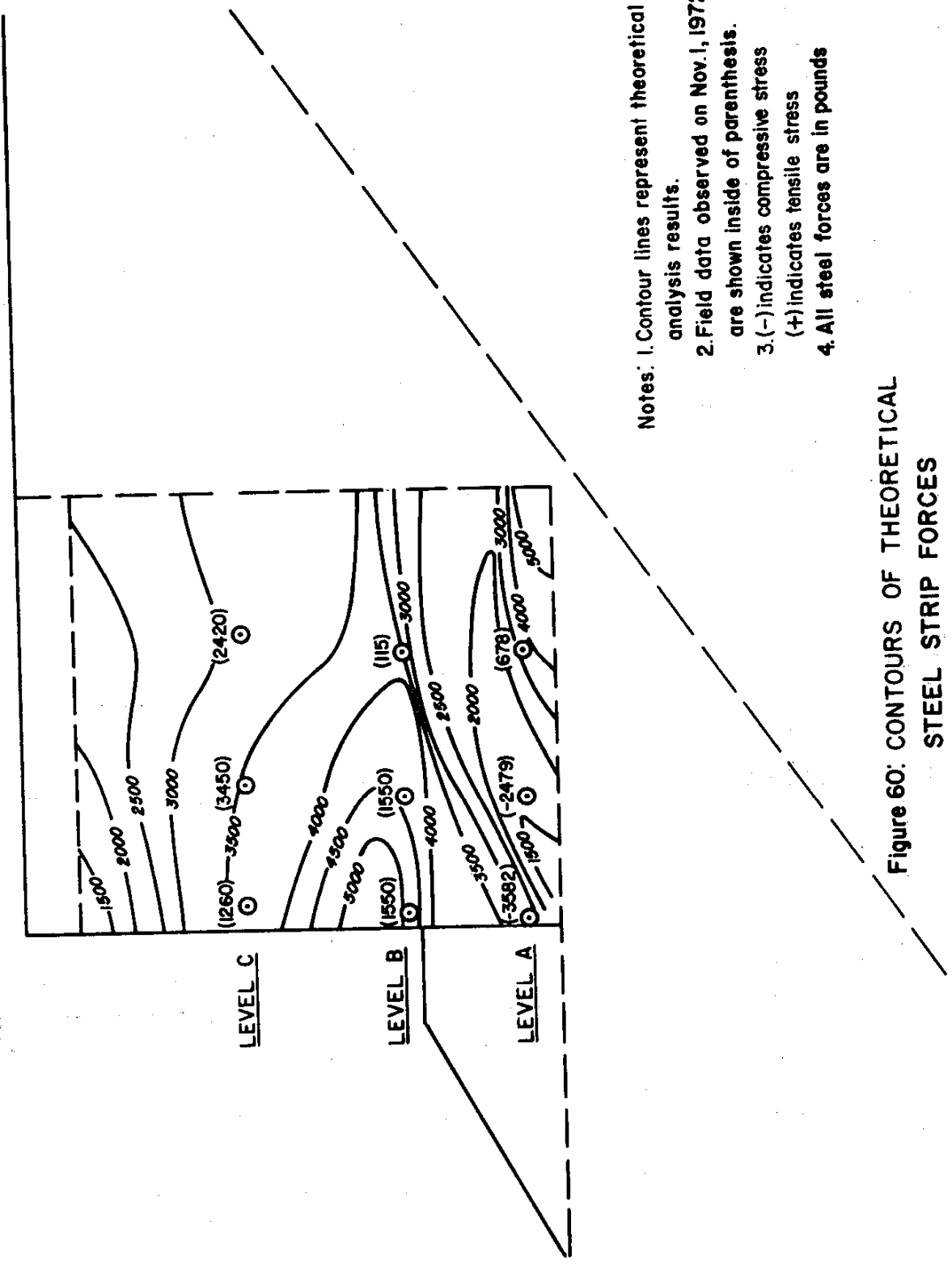
Figure 57: CONTOURS OF THEORETICAL STRESS RATIO, $K = \sigma_x / \sigma_y$



$$S.F. = \frac{C + \gamma H \tan \phi}{\text{Max. Shear Stress}}$$

Notes: | Contour lines represent theoretical analysis results.

Figure 59: CONTOURS OF THEORETICAL FACTOR OF SAFETY



- Notes:
1. Contour lines represent theoretical analysis results.
 2. Field data observed on Nov. 1, 1972 are shown inside of parenthesis.
 3. (-) indicates compressive stress (+) indicates tensile stress
 4. All steel forces are in pounds

Figure 60: CONTOURS OF THEORETICAL STEEL STRIP FORCES

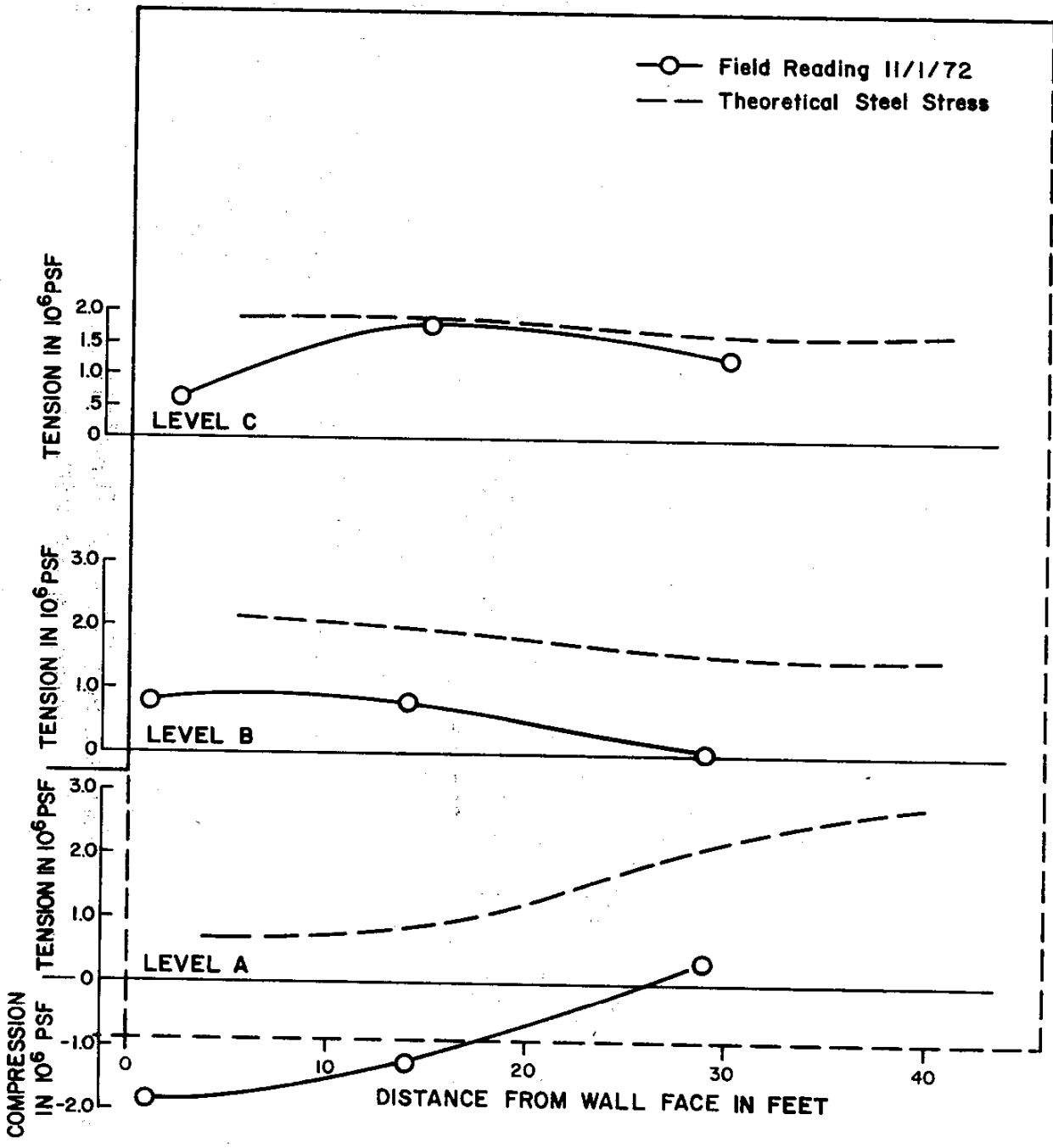


Figure 6I: DISTRIBUTION OF STEEL STRIP STRESS, STATION 551 + 75

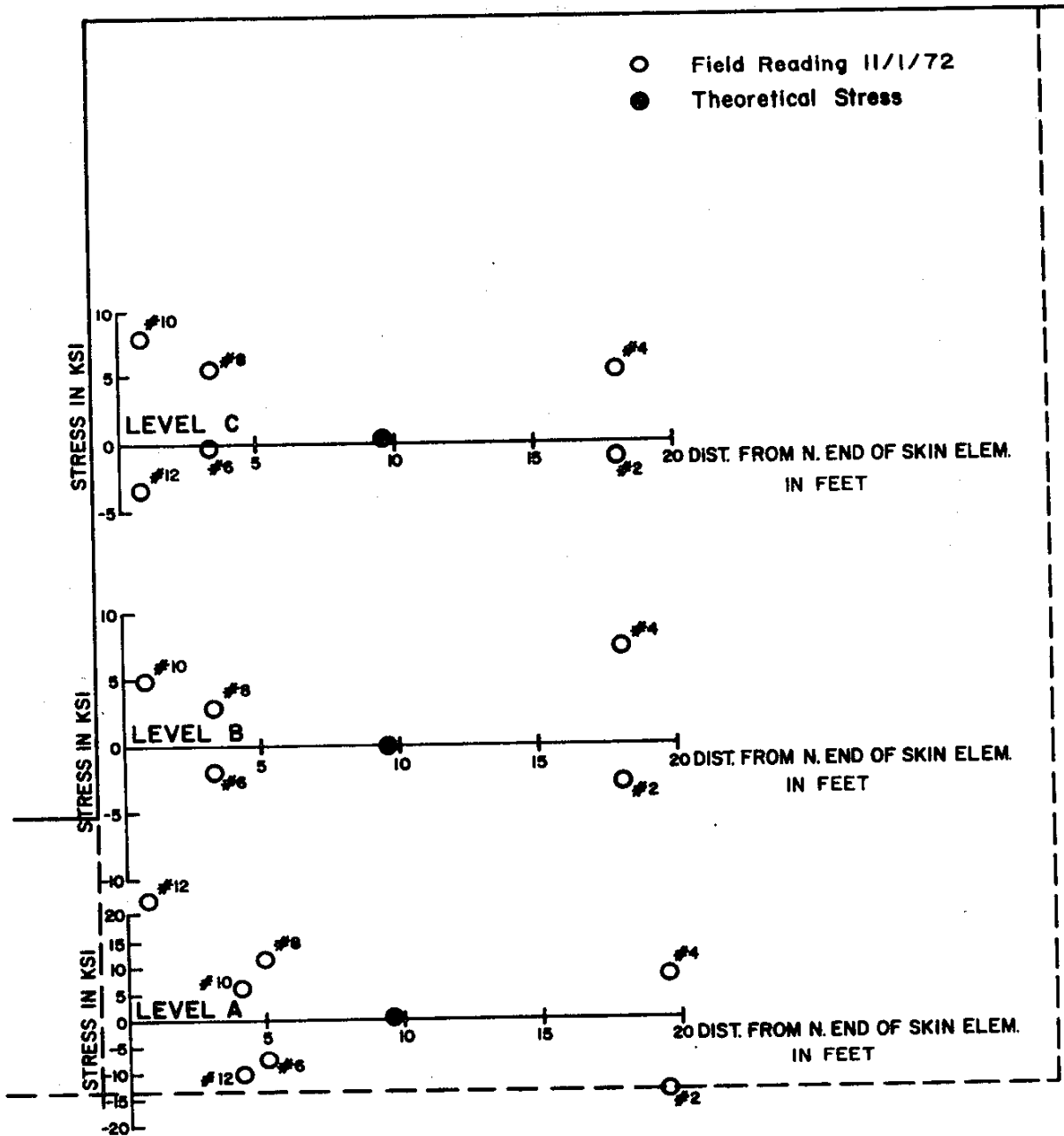


Figure 62: COMPARISON OF THEORETICAL AND FIELD STRESS IN SKIN PLATE

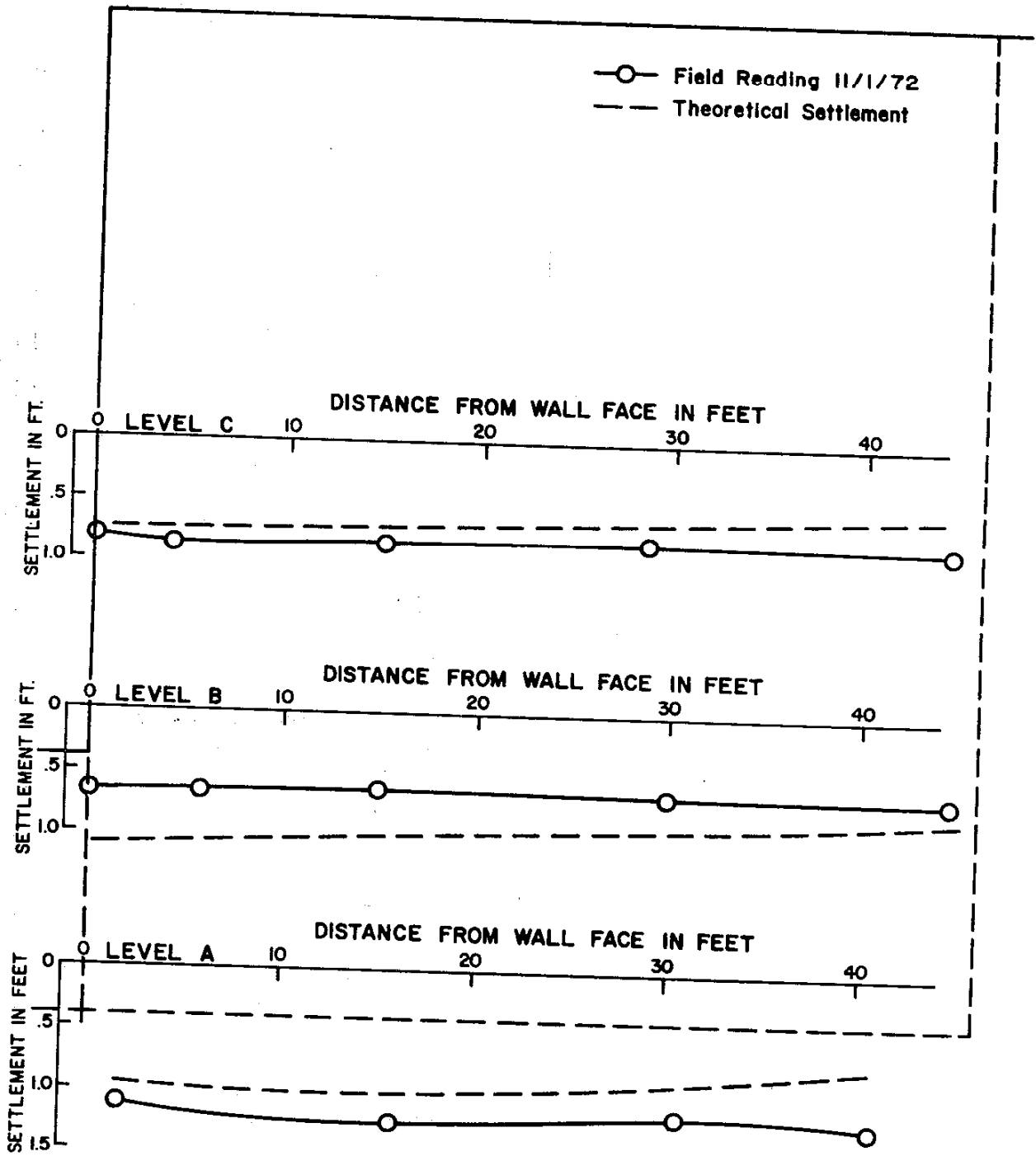


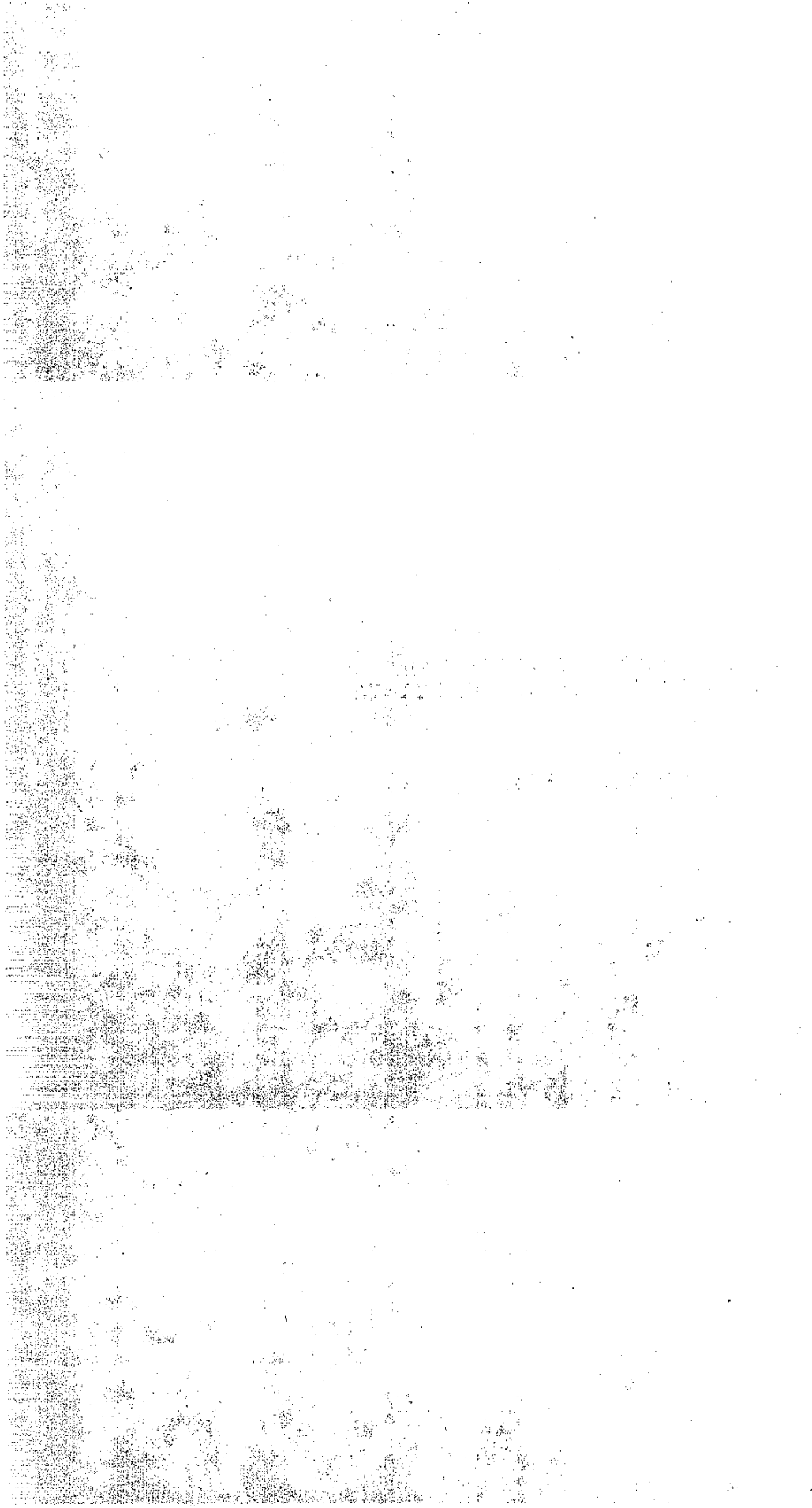
Figure 63: SETTLEMENT WITH RESPECT TO BERM READOUT POINT, STA. 551 + 75

APPENDIX A

DERIVATION OF EQUATIONS FOR
ANALYSIS OF STRESSES IN SKIN PLATE

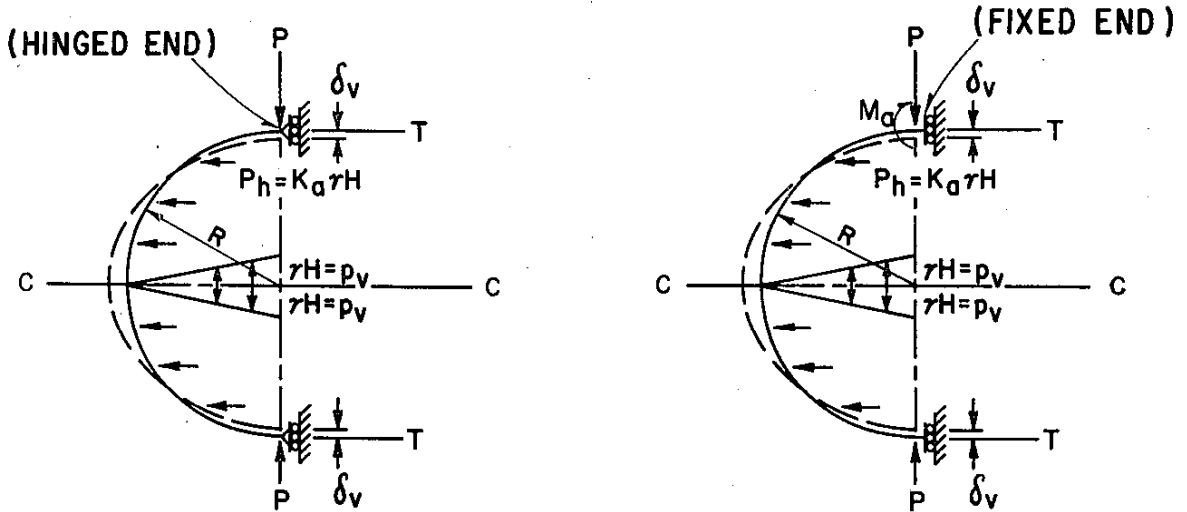
by

JERRY C. CHANG



DERIVATION OF EQUATIONS FOR ANALYSIS
OF STRESSES IN SKIN PLATE

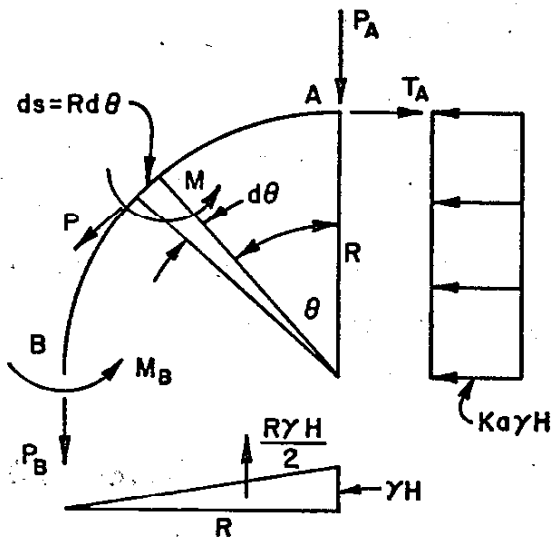
In order to analyze the stress in the skin plate, the redundant force, P , for the hinged end condition and additional redundant moment, M_a , for the fixed end condition must be solved (Figure A-1). The solutions of these two unknown are derived as follows:



LOADING DIAGRAM ON SKIN PLATE

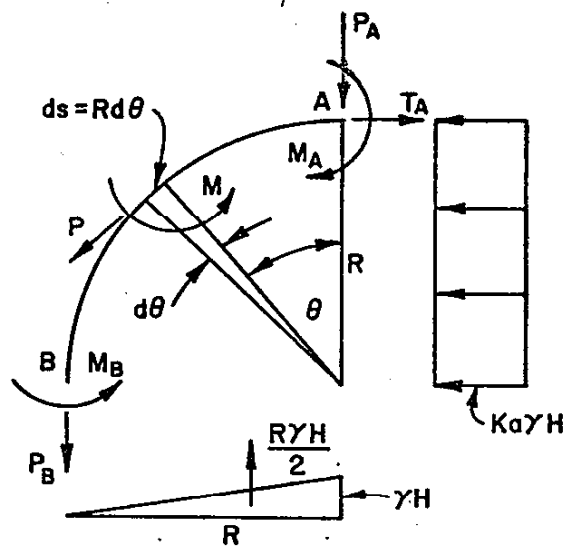
FIGURE A-1

A free body is cut through Section C-C (Figure A-1) and is shown in Figure A-2 for the hinged end condition and Figure A-3 for the fixed end condition. Due to symmetry, only one-half of the semi-circle needs to be analyzed.



HINGED END

FIGURE A-2



FIXED END

FIGURE A-3

Using the strain energy principles described by any text book of structural theory, for example, Seely and Smith (27)* strain energy, U , is equal to

$$U = \int \frac{M^2 R d\theta}{2EI}, \quad \text{-----} \quad (1)$$

and the deflection δ is equal to

$$\delta v = \int \frac{M}{EI} \frac{\partial M}{\partial P_A} ds, \quad \text{-----} \quad (2)$$

For the hinged end condition, using the notation and loading shown in Figure A-2, it can be shown that the moment, M , at any where in the quadrant is equal to

*Reference of the main body of this report.

$$\begin{aligned}
M = & P_A R \sin \theta + T_A R(1 - \cos \theta) - \frac{K\alpha \gamma H R^2}{2} (1 - \cos \theta)^2 \\
& - \gamma H (1 - \sin \theta) \frac{R^2 \sin^2 \theta}{2} \\
& - \frac{R \sin \theta}{2} \gamma H \sin \theta \frac{2}{3} R \sin \theta \quad \text{-----} \quad (3)
\end{aligned}$$

Substituting $ds = R d\theta$ into equation 2, yields

$$\delta v_A = \frac{R}{EI} \int_0^{\pi/2} M \frac{\partial M}{\partial P_A} d\theta \quad \text{-----} \quad (4)$$

Substituting Equation 3 into Equation 4 and integrating over the quadrant, Equation 4 yields

$$\delta v_A = \frac{P_A \pi R^3}{4EI} + \frac{K\alpha \gamma H R^4}{3EI} + \frac{\gamma H R^4}{96EI} (3\pi - 32) \quad \text{-----} \quad (5)$$

Solving Equation 5 in terms of P_A , then

$$P_A = \frac{4EI \delta v_A}{\pi R^3} - \frac{4K\alpha \gamma H R}{3\pi} - \frac{\gamma H R}{24\pi} (3\pi - 32) \quad \text{-----} \quad (6)$$

For the fixed end condition, using the notation and loading shown in Figure A-3, the moment, M , at any where in the quadrant is

$$\begin{aligned}
M = & P_A R \sin \theta + T_A R(1 - \cos \theta) + M_A \\
& - \frac{K\alpha \gamma H R^2}{2} (1 - 2 \cos \theta + \cos^2 \theta) \\
& - \frac{R^2 \gamma H}{2} (\sin^2 \theta - \sin^3 \theta) - \frac{\gamma H R^2}{3} \sin^3 \theta \quad \text{-----} \quad (7)
\end{aligned}$$

Substituting Equation 7 into Equation 4 and integrating over the quadrant, then

$$\delta v_A = \frac{M_A R^2}{EI} + \frac{R^3}{4EI} (P_A \pi + 2 T_A) + \frac{R^4 \gamma H}{96EI} (3\pi - 16Ka - 32) \quad \text{-----} \quad (8)$$

At the fixed end, A, the angle of rotation, θ_A , is expressed as

$$\theta_A = \int_0^{\pi/2} \frac{M}{EI} \frac{\partial M}{\partial M_A} ds = \frac{R}{EI} \int_0^{\pi/2} M d\theta = 0 \quad \text{-----} \quad (9)$$

Substituting Equation 7 into Equation 9 and integrating over the quadrant, then

$$\theta_A = \frac{P_A R^2}{EI} + \frac{T_A R^2}{EI} \left(\frac{\pi}{2} - 1\right) + \frac{\pi M_A R}{2EI} + \frac{Ka \gamma H R^3}{8EI} (8 - 3\pi) - \frac{\gamma H R^3}{24EI} (3\pi - 8) - \frac{2\gamma H R^3}{9EI} = 0 \quad \text{-----} \quad (10)$$

Solve Equation 8 and 10 simultaneously for P_A and M_A , then

$$P_A = \frac{\delta v_A EI}{\pi R^3} \left(4 - \frac{32}{8 - \pi^2}\right) + \gamma H R \left(\frac{4 - 4Ka}{3\pi} - \frac{1}{8}\right) - \frac{8\gamma H R}{8 - \pi^2} \left(\frac{4 - 4Ka}{3\pi} - \frac{(1 + \pi - \pi Ka)}{8} + \frac{1}{9}\right), \quad \text{-----} \quad (11)$$

and

$$M_A = \frac{8 \delta v_A EI}{R^2 (8 - \pi^2)} + \frac{2\pi\gamma HR^2}{(8 - \pi^2)} \left(\frac{4 - 4K\alpha}{3\pi} - \frac{(1 + \pi - \pi K\alpha)}{8} + \frac{1}{9} \right) . \quad \text{-----} \quad (12)$$

In summary:

For hinged end conditions,

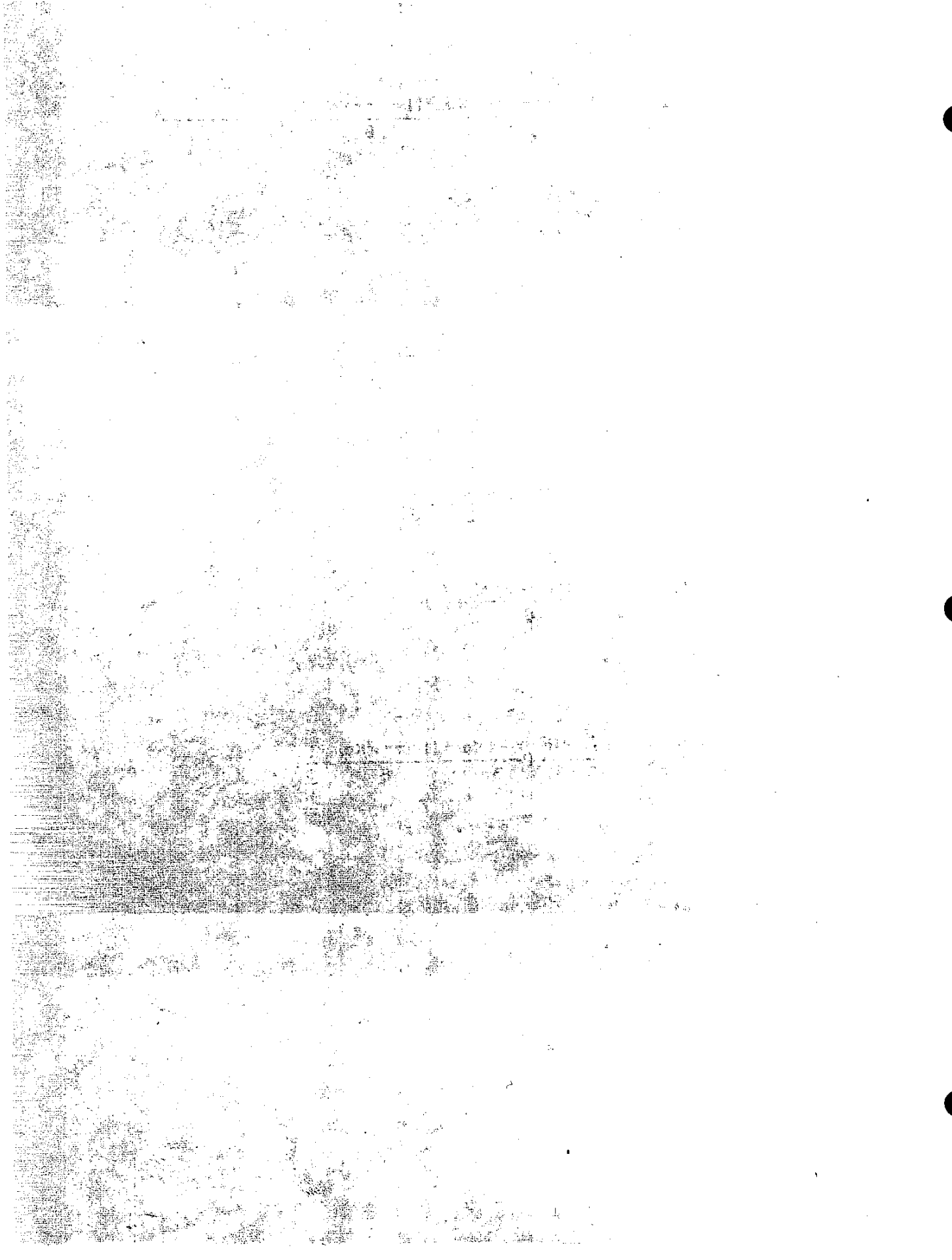
$$P_A = \frac{4EI \delta v_A}{\pi R^3} - \frac{4K\alpha\gamma HR}{3\pi} - \frac{\gamma HR}{24\pi} (3\pi - 32) ;$$

and for fixed end conditions,

$$P_A = \frac{\delta v_A EI}{\pi R^3} \left(4 - \frac{32}{8 - \pi^2} \right) + \gamma HR \left(\frac{4 - 4K\alpha}{3\pi} - \frac{1}{8} \right) - \frac{8\gamma HR}{8 - \pi^2} \left(\frac{4 - 4K\alpha}{3\pi} - \frac{(1 + \pi - \pi K\alpha)}{8} + \frac{1}{9} \right) ;$$

and

$$M_A = \frac{8 \delta v_A EI}{R^2 (8 - \pi^2)} + \frac{2\pi\gamma HR^2}{(8 - \pi^2)} \left(\frac{4 - 4K\alpha}{3\pi} - \frac{(1 + \pi - \pi K\alpha)}{8} + \frac{1}{9} \right) .$$

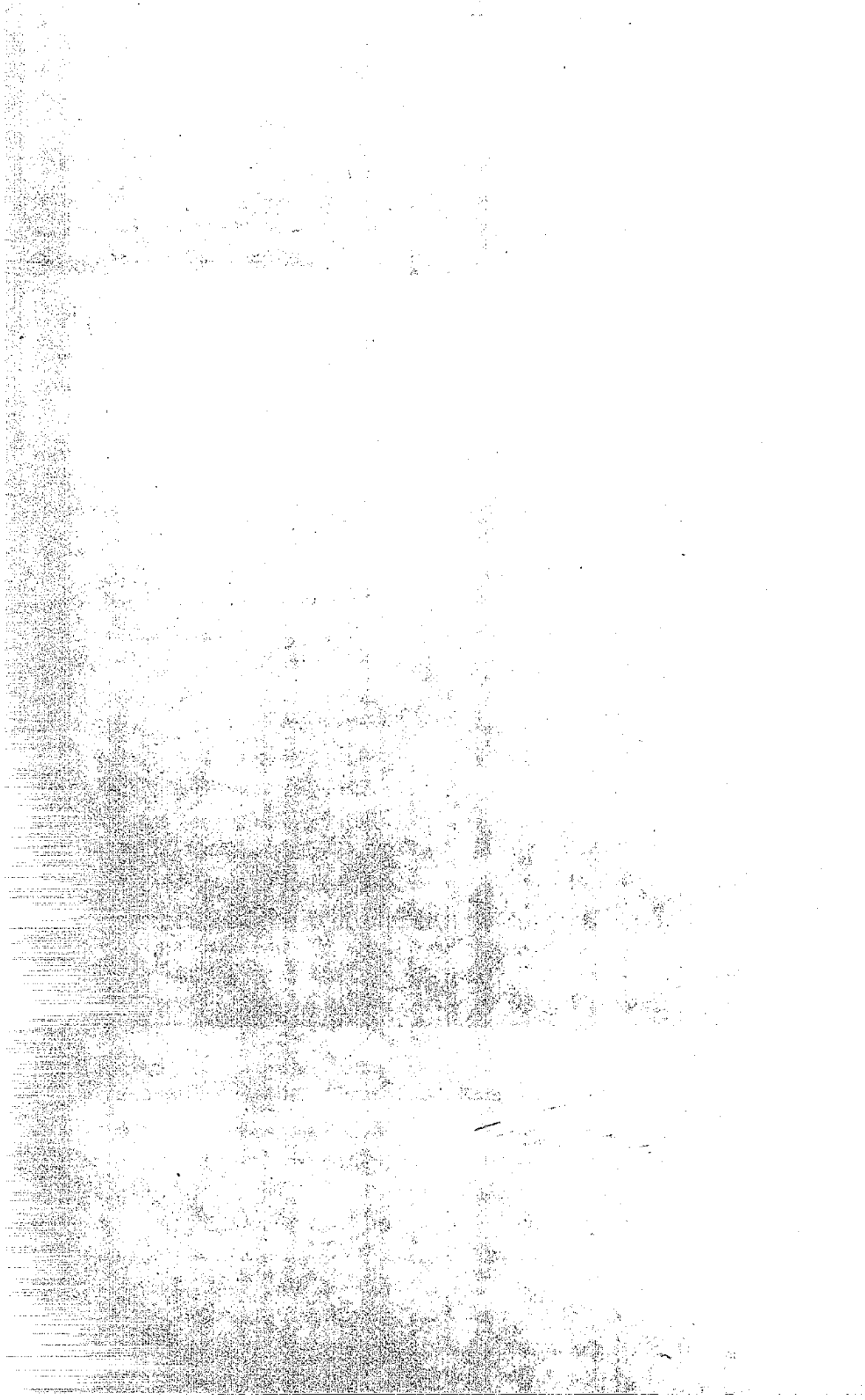


APPENDIX B
MATERIAL PROPERTIES OF
REINFORCED EARTH

By

K. M. ROMSTAD

L. R. HERRMANN



INTRODUCTION

In order to be able to quickly and economically evaluate the structural reliability of proposed reinforced earth structures it is necessary that analysis procedures applicable to such structures be available. There are two obvious approaches to the analysis of such reinforced structures: One possible approach is to attempt to analyze the structure in such a way that each and every reinforcing element is considered in detail. Due to projected excessive computer costs and the high probability of numerical difficulties such detailed analyses appear not to be feasible for real structures. The second approach involves the consideration of the reinforced earth as a "composite material" with associated "composite properties" which represent the overall structural response of the material. This latter approach may be applied with relative ease to very complicated structures and is the one pursued herein.

The use of composite materials for Civil Engineering applications is ages old, e.g., plain concrete (i.e., mortar reinforced with aggregate) and reinforced concrete. Correspondingly "strength of materials" theories have long been available for the analysis of structures made of such materials. During the past 15 years the use of new and exotic composite materials has become commonplace for aerospace applications and extensive theories have been developed for explaining their behaviors. Although on the surface

the bases for these theories may appear to differ from those used for the strength of materials theories for concrete structures, in reality they do not. The work reported herein follows directly from that reported in reference (1); an introduction to some of the extensive literature in this field may be found in reference(2).

The theory of composite material behavior may be derived from several different points of view (all leading to substantially the same result). The approach followed herein is to recognize that if the reinforcing pattern is repeated a sufficiently large number of times the material can be considered homogeneous at the phenomenological level (or as an inhomogeneous material in which the changing properties reflect only changes in the reinforcing pattern). The consideration of the reinforced material as homogeneous at the phenomenological level is analogous to the consideration of a microscopically crystalline material as macroscopically homogeneous (e.g., the treatment of steel as a homogeneous isotropic material) or to the accounting for the reinforcement in a concrete beam by the use of transformed section properties, etc. The reinforced material when viewed at the composite level will, in general, exhibit anisotropic behavior. Once the appropriate composite properties are determined standard analysis procedures (e.g., finite element procedures) may be used to analyze reinforced earth structures.

REINFORCED EARTH UNIT CELL

The experimental determination of the complete array of composite properties is often very difficult and expensive, fortunately a well developed theory exists for the relating of these properties to the known properties of the individual component materials (soil and steel in this case) and to the geometric arrangement of the reinforcement.

For a material that has a regular reinforcing pattern one can, in general, find a small unit of the material which when repeated in all directions results in the actual configuration of the composite material; in this report this fundamental building block is called the "unit cell". The average values of the stresses distributed over the cell faces are equal to the stresses in the equivalent composite material and thus the average response of the unit cell to a state of stress or strain is the same as the composite response of the material. Hence, the desired composite properties may be calculated from a consideration of the behavior of the unit cell and once the composite stress state is determined at a particular point in a reinforced earth structure the corresponding constituent stress state may be determined by returning to the unit cell. Figure B-1 illustrates a particular composite stress state and the corresponding stress state at the constituent level of the reinforced material.

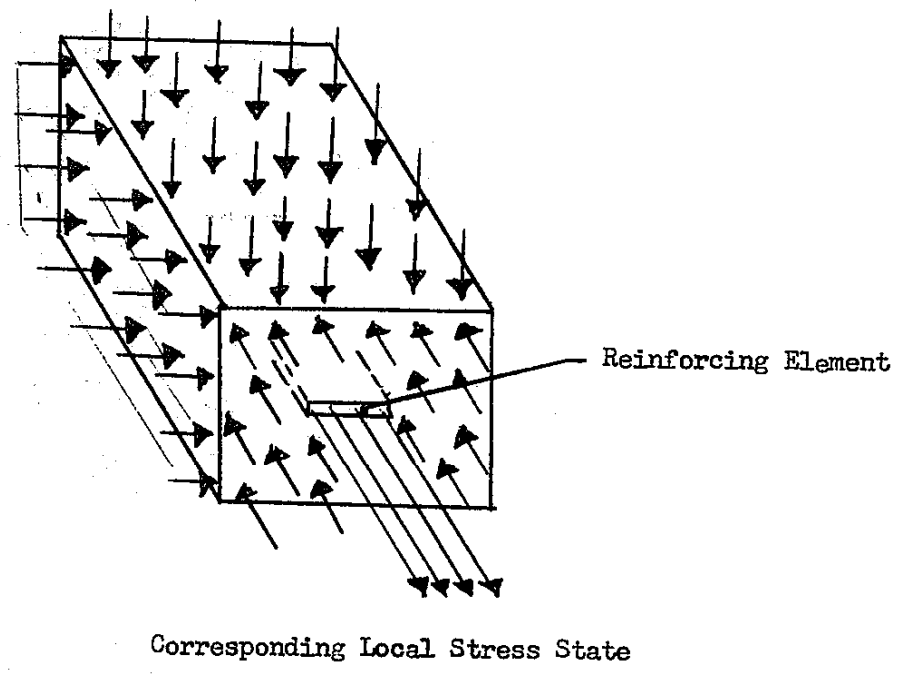
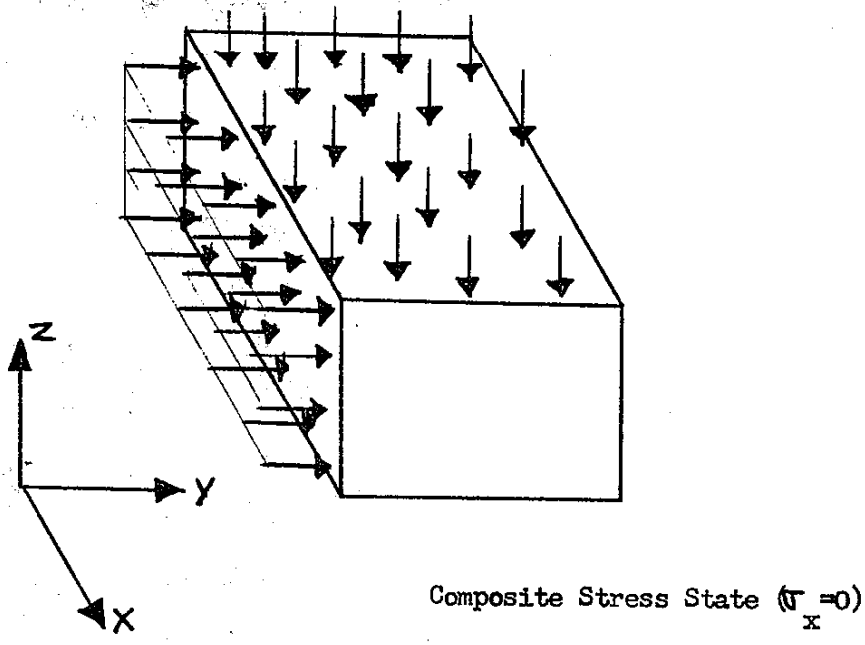


Figure B-1 Illustration of Composite Stress Concept

The unit cell for the reinforced earth structures under consideration is shown in Figure B-2. The composite material considered consists of a soil with thin steel strips parallel to each other at chosen spacings and extending deep into the soil mass. The 1 axis in Figure B-2 is chosen parallel to the strips and the 2 and 3 axes form a plane perpendicular to the longitudinal axis of the strips and are aligned with the principle axes of the strips. For a given reinforcing pattern all strips in a given 1-3 plane are assumed to be equally spaced, b , and the 1-3 planes containing the strips in the reinforced earth are present in parallel layers of spacing, d , (where b and d may vary from layer to layer). When the composite material is subjected to a homogeneous stress or strain state, those cells which are sufficiently far removed from the surface of the material to avoid surface effects must satisfy the conditions, (1) all unit cells will exhibit identical deformation and stress states, (2) the averages of the unit cell stresses and strains are equal to the phenomenological stresses and strains of the composite and (3) there must be continuity of the displacement and traction vectors across all cell interfaces.

COMPOSITE STRESS-STRAIN RELATIONSHIP FOR REINFORCED EARTH

The anisotropic phenomenological behavior of the composite material (i.e., reinforced earth) may be described by the equations:

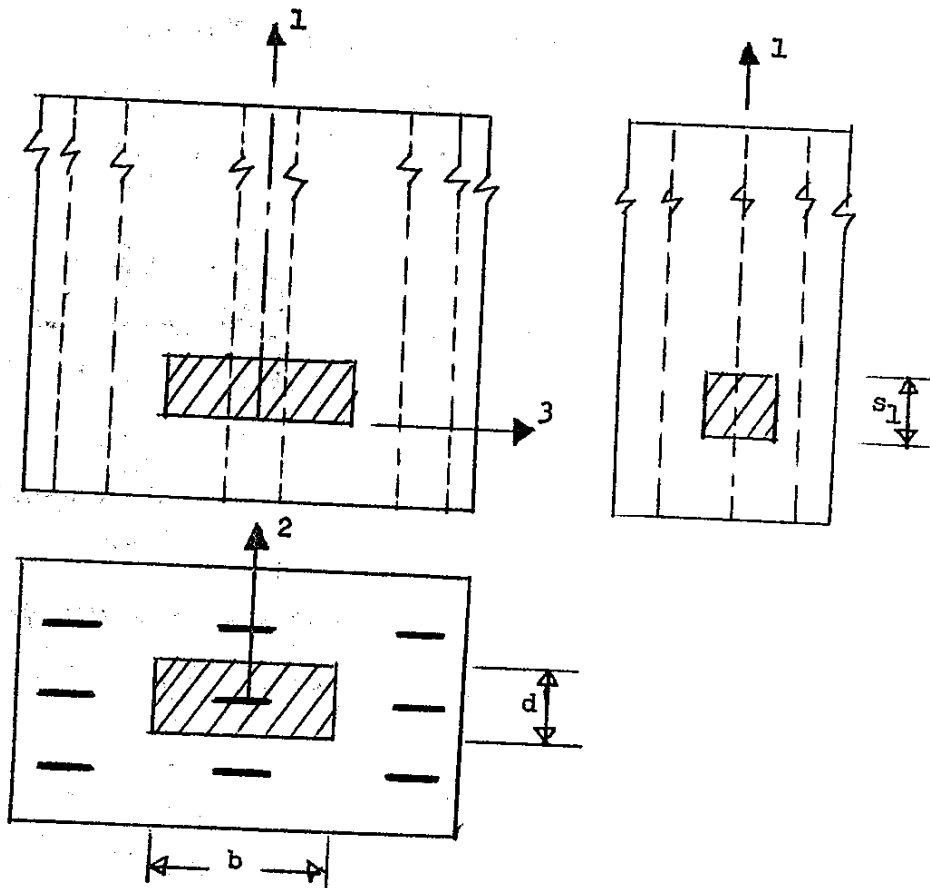
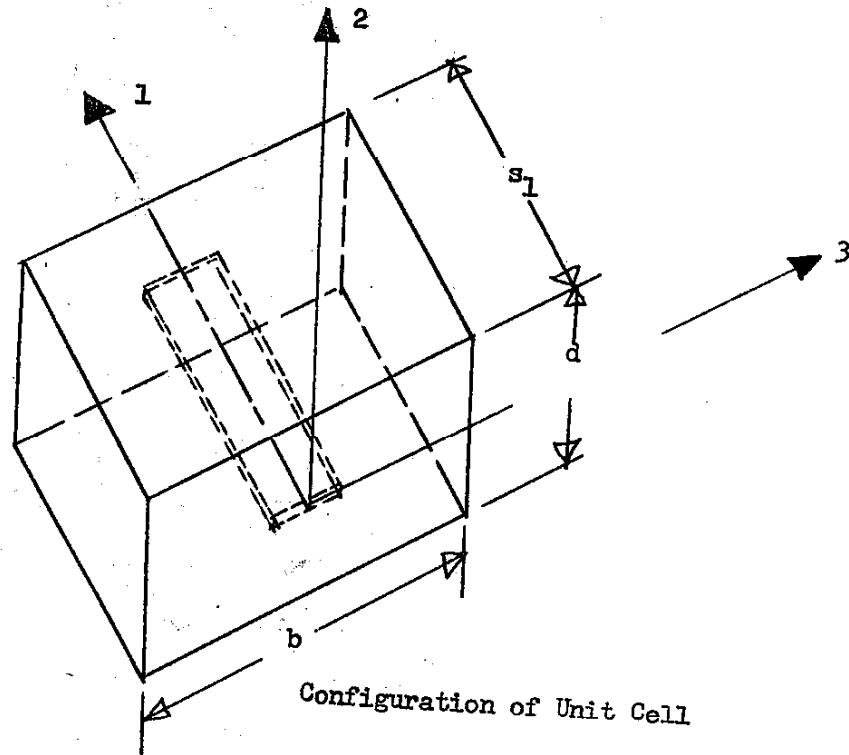


Figure B-2 Unit Cell Representation of Reinforced Earth

Strain - Stress Relationship

$$\begin{bmatrix} \epsilon_1 \\ \epsilon_2 \\ \epsilon_3 \\ \gamma_{12} \\ \gamma_{13} \\ \gamma_{23} \end{bmatrix} = \begin{bmatrix} c_{11} & c_{12} & c_{13} & & & \\ c_{12} & c_{22} & c_{23} & & & \\ c_{13} & c_{23} & c_{33} & & & \\ & & & c_{44} & & \\ & & & & c_{55} & \\ & & & & & c_{66} \end{bmatrix} \begin{bmatrix} \sigma_1 \\ \sigma_2 \\ \sigma_3 \\ \sigma_{12} \\ \sigma_{13} \\ \sigma_{23} \end{bmatrix} \quad (1)$$

The composite properties may be theoretically predicted by determining the average response of the unit cell to various applied homogeneous composite stress or strain states. The most accurate solution to this problem would require a detailed solution of a complicated three-dimensional boundary value problems, possibly by the finite element method. Fortunately however, the characteristics of the reinforced earth unit cell make some approximations possible which greatly simplify the problem. The most significant characteristic is that the percentage of reinforcement is extremely small (much less than 1% by volume). This characteristic leads to the assumption of the strains in the composite being equal to the strains in the soil.

The composite properties were predicted by considering the response of the unit cell to an arbitrary composite stress state and predicting the resulting composite strain state. The most significant considerations utilized in developing the properties were

the assumptions that the composite stress-strain state in the 2 and 3 directions equaled the soil stress-strain state and the displacements of all points in any 2-3 plane are equal for both soil and strip.

Any arbitrary composite stress state may be expressed as the sum of a series of simple stress states, i.e.,

$$\begin{bmatrix} \sigma_1 \\ \sigma_2 \\ \sigma_3 \\ \sigma_{12} \\ \sigma_{13} \\ \sigma_{23} \end{bmatrix} \text{arbitrary} = \begin{bmatrix} \sigma_1 \\ \sigma_0 \\ \sigma_0 \\ \sigma_0 \\ \sigma_0 \\ \sigma_0 \end{bmatrix} + \begin{bmatrix} \sigma_0 \\ \sigma_2 \\ \sigma_0 \\ \sigma_0 \\ \sigma_0 \\ \sigma_0 \end{bmatrix} + \dots + \begin{bmatrix} \sigma_0 \\ \sigma_0 \\ \sigma_0 \\ \sigma_0 \\ \sigma_0 \\ \sigma_{12} \end{bmatrix}$$

Consider the first of these simple stress states, i.e.,

$$\sigma_1 = \sigma; \quad \sigma_2 = \sigma_3 = \sigma_{12} = \sigma_{13} = \sigma_{23} = 0 \quad (2)$$

Equation (1) then yields

$$c_{11} = \epsilon_1 / \sigma \quad (3)$$

$$c_{12} = \epsilon_2 / \sigma \quad (4)$$

$$c_{13} = \epsilon_3 / \sigma \quad (5)$$

The applied composite stress σ acting over the composite area bd must equal the sum of the strip stress, σ^{st} , acting over the strip area, A^{st} , and the soil stress, σ^{so} acting over the soil area, A^{so}

(Fig.B1). Note that the soil area and the composite area are essentially equal for the reinforced earth systems under consideration ($bd = A^C = A^{SO}$)

$$\sigma A^C = \sigma_1^{SO} A^C + \sigma_1^{st} A^{st} \quad (6)$$

$$\sigma_2 = \sigma_2^{SO} = 0 \quad (7)$$

$$\sigma_3 = \sigma_3^{SO} = 0 \quad (8)$$

The superscripts c, so, and st refer to composite, soil and strip respectively.

It follows from the strain displacement relationships and the previous assumptions that

$$\epsilon_1 = \epsilon_1^{SO} = \epsilon_1^{st} \quad (9)$$

$$\epsilon_2 = \epsilon_2^{SO} \quad (10)$$

$$\epsilon_3 = \epsilon_3^{SO} \quad (11)$$

The constitutive equations for the soil and strip must be satisfied which, consistent with the assumptions made, become

$$\epsilon_1^{SO} = (1/E^{SO}) \sigma_1^{SO} \quad (12)$$

$$\epsilon_1^{st} = (1/E^{st}) \sigma_1^{st} \quad (13)$$

Substitute the strain-stress Equations 12 and 13 into Equation 9 to obtain the relationship

$$\sigma_1^{SO} = \frac{E^{SO}}{E^{St}} \sigma_1^{St} \quad (14)$$

which may then be substituted into Equation 6 to yield the relationships

$$\sigma_1^{St} = \frac{A^C E^{St}}{A^C E^{SO} + A^{St} E^{St}} \quad (15)$$

$$\sigma_1^{SO} = \frac{A^C E^{SO}}{A^C E^{SO} + A^{St} E^{St}} \quad (16)$$

Using Equations (3), (4) and (5) the composite material properties C_{11} , C_{12} , and C_{13} may then be solved for from the relationships

$$C_{11} = \frac{\epsilon_1}{\sigma} = \frac{\epsilon_1^{SO}}{\sigma} = \frac{\sigma_1^{SO}}{\sigma E^{SO}} = \frac{A^C}{A^C E^{SO} + A^{St} E^{St}} \quad (17)$$

$$C_{12} = \frac{\epsilon_2}{\sigma} = \frac{\epsilon_2^{SO}}{\sigma} = \frac{-\nu^{SO} \sigma_1^{SO}}{\sigma E^{SO}} = \frac{-\nu^{SO} A^C}{A^C E^{SO} + A^{St} E^{St}} \quad (18)$$

$$C_{13} = \frac{\epsilon_3}{\sigma} = \frac{\epsilon_3^{St}}{\sigma} = \frac{-\nu^{SO} \sigma_1^{SO}}{\sigma E^{SO}} = \frac{-\nu^{SO} A^C}{A^C E^{SO} + A^{St} E^{St}} \quad (19)$$

Considering in a similar manner the other five simple stress states into which the arbitrary composite stress state was decomposed yields the values of the other composite properties, i.e., C_{22} , C_{23} , C_{33} , C_{44} , C_{55} , and C_{66} . The final results are:

$$\begin{bmatrix} \epsilon_1 \\ \epsilon_2 \\ \epsilon_3 \end{bmatrix} = \frac{1}{E^{SO}(1+\alpha)} \begin{bmatrix} 1 & -\nu^{SO} & & -\nu^{SO} \\ -\nu^{SO} & 1+\alpha(1-\nu^{SO2}) & & -\nu^{SO} [1+\alpha(1+\nu^{SO})] \\ & & & \\ -\nu^{SO} & -\nu^{SO} [1+\alpha(1+\nu^{SO})] & & 1+\alpha(1-\nu^{SO2}) \end{bmatrix} \begin{bmatrix} \sigma_1 \\ \sigma_2 \\ \sigma_3 \end{bmatrix} \quad (20)$$

$$\begin{bmatrix} \gamma_{12} \\ \gamma_{13} \\ \gamma_{23} \end{bmatrix} = \begin{bmatrix} G^{SO} & & \\ & G^{SO} & \\ & & G^{SO} \end{bmatrix} \begin{bmatrix} \sigma_{12} \\ \sigma_{13} \\ \sigma_{23} \end{bmatrix} ; \quad \alpha = \frac{A^{st} E^{st}}{A^C E^{SO}}$$

This matrix is inverted to obtain the stress-strain coefficients in a form suitable for use in a finite element displacement formulation.

Reinforced earth structures will generally exhibit behavior assumed in elasticity as plain strain response where the strains ϵ_3 , γ_{13} , and γ_{23} are taken to be zero. In the accompanying computer program these strains are assumed to be zero and the resulting stress-strain matrix utilized is of the form,

$$\begin{bmatrix} \sigma_1 \\ \sigma_2 \\ \sigma_{12} \end{bmatrix} = \begin{bmatrix} a_{11} & a_{12} & 0 \\ a_{12} & a_{22} & 0 \\ 0 & 0 & a_{44} \end{bmatrix} \begin{bmatrix} \epsilon_1 \\ \epsilon_2 \\ \gamma_{12} \end{bmatrix} \quad (21)$$

where the a_{ij} coefficients are directly obtained from the inversion of the (C) matrix.

For a given problem if the 1-2 axes do not coincide with the x-y axes the a_{ij} coefficients are appropriately transformed by the program.

STRESS-STRAIN STATE IN SOIL, STRIP, AND SKIN PLATE

The finite element program utilizes Equation (21) in performing analyses for the composite stresses and strains in a reinforced earth structure. The corresponding strains and stresses in the component materials are obtained in the following manner. The x-y composite stress and strain components are transformed into 1-2 components. Since the composite strain in the 1 direction equals the axial strain in the strip (Equation 9), the force in the strip may be obtained from

$$F^{st} = A^{st} E^{st} \epsilon_1 \quad (22)$$

When the axial force in the strip has been determined, the stress in the soil in the 1 direction may be obtained from the equilibrium relationship (Equation 6) as

$$\sigma_1^{so} = \sigma_1 - F^{st}/A^c \quad (23)$$

The normal soil stresses in the 2 and 3 directions and the soil shear stress are assumed to be equal to the composite stresses and all soil strains are assumed to equal the composite strains.

The results from a detailed finite element analysis of the soil, reinforcing strip and skin plate for a small zone of reinforced earth indicated that the bending induced in the skin plate is negligible, and that the only significant stress in the skin plate is the membrane stress. Accordingly, in the accompanying computer program the membrane stress in the skin plate is estimated by approximating it as a circular membrane subjected to the pressure calculated to be acting in the soil at the point in question. If for a particular situation it should be desired to estimate the moment in the skin plate this may be done by a simple subsidiary calculation based on the predicted relative displacements of the membrane edges.

The calculation of moments in the strips is discussed in the following section.

HIGHER ORDER EFFECTS

The developments of the previous sections are all in the realm of conventional elasticity theory. There exist, however, higher order elasticity theories which in addition to the usual effects account for the so-called "couple-stresses" (e.g., see reference (3)).

That is, not only normal and shear stresses are admitted on an infinitesimal element but also stress couples; beam theory may in fact in some sense be interpreted as a special case of these theories. Experience has shown that for structures of practical interest made of isotropic materials, any effects due to "couple-stresses" are completely unimportant (this is indeed fortuitous as the application of the theory is considerably more complicated than the application of the conventional theory). It appears that this may not be the case for certain composite materials; fortunately reinforced earth does not appear to be one of the composite materials for which the "couple-stress" effects are significant.

The purpose of the steel reinforcing strips in reinforced earth is to develop tensile axial forces and thus to provide tensile strength for the material. However, it is possible, that in addition to the anticipated axial forces, shears and moments may also be developed in the strips. The accounting for the additional stiffness of the reinforced earth which results from the development of these moments and shears would apparently require the use of a "couple-stress" elasticity theory, however, because of the low percentage of reinforcement and because of the strip's small bending rigidity these effects appear to be negligible.

Even though the effects of the moments and shears in the reinforcement are not accounted for in the calculations of the stiffness

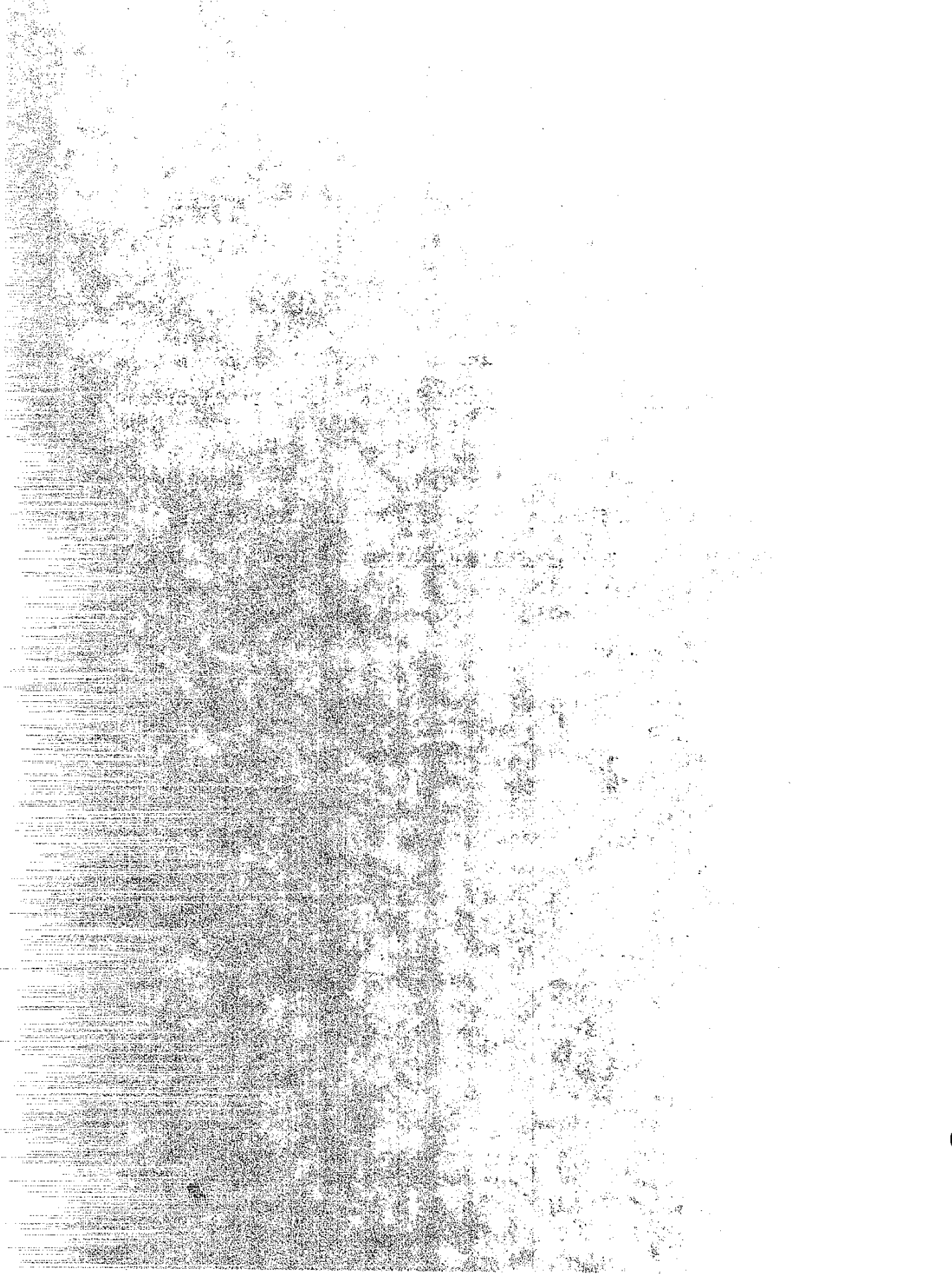
of the composite a knowledge of their values is of interest. Using the results of a conventional analysis (based on the use of the appropriate composite properties) of a reinforced earth structure it is possible to estimate their values. These calculations require only the predicted deformed shape of a reinforcing strip and the bending properties of the strip. In the accompanying finite element computer program quadratic displacement elements (linear strain elements) are used, thus, the curvatures of the reinforcing strips may be simply estimated and hence the resulting moments in the strips are determined. The use of a quadratic displacement element does not make it possible to directly compute the third derivatives of the strip deflections and hence estimates of the strip shears are not obtained. It would appear that they would be rather insignificant.

A second higher order effect which appears to be significant for certain composite materials is the so-called edge effect (it appears that this effect could also be accounted for by the use of a "couple-stress" theory). The edge effect arises because disturbances on the edges of the structure, due to self equilibrating stress distributions, may propagate far into the interior of the structure. For most structures made of isotropic homogeneous materials such disturbances quickly dampen out (St. Venant's principle), however, apparently this is not the case for certain composite materials (it appears that these effects are particularly pronounced when the modulus of the reinforcing element is orders

of magnitude greater than for the matrix material). In reinforced earth the presence of the skin plate would appear to essentially negate the edge effects that would otherwise be present and thus it was not necessary to consider these effects.

REFERENCES

- (1) Herrmann, L. R. and K. S. Pister, "Composite Properties of Filament-Resin Systems", ASME Paper No. 63-WA-239, pp. 1-8, Nov. 1963.
- (2) Pagano, N. J., S. W. Tsai, "Micromechanics of Composite Media", Composite Materials Workshop, Technomic Publications, Stamford, Conn., 1966.
- (3) Mindlin, R. D., "Influence of Couple-Stresses on Stress Concentrations", Experimental Mechanics, 3, 1963.



-



APPENDIX C

USER'S MANUAL FOR

PLANE STRAIN FINITE ELEMENT INCREMENTAL CONSTRUCTION PROGRAM
FOR EMBANKMENT AND/OR REINFORCED EARTH ANALYSIS
WITH BEAM ELEMENT AND MATERIAL PROPERTY OPTIONS

by

L. R. Herrmann

University of California
Davis, California

July 1972
Revised April 1974

[The page contains extremely faint and illegible text, likely due to heavy noise or low resolution. The text is organized into several paragraphs, but the individual words and sentences are not discernible.]



- I. CAPABILITIES OF PROGRAM: A brief discussion of the program is given in Commentary B.
- II. INPUT*: The input data is entered by means of the following groups of cards.

A1. Title Card (12A6) - Columns 1 to 72 - Any information that is to be printed as a title for the problem.

A2. Control Card (I5, E10.3, 2I5, A4, 2A8)

Columns 1 - 5 Number of construction increments

Columns 6 - 15 Plot width (max. 30)

Columns 6 - 20 Output desired

0 = complete analysis
1 = node point coordinates only

Columns 21 - 25 Change number of construction increments

Columns 26 - 29 Labor cost code

Columns 30 - 37 Name of user

Columns 38 - 45 User's phone number

A3. Material Cards - For each material type the following information must be supplied:

1st card (1X, I4, I2, I3, 6E10.5)

Columns 2 - 5 Material Number**

Col. 7 ITYP = 0 - Isotropic Material
2 - Orthotropic Material
3 - Reinforced Earth Material
4 - Strip Plate (beam)

*The numbers in the right-hand column refer to explanatory comments listed in Commentary A. The input and results for a sample problem are given in Commentary C and the program listing in Commentary D.

**If excavation is to be included in the analysis, see comment number 19 in Commentary A.

3

2,4

4

17

	ITYP = 0			ITYP = 2	ITYP = 3		ITYP = 4	
10**	-	1	NP	-	-	1	-	
11 - 20	Unit weight (γ)			Unit weight	Unit weight		A	1
21 - 30	-	B	h_1	C_{11}	-	B	I	
31 - 40	E	A	E_1	C_{12}	E_{soil}	A	E	
41 - 50	ν	ν	ν_1	C_{22}	ν_{soil}	ν	ν	
51 - 60	-	ϕ	-	C_{33}	-	ϕ	n_{max}	
61 - 70	-	c	-	TH(θ)	-	c	n_{min}	
71 - 80	-	-	-	-	-	-	τ_r	

If ITYP = 3 then the above card is immediately followed by a card giving the properties of the reinforcing strips. Whenever any of the strip properties change a new material must be defined.

REINFORCED EARTH DEFINITION (7E10.5)

Columns 1 - 10 EB = Young's modulus of strip
 11 - 20 AB = Width of strip
 21 - 30 XIB = Thickness of strip
 31 - 40 BE = Horizontal spacing of strips
 41 - 50 DE = Vertical spacing of strips
 51 - 60 TE = Angle (in degrees) the strip makes with x-axis
 61 - 70 TK = Thickness of skin plate

**Overburden code, i.e., 1 - indicates overburden properties description A; NP > 1 - indicates overburden properties description B (see note 4).

If NP > 1 then the previous card is immediately followed by $M = (NP-1)$ cards which describe the plots of properties vs. overburden, i.e., Type B description. These M cards successively contain the values of h_n (columns 1-10), E_n (columns 11-20), and ν_n (columns 21-30) ($n = 2 \rightarrow NP$) which define the modulus and Poisson's ratio curves vs. overburden $h = \gamma H$. If the value of Poisson's ratio is omitted from a card, the value is taken to be equal to the last specified value. The value of NP may not exceed 10.

B1. A card with 1 punched in column 1, followed by:

NODE POINT ARRAY - (1X, I4, 2E10.5, I5, 2E10.5, I5, E10.5)

1,2

As many cards as are necessary to specify the locations of all nodes in the system.

6,8

Columns 2 - 5 N - Node point number

5

6 - 15 x - coordinate

16 - 25 y - coordinate

26 - 30 N' - final point in st.
line sequence

31 - 40 x'

41 - 50 y'

51 - 55 INC-Numbering Increment

56 - 65 D - Spacing Ratio

} quantities associated
with straight line
generation option

6

7

B2. A card with 2 punched in column 1, followed by:

ELEMENT ARRAY - (1X, I4, 10I5) As many cards as necessary to
define all elements in the system.

Columns	2 - 5			
	6 - 10	The numbers of the four node points which describe the element (reading <u>counter clockwise</u> around the element).		
	11 - 15	For a <u>triangular element</u> the fourth number is <u>left blank</u> . For a <u>bending</u>		
	16 - 20	<u>element</u> the <u>third</u> and <u>fourth numbers</u> are left <u>blank</u> .		
	21 - 25	MN - Material number (corresponding to the material description in Section A3)		9
	26 - 30	IN - Construction increment number (i.e., the number of the construction incre- ment when the element becomes part of the structure)		9
	31 - 35	NMIS - Number of additional elements in the sequence		
	36 - 40	INC - Numbering Increment		
	41 - 45	NMISP - Number of additional layers	quantities asso- ciated with the	10
	46 - 50	INCP - Numbering Increment for the layers	data generation option	
	55	IPRNT = 0 Element does not have skin plate 1 Element includes skin plate		15
	56 - 60	IOUT = Excavation increment number		19

The order of the element cards need bear no relationship to the
locations of the elements in the body.

B3. A card with 3 punched in column 1, followed by:

BOUNDARY ARRAY - (1X, I4, I5, E10.5, I5, 2E10.5, 3I5, 2E10.3)

2,18

As many cards as necessary to specify displacement or non-zero stress boundary conditions. Pressure specification cards must precede all other cards in the Boundary Array.

Columns

2 - 5	N	- Node point number	
10	IF ₁	= $\begin{Bmatrix} 0 \\ 1 \end{Bmatrix}$ indicates $\begin{Bmatrix} \text{force} \\ \text{displacement} \end{Bmatrix}$ specified in 1 direction	11 12
11 - 20	V ₁	= value of $\begin{Bmatrix} \text{force} \\ \text{displacement} \end{Bmatrix}$ specified in 1 direction	
25	IF ₂	= $\begin{Bmatrix} 0 \\ 1 \end{Bmatrix}$ indicates $\begin{Bmatrix} \text{force} \\ \text{displacement} \end{Bmatrix}$ specified in 2 direction	
26 - 35	V ₂	= value of $\begin{Bmatrix} \text{force} \\ \text{displacement} \end{Bmatrix}$ specified in 2 direction	
36 - 45	θ	- angle (in degrees) between x ₁ -axis and x-axis (see Figure 1)	12
46 - 50	IN	- Construction increment in which the non-zero boundary conditions are to be applied	11
51 - 55	N'	- final point in sequence	13
56 - 60	INC	- Numbering Increment	
61 - 70	P _N	Pressure magnitudes at points N and N' respectively	14
71 - 80	P _{N'}		

B4. END CARD - Card with 4 punched in column 1

The above sequence of cards is repeated for the next analysis, etc.

III. OUTPUT:

The items appearing in the output are listed below:

- A. The input data is printed
- B. For each construction increment the following items are printed
(Note: All of the following items are total values, i.e., values accumulated during all the previous and present construction increments; incremental values can of course be found by subtracting values printed for successive increments.)

1. For each element, the following items are printed: (Note: The units are determined by the units employed in the input.)
Element No. = The element numbers are defined by the order of printing of the element input information.

a) For continuum Elements:

$\left. \begin{array}{l} X \\ Y \end{array} \right\}$ = Coordinates of the point in the element for which stresses and strains are printed

EPSILON-X = Soil strain in x direction

EPSILON-Y = Soil strain in y direction

GAMA-XY = Shear strain in soil

SIGMA-X = Soil stress in x direction

SIGMA-Y = Soil stress in y direction

TAU-XY = Shear stress in soil

SIGMA-1 = Max. Principal stress in soil

SIGMA-2 = Min. Principal stress in soil

ANG = Angle (in degrees) between direction of maximum principal stress and x axis

In addition if the element is reinforced earth the following items are printed:

STRIP AXIAL FORCE = Force in reinforcing strip

MOMENT = Moment in reinforcing strip

In addition if the reinforced earth element has a skin plate and is on the edge of the structure

SKIN MEMBRANE STRESS = Membrane stress in skin plate

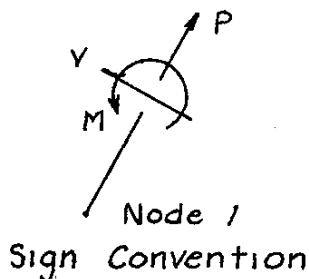
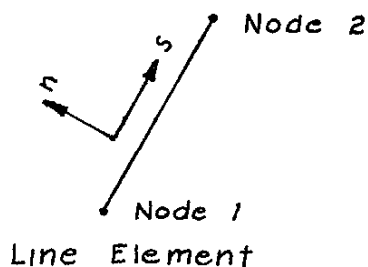
b) For beam elements (for plane strain these quantities are per unit of width)

P = Axial force at the center of element

V = Shear force at the center of element

M = Moment at the center of element

The sign convention used for the bending element is:



The stress calculation for the beam element requires values for n_{\max} (distance from N.A. to extreme fiber, for positive n), n_{\min} (distance from N.A. to extreme fiber, for negative n) and Tau_r (ratio of maximum shear stress to average value). If n_{\max} is left blank it is assumed that the section is rectangular and the program sets $n_{\max} = h/2$, $n_{\min} = -h/2$ and $\text{Tau}_r = 1.5$, where $\frac{h}{2} = \sqrt{\frac{3I}{A}}$. The normal stresses and strains are denoted by the symbols S and E respectively; the shear stress by the symbol TAU.

2. For each node in the system the x-y displacement components are printed.

COMMENTARY A

Explanatory Comments Concerning the Input

1. The cross-section of the body is assumed to lie in the x-y plane with the gravity loading acting in the negative y-direction, see Figure C-1. In the application of the analysis the cross-section of the body is described by a series of quadrilateral and/or triangular continuum elements and line (bending) elements. The quadrilateral elements may have arbitrary shapes. Because the triangular elements are of lower order than the quadrilateral elements they should be used sparingly. The numbering of the nodes for a simple element representation is shown in Figure C-2.

Considering any two of the two or three or four nodes which describe an element (line or triangle or quadrilateral) denote the bandwidth span between them as N_i . The value of N_i is equal to 2 plus twice the difference in their node numbers plus the number of nodes in this "range" which have bending elements associated with them minus twice the number of nodes in this "range" which are not part of the structure (see note 5). If the two nodes under consideration are 17 and 45, the "range" of nodes referred to is 17 → 45. For a given element denote the maximum value of N_i as NE_j . Considering all elements in the system denote the maximum value of NE_j as NE_{max} ("bandwidth" of simultaneous equations). For a minimization of computational cost, for a given analysis, it is important that the node points be numbered so as to minimize the value of NE_{max} (the numbering used in Figure C-2 gives a value of $NE_{max} = 12$; if the numbering had instead proceeded from left to right a value of $NE_{max} = 22$ would have been obtained).

The program checks the area of each element, if any one of these values should be non-positive, an error message ("data error in element n") is printed. This error is normally a result of one of the following causes: i) the nodes describing the element were entered in a clockwise manner instead of counter clockwise; ii) one of the node numbers describing the element was entered incorrectly or; iii) the coordinates of one of the nodes describing the element was entered incorrectly.

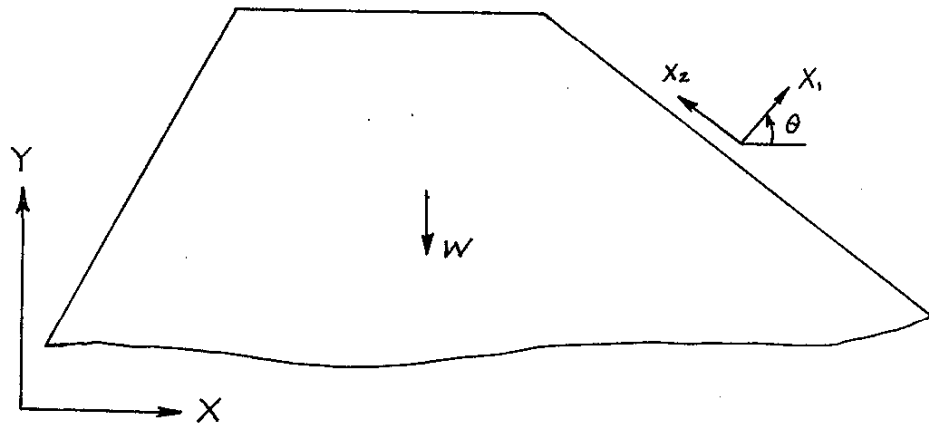


Figure C-1 - Sketch of typical body

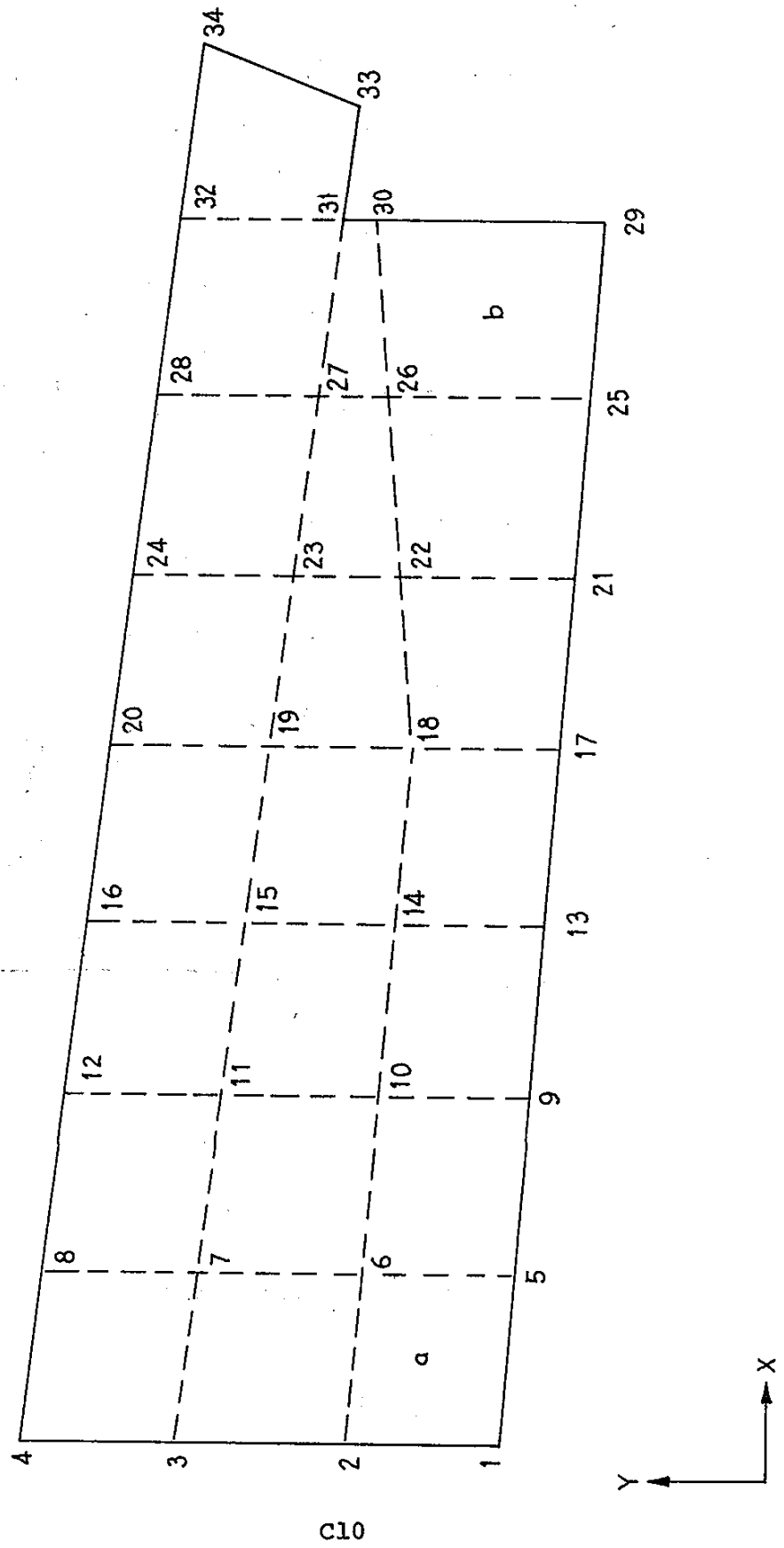


Figure C-2 - Representation by quadrilateral elements.

2. As the program is now dimensioned the value of NE_{max} (see comment 1) may not exceed 56, the maximum node number (NPT) may not exceed 700, the number of elements (NELEM) may not exceed 599, the number of boundary condition specifications (NBPTC) may not exceed 199, the number of different materials (NMAT) may not exceed 10, and the number of points used to specify overburden properties may not exceed 10. These limitations may be modified by changing the dimensions of the program. If any one of these restrictions is violated, an error message is printed and the program proceeds to the consideration of the next problem.

When changing the dimensions of the program three areas must be considered:

- i) Common blocks (see Table C-1)
- ii) The value of $NEQ = N4$ specified at the beginning of the program
- iii) The dimension checks at the end of the subroutine PREP

The dimensions in the program which are related to the size of the problem are indicated below:

$X(N_1), Y(N_1), NQ(N_1+1), U(N_1), V(N_1)$
 $NOD(N_2, 4), MNO(N_2), ST(N_2, 17), INCOUT(N_2)$
 $NODB(N_3), BIV(N_3, 3)$
 $SL(2*N_4), S(2*N_4, N_4)$
 $DEN(N_5), NON(N_5), GNU(N_5, N_6), E(N_5, N_6), H(N_5, N_6)$
 $AB(N_5), EB(N_5), XIB(N_5), BE(N_5), DE(N_5), TE(N_5), TK(N_5)$

where

- N_1 = maximum node number
 $N_2 - 1$ = maximum number of elements
 $N_3 - 1$ = maximum number of boundary conditions

SUBROUTINE	COMMON BLOCK					
	1	2	3	4	5	6
MAIN	X	X	X	X	X	X
STRESS	X	X	X	X	X	X
PREP	X	X			X	X
CONVT					X	
ANISP					X	
INTPI	X				X	
STIFNS	X	X	X	X	X	
GEOM			X			
STFSUB	X		X		X	
REDUCI				X		
BAKSUB				X		
PRINC						
ESTAB			X			
REINF						X
STREH			X			X

Table C-1 - Common Blocks - Subroutine Association

$$N_4 \geq 2*(NE_{\max} + 1)$$

N_5 = maximum number of different materials

N_6 = maximum number of points describing a Type B material

3. The program may be utilized for a non-incremental construction analysis by specifying the number of construction increments to be one.
4. The length units used to describe the material properties must be consistent with the units used to describe the geometry of the body.

The overburden dependence of a soil's modulus may be accounted for by one of two different means. "Type A" description is specified by punching a 1 in Col. 10 of the appropriate "material card." The overburden dependence of the modulus is modeled by using the relationship reported in Equ. (27) of the Highway Research Report by Travis Smith, et. al.*, i.e.,

$$E_t = [A + B(1-\sin\phi)\gamma H] \left[1 - \frac{\gamma H (1-\sin\phi) \sin\phi}{2c \cos\phi + 2 \sin\phi \left(\frac{\gamma H}{N_\phi} - \frac{2c}{(N_\phi)^{1/2}} \right)} \right]^2$$

where

$$N_\phi = \tan^2 \left(45^\circ + \frac{\phi}{2} \right)$$

$$E_i = A + B\sigma_3$$

γ = Density

c = Cohesion

ϕ = Friction angle (degrees)

H = Overburden depth

*"Stresses and Deformations in Jail Gulch Embankment," Interim report prepared by the Materials and Research Department, California Division of Highways, February 1972.

For a given construction increment, the program takes the overburden depth to be the vertical distance between the center of the element and the surface of the soil directly above this point. The value of γ that is used in the above and following equations is determined as follows: The average of all specified values of γ , for the several materials in the problem, which are non-zero are used; if no non-zero values are specified, a value of 130 pcf is assumed.

The "Type B" description interpolates plots of E and ν vs. overburden pressure ($h = H\gamma$), see Figure C-2a. This description is specified by assigning appropriate values for $h_1, E_1, \nu_1; h_2, E_2, \nu_2$; etc.

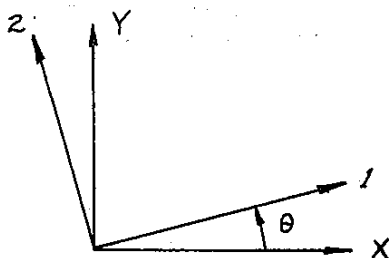
If the program is to be used for a plane stress analysis the "equivalent" plane stress properties are used, i.e., for isotropic materials the values of \bar{E} and $\bar{\nu}$ are used for E and ν .

$$\bar{E} = E \frac{(1 + 2\nu)}{(1 + \nu)^2}$$

$$\bar{\nu} = \frac{\nu}{1 + \nu}$$

Linear orthotropic material are described by the following stress-strain law:

$$\begin{bmatrix} \sigma_1 \\ \sigma_2 \\ \tau_{12} \end{bmatrix} = \begin{bmatrix} C_{11} & C_{12} & \\ C_{12} & C_{22} & \\ & & C_{33} \end{bmatrix} \begin{bmatrix} \epsilon_1 \\ \epsilon_2 \\ \gamma_{12} \end{bmatrix}$$



C14

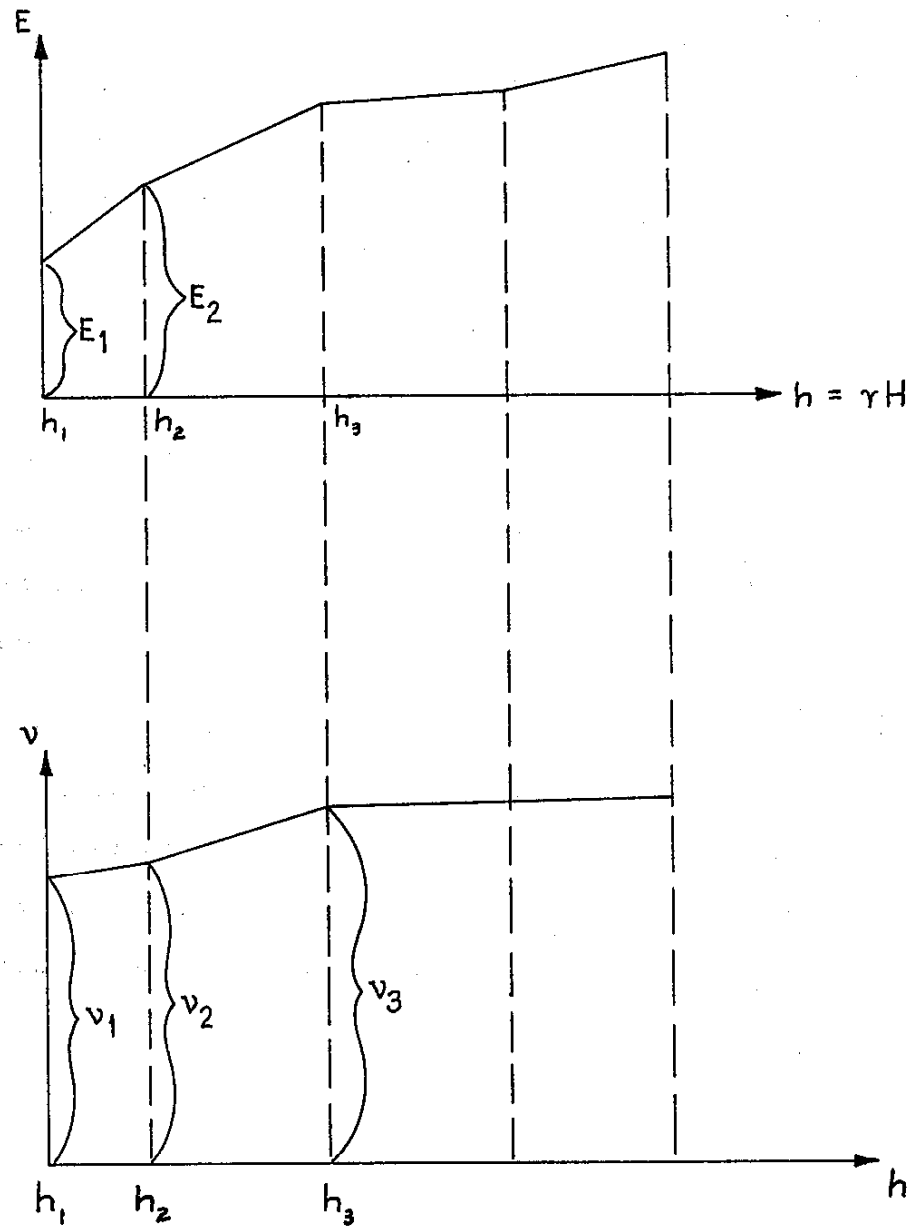


Figure C-2a - Typical plots of E and ν - Overburden

Reinforced earth materials are described by: a) specifying the appropriate properties for the soil and b) specifying the size, spacing and elastic properties of the reinforcing strips.

The quantities which define the reinforcing strips are illustrated in Figure C-3.

5. Not all numbers between 1 and the maximum node number need correspond to actual nodes in the body, e.g, the grid shown in Figure C-4 is permissible; coordinates may or may not be specified for the nonexistent nodes 15 and 21. This feature facilitates the use of the various data generation options (e.g., see "Comment 7").

6. The program has available two generation procedures to assist the User in describing the location of the node points. These generation options are described in the following two "comments." The use of these options can, for instance, permit one to describe the location of the nodes for an arbitrarily large grid by as few as four cards.

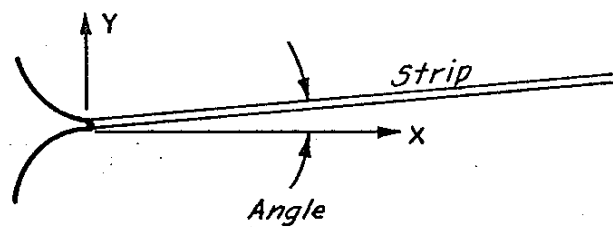
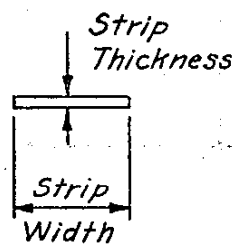
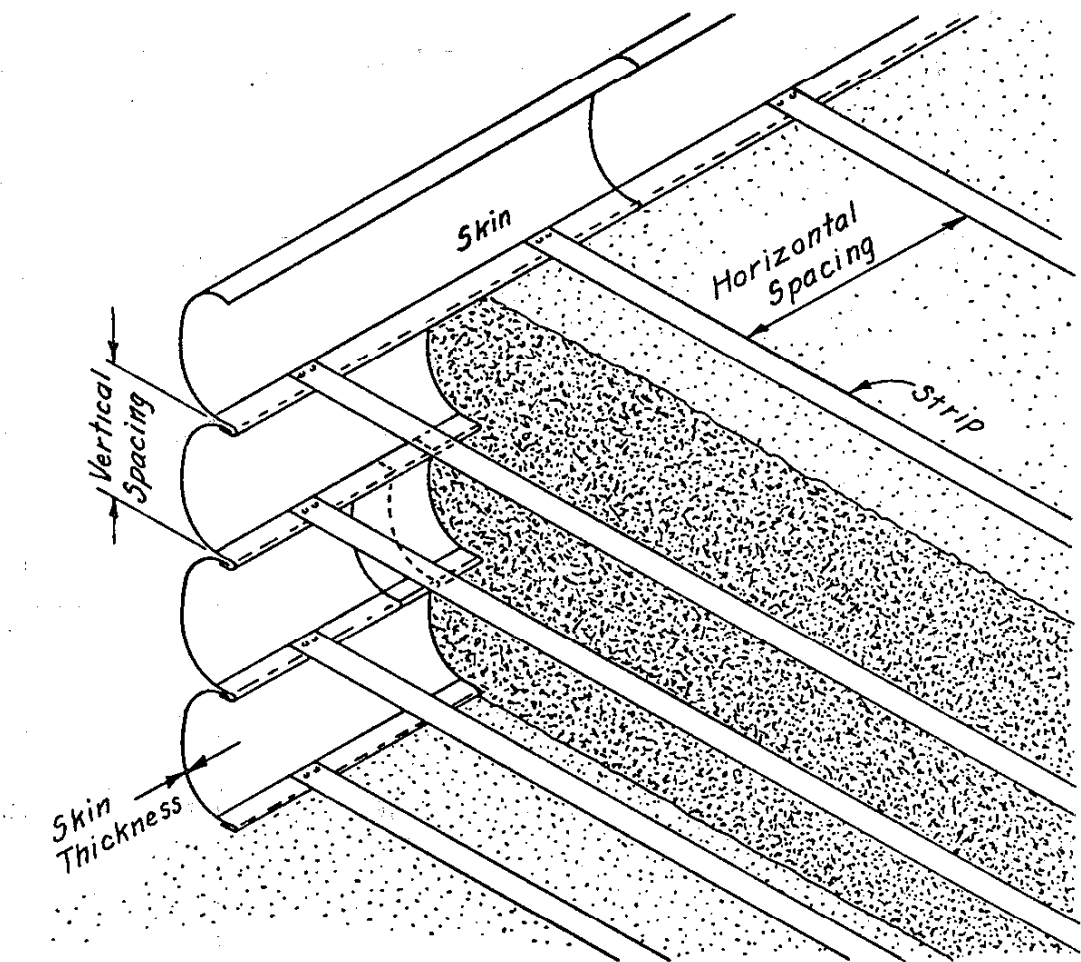


Figure C-3 - Reinforced Earth Input Properties

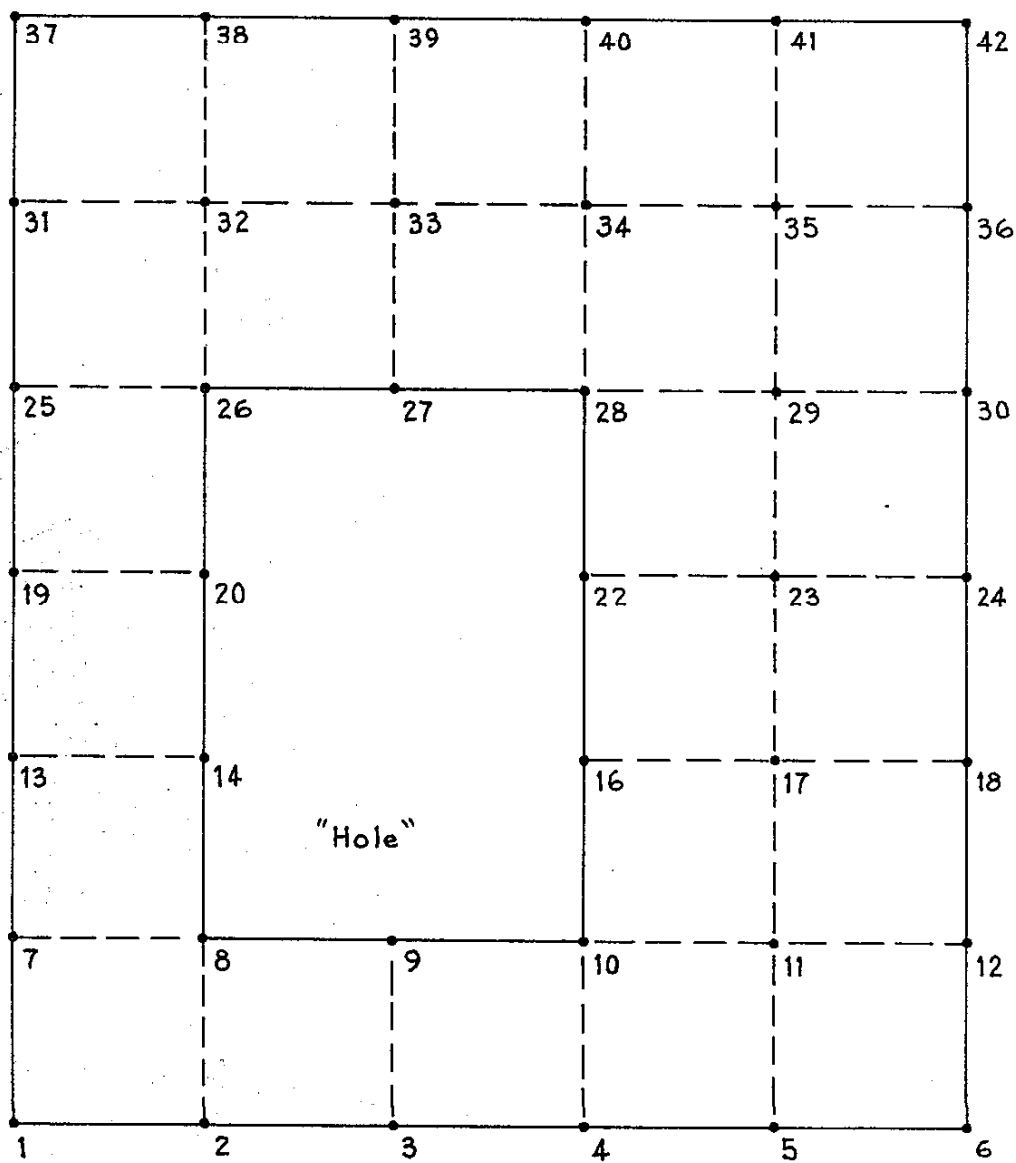


Figure C-4 - Example of grid with missing node numbers.

7. The "straight line coordinate generation option" may be used whenever several sequential points lie along a straight line. For such points it is only necessary to enter data for the end points (denoted as N and N') of the sequence and values for INC and D. INC is the difference between two successive node numbers in the sequence and D is the ratio of the distances between successive pairs of points. The end points of the segment may be entered in any order, i.e. the line segment shown in Figure C-5 may be defined by specifying the end-points in order 7 → 22 or 22 → 7. The spacing of the intermediate points is controlled by the value of the spacing ratio D. D is equal to the ratio of the lengths of the successive segments defined by the intermediate points. A value of $D = 1.0$ gives equally spaced points. The locations of the intermediate points 12 and 17 (see Figure C-5) could be generated by either specifying points 7 → 22 and $D = 2.0$ (Note: $D = 2.0/1.0 = 4.0/2.0$), or 22 → 7 and $D = 0.5$ (Note: $D = 2.0/4.0 = 1.0/2.0$); the value of INC would be 5.

For the grid shown in Figure C-2 the coordinates could be generated for the points lying between 1-4, 5-8, 9-12, etc., or between 1-29, 2-18, 18-30, 3-31 etc. Note that the line 3-31 cannot be extended to point 33 as the value of INC changes at point 31, however, if nodes 33 and 34 had been instead numbered 35 and 36 (there would then have been no nodes numbered 33 and 34, see "comment 5") it would be possible to generate all the nodes along the line with a single card.

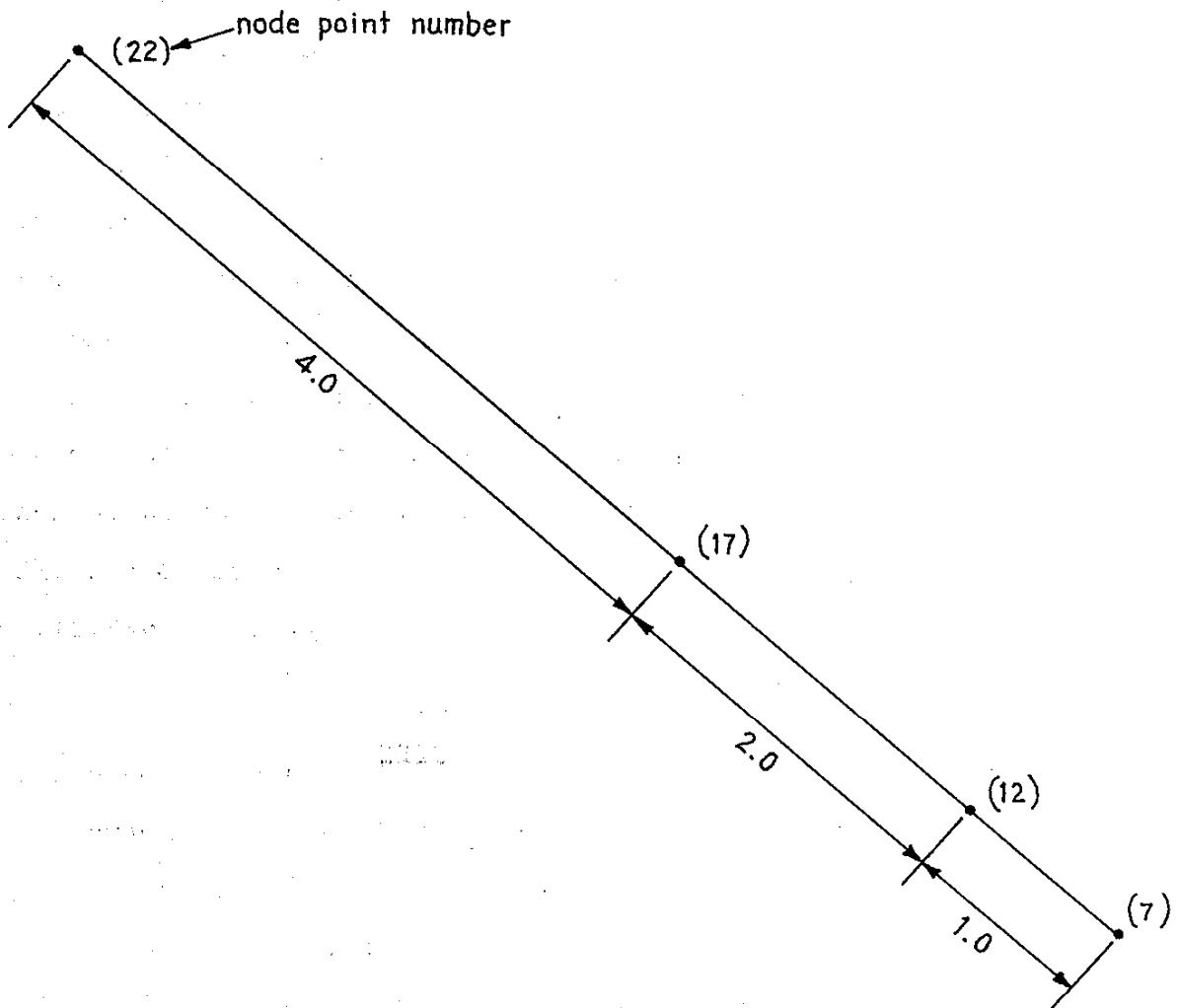
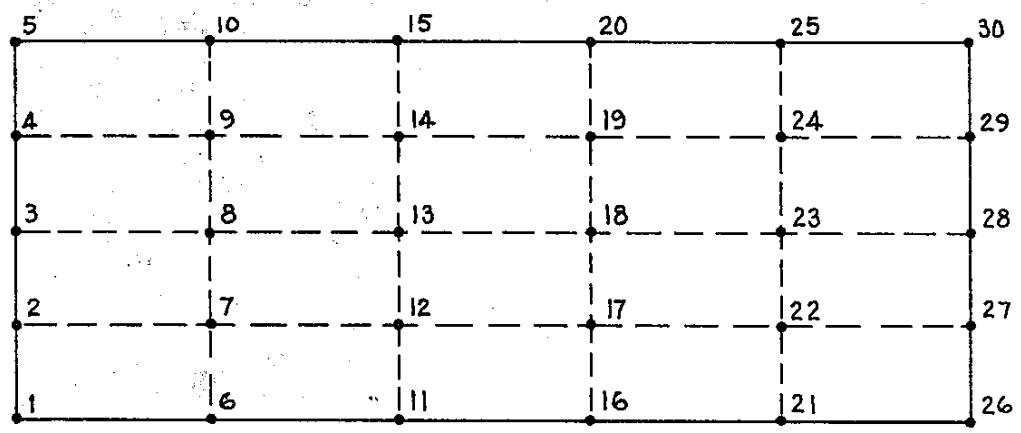


Figure C-5 - Node points lying on straight line.

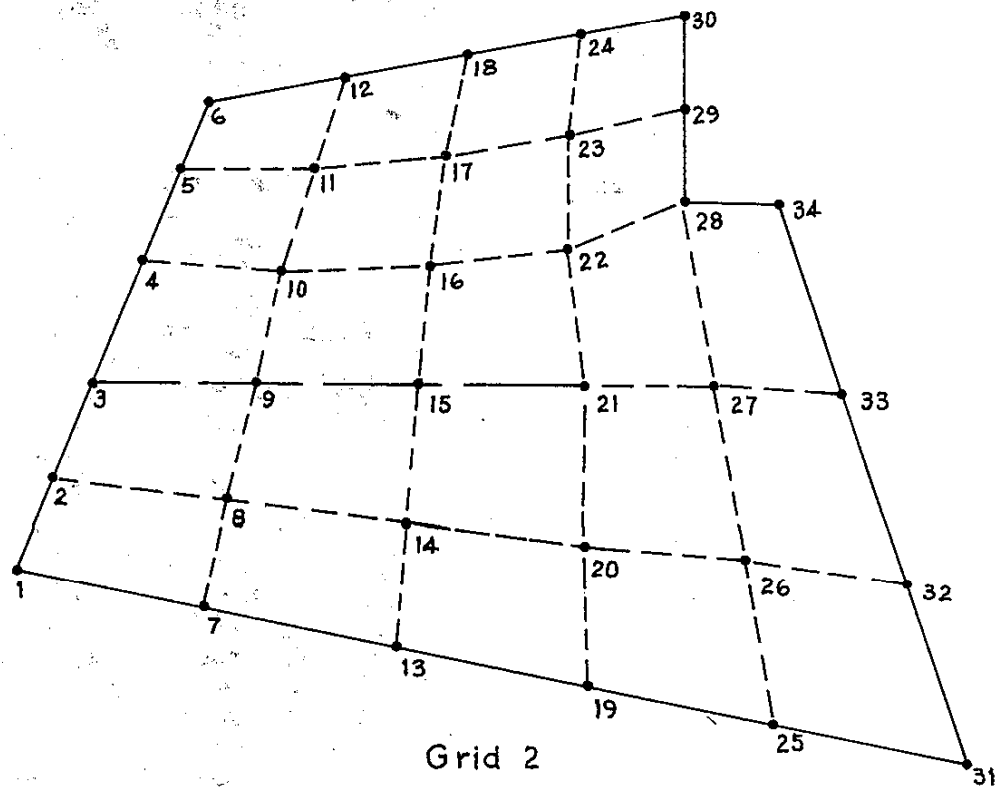
8. The "interior node point generation option" locates all nodes interior to the body whose coordinates have not been specifically specified by the user (i.e. all points not specifically treated in Section B1). The location of the interior nodes is accomplished by the so called "Laplacian generation scheme", i.e., the coordinates of an interior node point are selected so that they are equal to the average of the coordinates of the neighboring nodes. Note that all nodes on the boundaries of the body must be either directly specified or generated by means of the straight line generation scheme (described in "comment 7"). Figure C-6 illustrates two grids which have been prepared with the aid of this generation scheme. Grid 1 was prepared by specifying the locations of the exterior nodes by means of the straight line generation scheme; the interior nodes were left unspecified and hence were "generated" as described above. Grid 2 was prepared in a similar way with the exception that the interior sequence of nodes lying on the line 3-21 were generated with the "straight line generation scheme".

9. When the values of MN, and/or IN remain constant for a number of sequential element cards, it is only necessary to specify MN and/or IN for the first card in the group (the appropriate columns are left blank for the remainder of the cards in the group).

10. If the body is divided into layers of elements, and the quantities MN and IN remain the same for a number of elements within a layer (and possibly the same for a number of layers), the node numbers for these elements may be simply specified by



Grid 1



Grid 2

Figure C-6 - Grids prepared with the aid of the generation options.

using the "element data generation option". To use the generation option for the elements in a single layer the data is supplied for the first element in the layer and the appropriate values are specified for NMIS and INC. The quantity NMIS indicates the number of additional elements in the sequence. The quantity INC indicates the amount by which the node numbers of successive elements differ.

For example the bottom row of elements in Figure C-2 could be specified by giving the node numbers for element "a" and the values NMIS = 6 and INC = 4 or the information for element "b" and the values NMIS = 6 and INC = -4 (in order to use this option all the elements from a → b must, however, have the same values of MN and IN). Alternatively if one wished to generate the element information for the elements in the left hand column (all these elements would need to have the same values of MN and IN), one could do this by giving the node numbers for element "a" and the values NMIS = 2 and INC = 1, etc.

In addition, if the values of MN and IN remain unchanged for a number of layers the data information for all the elements in these layers may be generated with a single card by supplying, in addition to the values of NMIS and INC (for the first layer), the values of NMISP and INCP. NMISP denotes the number of additional layers for which the element data is to be generated and INCP indicates the difference between the node numbers of the successive layers. For example, if the bottom two layers of elements in Figure C-2 all had identical values of MN and IN the data for all these elements could be generated by giving the appropriate data for element "a" and the values

```
NMIS = 6  
INC = 4  
NMISP = 1  
INCP = 1
```

or alternatively

```
NMIS = 1  
INC = 1  
NMISP = 6  
INCP = 4
```

As a second example if the elements of Grid 1 of Figure C-6 all had identical values of MN and IN they all could be described by giving the appropriate data for the lower left element and

```
NMIS = 3  
INC = 1  
NMISP = 4  
INCP = 5
```

11. For each of the two directions (see "comment 12") one either specifies the displacement by setting "IF" equal to one and "V" equal to the specified displacement or adds in the "boundary load" by leaving "IF" blank and setting "V" equal to the boundary load (i.e. resultant of specified boundary stress). Boundary displacements and forces are positive when they have the same sense as the positive coordinate direction. If a boundary point is not constrained and has no load applied to it, it is not necessary and is in fact economically not desirable to include the point in the boundary array.

A point load may be applied at any node point within the structure by treating it as a boundary point.

Specified loads are applied to the structure during construction increment IN. A specified displacement is applied during construction increment IN, during all other increments, the incremental displacement for that point is taken to be zero. If at a given point, loads are applied during more than one of the construction increments, this may be achieved by specifying the point more than once in the boundary array.

12. If $\theta = 0$ the subscripts 1 and 2 refer to x and y, if $\theta \neq 0$ (see Figure C-1) they refer to X_1 and X_2 , (i.e. $IF_1 = IF_{X_1}$, etc.).

13. If several sequential points have identical boundary conditions, they may all be considered with a single card by supplying the proper values for the quantities N' and INC. The quantity N' denotes the number of the last point in the sequence. The quantity INC specifies the difference between the node numbers of successive points.

If for example the points 1 → 21 on the bottom boundary of the structure shown in Figure C-2 all had the same boundary condition specifications, this could be accomplished by specifying the appropriate boundary conditions and $N = 1$, $N' = 21$, $INC = 4$.

14. Uniform or linearly varying pressure may be applied to a straight or curved boundary by using the boundary condition generation option (see "comment 13" - leaving the spaces for IF_1 , IF_2 , V_1 , V_2 and TH blank) for the points involved and specifying appropriate values for P_N and $P_{N'}$ (if the pressure is uniform $P_N = P_{N'}$). For example, for the boundary shown in Figure C-7 one would specify:

$N = 11$
 $N' = 2$
 $INC = -3$
 $P_N = 100$
 $P_{N'} = 50$

The points $N \rightarrow N'$ must be specified in a counterclockwise order as one proceeds along an external boundary and clockwise along internal boundaries (i.e., inside holes in the body). Pressure specification cards must precede all others in the "Boundary Condition Array".

15. Those reinforced earth elements which are on the edge of the earth structure where a "skin plate" is present are flagged by setting $IPRNT = 1$.

16. A bending (and stretching) element (stripplate element for plane strain, beam element for plane stress) may be placed between any two nodes in the system. If two or more bending elements intersect at a node the connection between them is treated as rigid. Curved members may be approximated by a series of straight elements. In the element array bending elements are designated by leaving their 3rd and 4th node numbers blank.

17. The section properties of a bending element are described by specifying values of area (A) and moment of inertia (I). For plane stress analyses A and I are the appropriate values for a unit width of the bending element. The Young's modulus of the material is denoted by E . For plane strain the values of Poisson's ratio is supplied for ν while the plane stress $\bar{\nu}$ is assigned a value of zero. The quantities n_{max} , n_{min} and Tau_r are described in Section III-B-1-b (i.e., description of output for beam element).

18. Slope boundary conditions for bending elements are specified automatically by the program as follows: If no displacement boundary conditions are specified for a node at the end of a bending member the moment at the end of the bending member is taken to be zero; if one or both of the displacements are specified the slope of the bending element is set equal to zero.

19. The "Element Excavation Increment Number" specifies the increment during which the material in the element is to be excavated. If the material is not to be excavated the number is left blank (the program then sets it equal to 99).

For a given analysis if there is to be excavation all "Type B" materials (see note 4 and Figure C-2a) require additional input. For excavation problems "Type B" materials require that two plots of "E and $v \sim$ overburden" be specified.

The first (loading behavior) is used in all increments prior to the first excavation increment for the problem. The second description (unloading behavior) is used for all subsequent increments. Both descriptions must have the same number of points in the specifications of the "E & $v \sim$ " curves. For example, for an excavation problem if material number 3 is of type B with 6 points defining the E & v curves, then material 4 must be a dummy material that is used to record the unloading behavior for material 3 (6 points must also be used to describe the unloading curves). All elements made of this material are given material number 3.

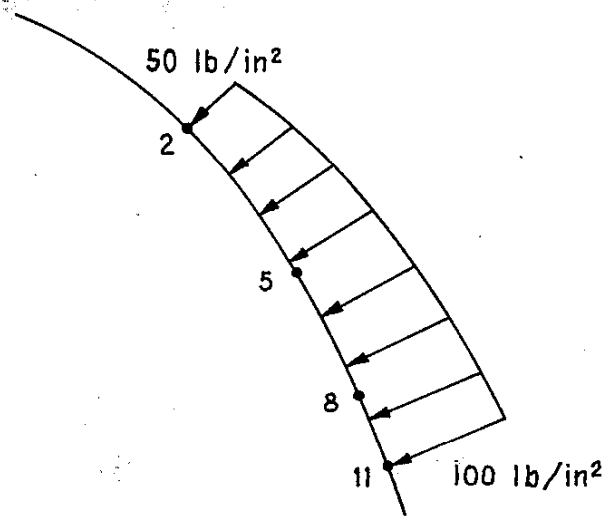


Figure C-7 - Pressurized boundary.

COMMENTARY B

Discussion of Program

In this appendix very brief descriptions of the uses and special features of the program are given. The theory of the finite element procedure is, however, not discussed; instead the reader is referred to standard works on the subject such as the book by Zienkiewicz*.

This finite element program may be applied to a wide range of problems in structural engineering and mechanics. The program may be directly, or with only minor modification, applied to any elasticity problem that may be characterized as plane stress or plane strain. The program is specifically set up for plane strain problems; the use of the program for plane stress problems is described in comment 4 of Commentary A. In addition the program has certain unique features which make it particularly suitable for the analysis of ordinary and reinforced earth structures (e.g., embankments) situated on soil or rock foundations. These special features include provisions for the consideration of:

1. The incremental construction sequence
2. Overburden dependent material properties
3. Orthotropic material behavior
4. Reinforced earth construction
5. Bending members

The basic theory underlying an incremental construction analysis may be found in the paper by Clough and Woodward**. Basically such

*The Finite Element Method in Engineering Science, McGraw-Hill, London, 1971.

**"Analysis of Embankment Stresses and Deformations," J. of the Soil Mech. and Foundations Div. of the ASCE, Vol. 93. No. SM4, July 1967, pp. 529-549.

analyses permit account to be taken of the fact that an earth embankment is not formed in one operation but is instead placed as a sequence of layers. Thus the program may be used to predict the stresses and deformations developed in all existing layers as each new layer is placed.

For soils whose properties are functions of the overburden their properties may be modeled by utilizing (see comment 4 in Commentary A) the special provision in the program for the description of this dependence.

The inclusion of the option of prescribing an orthotropic stress-strain law permits the characterization of layers which exhibit directionally dependent material properties.

The program is specially designed for the analysis of reinforced earth structures. The user supplies to the program a description of the spacing, size and elastic properties of the reinforcing strips and the properties of the soil. Utilizing these properties the program calculates "composite properties" for the reinforced earth (these calculations are based upon the model developed by Romstad and Herrmann*). Utilizing these "composite properties" for the reinforced earth a finite element analysis of the structure subjected to the loads prescribed by the user is performed. From the finite element analysis the composite stresses and strains developed in the reinforced earth are obtained. The program then uses the composite stresses and strains in calculations which yield the corresponding stresses and strains in the soil and the axial forces and moments developed in the reinforcing strips (these calculations follow from the above mentioned model*).

*"Material Properties of Reinforced Earth," Consulting Report to California Division of Highways, July 1972.

The bending (and stretching) element may be used, for example, to model cross-sections of culverts or bridges which pass through the embankment.

The finite element analysis utilizes a recently developed element that is considerably more accurate than previously available simple elements. The derivation and characteristics of this element are described in detail in a paper by Herrmann*.

The "Input" procedures used in the program represent an attempt to minimize the effort required by the user for data preparation and represents a combination of numerous suggestions made to the authors by users of related finite element programs over the past years.

*"Efficiency Evaluation of a Two-Dimensional Incompatible Finite Element," J. of Computers and Structures, June 1972.

COMMENTARY C

Sample Problem

In this commentary the input and output for a sample problem are given. The problem is intended to serve as an example of the input and output formats, and a check-problem that may be used to determine if the program is functioning properly. For the sake of simplicity a very much coarser grid is used for this sample problem than would be used in an actual analysis.

The configuration of the problem is shown in Figure C-8. The first number contained within parentheses within an element indicates the material type, the second, the incremental construction number. The number in parentheses next to the external load, indicates the construction increment during which this load is applied. Material 1 is taken to have been in place prior to construction, hence, its weight is not a new factor and thus its density is set equal to zero.

The input data and the output from the program follow (Note: Units of lbs. and ft. were used in this example, e.g., moduli and stress are expressed in psf):

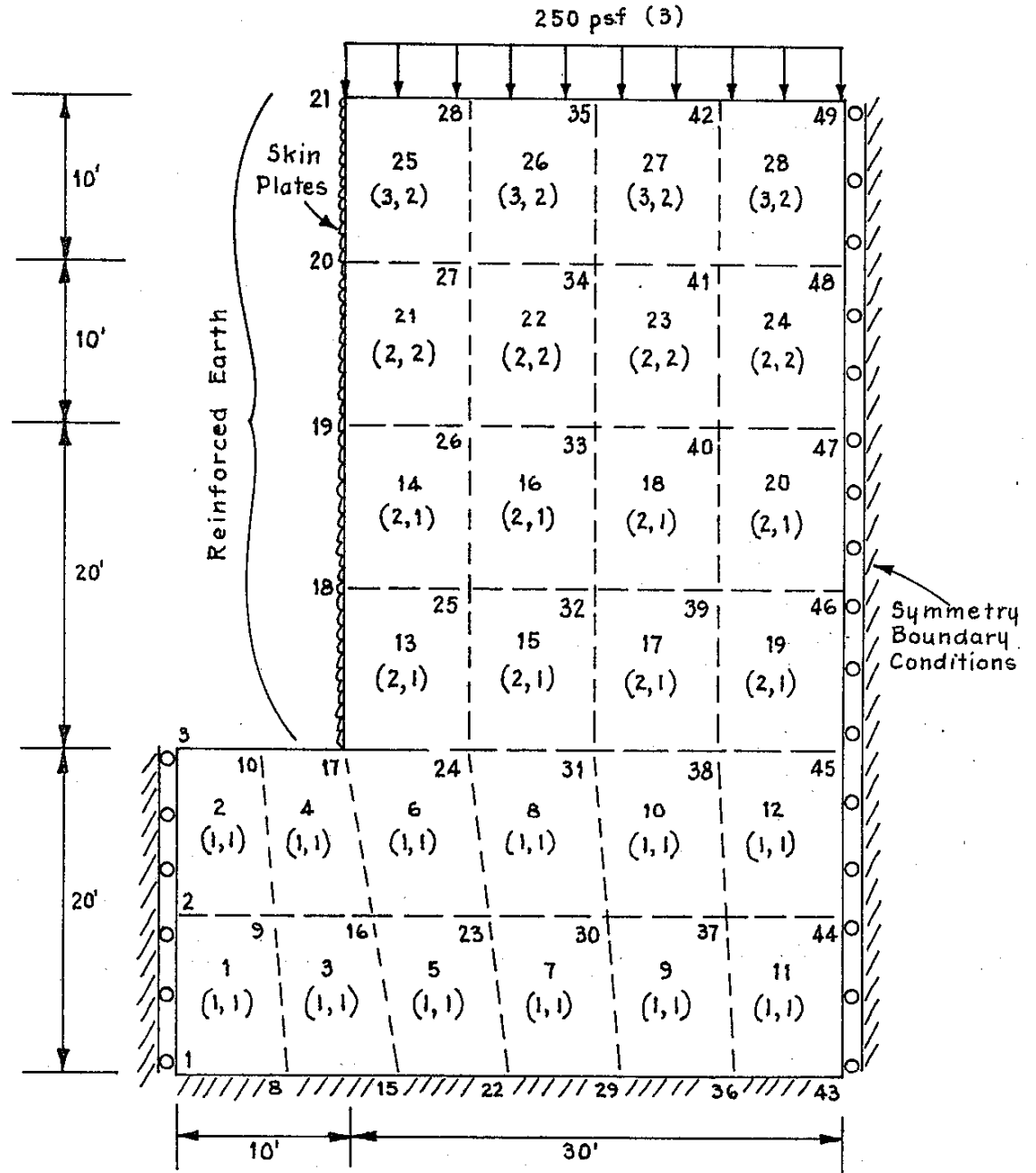
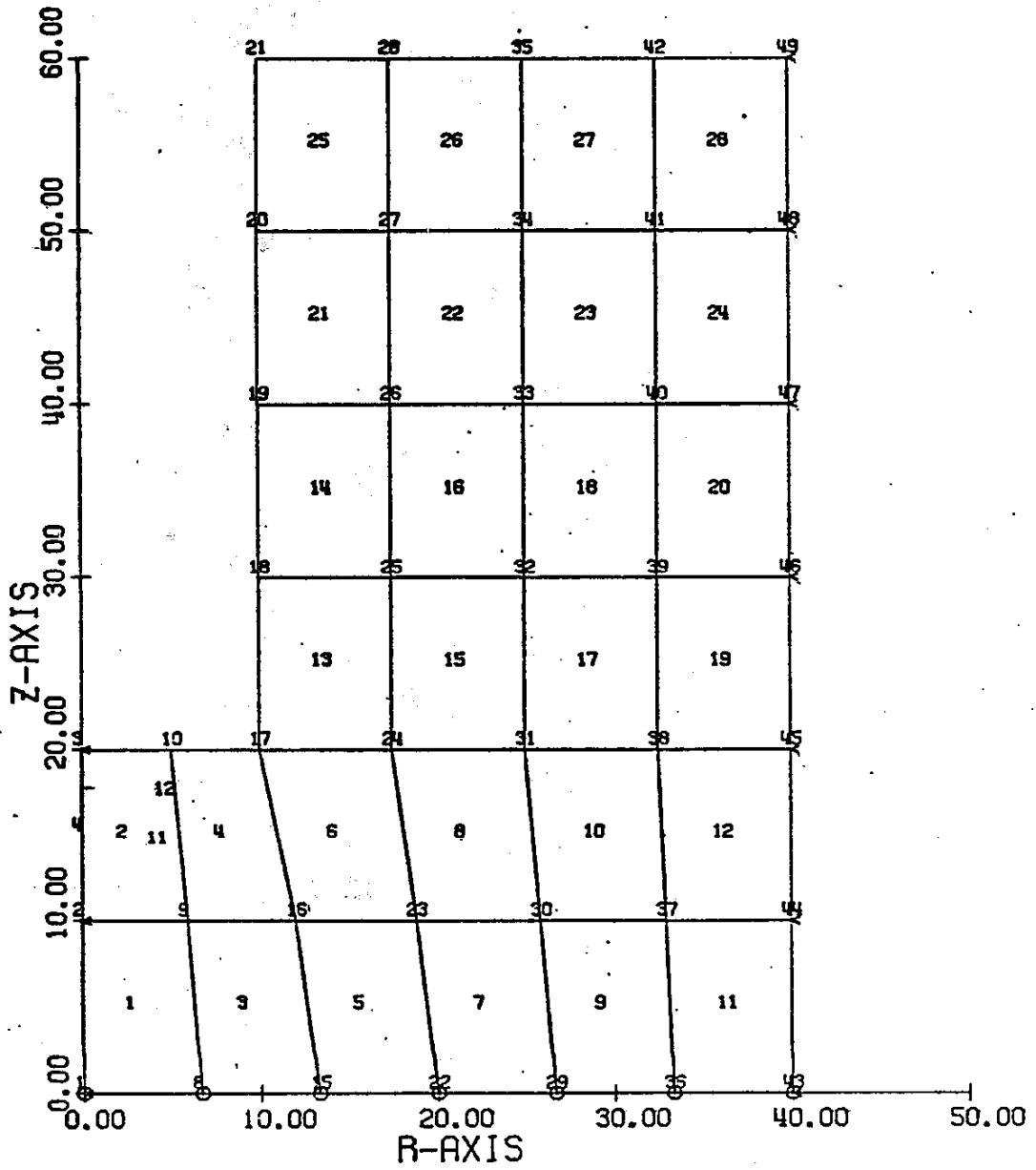


Figure C-8 - Sample problem.



END OF PLOT TAPE011549 DATED 02/23/73

REINFORCED EARTH EXAMPLE--VERY COARSE GRID

INPUT DATA CARD IMAGE ****

REINFORCED EARTH EXAMPLE--VERY COARSE GRID

3 6.15 0 OE132 CLETUS 6964

1				15000000.	.3		
2 3 4	130.			3000000.	.4		
4.32E+09	.131	.00985	3.28	.833		.0104	
2000.	4200000.	.4					
4000.	5200000.	.4					
10000.	6700000.	.4					
3 3 4	130.			3000000.	.4		
4.32E+09	.131	.00985	4.92	.833		.0104	
2000.	4200000.	.4					
4000.	5200000.	.4					
10000.	6700000.	.4					

1

1			43	40.			7
2		10.					
44	40.	10.					
3		20.	17	10.	20.		7
17	10.	20.	45	40.	20.		7
17	10.	20.	20	10.	50.		1
45	40.	20.	48	40.	50.		1
20	10.	50.	48	40.	50.		7
21	10.	60.	49	40.	60.		7

2

1	8	9	2	1	1	5	7	1	1	
17	24	25	18	2	1	1	1			1
24	31	32	25	2	1	2	7	1	1	
19	26	27	20	2	2					1
26	33	34	27	2	2	2	7			
20	27	28	21	3	2					1
27	34	35	28	3	2	2	7			

3

49								3	21	-7	250.	250
1	1								3			
1	1		1						43	7		
43	1								49	1		

4

REINFORCED EARTH EXAMPLE--VERY COARSE GRID

NUMBER OF CONSTRUCTION INCREMENTS = 3

PROPERTIES FOR MATERIAL 1 *****

DENSITY = 0.0

YOUNGS MODULUS= 0.1500E 08
POISSONS RATIO= 0.3000E 00

PROPERTIES FOR MATERIAL 2 *****

DENSITY = 1.30000E 02

REINFORCED EARTH

STRIP YOUNGS MODULUS= 0.4320E 10
STRIP WIDTH= 0.1310E 00
STRIP THICKNESS= 0.9850E-02
HORIZONTAL SPACING= 0.3280E 01
VERTICAL SPACING= 0.8330E 00
ANGLE= 0.0
SKIN THICKNESS IF BOUNDARY ELEMENT= 0.1040E-01
SOIL PROPERTIES

ELASTIC PROPERTIES - OVERBURDEN

OVERBURDEN	YOUNGS MODULUS	POISSONS RATIO
0.0	3.00E 06	4.00E-01
2.00E 03	4.20E 06	4.00E-01
4.00E 03	5.20E 06	4.00E-01
1.00E 04	6.70E 06	4.00E-01

PROPERTIES FOR MATERIAL 3 *****

DENSITY = 1.30000E 02

REINFORCED EARTH

STRIP YOUNGS MODULUS= 0.4320E 10
 STRIP WIDTH= 0.1310E 00
 STRIP THICKNESS= 0.9850E-02
 HORIZONTAL SPACING= 0.4920E 01
 VERTICAL SPACING= 0.8330E 00
 ANGLE= 0.0
 SKIN THICKNESS IF BOUNDARY ELEMENT= 0.1040E-01

SOIL PROPERTIES

ELASTIC PROPERTIES - OVERBURDEN

OVERBURDEN	YOUNGS MODULUS	POISSONS RATIO
0.0	3.00E 06	4.00E-01
2.00E 03	4.20E 06	4.00E-01
4.00E 03	5.20E 06	4.00E-01
1.00E 04	6.70E 06	4.00E-01

NODAL POINT	X COORDINATE	Y COORDINATE	NODAL POINT	X COORDINATE	Y COORDINATE
1	0.0	0.0	17	10.00	20.00
2	0.0	10.00	18	10.00	30.00
3	0.0	20.00	19	10.00	40.00
4	0.0	15.00	20	10.00	50.00
5	0.0	17.50	21	10.00	60.00
6	0.0	16.25	22	20.00	0.0
7	0.0	16.88	23	18.85	10.00
8	6.67	0.0	24	17.50	20.00
9	5.92	10.00	25	17.50	30.00
10	5.00	20.00	26	17.50	40.00
11	4.17	14.22	27	17.50	50.00
12	4.58	17.11	28	17.50	60.00
13	4.37	15.66	29	26.67	0.0
14	4.48	16.39	30	25.86	10.00
15	13.33	0.0	31	25.00	20.00
16	12.03	10.00	32	25.00	30.00
33	25.00	40.00			
34	25.00	50.00			
35	25.00	60.00			
36	33.33	0.0			
37	32.92	10.00			
38	32.50	20.00			
39	32.50	30.00			
40	32.50	40.00			
41	32.50	50.00			
42	32.50	60.00			
43	40.00	0.0			
44	40.00	10.00			
45	40.00	20.00			
46	40.00	30.00			
47	40.00	40.00			
48	40.00	50.00			
49	40.00	60.00			

ELEM NO.	ELEMENT NODAL POINTS				MAT NO.	CONST INCR.	ELEM NO.	ELEMENT NODAL POINTS				MAT NO.	CONST INCR.
1	1	8	9	2	1	1	10	37	38	31	30	1	1
2	2	9	10	3	1	1	11	43	44	37	36	1	1
3	8	15	16	9	1	1	12	37	44	45	38	1	1
4	16	17	10	9	1	1	13	17	24	25	18	2	1
5	15	22	23	16	1	1	14	18	25	26	19	2	1
6	16	23	24	17	1	1	15	24	31	32	25	2	1
7	29	30	23	22	1	1	16	32	33	26	25	2	1
8	23	30	31	24	1	1	17	31	38	39	32	2	1
9	36	37	30	29	1	1	18	32	39	40	33	2	1

ELEM NO.	ELEMENT NODAL POINTS				MAT NO.	CONST INCR.
19	38	45	46	39	2	1
20	39	46	47	40	2	1
21	19	26	27	20	2	2
22	26	33	34	27	2	2
23	33	40	41	34	2	2
24	47	48	41	40	2	2
25	20	27	28	21	3	2
26	27	34	35	28	3	2
27	34	41	42	35	3	2
28	41	48	49	42	3	2

*****BOUNDARY CONDITIONS*****

BOUNDARY NODE		INCREMENT NO.			
49	P-X= 0.0	P-Y= -9.38E 02	ANG= 0.0	3	
42	P-X= 0.0	P-Y= -1.88E 03	ANG= 0.0	3	
35	P-X= 0.0	P-Y= -1.88E 03	ANG= 0.0	3	
28	P-X= 0.0	P-Y= -1.88E 03	ANG= 0.0	3	
21	P-X= 0.0	P-Y= -9.38E 02	ANG= 0.0	3	
1	U-X= 0.0	P-Y= 0.0	ANG= 0.0	1	
2	U-X= 0.0	P-Y= 0.0	ANG= 0.0	1	
3	U-X= 0.0	P-Y= 0.0	ANG= 0.0	1	
1	U-X= 0.0	U-Y= 0.0	ANG= 0.0	1	
8	U-X= 0.0	U-Y= 0.0	ANG= 0.0	1	
15	U-X= 0.0	U-Y= 0.0	ANG= 0.0	1	
22	U-X= 0.0	U-Y= 0.0	ANG= 0.0	1	
29	U-X= 0.0	U-Y= 0.0	ANG= 0.0	1	
36	U-X= 0.0	U-Y= 0.0	ANG= 0.0	1	
43	U-X= 0.0	U-Y= 0.0	ANG= 0.0	1	
44	U-X= 0.0	P-Y= 0.0	ANG= 0.0	1	
45	U-X= 0.0	P-Y= 0.0	ANG= 0.0	1	
46	U-X= 0.0	P-Y= 0.0	ANG= 0.0	1	
47	U-X= 0.0	P-Y= 0.0	ANG= 0.0	1	
48	U-X= 0.0	P-Y= 0.0	ANG= 0.0	1	
49	U-X= 0.0	P-Y= 0.0	ANG= 0.0	1	

CONSTRUCTION INCREMENT 1

ELEMENT NO.	X	Y	EPSILON-X	EPSILON-Y	GAMA-XY
1	3.33E 00	5.00E 00	-2.60E-05	-4.57E-05	-4.00E-05
2	2.96E 00	1.50E 01	-5.00E-05	5.17E-06	-3.16E-05
3	9.63E 00	5.00E 00	-5.30E-06	-7.17E-05	-5.63E-05
4	7.96E 00	1.50E 01	-3.85E-05	-4.54E-05	-1.30E-04
5	1.60E 01	5.00E 00	3.01E-06	-9.64E-05	-5.72E-05
6	1.44E 01	1.50E 01	1.03E-05	-1.08E-04	-8.07E-05
7	2.29E 01	5.00E 00	9.35E-06	-1.15E-04	-3.87E-05
8	2.17E 01	1.50E 01	1.67E-05	-1.27E-04	-2.95E-05
9	2.98E 01	5.00E 00	8.85E-06	-1.22E-04	-1.94E-05
10	2.92E 01	1.50E 01	1.93E-05	-1.31E-04	-1.39E-05
11	3.67E 01	5.00E 00	8.53E-06	-1.24E-04	-6.36E-06
12	3.63E 01	1.50E 01	1.97E-05	-1.33E-04	-3.71E-06
13	1.38E 01	2.50E 01	9.88E-05	-3.31E-04	-2.45E-04
STRIP AXIAL FORCE=			5.510E 02	MOMENT= 5.548E-03	
SKIN MEMBRANE STRESS=			0.374E 05		
14	1.37E 01	3.50E 01	7.07E-05	-1.32E-04	8.80E-05
STRIP AXIAL FORCE=			3.942E 02	MOMENT= 8.052E-03	
SKIN MEMBRANE STRESS=			0.470E 04		
15	2.12E 01	2.50E 01	6.07E-05	-2.89E-04	-1.27E-04
STRIP AXIAL FORCE=			3.385E 02	MOMENT= 5.894E-03	
16	2.12E 01	3.50E 01	7.64E-05	-1.56E-04	2.98E-05
STRIP AXIAL FORCE=			4.259E 02	MOMENT= 7.309E-03	
17	2.87E 01	2.50E 01	4.73E-05	-2.83E-04	-5.28E-05
STRIP AXIAL FORCE=			2.635E 02	MOMENT= 6.068E-03	
18	2.87E 01	3.50E 01	6.59E-05	-1.39E-04	3.74E-06
STRIP AXIAL FORCE=			3.675E 02	MOMENT= 7.107E-03	
19	3.62E 01	2.50E 01	4.23E-05	-2.78E-04	-1.59E-05
STRIP AXIAL FORCE=			2.357E 02	MOMENT= 6.126E-03	
20	3.62E 01	3.50E 01	6.37E-05	-1.38E-04	-2.45E-07
STRIP AXIAL FORCE=			3.554E 02	MOMENT= 7.024E-03	

ELEMENT NO.	SIGMA-X	SIGMA-Y	TAU-XY	SIGMA-1	SIGMA-2	ANG
1	-9.21E 02	-1.15E 03	-2.31E 02	-7.77E 02	-1.29E 03	-3.19E 01
2	-9.65E 02	-3.28E 02	-1.82E 02	-2.80E 02	-1.01E 03	1.05E 02
3	-7.28E 02	-1.49E 03	-3.25E 02	-6.09E 02	-1.61E 03	-2.02E 01
4	-1.17E 03	-1.25E 03	-7.47E 02	-4.62E 02	-1.96E 03	-4.35E 01
5	-7.73E 02	-1.92E 03	-3.30E 02	-6.85E 02	-2.01E 03	-1.50E 01
6	-7.29E 02	-2.09E 03	-4.66E 02	-5.85E 02	-2.24E 03	-1.71E 01
7	-8.04E 02	-2.24E 03	-2.23E 02	-7.70E 02	-2.27E 03	-8.67E 00
8	-7.66E 02	-2.43E 03	-1.70E 02	-7.49E 02	-2.45E 03	-5.77E 00
9	-8.78E 02	-2.39E 03	-1.12E 02	-8.70E 02	-2.40E 03	-4.21E 00
10	-7.45E 02	-2.48E 03	-8.01E 01	-7.41E 02	-2.48E 03	-2.64E 00
11	-9.01E 02	-2.43E 03	-3.67E 01	-9.01E 02	-2.43E 03	-1.37E 00
12	-7.53E 02	-2.52E 03	-2.14E 01	-7.53E 02	-2.52E 03	-6.96E-01
13	-9.33E 02	-2.03E 03	-3.14E 02	-8.50E 02	-2.12E 03	-1.49E 01
14	-1.17E 02	-5.79E 02	1.00E 02	-9.65E 01	-6.00E 02	1.17E 01
15	-1.01E 03	-1.91E 03	-1.63E 02	-9.85E 02	-1.94E 03	-9.99E 00
16	-1.89E 02	-7.19E 02	3.40E 01	-1.86E 02	-7.21E 02	3.65E 00
17	-1.09E 03	-1.94E 03	-6.76E 01	-1.08E 03	-1.94E 03	-4.54E 00
18	-1.82E 02	-6.49E 02	4.27E 00	-1.82E 02	-6.49E 02	5.23E-01
19	-1.10E 03	-1.92E 03	-2.04E 01	-1.10E 03	-1.92E 03	-1.42E 00
20	-1.93E 02	-6.52E 02	-2.80E-01	-1.93E 02	-6.52E 02	-3.49E-02

NODAL POINT	X DISPLCEMNT	Y DISPLCEMNT	NODAL POINT	X DISPLCEMNT	Y DISPLCEMNT
1	0.0	0.0	17	-5.61E-04	-1.53E-03
2	0.0	-3.06E-04	18	-3.18E-03	-5.25E-03
3	0.0	-3.15E-04	19	-9.75E-04	-6.14E-03
4	0.0	0.0	20	0.0	0.0
5	0.0	0.0	21	0.0	0.0
6	0.0	0.0	22	0.0	0.0
7	0.0	0.0	23	-3.65E-04	-1.07E-03
8	0.0	0.0	24	-4.47E-04	-2.29E-03
9	-3.35E-04	-5.77E-04	25	-1.81E-03	-5.19E-03
10	-2.09E-04	-4.38E-04	26	-1.28E-03	-6.92E-03
11	0.0	0.0	27	0.0	0.0
12	0.0	0.0	28	0.0	0.0
13	0.0	0.0	29	0.0	0.0
14	0.0	0.0	30	-2.37E-04	-1.20E-03
15	0.0	0.0	31	-3.31E-04	-2.48E-03
16	-4.06E-04	-8.12E-04	32	-1.01E-03	-5.37E-03
33	-9.33E-04	-6.75E-03			
34	0.0	0.0			
35	0.0	0.0			
36	0.0	0.0			
37	-1.17E-04	-1.23E-03			
38	-1.71E-04	-2.57E-03			
39	-4.63E-04	-5.35E-03			
40	-4.93E-04	-6.75E-03			
41	0.0	0.0			
42	0.0	0.0			
43	0.0	0.0			
44	0.0	-1.25E-03			
45	0.0	-2.58E-03			
46	0.0	-5.36E-03			
47	0.0	-6.72E-03			
48	0.0	0.0			
49	0.0	0.0			

CONSTRUCTION INCREMENT 2

ELEMENT NO.	X	Y	EPSILON-X	EPSILON-Y	GAMA-XY
1	3.33E 00	5.00E 00	-5.40E-05	-1.02E-04	-8.54E-05
2	2.96E 00	1.50E 01	-1.09E-04	1.10E-05	-7.05E-05
3	9.63E 00	5.00E 00	-7.96E-06	-1.52E-04	-1.09E-04
4	7.96E 00	1.50E 01	-8.36E-05	-1.02E-04	-2.86E-04
5	1.60E 01	5.00E 00	6.87E-06	-1.96E-04	-1.09E-04
6	1.44E 01	1.50E 01	1.77E-05	-2.22E-04	-1.60E-04
7	2.29E 01	5.00E 00	1.75E-05	-2.26E-04	-7.07E-05
8	2.17E 01	1.50E 01	3.19E-05	-2.49E-04	-7.10E-05
9	2.98E 01	5.00E 00	1.68E-05	-2.36E-04	-3.70E-05
10	2.92E 01	1.50E 01	4.52E-05	-2.57E-04	-4.49E-05
11	3.67E 01	5.00E 00	1.77E-05	-2.39E-04	-1.31E-05
12	3.62E 01	1.50E 01	4.96E-05	-2.64E-04	-1.40E-05
13	1.37E 01	2.50E 01	2.31E-04	-6.95E-04	-5.94E-04
			STRIP AXIAL FORCE= 1.285E 03	MOMENT= 4.430E-03	
			SKIN MEMBRANE STRESS= 0.840E 05		
14	1.37E 01	3.50E 01	3.05E-04	-5.45E-04	4.77E-05
			STRIP AXIAL FORCE= 1.699E 03	MOMENT= 8.246E-03	
			SKIN MEMBRANE STRESS= 0.194E 05		
15	2.12E 01	2.50E 01	1.59E-04	-5.89E-04	-3.89E-04
			STRIP AXIAL FORCE= 8.868E 02	MOMENT= 5.140E-03	
16	2.12E 01	3.50E 01	2.90E-04	-6.03E-04	-8.68E-05
			STRIP AXIAL FORCE= 1.619E 03	MOMENT= 7.021E-03	
17	2.87E 01	2.50E 01	1.44E-04	-5.94E-04	-1.89E-04
			STRIP AXIAL FORCE= 8.032E 02	MOMENT= 5.516E-03	
18	2.87E 01	3.50E 01	2.51E-04	-5.62E-04	-6.05E-05
			STRIP AXIAL FORCE= 1.401E 03	MOMENT= 6.860E-03	

ELEMENT NO.	SIGMA-X	SIGMA-Y	TAU-XY	SIGMA-1	SIGMA-2	ANG
1	-1.97E 03	-2.52E 03	-4.93E 02	-1.68E 03	-2.81E 03	-3.04E 01
2	-2.11E 03	-7.24E 02	-4.07E 02	-6.14E 02	-2.23E 03	1.05E 02
3	-1.48E 03	-3.15E 03	-6.27E 02	-1.27E 03	-3.36E 03	-1.85E 01
4	-2.57E 03	-2.78E 03	-1.65E 03	-1.02E 03	-4.33E 03	-4.32E 01
5	-1.56E 03	-3.90E 03	-6.27E 02	-1.40E 03	-4.06E 03	-1.41E 01
6	-1.57E 03	-4.34E 03	-9.22E 02	-1.29E 03	-4.62E 03	-1.68E 01
7	-1.60E 03	-4.42E 03	-4.08E 02	-1.55E 03	-4.47E 03	-8.09E 00
8	-1.51E 03	-4.75E 03	-4.10E 02	-1.46E 03	-4.80E 03	-7.09E 00
9	-1.70E 03	-4.62E 03	-2.14E 02	-1.69E 03	-4.64E 03	-4.16E 00
10	-1.32E 03	-4.81E 03	-2.59E 02	-1.30E 03	-4.83E 03	-4.22E 00
11	-1.71E 03	-4.67E 03	-7.53E 01	-1.71E 03	-4.67E 03	-1.46E 00
12	-1.28E 03	-4.89E 03	-8.08E 01	-1.28E 03	-4.89E 03	-1.26E 00
13	-2.10E 03	-4.92E 03	-9.21E 02	-1.82E 03	-5.20E 03	-1.65E 01
14	-4.84E 02	-2.85E 03	4.10E 01	-4.83E 02	-2.86E 03	9.90E-01
15	-2.06E 03	-4.32E 03	-6.11E 02	-1.91E 03	-4.48E 03	-1.42E 01
16	-9.46E 02	-3.46E 03	-1.41E 02	-9.38E 02	-3.47E 03	-3.20E 00
17	-2.23E 03	-4.48E 03	-3.02E 02	-2.19E 03	-4.52E 03	-7.51E 00
18	-1.05E 03	-3.33E 03	-9.14E 01	-1.04E 03	-3.33E 03	-2.29E 00

ELEMENT NO.	X	Y	EPSILON-X	EPSILON-Y	GAMA-XY
19	3.62E 01	2.50E 01	1.37E-04	-5.89E-04	-6.02E-05
	STRIP AXIAL FORCE=		7.641E 02	MOMENT= 5.643E-03	
20	3.62E 01	3.50E 01	2.37E-04	-5.56E-04	-2.02E-05
	STRIP AXIAL FORCE=		1.323E 03	MOMENT= 6.797E-03	
21	1.37E 01	4.50E 01	1.78E-04	-3.36E-04	8.20E-05
	STRIP AXIAL FORCE=		9.910E 02	MOMENT= 6.618E-03	
	SKIN MEMBRANE STRESS=		0.142E 05		
22	2.12E 01	4.50E 01	2.03E-04	-3.96E-04	1.02E-04
	STRIP AXIAL FORCE=		1.132E 03	MOMENT= 6.690E-03	
23	2.87E 01	4.50E 01	1.89E-04	-3.96E-04	5.42E-05
	STRIP AXIAL FORCE=		1.053E 03	MOMENT= 6.520E-03	
24	3.62E 01	4.50E 01	1.79E-04	-3.87E-04	1.97E-05
	STRIP AXIAL FORCE=		9.984E 02	MOMENT= 6.480E-03	
25	1.38E 01	5.50E 01	6.14E-05	-1.24E-04	7.51E-05
	STRIP AXIAL FORCE=		3.424E 02	MOMENT= 7.874E-03	
	SKIN MEMBRANE STRESS=		0.582E 04		
26	2.13E 01	5.50E 01	9.83E-05	-1.62E-04	1.15E-04
	STRIP AXIAL FORCE=		5.481E 02	MOMENT= 7.697E-03	
27	2.88E 01	5.50E 01	1.25E-04	-1.84E-04	7.46E-05
	STRIP AXIAL FORCE=		6.993E 02	MOMENT= 7.496E-03	
28	3.63E 01	5.50E 01	1.36E-04	-1.91E-04	2.30E-05
	STRIP AXIAL FORCE=		7.581E 02	MOMENT= 7.351E-03	

ELEMENT NO.	SIGMA-X	SIGMA-Y	TAU-XY	SIGMA-1	SIGMA-2	ANG
19	-2.26E 03	-4.48E 03	-9.65E 01	-2.26E 03	-4.48E 03	-2.49E 00
20	-1.13E 03	-3.36E 03	-3.01E 01	-1.13E 03	-3.36E 03	-7.75E 00
21	-3.54E 02	-1.67E 03	1.05E 02	-3.46E 02	-1.68E 03	4.53E 00
22	-4.69E 02	-2.00E 03	1.31E 02	-4.58E 02	-2.01E 03	4.85E 00
23	-5.76E 02	-2.07E 03	6.94E 01	-5.73E 02	-2.08E 03	2.65E 00
24	-6.06E 02	-2.06E 03	2.52E 01	-6.05E 02	-2.06E 03	9.98E-01
25	-1.45E 02	-5.68E 02	8.57E 01	-1.29E 02	-5.85E 02	1.10E 01
26	-6.69E 01	-6.61E 02	1.31E 02	-3.94E 01	-6.89E 02	1.19E 01
27	1.97E 01	-6.86E 02	8.51E 01	2.98E 01	-6.96E 02	6.78E 00
28	6.12E 01	-6.84E 02	2.62E 01	6.21E 01	-6.85E 02	2.01E 00

NODAL POINT	X DISPLCEMNT	Y DISPLCEMNT	NODAL POINT	X DISPLCEMNT	Y DISPLCEMNT
1	0.0	0.0	17	-1.31E-03	-3.35E-03
2	0.0	-6.86E-04	18	-8.76E-03	-1.15E-02
3	0.0	-7.22E-04	19	-7.50E-03	-1.60E-02
4	0.0	0.0	20	-4.71E-03	-1.27E-02
5	0.0	0.0	21	-1.61E-03	-1.37E-02
6	0.0	0.0	22	0.0	0.0
7	0.0	0.0	23	-7.08E-04	-2.15E-03
8	0.0	0.0	24	-1.13E-03	-4.57E-03
9	-6.95E-04	-1.28E-03	25	-5.47E-03	-1.03E-02
10	-4.95E-04	-9.64E-04	26	-6.22E-03	-1.68E-02
11	0.0	0.0	27	-3.64E-03	-1.37E-02
12	0.0	0.0	28	-1.76E-03	-1.52E-02
13	0.0	0.0	29	0.0	0.0
14	0.0	0.0	30	-4.70E-04	-2.34E-03
15	0.0	0.0	31	-9.08E-04	-4.84E-03
16	-8.03E-04	-1.69E-03	32	-3.31E-03	-1.08E-02
33	-4.02E-03	-1.65E-02			
34	-2.43E-03	-1.38E-02			
35	-1.49E-03	-1.55E-02			
36	0.0	0.0			
37	-2.42E-04	-2.38E-03			
38	-4.80E-04	-5.01E-03			
39	-1.58E-03	-1.09E-02			
40	-1.98E-03	-1.65E-02			
41	-1.20E-03	-1.36E-02			
42	-8.44E-04	-1.55E-02			
43	0.0	0.0			
44	0.0	-2.40E-03			
45	0.0	-5.03E-03			
46	0.0	-1.09E-02			
47	0.0	-1.64E-02			
48	0.0	-1.36E-02			
49	0.0	-0.02			

CONSTRUCTION INCREMENT 3

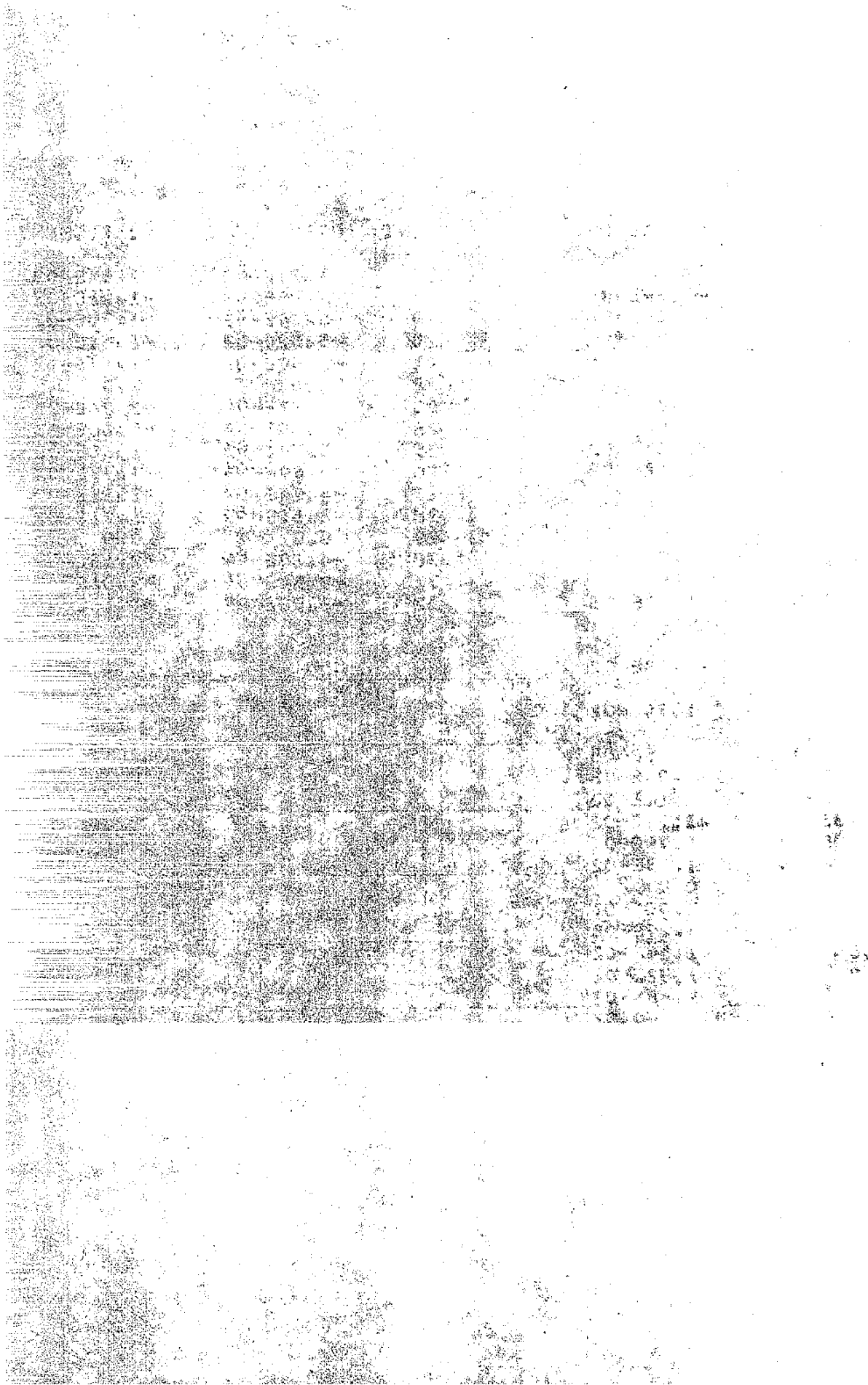
ELEMENT NO.	X	Y	EPSILON-X	EPSILON-Y	GAMA-XY
1	3.33E 00	5.00E 00	-5.66E-05	-1.07E-04	-8.99E-05
2	2.96E 00	1.50E 01	-1.15E-04	1.15E-05	-7.43E-05
3	9.63E 00	5.00E 00	-8.05E-06	-1.60E-04	-1.14E-04
4	7.96E 00	1.50E 01	-8.76E-05	-1.08E-04	-3.02E-04
5	1.60E 01	5.00E 00	7.40E-06	-2.06E-04	-1.13E-04
6	1.44E 01	1.50E 01	1.89E-05	-2.34E-04	-1.67E-04
7	2.29E 01	5.00E 00	1.83E-05	-2.37E-04	-7.31E-05
8	2.17E 01	1.50E 01	3.35E-05	-2.61E-04	-7.36E-05
9	2.98E 01	5.00E 00	1.74E-05	-2.47E-04	-3.81E-05
10	2.92E 01	1.50E 01	4.73E-05	-2.69E-04	-4.68E-05
11	3.67E 01	5.00E 00	1.83E-05	-2.49E-04	-1.35E-05
12	3.62E 01	1.50E 01	5.18E-05	-2.75E-04	-1.46E-05
13	1.37E 01	2.50E 01	2.44E-04	-7.30E-04	-6.23E-04
			STRIP AXIAL FORCE= 1.359E 03	MOMENT= 4.322E-03	
			SKIN MEMBRANE STRESS= 0.886E 05		
14	1.37E 01	3.50E 01	3.28E-04	-5.86E-04	4.75E-05
			STRIP AXIAL FORCE= 1.829E 03	MOMENT= 8.263E-03	
			SKIN MEMBRANE STRESS= 0.209E 05		
15	2.12E 01	2.50E 01	1.68E-04	-6.16E-04	-4.07E-04
			STRIP AXIAL FORCE= 9.356E 02	MOMENT= 5.074E-03	
16	2.12E 01	3.50E 01	3.10E-04	-6.41E-04	-9.59E-05
			STRIP AXIAL FORCE= 1.727E 03	MOMENT= 6.989E-03	
17	2.87E 01	2.50E 01	1.52E-04	-6.20E-04	-1.98E-04
			STRIP AXIAL FORCE= 8.475E 02	MOMENT= 5.471E-03	
18	2.87E 01	3.50E 01	2.68E-04	-5.97E-04	-6.65E-05
			STRIP AXIAL FORCE= 1.495E 03	MOMENT= 6.825E-03	

ELEMENT NO.	SIGMA-X	SIGMA-Y	TAU-XY	SIGMA-1	SIGMA-2	ANG
1	-2.07E 03	-2.65E 03	-5.19E 02	-1.77E 03	-2.96E 03	-3.03E 01
2	-2.22E 03	-7.63E 02	-4.29E 02	-6.47E 02	-2.34E 03	1.05E 02
3	-1.55E 03	-3.31E 03	-6.55E 02	-1.33E 03	-3.53E 03	-1.63E 01
4	-2.70E 03	-2.94E 03	-1.74E 03	-1.07E 03	-4.56E 03	-4.31E 01
5	-1.63E 03	-4.10E 03	-6.53E 02	-1.47E 03	-4.26E 03	-1.40E 01
6	-1.64E 03	-4.56E 03	-9.63E 02	-1.36E 03	-4.85E 03	-1.67E 01
7	-1.68E 03	-4.63E 03	-4.22E 02	-1.62E 03	-4.68E 03	-7.99E 00
8	-1.58E 03	-4.98E 03	-4.25E 02	-1.53E 03	-5.03E 03	-7.02E 00
9	-1.78E 03	-4.83E 03	-2.20E 02	-1.77E 03	-4.85E 03	-4.10E 00
10	-1.37E 03	-5.02E 03	-2.70E 02	-1.35E 03	-5.04E 03	-4.20E 00
11	-1.79E 03	-4.88E 03	-7.76E 01	-1.79E 03	-4.88E 03	-1.44E 00
12	-1.33E 03	-5.11E 03	-8.41E 01	-1.33E 03	-5.11E 03	-1.28E 00
13	-2.21E 03	-5.23E 03	-9.76E 02	-1.92E 03	-5.51E 03	-1.65E 01
14	-5.22E 02	-3.11E 03	4.07E 01	-5.21E 02	-3.11E 03	9.01E-01
15	-2.16E 03	-4.56E 03	-6.47E 02	-2.00E 03	-4.72E 03	-1.42E 01
16	-1.01E 03	-3.73E 03	-1.57E 02	-9.99E 02	-3.74E 03	-3.30E 00
17	-2.33E 03	-4.71E 03	-3.19E 02	-2.29E 03	-4.75E 03	-7.51E 00
18	-1.11E 03	-3.57E 03	-1.02E 02	-1.11E 03	-3.57E 03	-2.37E 00

ELEMENT NO.	X	Y	EPSILON-X	EPSILON-Y	GAMA-XY
19	3.62E 01	2.50E 01	1.45E-04	-6.14E-04	-6.32E-05
	STRIP AXIAL FORCE=		8.062E 02	MOMENT= 5.604E-03	
20	3.62E 01	3.50E 01	2.53E-04	-5.90E-04	-2.23E-05
	STRIP AXIAL FORCE=		1.411E 03	MOMENT= 6.761E-03	
21	1.37E 01	4.50E 01	2.02E-04	-3.81E-04	8.21E-05
	STRIP AXIAL FORCE=		1.128E 03	MOMENT= 6.590E-03	
	SKIN MEMBRANE STRESS= 0.161E 05				
22	2.12E 01	4.50E 01	2.28E-04	-4.41E-04	1.02E-04
	STRIP AXIAL FORCE=		1.271E 03	MOMENT= 6.673E-03	
23	2.87E 01	4.50E 01	2.13E-04	-4.39E-04	5.16E-05
	STRIP AXIAL FORCE=		1.185E 03	MOMENT= 6.492E-03	
24	3.62E 01	4.50E 01	2.02E-04	-4.29E-04	1.88E-05
	STRIP AXIAL FORCE=		1.127E 03	MOMENT= 6.451E-03	
25	1.37E 01	5.50E 01	9.17E-05	-1.79E-04	7.52E-05
	STRIP AXIAL FORCE=		5.113E 02	MOMENT= 7.851E-03	
	SKIN MEMBRANE STRESS= 0.765E 04				
26	2.12E 01	5.50E 01	1.28E-04	-2.17E-04	1.14E-04
	STRIP AXIAL FORCE=		7.149E 02	MOMENT= 7.669E-03	
27	2.87E 01	5.50E 01	1.55E-04	-2.38E-04	7.39E-05
	STRIP AXIAL FORCE=		8.647E 02	MOMENT= 7.470E-03	
28	3.62E 01	5.50E 01	1.65E-04	-2.44E-04	2.24E-05
	STRIP AXIAL FORCE=		9.215E 02	MOMENT= 7.323E-03	

ELEMENT NO.	SIGMA-X	SIGMA-Y	TAU-XY	SIGMA-1	SIGMA-2	ANG
19	-2.36E 03	-4.70E 03	-1.02E 02	-2.36E 03	-4.71E 03	-2.50E 00
20	-1.20E 03	-3.60E 03	-3.37E 01	-1.20E 03	-3.60E 03	-8.06E-01
21	-4.02E 02	-1.92E 03	1.05E 02	-3.95E 02	-1.92E 03	3.95E 00
22	-5.13E 02	-2.26E 03	1.30E 02	-5.04E 02	-2.27E 03	4.24E 00
23	-6.24E 02	-2.33E 03	6.54E 01	-6.22E 02	-2.33E 03	2.20E 00
24	-6.54E 02	-2.30E 03	2.38E 01	-6.54E 02	-2.30E 03	8.28E-01
25	-1.91E 02	-8.18E 02	8.58E 01	-1.79E 02	-8.29E 02	7.66E 00
26	-1.13E 02	-9.12E 02	1.31E 02	-9.24E 01	-9.33E 02	9.05E 00
27	-2.66E 01	-9.36E 02	8.42E 01	-1.88E 01	-9.44E 02	5.24E 00
28	1.39E 01	-9.34E 02	2.55E 01	1.46E 01	-9.34E 02	1.54E 00

NODAL POINT	X DISPLCEMNT	Y DISPLCEMNT	NODAL POINT	X DISPLCEMNT	Y DISPLCEMNT
1	0.0	0.0	17	-1.37E-03	-3.54E-03
2	0.0	-7.24E-04	18	-9.25E-03	-1.21E-02
3	0.0	-7.64E-04	19	-8.14E-03	-1.70E-02
4	0.0	0.0	20	-5.52E-03	-1.41E-02
5	0.0	0.0	21	-2.59E-03	-1.57E-02
6	0.0	0.0	22	0.0	0.0
7	0.0	0.0	23	-7.37E-04	-2.26E-03
8	0.0	0.0	24	-1.19E-03	-4.80E-03
9	-7.29E-04	-1.35E-03	25	-5.78E-03	-1.08E-02
10	-5.21E-04	-1.02E-03	26	-6.69E-03	-1.77E-02
11	0.0	0.0	27	-4.24E-03	-1.51E-02
12	0.0	0.0	28	-2.50E-03	-1.71E-02
13	0.0	0.0	29	0.0	0.0
14	0.0	0.0	30	-4.88E-04	-2.45E-03
15	0.0	0.0	31	-9.54E-04	-5.06E-03
16	-8.38E-04	-1.78E-03	32	-3.50E-03	-1.13E-02
33	-4.32E-03	-1.73E-02			
34	-2.83E-03	-1.51E-02			
35	-1.97E-03	-1.74E-02			
36	0.0	0.0			
37	-2.50E-04	-2.48E-03			
38	-5.04E-04	-5.23E-03			
39	-1.67E-03	-1.14E-02			
40	-2.13E-03	-1.73E-02			
41	-1.39E-03	-1.49E-02			
42	-1.09E-03	-1.73E-02			
43	0.0	0.0			
44	0.0	-2.50E-03			
45	0.0	-5.25E-03			
46	0.0	-1.14E-02			
47	0.0	-1.72E-02			
48	0.0	-1.48E-02			
49	0.0	-0.02			

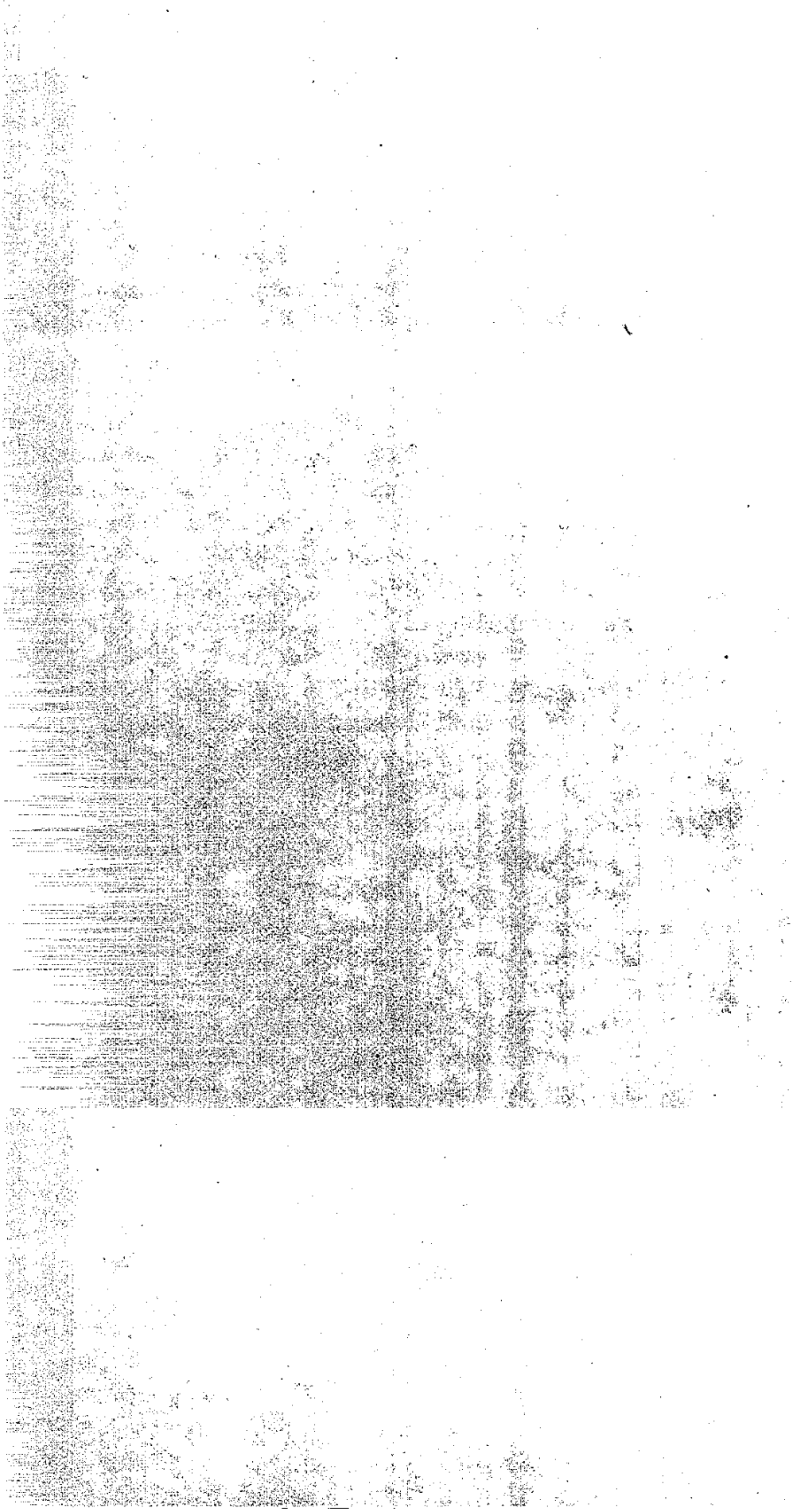


APPENDIX D

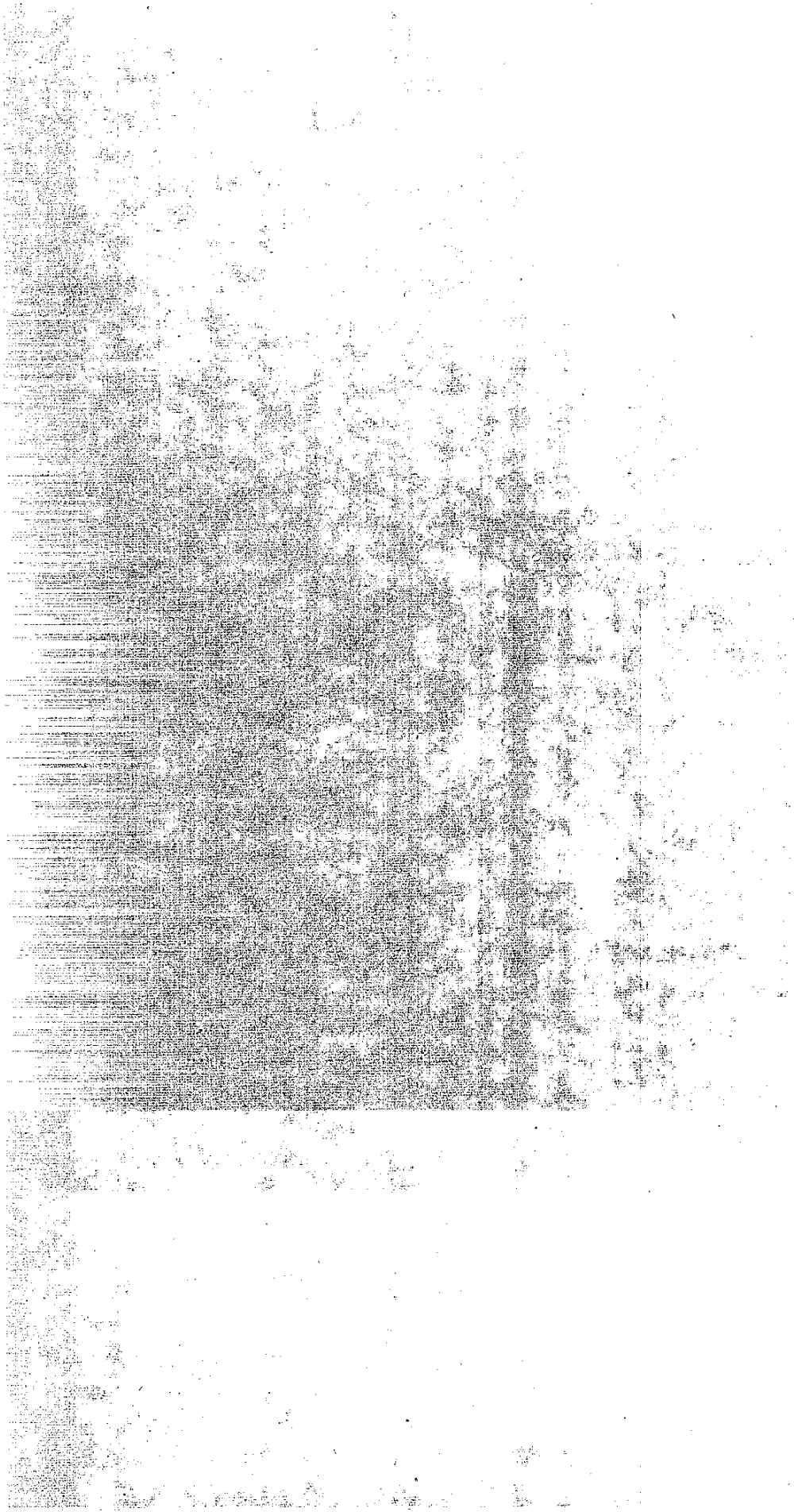
LIST OF THE FINITE ELEMENT COMPUTOR PROGRAM

AND

EXAMPLE OF INPUT AND OUTPUT DATA

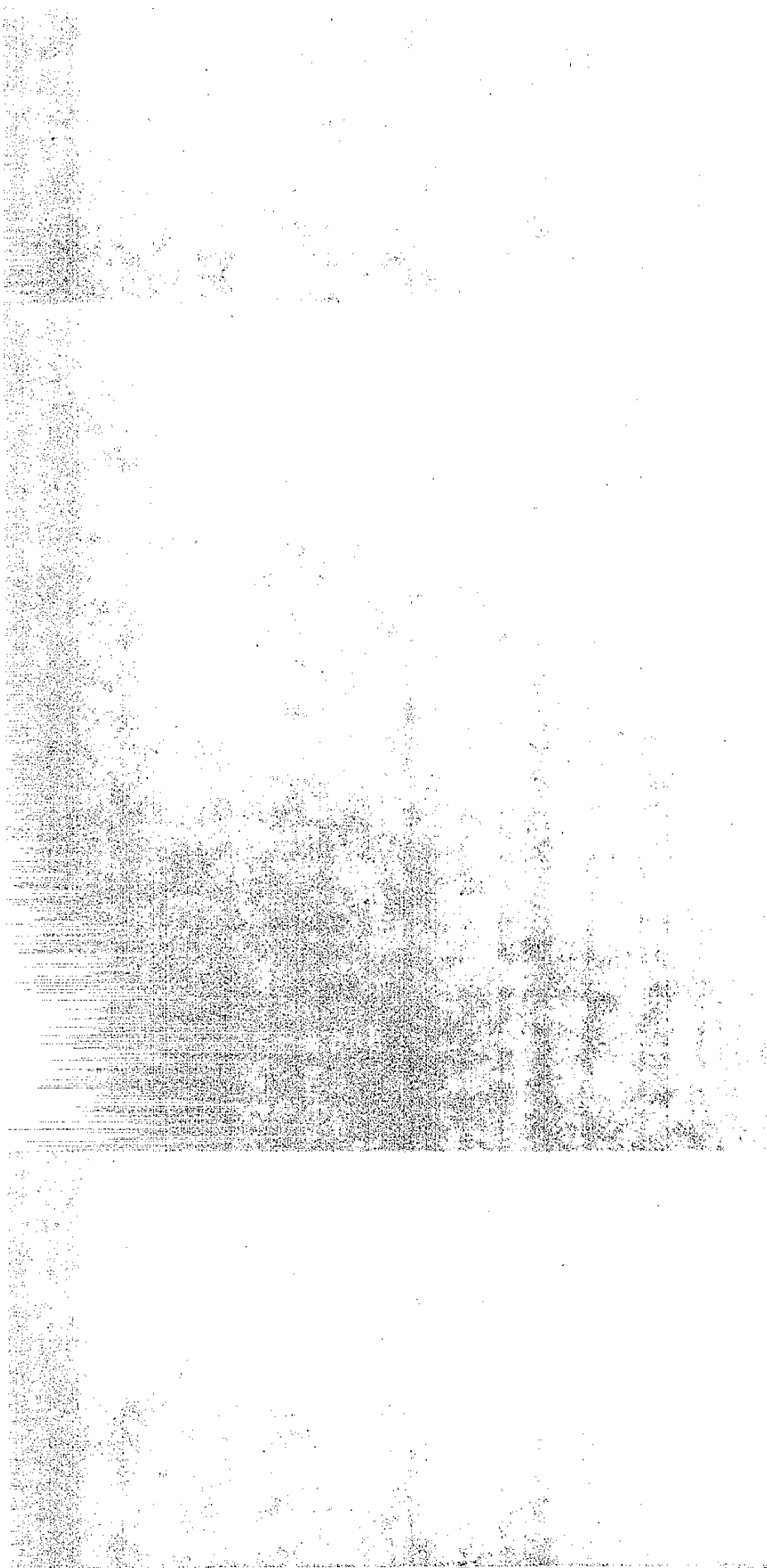


INPUT EXAMPLE



1	2	3	4	5	6	7	8	9	10	11	12	13	14	15	16	17	18	19	20	21	22	23	24	25	26	27	28	29	30	31	32	33	34	35	36	37	38	39	40	41	42	43	44	45	46	47	48	49	50	51	52	53	54	55	56	57	58	59	60	61	62	63	64	65	66	67	68	69	70	71	72	73	74	75	76	77	78	79	80																																																																																																																																																																																																																																																																																																																																																																																																																																																																																																																																																																																																																																																																																																																							
294	211	232	253	295	311	312	233	234	235	236	237	238	239	240	241	242	243	244	245	246	247	248	249	250	251	252	253	254	255	256	257	258	259	260	261	262	263	264	265	266	267	268	269	270	271	272	273	274	275	276	277	278	279	280	281	282	283	284	285	286	287	288	289	290	291	292	293	294	295	296	297	298	299	300	301	302	303	304	305	306	307	308	309	310	311	312	313	314	315	316	317	318	319	320	321	322	323	324	325	326	327	328	329	330	331	332	333	334	335	336	337	338	339	340	341	342	343	344	345	346	347	348	349	350	351	352	353	354	355	356	357	358	359	360	361	362	363	364	365	366	367	368	369	370	371	372	373	374	375	376	377	378	379	380	381	382	383	384	385	386	387	388	389	390	391	392	393	394	395	396	397	398	399	400	401	402	403	404	405	406	407	408	409	410	411	412	413	414	415	416	417	418	419	420	421	422	423	424	425	426	427	428	429	430	431	432	433	434	435	436	437	438	439	440	441	442	443	444	445	446	447	448	449	450	451	452	453	454	455	456	457	458	459	460	461	462	463	464	465	466	467	468	469	470	471	472	473	474	475	476	477	478	479	480	481	482	483	484	485	486	487	488	489	490	491	492	493	494	495	496	497	498	499	500	501	502	503	504	505	506	507	508	509	510	511	512	513	514	515	516	517	518	519	520	521	522	523	524	525	526	527	528	529	530	531	532	533	534	535	536	537	538	539	540	541	542	543	544	545	546	547	548	549	550	551	552	553	554	555	556	557	558	559	560	561	562	563	564	565	566	567	568	569	570	571	572	573	574	575	576	577	578	579	580	581	582	583	584	585	586	587	588	589	590	591	592	593	594	595	596	597	598	599	600	601	602	603	604	605	606	607	608	609	610	611	612	613	614	615	616	617	618	619	620	621	622	623	624	625	626	627	628	629	630	631	632	633	634	635	636	637	638	639	640	641	642	643	644	645	646	647	648	649	650	651	652	653	654	655	656	657	658	659	660	661	662	663	664	665	666	667	668	669	670	671	672	673	674	675	676	677	678	679	680	681	682	683	684	685	686	687	688	689	690	691	692	693	694	695	696	697	698	699	700	701	702	703	704	705	706	707	708	709	710	711	712	713	714	715	716	717	718	719	720	721	722	723	724	725	726	727	728	729	730	731	732	733	734	735	736	737	738	739	740	741	742	743	744	745	746	747	748	749	750	751	752	753	754	755	756	757	758	759	760	761	762	763	764	765	766	767	768	769	770	771	772	773	774	775	776	777	778	779	780	781	782	783	784	785	786	787	788	789	790	791	792	793	794	795	796	797	798	799	800	801	802	803	804	805	806	807	808	809	810	811	812	813	814	815	816	817	818	819	820	821	822	823	824	825	826	827	828	829	830	831	832	833	834	835	836	837	838	839	840	841	842	843	844	845	846	847	848	849	850	851	852	853	854	855	856	857	858	859	860	861	862	863	864	865	866	867	868	869	870	871	872	873	874	875	876	877	878	879	880	881	882	883	884	885	886	887	888	889	890	891	892	893	894	895	896	897	898	899	900	901	902	903	904	905	906	907	908	909	910	911	912	913	914	915	916	917	918	919	920	921	922	923	924	925	926	927	928	929	930	931	932	933	934	935	936	937	938	939	940	941	942	943	944	945	946	947	948	949	950	951	952	953	954	955	956	957	958	959	960	961	962	963	964	965	966	967	968	969	970	971	972	973	974	975	976	977	978	979	980	981	982	983	984	985	986	987	988	989	990	991	992	993	994	995	996	997	998	999	1000

INPUT DATA DESCRIPTION



REINFORCED EARTH PROJECT 39 STA 551+75

NUMBER OF CONSTRUCTION INCREMENTS = 12

PROPERTIES FOR MATERIAL 1 *****

DENSITY = 0.0

PROPERTIES ARE OVERBURDEN DEPENDENT

MODULUS VS CONFINING PRESSURE - A (INTERCEPT)= 0.1000E 07
B (SLOPE)= 0.7370E 03

FRICTION ANGLE= 0.4000E 02

COHESION= 0.9000E 03

POISSONS RATIO= 0.3000E 00

PROPERTIES FOR MATERIAL 2 *****

DENSITY = 0.0

PROPERTIES ARE OVERBURDEN DEPENDENT

MODULUS VS CONFINING PRESSURE - A(INTERCEPT)= 0.5550E 06
B(SLOPE)= 0.1680E 03

FRICTION ANGLE= 0.4000E 02

COHESION= 0.5000E 00

POISSONS RATIO= 0.3000E 00

PROPERTIES FOR MATERIAL 3 *****

DENSITY = 1.43000E 02

PROPERTIES ARE OVERBURDEN DEPENDENT

MODULUS VS CONFINING PRESSURE - A(INTERCEPT)= 0.1000E 07
B(SLOPE)= 0.7370E 03

FRICTION ANGLE= 0.4000E 02

COHESION= 0.9000E 03

POISSONS RATIO= 0.3000E 00

PROPERTIES FOR MATERIAL 4 *****

DENSITY = 1.43000E 02

REINFORCED EARTH

STRIP YOUNGS MODULUS= 0.4104E 10

STRIP WIDTH= 0.1970E 00

STRIP THICKNESS= 0.9830E-02

HORIZONTAL SPACING= 0.1640E 01

VERTICAL SPACING= 0.8330E 00

ANGLE= 0.0

SKIN THICKNESS IF BOUNDARY ELEMENT= 0.1000E-01

SOIL PROPERTIES

PROPERTIES ARE OVERBURDEN DEPENDENT

MODULUS VS CONFINING PRESSURE - A(INTERCEPT)= 0.1440E 07
B(SLOPE)= 0.3350E 03

FRICTION ANGLE= 0.3950E 02

COHESION= 0.1000E 04

POISSONS RATIO= 0.3000E 00

PROPERTIES FOR MATERIAL 5 *****

DENSITY = 1.43000E 02

REINFORCED EARTH

STRIP YOUNGS MODULUS= 0.4104E 10

STRIP WIDTH= 0.1970E 00

STRIP THICKNESS= 0.9830E-02

HORIZONTAL SPACING= 0.3280E 01

VERTICAL SPACING= 0.8330E 00

ANGLE= 0.0

SKIN THICKNESS IF BOUNDARY ELEMENT= 0.1000E-01

SOIL PROPERTIES

PROPERTIES ARE OVERBURDEN DEPENDENT

MODULUS VS CONFINING PRESSURE - A(INTERCEPT)= 0.1440E 07
B(SLOPE)= 0.3350E 03

FRICTION ANGLE= 0.3950E 02

COHESION= 0.1000E 04

POISSONS RATIO= 0.3000E 00

PROPERTIES FOR MATERIAL 6 *****

DENSITY = 1.43000E 02

REINFORCED EARTH

STRIP YOUNGS MODULUS= 0.4104E 10

STRIP WIDTH= 0.1970E 00

STRIP THICKNESS= 0.9830E-02

HORIZONTAL SPACING= 0.4920E 01

VERTICAL SPACING= 0.8330E 00

ANGLE= 0.0

SKIN THICKNESS IF BOUNDARY ELEMENT= 0.1000E-01

SOIL PROPERTIES

PROPERTIES ARE OVERBURDEN DEPENDENT

MODULUS VS CONFINING PRESSURE - A(INTERCEPT)= 0.1440E 07
B(SLOPE)= 0.3350E 03

FRICTION ANGLE= 0.3950E 02

COHESION= 0.1000E 04

POISSONS RATIO= 0.3000E 00

NODAL POINT	X COORDINATE	Y COORDINATE	NODAL POINT	X COORDINATE	Y COORDINATE
1	0.0	50.00	38	125.00	146.67
2	0.0	95.00	39	122.00	155.00
3	0.0	140.00	40	113.67	176.00
4	0.0	150.00	41	104.78	196.73
5	0.0	178.00	42	97.00	218.00
6	0.0	164.00	43	200.00	50.00
7	0.0	171.00	44	170.67	101.68
8	33.33	50.00	45	148.00	150.00
9	29.80	95.03	46	139.50	167.50
10	26.33	140.00	47	131.00	185.00
11	27.00	150.00	48	121.00	205.50
12	26.33	162.67	49	111.00	226.00
13	25.00	188.00	50	116.00	215.75
14	25.66	175.33	51	113.50	220.88
15	66.67	50.00	52	215.07	61.20
16	59.52	95.14	53	189.79	107.92
17	52.67	140.00	54	166.33	153.67
18	60.00	150.00	55	156.29	173.30
19	55.00	175.00	56	146.29	192.86
20	50.00	200.00	57	135.78	213.76
21	52.50	187.50	58	125.27	234.67
22	100.00	50.00	59	140.53	202.39
23	88.96	95.51	60	132.90	218.50
24	79.00	140.00	61	230.13	72.40
25	75.00	160.00	62	207.08	115.14
26	70.61	180.61	63	184.67	157.33
27	65.00	200.00	64	173.04	179.18
28	71.00	175.00	65	161.57	200.71
29	133.33	50.00	66	150.55	222.02
30	117.30	96.92	67	139.53	243.33
31	102.00	143.33	68	155.93	209.69
32	94.40	165.40	69	147.73	226.51
33	87.45	187.44	70	245.20	83.60
34	80.00	207.00	71	223.72	122.91
35	89.10	180.68	72	203.00	161.00
36	166.67	50.00	73	189.62	185.36
37	144.91	98.82	74	176.86	208.57

NODAL POINT	X COORDINATE	Y COORDINATE	NODAL POINT	X COORDINATE	Y COORDINATE
75	165.33	230.29	112	219.93	271.13
76	153.80	252.00	113	210.90	286.70
77	171.05	217.65	114	215.42	278.92
78	162.42	234.82	115	320.53	139.60
79	260.27	94.80	116	302.14	169.55
80	239.61	131.90	117	283.83	199.33
81	219.17	168.67	118	268.10	224.48
82	205.57	192.71	119	252.38	249.63
83	192.14	216.43	120	243.31	264.85
84	180.10	238.55	121	234.23	280.09
85	168.07	260.67	122	225.13	295.33
86	185.88	226.13	123	240.72	269.34
87	176.97	243.40	124	335.60	150.80
88	275.33	106.00	125	317.63	179.21
89	255.30	141.21	126	300.00	207.00
90	235.33	176.33	127	287.39	226.85
91	221.35	200.37	128	274.78	246.71
92	207.43	224.29	129	266.75	259.25
93	194.88	246.81	130	257.65	274.14
94	182.33	269.33	131	248.54	289.05
95	200.71	234.62	132	239.40	304.00
96	191.52	251.97	133	350.66	162.00
97	290.40	117.20	134	332.78	189.50
98	270.94	150.62	135	315.00	216.83
99	251.50	184.00	136	302.16	236.63
100	237.07	208.14	137	289.32	256.42
101	222.71	232.14	138	281.13	268.88
102	209.65	255.07	139	272.00	283.43
103	196.60	278.00	140	262.84	298.03
104	203.13	266.53	141	253.66	312.66
105	199.86	272.27	142	365.73	173.20
106	305.46	128.40	143	347.85	199.95
107	286.55	160.06	144	330.00	226.67
108	267.67	191.67	145	316.92	246.40
109	252.71	216.07	146	303.85	266.14
110	238.00	240.00	147	295.50	278.50
111	228.97	255.57	148	286.33	292.74

NODAL POINT	X COORDINATE	Y COORDINATE	NODAL POINT	X COORDINATE	Y COORDINATE
149	277.14	307.02	186	346.00	326.75
150	267.93	321.33	187	339.00	336.50
151	380.80	184.40	188	332.00	346.25
152	362.87	210.44	189	325.00	356.00
153	345.00	236.50	190	338.00	356.00
154	331.68	256.17	191	338.00	360.00
155	318.39	275.85	192	332.00	360.00
156	309.88	288.13	193	343.00	364.00
157	300.67	302.05	194	342.00	365.50
158	291.44	316.01	195	347.00	338.50
159	282.19	329.99	196	347.00	346.50
160	395.86	195.60	197	347.00	356.00
161	377.83	220.92	198	347.00	360.00
162	360.00	246.34	199	350.00	365.00
163	346.41	265.94	200	350.00	370.00
164	332.92	285.57	201	436.44	225.81
165	324.25	297.75	202	418.05	249.83
166	315.00	311.37	203	400.38	274.22
167	305.74	325.01	204	386.05	293.36
168	296.46	338.66	205	372.69	312.88
169	410.93	206.80	206	364.13	324.50
170	392.61	231.29	207	360.00	338.50
171	375.00	256.17	208	360.00	346.50
172	361.05	275.70	209	360.00	356.00
173	347.46	295.28	210	360.00	360.00
174	340.00	340.00	211	360.00	365.00
175	338.00	346.50	212	360.00	370.00
176	338.63	307.38	213	360.00	373.00
177	329.33	320.70	214	360.00	377.00
178	320.03	334.01	215	360.00	381.00
179	310.73	347.33	216	360.00	385.00
180	426.00	218.00	217	360.00	388.00
181	406.66	241.28	218	360.00	393.50
182	390.00	266.00	219	360.00	399.00
183	375.34	285.41	220	360.00	404.50
184	362.00	305.00	221	363.71	410.00
185	353.00	317.00	222	446.88	233.63

NODAL POINT	X COORDINATE	Y COORDINATE	NODAL POINT	X COORDINATE	Y COORDINATE
223	428.72	257.99	260	383.00	393.50
224	410.75	282.45	261	383.00	399.00
225	396.75	301.31	262	383.00	404.50
226	383.38	320.75	263	383.00	410.00
227	375.25	332.00	264	467.75	249.25
228	371.00	338.50	265	449.62	274.07
229	371.00	346.50	266	431.50	298.90
230	371.00	356.00	267	418.17	317.20
231	371.00	360.00	268	404.75	336.50
232	371.00	365.00	269	397.50	347.00
233	371.00	370.00	270	401.13	341.75
234	371.00	373.00	271	399.31	344.38
235	371.00	377.00	272	395.00	356.00
236	371.00	381.00	273	395.00	360.00
237	371.00	385.00	274	395.00	365.00
238	371.00	388.00	275	395.00	370.00
239	371.00	393.50	276	395.00	373.00
240	371.00	399.00	277	395.00	377.00
241	371.00	404.50	278	395.00	381.00
242	371.00	410.00	279	395.00	385.00
243	457.31	241.44	280	395.00	388.00
244	439.19	266.04	281	395.00	393.50
245	421.13	290.67	282	395.00	399.00
246	407.46	309.26	283	395.00	404.50
247	394.06	328.63	284	395.00	410.00
248	386.38	339.50	285	478.19	257.06
249	380.00	341.00	286	460.04	282.10
250	383.00	346.50	287	441.88	307.12
251	383.00	356.00	288	428.88	325.15
252	383.00	360.00	289	415.44	344.38
253	383.00	365.00	290	408.63	354.50
254	383.00	370.00	291	406.00	356.00
255	383.00	373.00	292	407.31	355.25
256	383.00	377.00	293	406.66	355.63
257	383.00	381.00	294	406.00	360.00
258	383.00	385.00	295	406.00	365.00
259	383.00	388.00	296	406.00	370.00

NODAL POINT	X COORDINATE	Y COORDINATE	NODAL POINT	X COORDINATE	Y COORDINATE
297	406.00	373.00	334	432.36	367.16
298	406.00	377.00	335	433.10	365.98
299	406.00	381.00	336	432.73	366.57
300	406.00	385.00	337	432.92	366.28
301	406.00	388.00	338	432.82	366.42
302	406.00	393.50	339	427.00	373.00
303	406.00	399.00	340	432.00	377.00
304	406.00	404.50	341	429.00	381.00
305	406.00	410.00	342	429.00	385.00
306	488.63	264.88	343	429.00	389.00
307	470.49	290.15	344	429.00	393.50
308	452.25	315.35	345	429.00	399.00
309	439.58	333.10	346	429.00	404.50
310	426.13	352.25	347	429.00	410.00
311	419.75	362.00	348	509.50	280.50
312	422.94	357.13	349	492.04	306.68
313	421.34	359.56	350	473.00	331.80
314	422.14	358.34	351	461.00	349.00
315	421.74	358.95	352	447.50	368.00
316	413.00	365.00	353	442.00	377.00
317	419.00	369.00	354	440.00	381.00
318	417.00	373.00	355	446.00	385.00
319	417.00	377.00	356	441.00	389.00
320	417.00	381.00	357	441.00	393.50
321	417.00	385.00	358	441.00	399.00
322	417.00	388.00	359	441.00	404.50
323	417.00	393.50			
324	417.00	399.00			
325	417.00	404.50			
326	417.00	410.00			
327	499.06	272.69			
328	481.05	298.27			
329	462.63	323.57			
330	450.29	341.05			
331	436.81	360.13			
332	430.88	369.50			
333	433.84	364.81			

NODAL POINT	X COORDINATE	Y COORDINATE	NODAL POINT	X COORDINATE	Y COORDINATE
360	441.00	410.00	386	470.00	408.28
361	522.63	290.42	387	548.88	310.26
362	504.59	316.15	388	530.72	335.71
363	486.13	341.60	389	512.38	361.20
364	474.00	358.50	390	500.00	377.50
365	459.50	377.50	391	483.50	396.50
366	454.00	385.25	392	478.00	401.75
367	450.00	389.00	393	480.75	399.13
368	455.00	393.50	394	479.38	400.44
369	455.00	399.00	395	480.06	399.78
370	455.00	404.50	396	479.72	400.11
371	455.00	410.00	397	479.89	399.95
372	455.00	407.25	398	479.80	400.03
373	455.00	408.62	399	479.85	399.99
374	535.75	300.34	400	562.00	320.17
375	517.58	325.90	401	544.05	345.47
376	499.25	351.40	402	525.50	371.00
377	487.00	368.00	403	513.00	387.00
378	471.50	387.00	404	495.50	406.00
379	466.00	393.50	405	490.00	410.00
380	465.00	399.00	406	575.00	330.00
381	470.00	404.50	407	558.00	355.00
382	470.00	410.00	408	540.00	381.00
383	470.00	407.25	409	528.00	399.00
384	470.00	408.63	410	520.00	410.00
385	470.00	407.94	411	547.50	410.00
			412	575.00	410.00
			413	575.00	367.00

ELEM NO.	ELEMENT NODAL POINTS				MAT NO.	CONST INCR.	ELEM NO.	ELEMENT NODAL POINTS				MAT NO.	CONST INCR.
1	1	8	9	2	1	1	38	161	162	153	152	1	1
2	9	10	3	2	1	1	39	169	170	161	160	1	1
3	8	15	16	9	1	1	40	170	171	162	161	1	1
4	16	17	10	9	1	1	41	180	181	170	169	1	1
5	15	22	23	16	1	1	42	170	181	182	171	1	1
6	23	24	17	16	1	1	43	201	202	181	180	1	1
7	22	29	30	23	1	1	44	181	202	203	182	1	1
8	23	30	31	24	1	1	45	222	223	202	201	1	1
9	29	36	37	30	1	1	46	202	223	224	203	1	1
10	30	37	38	31	1	1	47	243	244	223	222	1	1
11	36	43	44	37	1	1	48	223	244	245	224	1	1
12	37	44	45	38	1	1	49	264	265	244	243	1	1
13	43	52	53	44	1	1	50	265	266	245	244	1	1
14	53	54	45	44	1	1	51	285	286	265	264	1	1
15	52	61	62	53	1	1	52	286	287	266	265	1	1
16	62	63	54	53	1	1	53	306	307	286	285	1	1
17	70	71	62	61	1	1	54	307	308	287	286	1	1
18	71	72	63	62	1	1	55	327	328	307	306	1	1
19	79	80	71	70	1	1	56	307	328	329	308	1	1
20	80	81	72	71	1	1	57	348	349	328	327	1	1
21	88	89	80	79	1	1	58	328	349	350	329	1	1
22	89	90	81	80	1	1	59	361	362	349	348	1	1
23	97	98	89	88	1	1	60	349	362	363	350	1	1
24	98	99	90	89	1	1	61	374	375	362	361	1	1
25	106	107	98	97	1	1	62	362	375	376	363	1	1
26	107	108	99	98	1	1	63	387	388	375	374	1	1
27	115	116	107	106	1	1	64	375	388	389	376	1	1
28	116	117	108	107	1	1	65	387	400	401	388	1	1
29	124	125	116	115	1	1	66	388	401	402	389	1	1
30	125	126	117	116	1	1	67	400	406	407	401	1	1
31	133	134	125	124	1	1	68	407	408	402	401	1	1
32	134	135	126	125	1	1	69	406	413	407	407	1	1
33	142	143	134	133	1	1	70	413	412	408	407	1	1
34	143	144	135	134	1	1	71	3	10	11	4	2	1
35	151	152	143	142	1	1	72	10	17	18	11	2	1
36	152	153	144	143	1	1	73	17	24	25	18	2	1
37	160	161	152	151	1	1	74	24	31	32	25	2	1

ELEM NO.	ELEMENT NODAL POINTS				MAT NO.	CONST INCR.	ELEM NO.	ELEMENT NODAL POINTS				MAT NO.	CONST INCR.
75	31	38	39	39	2	1	112	164	173	176	165	2	1
76	39	40	32	31	2	1	113	171	182	183	172	2	1
77	38	45	46	39	2	1	114	172	183	184	173	2	1
78	46	47	40	39	2	1	115	184	185	176	173	2	1
79	45	54	55	46	2	1	116	182	203	204	183	2	1
80	46	55	56	47	2	1	117	204	205	184	183	2	1
81	54	63	64	55	2	1	118	184	205	206	185	2	1
82	55	64	65	56	2	1	119	203	224	225	204	2	1
83	63	72	73	64	2	1	120	225	226	205	204	2	1
84	64	73	74	65	2	1	121	205	226	227	206	2	1
85	81	82	73	72	2	1	122	224	245	246	225	2	1
86	73	82	83	74	2	1	123	225	246	247	226	2	1
87	81	90	91	82	2	1	124	226	247	248	227	2	1
88	82	91	92	83	2	1	125	245	266	267	246	2	1
89	90	99	100	91	2	1	126	246	267	268	247	2	1
90	91	100	101	92	2	1	127	247	268	269	248	2	1
91	99	108	109	100	2	1	128	266	287	288	267	2	1
92	100	109	110	101	2	1	129	288	289	268	267	2	1
93	108	117	118	109	2	1	130	268	289	290	269	2	1
94	109	118	119	110	2	1	131	287	308	309	288	2	1
95	126	127	118	117	2	1	132	288	309	310	289	2	1
96	127	128	119	118	2	1	133	289	310	311	290	2	1
97	128	129	119	119	2	1	134	308	329	330	309	2	1
98	126	135	136	127	2	1	135	309	330	331	310	2	1
99	127	136	137	128	2	1	136	310	331	332	311	2	1
100	128	137	138	129	2	1	137	329	350	351	330	2	1
101	135	144	145	136	2	1	138	330	351	352	331	2	1
102	136	145	146	137	2	1	139	331	352	353	332	2	1
103	137	146	147	138	2	1	140	363	364	351	350	2	1
104	144	153	154	145	2	1	141	351	364	365	352	2	1
105	145	154	155	146	2	1	142	365	366	353	352	2	1
106	146	155	156	147	2	1	143	376	377	364	363	2	1
107	153	162	163	154	2	1	144	364	377	378	365	2	1
108	154	163	164	155	2	1	145	378	379	366	365	2	1
109	155	164	165	156	2	1	146	389	390	377	376	2	1
110	162	171	172	163	2	1	147	377	390	391	378	2	1
111	163	172	173	164	2	1	148	391	392	379	378	2	1

ELEM NO.	ELEMENT				MAT NO.	CONST INCR.	ELEM NO.	ELEMENT				MAT NO.	CONST INCR.
	NODAL	POINTS					NODAL	POINTS					
149	402	403	390	389	2	1	186	121	122	113	112	3	2
150	390	403	404	391	2	1	187	129	130	120	119	3	2
151	404	405	392	391	2	1	188	130	131	121	120	3	2
152	408	409	403	402	2	1	189	131	132	122	121	3	2
153	403	409	410	404	2	1	190	138	139	130	129	3	2
154	404	410	405	405	2	1	191	139	140	131	130	3	2
155	412	411	409	408	2	1	192	140	141	132	131	3	2
156	409	411	410	410	2	1	193	147	148	139	138	3	2
157	4	11	12	12	3	2	194	148	149	140	139	3	2
158	12	13	5	4	3	2	195	149	150	141	140	3	2
159	11	18	19	12	3	2	196	156	157	148	147	3	2
160	12	19	20	13	3	2	197	157	158	149	148	3	2
161	25	26	19	18	3	2	198	158	159	150	149	3	2
162	26	27	20	19	3	2	199	165	166	157	156	3	2
163	25	32	33	26	3	2	200	166	167	158	157	3	2
164	26	33	34	27	3	2	201	167	168	159	158	3	2
165	40	41	33	32	3	2	202	176	177	166	165	3	2
166	41	42	34	33	3	2	203	177	178	167	166	3	2
167	40	47	48	41	3	2	204	178	179	168	167	3	2
168	41	48	49	42	3	2	205	176	185	186	186	3	2
169	47	56	57	48	3	2	206	186	187	177	176	3	2
170	48	57	58	49	3	2	207	187	188	178	177	3	2
171	56	65	66	57	3	2	208	188	189	179	178	3	2
172	57	66	67	58	3	2	209	185	206	186	186	3	2
173	65	74	75	66	3	2	210	195	174	187	186	3	2
174	66	75	76	67	3	2	211	186	206	207	195	3	2
175	74	83	84	75	3	2	212	227	228	207	206	3	2
176	75	84	85	76	3	2	213	248	249	228	227	3	2
177	83	92	93	84	3	2	214	187	174	175	188	3	2
178	84	93	94	85	3	2	215	195	196	175	174	3	2
179	92	101	102	93	3	2	216	195	207	208	196	3	2
180	93	102	103	94	3	2	217	207	228	229	208	3	2
181	110	111	102	101	3	2	218	228	249	250	229	3	2
182	111	112	103	102	3	2	219	248	269	250	249	3	2
183	112	113	103	103	3	2	220	188	175	190	189	3	2
184	119	120	111	110	3	2	221	175	196	197	190	3	2
185	120	121	112	111	3	2	222	196	208	209	197	3	2

ELEM NO.	ELEMENT NODAL POINTS				MAT NO.	CONST INCR.	ELEM NO.	ELEMENT NODAL POINTS				MAT NO.	CONST INCR.
223	208	229	230	209	3	2	257	297	318	319	298	3	7
224	229	250	251	230	3	2	258	298	319	320	299	3	7
225	269	272	251	250	3	2	259	339	340	319	318	3	7
226	290	291	272	269	3	2	260	319	340	341	320	3	7
227	209	230	231	210	4	3	261	332	353	340	339	3	7
228	230	251	252	231	4	3	262	340	353	354	341	3	7
229	251	272	273	252	4	3	263	215	236	237	216	5	8
230	272	291	294	273	4	3	264	216	237	238	217	5	8
231	290	311	294	291	3	3	265	236	257	258	237	5	8
232	210	231	232	211	4	4	266	237	258	259	238	5	8
233	231	252	253	232	4	4	267	257	278	279	258	5	8
234	252	273	274	253	4	4	268	258	279	280	259	5	8
235	273	294	295	274	4	4	269	278	299	300	279	5	8
236	311	316	295	294	3	4	270	279	300	301	280	5	8
237	211	232	233	212	4	5	271	299	320	321	300	3	8
238	232	253	254	233	4	5	272	300	321	322	301	3	8
239	253	274	275	254	4	5	273	320	341	342	321	3	8
240	274	295	296	275	4	5	274	321	342	343	322	3	8
241	295	316	317	296	3	5	275	341	354	355	342	3	8
242	332	317	316	311	3	5	276	342	355	356	343	3	8
243	212	233	234	213	5	6	277	366	355	354	353	3	8
244	233	254	255	234	5	6	278	355	366	367	356	3	8
245	254	275	276	255	5	6	279	217	238	239	218	6	9
246	275	296	297	276	5	6	280	218	239	240	219	6	9
247	296	317	318	297	3	6	281	238	259	260	239	6	9
248	332	339	318	317	3	6	282	239	260	261	240	6	9
249	213	234	235	214	5	7	283	259	280	281	260	6	9
250	214	235	236	215	5	7	284	260	281	282	261	6	9
251	234	255	256	235	5	7	285	280	301	302	281	6	9
252	235	256	257	236	5	7	286	281	302	303	282	6	9
253	255	276	277	256	5	7	287	301	322	323	302	3	9
254	256	277	278	257	5	7	288	302	323	324	303	3	9
255	276	297	298	277	5	7	289	322	343	344	323	3	9
256	277	298	299	278	5	7	290	323	344	345	324	3	9

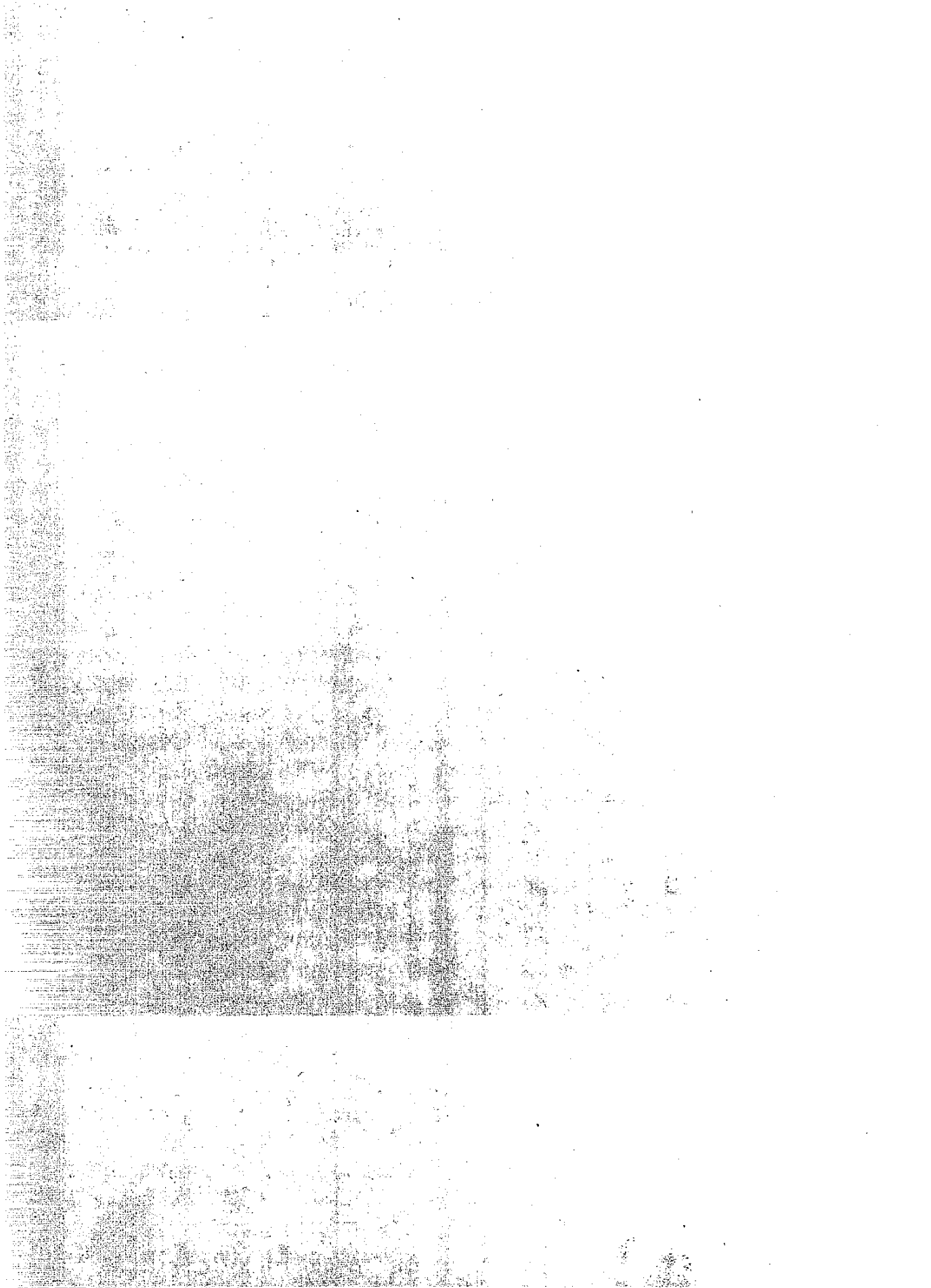
ELEM NO.	ELEMENT NODAL POINTS				MAT NO.	CONST INCR.
291	343	356	357	344	3	9
292	344	357	358	345	3	9
293	356	367	368	357	3	9
294	357	368	369	358	3	9
295	366	379	368	367	3	9
296	368	379	380	369	3	9
297	219	240	241	220	6	10
298	240	261	262	241	6	10
299	261	282	283	262	6	10
300	282	303	304	283	6	10
301	303	324	325	304	3	10
302	324	345	346	325	3	10
303	345	358	359	346	3	10
304	358	369	370	359	3	10
305	380	381	370	369	3	10
306	379	392	381	380	3	10
307	189	190	191	192	3	11
308	190	197	198	191	3	11
309	197	209	210	198	3	11
310	191	193	194	192	3	11
311	191	198	199	193	3	11
312	199	200	194	193	3	11
313	198	210	211	199	3	11
314	199	211	212	200	3	11
315	241	242	221	220	3	12
316	241	262	263	242	3	12
317	262	283	284	263	3	12
318	283	304	305	284	3	12
319	304	325	326	305	3	12
320	325	346	347	326	3	12
321	346	359	360	347	3	12
322	359	370	371	360	3	12
323	370	381	382	371	3	12
324	392	405	382	381	3	12

*****BOUNDARY CONDITIONS*****

BOUNDARY NODE				INCREMENT NO.
2	U-X= 0.0	P-Y= 0.0	ANG= 0.0	1
3	U-X= 0.0	P-Y= 0.0	ANG= 0.0	1
4	U-X= 0.0	P-Y= 0.0	ANG= 0.0	1
5	U-X= 0.0	P-Y= 0.0	ANG= 0.0	1
1	U-X= 0.0	U-Y= 0.0	ANG= 0.0	1
8	U-X= 0.0	U-Y= 0.0	ANG= 0.0	1
15	U-X= 0.0	U-Y= 0.0	ANG= 0.0	1
22	U-X= 0.0	U-Y= 0.0	ANG= 0.0	1
29	U-X= 0.0	U-Y= 0.0	ANG= 0.0	1
36	U-X= 0.0	U-Y= 0.0	ANG= 0.0	1
43	U-X= 0.0	U-Y= 0.0	ANG= 0.0	1
52	U-X= 0.0	U-Y= 0.0	ANG= 0.0	1
61	U-X= 0.0	U-Y= 0.0	ANG= 0.0	1
70	U-X= 0.0	U-Y= 0.0	ANG= 0.0	1
79	U-X= 0.0	U-Y= 0.0	ANG= 0.0	1
88	U-X= 0.0	U-Y= 0.0	ANG= 0.0	1
97	U-X= 0.0	U-Y= 0.0	ANG= 0.0	1
106	U-X= 0.0	U-Y= 0.0	ANG= 0.0	1
115	U-X= 0.0	U-Y= 0.0	ANG= 0.0	1
124	U-X= 0.0	U-Y= 0.0	ANG= 0.0	1

133	U-X= 0.0	U-Y= 0.0	ANG= 0.0	1
142	U-X= 0.0	U-Y= 0.0	ANG= 0.0	1
151	U-X= 0.0	U-Y= 0.0	ANG= 0.0	1
160	U-X= 0.0	U-Y= 0.0	ANG= 0.0	1
169	U-X= 0.0	U-Y= 0.0	ANG= 0.0	1
180	U-X= 0.0	U-Y= 0.0	ANG= 0.0	1
201	U-X= 0.0	U-Y= 0.0	ANG= 0.0	1
222	U-X= 0.0	U-Y= 0.0	ANG= 0.0	1
243	U-X= 0.0	U-Y= 0.0	ANG= 0.0	1
264	U-X= 0.0	U-Y= 0.0	ANG= 0.0	1
285	U-X= 0.0	U-Y= 0.0	ANG= 0.0	1
306	U-X= 0.0	U-Y= 0.0	ANG= 0.0	1
327	U-X= 0.0	U-Y= 0.0	ANG= 0.0	1
348	U-X= 0.0	U-Y= 0.0	ANG= 0.0	1
361	P-N= 0.0	U-S= 0.0	ANG= 3.71E 01	1
374	P-N= 0.0	U-S= 0.0	ANG= 3.71E 01	1
387	P-N= 0.0	U-S= 0.0	ANG= 3.71E 01	1
400	P-N= 0.0	U-S= 0.0	ANG= 3.71E 01	1
406	P-N= 0.0	U-S= 0.0	ANG= 3.71E 01	1
412	P-X= 0.0	P-Y= -1.24E 05	ANG= 0.0	1
411	P-X= 0.0	P-Y= -8.37E 04	ANG= 0.0	1
410	P-X= 0.0	P-Y= -4.44E 04	ANG= 0.0	1
405	P-X= 0.0	P-Y= -7.94E 03	ANG= 0.0	1

PROGRAM LISTING



PANVALET
THE PROGRAM MANAGEMENT AND SECURITY SYSTEM

PROGRAMS AND ALL SUPPORTING MATERIALS COPYRIGHT 1971, 1972 BY PANSOPH
SYSTEMS, INCORPORATED

```
++WRITE PRINT,ENG085A                                000191
C      DATA SET ENG085A      AT LEVEL 008 AS OF 01/17/74
SUBROUTINE FINEL(PAPSIZ)                                00001
COMMON /CNTRL/ WIDTH, INOUT, INCR2, LC1, PGM1, PGM2, PHON 00002
COMMON /HDLIN/ HED(18), DUM(2)                          00003
COMMON/BLK1/ R(700), Z(700), IX(600,4), IXXX            00004
COMMON/BLK2/MNO(6,3), NODB(200), BIV(200,3), JIFLG(3), BIVD(2) 00005
1, NUMEL, NUMNP, NUMPC, NUMC, NINC                       00006
DIMENSION IBUF(1024), IPS(5), INS(5), ISYMBL(3), PGMR(3) 00007
REAL*8 MSG(5) /'END OF P', 'LOT TAPE', 3* ' / , DATE/' DATED' / 00008
DATA LC /'E132' / , NT/5 / , NPLOTS/1 / , BLANK/' / , IBLNK/' / 00009
REAL*8 PAPER1 /'BLANK' / , PAPER2/'WHITE' /             00010
REAL*8 VOL, START /'ANYWHERE' / , NAME/'ENG085' /       00011
REAL*4 DOUT(6) /'RETU', 'RN -', ' DIS', 'TR.1', '5 BA', 'SKET' / 00012
REAL MRGN, MRGNT, MPGNB, NROUND, X(4), Y(4)             00013
REAL*4 XSYMB(3,2) / 0., .05, 0., .04, .08, 0. /        00014
REAL*4 XY (50, 2)                                       00015
DATA IPS/3, 2, 2, 2, 2 / , INS/1, 2, 3, 4, 1 / , ISYMBL/76, 18, 1/ 00016
DATA PGMR/'TRAN', 'SP.', 'LAB.' / , NPEN /3 / , VOL/'****' / 00017
REAL*4 PHON(3), PHONE(3) / 2* ' -', ' ' /              00018
IF (PAPSIZ .GT. 1.0 .AND. PAPSIZ .LT. 30.1) GOTO 51     00019
49 CONTINUE                                             00020
50 FORMAT( '1 *** IMPROPER PLOT WIDTH =', E16.7, ' ***' ) 00021
RETURN                                                  00022
51 CONTINUE                                             00023
    INCH = 11                                           00024
    IF ( PAPSIZ .GT. 11.1 ) INCH = 30                    00025
    WIDTH = INCH                                        00026
    CALL PLOTS (IBUF, 1024, 8)                            00027
    IF(LC1 .NE. IBLNK) LC=LC1                             00028
    IF(PGM1 .EQ. BLANK .AND. PGM2 .EQ. BLANK) GOTO 52    00029
    PGMR(1) = PGM1                                       00030
    PGMR(2) = PGM2                                       00031
    PGMR(3) = BLANK                                      00032
52 CONTINUE                                             00033
    IF (PHON(1) .NE. BLANK) PHONE(1) = PHON(1)          00034
    IF (PHON(2) .NE. BLANK) PHONE(2) = PHON(2)          00035
    IF (PHON(3) .NE. BLANK) PHONE(3) = PHON(3)          00036
C                                                       00037
    R1 = R(1)                                           00038
    R2 = R(1)                                           00039
    Z1 = Z(1)                                           00040
    Z2 = Z(1)                                           00041
    DO 100 I=1, NUMNP                                    00042
```

```

IF(R(I) .LT. R1) R1=R(I)
IF(Z(I) .LT. Z1) Z1=Z(I)
IF(R(I) .GT. R2) R2=R(I)
IF(Z(I) .GT. Z2) Z2=Z(I)
100 CONTINUE
RR = R2-R1
ZZ = Z2-Z1
MRGN = 0.
NROUND = 1
DO 60 ITR1 = 1, 7
SCL1 = ZZ/(PAPSIZ - MRGN)
IF ( SCL1 .LT. 1) GO TO 16
IF(SCL1 .GT. 19) NROUND = 5
IF(SCL1 .GT. 99) NROUND = 10
I = SCL1 / NROUND
SCL5 = I*NROUND
IF (SCL5 .LT. SCL1 ) SCL5 = SCL5+NROUND
16 CONTINUE
IF (SCL1 .LT. 1) SCL5 = SCL1
PAP5 = ZZ / SCL5
IF ( WIDTH .GT. (PAP5 +2.0) ) GOTO 61
MRGN = MRGN + .70 ** (ITR1-1)
60 CONTINUE
C *****
GOTO 49
61 MRGN = WIDTH - PAP5
MRGNB= MRGN * .61
MRGNT= MRGN - MRGNB
FACT = 1. /SCL5
C INITIALIZE PEN POSITION & DRAW AXES
CALL PLOT ( 2.5, -WIDTH ,23)
CALL PLOT (1.6,MRGNB,23)
RLEN = RR / SCL5 + 1.
RLEN = AINT(RLEN)
NF = RLEN /12. + 2.00
CALL AXIS (0.,0.,6HR-AXIS,-6,RLEN,0.,R1,SCL5)
IF (RLEN .GE. 15.0)
*CALL SYMBOL ( 0.0, -.85, .21, HED, 0.,72)
IF (RLEN .LT. 15.0)
*CALL SYMBOL ( 0.0, -.75, .14, HED, 0.,72)
ZLEN = AINT ( ZZ / SCL5 +.51)
CALL AXIS (0.,0.,6HZ-AXIS,+6,ZLEN,90.,Z1,SCL5,10.)
C *****
NP =1
DO 30 I = 1,NUMEL
DIV = 0.0
N1 = 0
XXX= 0

```

YYY= 0	0009
NP= NP+1	0009
DO 20 J = 1,5	0009
IP = IPS(J)	0009
JN = INS (J)	0009
N = IX(I,JN)	0009
XX = (R(N)-R1) * FACT	0009
YY = (Z(N)-Z1) * FACT	0009
CALL PLOT (XX,YY,IP)	0009
IF(N1.EQ. N)GOTO 20	0010
NI= N	0010
IF(J .GT. 4) GOTO 20	0010
IF (N .LT. 1) GOTO 20	0010
XXX = XXX+XX	0010
YYY = YYY+YY	0010
DIV = DIV+1.0	0010
X(J) = XX	0010
Y(J) = YY	0010
20 CONTINUE	0010
YYY = YYY/DIV-0.034	0011
XXX = XXX/DIV-0.07	0011
IF (NP .GT. 2) GOTO 34	0011
CMP = .0334	0011
IF (DIV .GT. 3.1) GOTO 25	0011
CMP= .061	0011
25 CONTINUE	0011
AREA2=X(1)*Y(2)+Y(1)*X(3)+Y(3)*X(2)-Y(2)*X(3)-Y(1)*X(2)-X(1)*Y(3)	0011
AREA2= ABS(AREA2) / 2.0	0011
IF (AREA2 .LT. CMP) GOTO 28	0011
GOTO 34	0012
28 CONTINUE	0012
CALL SYMBOL (XXX+ .03, YYY+.004,.07,14,0.,-1)	0012
GOTO 30	0012
34 FPN = I	0012
YYY = YYY + 0.025	0012
CALL NUMBER(XXX,YYY,.07,FPN,0., -1)	0012
NP = 0	0012
30 CONTINUE	0012
C *****	0012
CALL SERIAL(VOL,IER)	0013
DO 40 IN = 1,NUMPC	0013
I=NODE(IN)/10000	0013
NB=NODB(IN) - I*10000	0013
NB4= NB/100	0013
NB = NB - NB4 * 100	0013
IF(NB .LT. 1) GOTO 40	0013
K1 = 11/NB + 9/NB + 2*NB - 20	0013
IF (K1 .LT. 1 .OR. K1 .GT. 3) GO TO 40	0013

	XX = (R(I)-R1)*FACT -XSYMB(K1,1)	00139
	YY = (Z(I)-Z1)*FACT - XSYMB(K1,2)	00140
	INTEQ = ISYMBL(K1)	00141
70	FORMAT (4I12,7X,4F16.4)	00142
	CALL SYMBOL (XX, YY, 0.07, INTEQ, 0.0, -1)	00143
	CALL SYMBOL (XX, YY, 0.07, INTEQ, 0.0, -1)	00144
40	CONTINUE	00145
		00146
	N2 = 1	00147
	NXY = 0	00148
	NI = 1	00149
	DO 97 I=1,NUMNP	00150
	XX = (R(I)-R1)* FACT -0.046	00151
	YY = (Z(I)-Z1)* FACT +0.03	00152
	IF (I .LT. 2) GOTO 79	00153
	IF (NXY .GT. N2) N2 = NXY	00154
	DO 77 N = N1,N2	00155
	DIS2 = (XX - XY(N,1)) **2 + (YY - XY(N,2)) **2	00156
	IF (DIS2 .LT. 0.064) GOTO 97	00157
77	CONTINUE	00158
79	CONTINUE	00159
	FPN = I	00160
	NXY = NXY +1	00161
	CALL NUMBER(XX,YY,.07,FPN,0.,-1)	00162
	IF (NXY .LE. 50) GOTO 73	00163
	NXY = 1	00164
73	CONTINUE	00165
	XY (NXY,1) = XX	00166
	XY (NXY,2) = YY	00167
97	CONTINUE	00168
		00169
		END OF NODES
	RR =RR* FACT	00170
	MSG(3)= VOL	00171
	MSG(4)=DATE	00172
	CALL DHDATE(0,DATE)	00173
	MSG(5)=DATE	00174
	CALL PLOT (RR+1.5,0., -03)	00175
	ZMSG =0.73 * ZLEN	00176
	CALL SYMBOL (0., ZMSG, 0.14, MSG, 270.0, 40)	00177
	CALL PLOT(2.0,0.0,999)	00178
	XX = . NUMNP + NUMEL	00179
	TIME = .021* XX + RLEN * ZLEN / 70.0	00180
	NT = TIME+4.	00181
	WRITE(3,699)	00182
	* (VOL, I=1,7), NPEN, VOL, VOL, INCH, VOL, PAPER1 , PAPER2 , VOL,	00183
	* START , VOL, NT, VOL, DATE , VOL, NF, (VOL, I=1,5), PGMR, PHONE,	00184
		00185

```

* VOL,VOL,NAME,VOL,LC,(VOL,I=1,4),DOUT,VOL,VOL          00186
WRITE(8,699)                                              00187
* (VOL,I=1,7),NPEN,VOL,VOL,INCH,VOL,PAPER1,PAPER2,VOL,  00188
* START,VOL,NT,VOL,DATE,VOL,NF,(VOL,I=1,5),PGMR,PHONE,  00189
* VOL,VOL,NAME,VOL,LC,(VOL,I=1,4),DOUT,VOL,VOL          00190
699 FORMAT(1H1,19X,A6,59(1H*)/20X,A6,58X,1H*            00191
*/ 20X,A6,9X,40HINSTRUCTIONS TO CALCOMP PLOTTER OPERATOR,9X,1H*00192
*/ 20X,A6,58X,1H*/20X,A6,59(1H*)/20X,A6,58X,1H*        00193
*/ 20X,A6,21X,10HUSE NUMBER,12,4H PEN,21X,1H*/20X,A6,58X,1H* 00194
*/ 20X,A6,9X,10HPLOT WIDTH,15X,2H=,12,5H INCH,15X,1H*    00195
*/ 20X,A6,9X,13HTYPE OF PAPER,12X,2H=,2A8,6X,1H*        00196
*/ 20X,A6,9X,9HSTART PEN,16X,2H=,A8,14X,1H*             00197
*/ 20X,A6,9X,13HPLOTTING TIME,12X,1H=,I3,8H MINUTES,12X,1H* 00198
*/ 20X,A6,9X,15HDATE OF PLOT,10X,2H=,A8,14X,1H*         00199
*/ 20X,A6,9X,15HLENGTH OF PAPER,10X,1H=,I3,5H FEET,15X,1H* 00200
*/ 20X,A6,9X,18HLAST BLOCK ADDRESS,6X,6H=999,19X,1H*    00201
*/ 20X,A6,58X,1H*/20X,A6,59(1H*)/20X,A6,58X,1H*        00202
*/ 20X,A6,9X,13HSUBMITTED BY,3A4,5X,6HPHONE,3A4,2H*    00203
*/ 20X,A6,58X,1H*                                         00204
*/ 20X,A6,17X,7HPROGRAM,11(1H.),A6,17X,1H*              00205
*/ 20X,A6,17X,19HLABOR COST CODE.....A4,1HL,17X,1H*    00206
*/ 20X,A6,17X,18HREEL NUMBER.....A6,17X,1H*            00207
*/ 20X,A6,58X,1H*/20X,A6,17X,6A4,17X,1H*               00208
*/ 20X,A6,58X,1H*/20X,A6,59(1H*)                        00209
RETURN                                                    00210
END                                                        00211
SUBROUTINE STRESS(IA,NELEMT,HTOP,HTOPP)                 00212
COMMON/PLK1/X(700),Y(700),NOD(600,4),IX               00213
COMMON/PLK2/MNO(600),NODB(200),BIV(200,3),IIFLG(3),BIVD(3) 00214
1 ,NELEM,NPT,NBPTC,NINC                                00215
COMMON/BLK3/C1(17,17),ZY(17),RT(3),ZT(3),RQ(4),ZQ(4),  00216
1 NQ(700),U(700),V(700),ITDQ(2,3),ATOQ(2,3),EST(4,3)  00217
2 ,IS(5),BS(3),AS(3),RQ,J1,                          00218
3 AL(3,3),BT(3,3),GA(3,3),Z5(12,12),Z4(12)           00219
4 ,T(28,2),ITRW(28,2),NETCL(17,2),CTP(12,17),STORE(17) 00220
COMMON/PLK4/SL(112),S(112,56)                          00221
COMMON/BLK5/DEN(10),NON(10),GNU(10,10),E(10,10),H(10,10), 00222
1 ST(600,9),CP(3,3)                                    00223
COMMON/BLK6/AB(10),EB(10),XIB(10),RE(10),DE(10),TE(10),F(3) 00224
1 ,TK(10)                                               00225
DIMENSION DUMY(8)                                       00226
C                                                         00227
C                                                         00228
C FORMAT STATEMENTS                                     00229
C                                                         00230
917 FORMAT(1H1,22HCONSTRUCTION INCREMENT,14////)      00231
920 FORMAT(17,4X,1P11E11.2)                            00232
922 FORMAT(5X,7HELEMENT,45X,                           00233

```

1	28HELEMENT STRAINS AND STRESSES / ,6X,3HNO.,8X	00234
1	,1HX,10X,1HY,6X,9HEPSILON-X, 2X, 9HEPSILON-Y, 3X, 7HGAMA-XY, 4X,	00235
2	7HSIGMA-X, 4X, 7HSIGMA-Y,4X,6HTAU-XY,5X,7HSIGMA-1, 4X, 7HSIGMA-2,	00236
3	6X, 3HANG, /)	00237
924	FORMAT(1H1,4X,4HNODE, 7X, 13HDISPLACEMENTS, / 6X, 3HNO. , 8X,	00238
1	1HU, 10X, 1HV, /)	00239
925	FORMAT(1H1)	00240
926	FORMAT(10X,19HSTRIP AXIAL FORCE=,1PE11.3,3X,7HMOMENT=,E11.3)	00241
927	FORMAT(12X,21HSKIN MEMBRANE STRESS=,E11.3)	00242
929	FORMAT(1X)	00243
930	FORMAT(I7,5X, 9HBEAM— P=,1PE11.3,3X,2HV=,E11.3,3X,2HM=, E11.3)	00244
		00245
	BOUNDARY POINTS TRANSFORMED TO X-Y COORDINATE SYSTEM	00246
		00247
	DO 600 K=1,NBPTC	00248
	KK=IABS(NODB(K))	00249
	NODB(K)=KK	00250
	ANG=RIV(K,3)	00251
	IF(ANG .EQ. 0.0) GO TO 600	00252
	K1=KK/1000	00253
	JJ=NQ(K1)/100	00254
	IF(JJ.EQ.NO(K1+1)/100) GO TO 600	00255
	CT=COS(ANG)	00256
	SA=SIN(ANG)	00257
	D1=SL(JJ)	00258
	D2=SL(JJ+1)	00259
	SL(JJ)=D1*CT-D2*SA	00260
	SL(JJ+1)=D1*SA+D2*CT	00261
600	CONTINUE	00262
		00263
	FOR EACH ELEMENT FIND STRAINS AND STRESSES	00264
		00265
	REWIND 2	00266
	DO 726 III=1,NELEMT	00267
		00268
	RECALL ELEMENT STIFFNESS MATRIX	00269
		00270
	READ (2)(ZY(M),STORE(M),(C1(M,N),N=1,17),M=1,17),((CP(J,K),K=1,3),	00271
1	J=1,3)	00272
	I=STORE(17)+0.1	00273
	MN=MNO(I)/1000	00274
	ITYP=MCD(NON(MN),10)+1	00275
	NOD(I,1)=IABS(NOD(I,1))	00276
		00277
	CALCULATE ELEMENT UNKNOWNNS	00278
		00279
	L=1	00280
	DO 620 J=1,4	00281

	K=NOD(I,J)	00282
	ND=NQ(K)/100	00283
	DUMY (L) = -ZY (L)	00284
	DUMY (L+1) = -ZY (L+1)	00285
	ZY(L)=SL(ND)	00286
	ZY(L+1)=SL(ND+1)	00287
620	L=L+2	00288
	IF (I .NE. 280) GOTO 7215	00289
	DO 7025 J = 1, 8	00290
	DO 7025 K = 1, 8	00291
7025	DUMY (J) = DUMY (J) + C1 (J, K) * ZY (K)	00292
7215	CONTINUE	00293
	IF(ITYP.NE.5) GO TO 621	00294
	ZY(6)=SL(ND+2)	00295
	CALL BEAMST(I,MN)	00296
	GO TO 718	00297
621	JTRY=2	00298
	IF(NOD(I,3) .NE. NOD(I,4))GO TO 625	00299
	JTRY=1	00300
	DO 622 J=9,17	00301
622	ZY(J)=0.0	00302
	GO TO 658	00303
625	DO 630 J=1,8	00304
	DO 630 K=9,17	00305
630	ZY(K)=ZY(K)-C1(K,J)*ZY(J)	00306
	ZY(9)=ZY(9)/C1(9,9)	00307
	DO 650 J=10,17	00308
	KA=J-1	00309
	DO 645 K=9,KA	00310
645	ZY(J)=ZY(J)-ZY(K)*C1(J,K)	00311
650	ZY(J)=ZY(J)/C1(J,J)	00312
658	DO 660 K=1,4	00313
660	RO(K) =0.0	00314
C		00315
C	CALCULATE SUB-ELEMENT EXPANSION COEFFICIENTS	00316
C		00317
	DUXX=0.0	00318
	DUXY=0.0	00319
	DUYX=0.0	00320
	DVXX=0.0	00321
	DVXY=0.0	00322
	DVYY=0.0	00323
	DO 715 J1=1,JTRY	00324
	DO 670 K=1,12	00325
670	Z4(K)=0.0	00326
	M=6*J1-7	00327
	DO 675 K=1,3	00328
	M=M+2	00329

	RT(K)=STORE(M)	00330
675	ZT(K)=STORE(M+1)	00331
	J1P=J1	00332
	DU=0.5	00333
	IF (JTRY .EQ. 2)GO TO 677	00334
	DU=1.0	00335
	J1P=2	00336
677	CALL GEOM(AA,D1,D2,D3)	00337
	DU=DU/AA	00338
	MP=1	00339
	DO 680 K=1,17	00340
	KA=NETCL(K,J1)	00341
	DO 680 MM=1,KA	00342
	M=ITRW(MP,J1)	00343
	Z4(M)=Z4(M)+ZY(K)*T(MP,J1)	00344
680	MP=MP+1	00345
C		00346
C	STRAINS CALCULATED FOR SUBELEMENTS	00347
C		00348
	IF(ITYP .NE. 4)GO TO 697	00349
	DDI=0.5/AA/AA	00350
	DO 695 K=1,3	00351
	J1=IS(K+1)	00352
	K1=IS(K+2)	00353
	B1J1=BS(J1)	00354
	B1K1=BS(K1)	00355
	A1J1=AS(J1)	00356
	A1K1=AS(K1)	00357
	B1=Z4(K+6)	00358
	C1=Z4(K+9)	00359
	DUXX=DUXX+DD1*2.0*B1J1*B1K1*B1	00360
	DUXY=DUXY+DD1*(A1J1*B1K1+B1J1*A1K1)*B1	00361
	DUYX=DUYX+DD1*2.0*A1J1*A1K1*B1	00362
	DVXX=DVXX+DD1*2.0*B1J1*B1K1*C1	00363
	DVXY=DVXY+DD1*(A1J1*B1K1+B1J1*A1K1)*C1	00364
695	DVYY=DVYY+DD1*2.0*A1J1*A1K1*C1	00365
697	EX=0.	00366
	EY=0.0	00367
	GAMXY=0.0	00368
	DO 701 K=1,3	00369
	D1=AS(K)	00370
	D2=BS(K)	00371
	EX=EX+Z4(K)*D2	00372
	EY=EY+Z4(K+3)*D1	00373
701	GAMXY=GAMXY+Z4(K)*D1+Z4(K+3)*D2	00374
	RQ(1)=EX*DU+RQ(1)	00375
	RQ(2)=EY*DU+RQ(2)	00376
	RQ(3)=GAMXY*DU+RQ(3)	00377

	DU=(1.0-DU*AA)*0.5/AA	00371
	IF(J1 .EQ. 2)GO TO 705	00372
	RQ(1)=RQ(1)-DU*BS(1)*(Z4(7)-Z4(8)-Z4(9))	00373
	RQ(2)=RQ(2)-DU*AS(1)*(Z4(10)-Z4(11)-Z4(12))	00381
	RQ(3)=RQ(3)-DU*(AS(1)*(Z4(7)-Z4(8)-Z4(9)) +BS(1)*(Z4(10)-Z4(11)	00382
	1 -Z4(12)))	00383
	GO TO 715	00384
705	RQ(1)=RQ(1)-DU *BS(3)*(Z4(9)-Z4(8)-Z4(7))	00385
	RQ(2)=RQ(2)-DU *AS(3)*(Z4(12)-Z4(11)-Z4(10))	00386
	RQ(3)=RQ(3)-DU *(AS(3)*(Z4(9)-Z4(8)-Z4(7)) +BS(3)*(Z4(12)-Z4(11)	00387
	1 -Z4(10)))	00388
	715 CONTINUE	00389
C		00390
C	INCREMENTAL STRESSES CALCULATED	00391
C		00392
	DO 717 L=1,3	00393
	DU=0.0	00394
	DO 716 J=1,3	00395
716	DU=DU+RQ(J)*CP(L,J)	00396
717	ZQ(L)=DU	00397
C		00398
C	FORCES IN REINFORCING STRIP DETERMINED FROM COMPOSITE MATERIAL	00399
C		00400
	IF(ITYP.NE.4)GO TO 718	00401
	NP=NON(MN)/1000	00402
	IAC=MOD(MNO(I),1000)/10	00403
	ND=IAC-IA	00404
	CALL STREH(DUXX,DUXY,DUYX,DVXX,DVXY,DVYY,MN,HTOP,ND,HTOPP,I,NP)	00405
C		00406
C	INCREMENTAL STRESSES AND STRAINS ADDED TO TOTAL VALUES	00407
C		00408
718	DO 719 J=1,3	00409
	ST(I,J+6)=ST(I,J+6)+F(J)	00410
	ST(I,J+3)=ST(I,J+3)+ZQ(J)	00411
719	ST(I,J)=ST(I,J)+RQ(J)	00412
726	CONTINUE	00413
C		00414
C	PRINT ELEMENT STRAINS AND STRESSES	00415
C		00416
	WRITE (6,917) IA	00417
	WRITE(6,922)	00418
	IPG=8	00419
	DO 760 I=1,NELEM	00420
	N=MNO(I)	00421
	IAC=MOD(N,1000)/10	00422
	IF(IAC .GT. IA) GO TO 760	00423
	MN=N/1000	00424
	ITYP=MOD(NON(MN),10)+1	00425

	IF(ITYP.NE.5) GO TO 728	00426
	IPG=IPG+1	00427
	WRITE(6,930)I,(ST(I,K),K=1,3)	00428
	GO TO 760	00429
728	N1=NOD(I,1)	00430
	N2=NOD(I,2)	00431
	N3=NOD(I,3)	00432
	N4=NOD(I,4)	00433
	XC=(X(N2)+X(N4))*0.5	00434
	YC=(Y(N2)+Y(N4))*0.5	00435
	IF(N3.NE.N4)GO TO 730	00436
	XC=(XC*2.0+X(N1))/3.0	00437
	YC=(YC*2.0+Y(N1))/3.0	00438
730	DO 740 J=1,3	00439
740	RQ(J)=ST(I,J+3)	00440
		00441
	PRINCIPAL STRESSES CALCULATED	00442
		00443
	CALL PRINC (RQ,ZQ)	00444
	IF(IPG.LT.40) GO TO 744	00445
	WRITE(6,925)	00446
	WRITE(6,922)	00447
	IPG=4	00448
		00449
	WRITE ELEMENT STRESSES AND STRAINS	00450
		00451
744	WRITE(6,920) I, XC , YC, (ST(I,K) ,K=1,6), (ZQ(L),L=1,3)	00452
	IPG=IPG+1	00453
	IF(ITYP.NE.4)GO TO 760	00454
	WRITE(6,926) (ST(I,K),K=7,8)	00455
	IPG=IPG+2	00456
		00457
	MEMBRANE STRESS DETERMINATION EQUALS PR/T	00458
		00459
	IPRNT=MOD(N ,10)	00460
	IF(IPRNT.EQ.9)GO TO 755	00461
	TH=TE(MN)*.014533	00462
	CT=COS(TH)	00463
	SINT=SIN(TH)	00464
	S1=ST(I,4)*CT*CT+ST(I,5)*SINT*SINT+2.*ST(I,6)*CT*SINT	00465
	STRM=-S1*DE(MN)/(2.*TK(MN))	00466
	WRITE(6,927)STRM	00467
	IPG=IPG+1	00468
755	WRITE(6,929)	00469
760	CONTINUE	00470
C		00471
C	DISPLACEMENTS PRINTED	00472
C		00473

	DO 785 I=1,NPT	00474
	IF (MOD(NQ(I),100) .EQ. 0)GO TO 785	00475
	JJ=NQ(I)/100	00476
	DU=SL(JJ)	00477
	DV=SL(JJ+1)	00478
	X(I)=X(I)+DU	00479
	Y(I)=Y(I)+DV	00480
	U(I)=U(I)+DU	00481
	V(I)=V(I)+DV	00482
785	CONTINUE	00483
	CALL RESOUT(4)	00484
	REWIND 2	00485
	WRITE (6, 9421) (DUMY(J),J = 1, 8)	00486
9421	FORMAT (1P8E12.4)	00487
	RETURN	00488
	END	00489
	SUBROUTINE PREP	00490
C		00491
C	THIS SUBROUTINE SETS UP THE DESCRIPTION OF THE PROBLEM	00492
C		00493
	DIMENSION ANI(8),AN(3),TITLE(20) , IMAGE(20)	00494
	DIMENSION PHON (3)	00495
	COMMON /CNTRL/ WIDTH, INOUT, INCR2,LC1,PGM1,PGM2,PHON	00496
	COMMON /HDLIN/ TITLE	00497
	COMMON/BLK1/ X(700),Y(700),NDD(600,4),IX	00498
	COMMON/BLK2/MNO(600),NODB(200),BIV(200,3),IIFLG(3),BIVD(3)	00499
1	,NELEM, NPT, NBPTC, NINC	00500
	COMMON/BLK5/ DEN(10),NON(10),GNU(10,10),E(10,10),H(10,10),	00501
1	ST(600,9),CP(3,3)	00502
	COMMON/BLK6/AB(10),EB(10),XIB(10),BE(10),DE(10),TE(10),F(3)	00503
1	,TK(10)	00504
C		00505
C	FORMAT STATEMENTS	00506
C		00507
800	FORMAT (I5, F10.0, 2I5, 6A4)	00508
801	FORMAT (3E10.5)	00509
802	FORMAT (I1,I4,1E15)	00510
803	FORMAT (9X,20A4)	00511
805	FORMAT (20A4)	00512
806	FORMAT (I1,I4,I5,F10.0,I5,2F10.0,3I5 ,2F10.0)	00513
807	FORMAT (I1,I4,I2, I3, 6E10.5)	00514
808	FORMAT (I1,I4,2F10.0, I5,2F10.0,I5,F10.0)	00515
809	FORMAT(7E10.5)	00516
900	FORMAT (1H1 8X 20A4, ///)	00517
901	FORMAT(1H0,4X,35HNUMBER OF CONSTRUCTION INCREMENTS =,I4////////)	00518
902	FORMAT(1H1////////10X,29H*****ELEMENT INFORMATION*****//1X,	00519
1	7HELEMENT,10X, 7HELEMENT,13X,	00520
2	8HMATERIAL,4X,12HCONSTRUCTION/1X,6HNUMBER,	00521

3	10X,11HNODE POINTS,10X,6HNUMBER,6X,	00522
4	16HINCREMENT NUMBER)	00523
903	FORMAT(1H0,9X, 35HPROPERTIES ARE OVERBURDEN DEPENDENT // 20X,	00524
1	45HMODULUS VS CONFINING PRESSURE - A(INTERCEPT)=, E11.4, /,52X,	00525
2	9HF(SLOPE)=, E11.4, /, 20X, 15HFRICITION ANGLE=, E11.4, /,20X,	00526
3	9HCOHESION=, E11.4, /, 20X, 15HPOISSONS RATIO=, E11.4)	00527
904	FORMAT(1H0,10X,15HYOUNGS MODULUS=, E11.4, /, 11X,	00528
1	15HPOISSONS RATIO=, E11.4)	00529
905	FORMAT(1H0, 9X,5HC-11=, E11.4, /, 10X, 5HC-12=, E11.4, /,	00530
1	10X,5HC-22=, E11.4, /, 10X, 5HC-33=, E11.4, /,	00531
2	10X,3HTH=, E11.4)	00532
906	FORMAT(I7,6X,3(A6,1PE10.2,9X),I7//)	00533
907	FORMAT(1H0//5X,23HPROPERTIES FOR MATERIAL,I3,3X,8H*****//,10X,	00534
1	9HDENSITY =,1PE15.5)	00535
908	FORMAT(/////1H)	00536
909	FORMAT(I11,5X,1P2E10.2)	00537
911	FORMAT (//, 1X 23HERROR-TOO MANY MATERIALS)	00538
912	FORMAT (//, 1X 23HERROR-TOO MANY ELEMENTS)	00539
913	FORMAT (//, 1X 26HERROR-TOO MANY NODE POINTS)	00540
914	FORMAT (//, 1X,34HERROR-TOO MANY BOUNDARY CONDITIONS)	00541
915	FORMAT(1H1/////10X,29H*****BOUNDARY CONDITIONS*****//1X,	00542
1	13HBOUNDARY NODE,74X,13HINCREMENT NO./)	00543
916	FORMAT(1H ,9X,1P3E20.2)	00544
917	FORMAT(I5,5X, 4I5,2I12)	00545
918	FORMAT(1H0// 5X, 8HMATERIAL,I4,2X,21HREPRESENTS A BENDING ,	00546
	17HELEMENT, // ,11X, 5HAREA=,E11.4, //,11X,18HMOMENT OF INERTIA=,	00547
	2FE11.4, //,11X,15HYOUNGS MODULUS=,E11.4, //, 11X,	00548
3	15HPOISSONS RATIO=, E11.4)	00549
920	FORMAT(28H ERROR-DATA ERROR IN ELEMENT, I5)	00550
921	FORMAT(1H0/,6X,16HREINFORCED EARTH//,	00551
1	10X,21HSTRIP YOUNGS MODULUS=,E11.4, /,	00552
2	10X,12HSTRIP WIDTH=,E11.4, /,	00553
3	10X,16HSTRIP THICKNESS=,E11.4, /,	00554
4	10X,19HHORIZONTAL SPACING=,E11.4, /,	00555
5	10X,17HVERTICAL SPACING=,E11.4, /,	00556
6	10X,6HANGLE=,E11.4, /,	00557
7	10X,35HSKIN THICKNESS IF BOUNDARY ELEMENT=,E11.4, /,	00558
8	8X,15HSOIL PROPERTIES)	00559
923	FORMAT(1H0,9X,31HELASTIC PROPERTIES - OVERBURDEN//20X,	00560
1	10H0VERBURDEN,10X,14HYOUNGS MODULUS,6X,14HPOISSONS RATIO)	00561
	DATA ANI,AN(3)	00562
2	/4HU-X=, 4HP-X=, 4HU-Y=, 4HP-Y=, 4HU-N=, 4HP-N=,	00564
3	4HU-S=, 4HP-S=, 4HANG= /	00565
C		00566
C	INPUT DATA IS READ	00567
C		00568
	DO 1 I=1,3000	00569

1	ST(I,1)=0.0	00570
	IXP=1	00571
	READ(5,805,END=700) TITLE	00572
	WRITE(6,900) TITLE	00573
	WRITE(3,803) TITLE	00574
	READ(5,800) NINC, WIDTH, INOUT, INCL, LC1, PGM1, PGM2, PHON	00575
	READ(99,805) IMAGE	00576
	WRITE(3,803) IMAGE	00577
	IF(INCL.LT.1) NINC = NINC + INCL	00578
	IF(NINC.LT.1) NINC=1	00579
	WRITE(6,901) NINC	00580
C		00581
C	MATERIAL PROPERTIES	00582
C		00583
	NMAT=0	00584
2	PEAD(5,807) NSEC,I,ITYP,NOMI,D1,D2,D3,D4,D5,D6	00585
	READ(99,805) IMAGE	00586
	WRITE(3,803) IMAGE	00587
	IF(NSEC.NE.0) GO TO 106	00588
	NOMI=NOMI+1	00589
	NON(I)=NOMI*1000+ITYP	00590
	DEN(I)=D1	00591
	NMAT=NMAT+1	00592
	ITYP=ITYP+1	00593
	IF(ITYP.EQ.5) GO TO 95	00594
	WRITE(6,907) I, D1	00595
	GO TO (60,60,58,59),ITYP	00596
C		00597
C	ANISOTROPIC PROPERTIES	00598
C		00599
	58 WRITE(6,905) D2,D3,D4,D5,D6	00600
	CALL ANISP(D2,D3,D4,D5,D6)	00601
	GO TO 65	00602
C		00603
C	REINFORCED EARTH PROPERTIES	00604
C		00605
59	READ(5,839)(EB(I),AB(I),XIB(I),BE(I),DE(I),TE(I),TK(I))	00606
	READ(99,805) IMAGE	00607
	WRITE(3,803) IMAGE	00608
	WRITE(6,921)(EB(I),AB(I),XIB(I),BE(I),DE(I),TE(I),TK(I))	00609
	AB(I)=AB(I)*XIB(I)	00610
	XIB(I)=AB(I)*XIB(I)*XIB(I)/12.	00611
	60 IF (NOMI .GE. 2) GO TO 80	00612
C		00613
C	LINEAR ISOTROPIC PROPERTIES	00614
C		00615
	WRITE(6,904) D3,D4	00616
	E(I,1)=D3	00617

	GNU(I,1)=D4	00618
	IF(ITYP .EQ. 4) GO TO 2	00619
	CALL CONV(D3,D4)	00620
65	L=0	00621
	DO 70 J=1,3	00622
	DO 70 K=J,3	00623
	L=L+1	00624
70	H(I,L)=CP(J,K)	00625
	GO TO 2	00626
C		00627
C	OVERBURDEN DEPENDENT ISOTROPIC PROPERTIES - TYPE A	00628
C		00629
80	H(I,1)=D2	00630
	E(I,1)=D3	00631
	GNU(I,1)=D4	00632
	IF(NOMI .GT. 2) GO TO 82	00633
	H(I,2)=D5	00634
	H(I,3)=D6	00635
	WRITE(6,903) D3,D2,D5,D6,D4	00636
	GO TO 2	00637
C		00638
C	OVERBURDEN DEPENDENT ISOTROPIC PROPERTIES - TYPE B	00639
C		00640
82	NOMI=NOMI-1	00641
	DO 90 N=2,NOMI	00642
	READ(5,801) H(I,N),E(I,N),GNU(I,N)	00643
	READ(99,805) IMAGE	00644
	WRITE(3,803) IMAGE	00645
90	IF(GNU(I,N).EQ.0.0) GNU(I,N)=GNU(I,N-1)	00646
	WRITE(6,923)	00647
	WRITE(6,916) (H(I,N),E(I,N),GNU(I,N),N=1,NOMI)	00648
	GO TO 2	00649
C		00650
C	BEAM PROPERTIES	00651
C		00652
95	E(I,1)=D3	00653
	GNU(I,1)=D4	00654
	H(I,1)=D1	00655
	H(I,2)=D2	00656
	WRITE(6,918) I,D1,D2,D3,D4	00657
	GO TO 2	00658
C		00659
C	INPUT CONTROL UNIT	00660
C		00661
106	GO TO (107,112,175,195),NSEC	00662
C		00663
C	NODE POINT COORDINATES	00664
C		00665

107	NPT=0	00666
108	READ(5,808) NSEC,N,XS ,YS ,NP,XP,YP,INCR,D	00667
	READ(99,805) IMAGE	00668
	WRITE(3,803) IMAGE	00669
	IF(NSEC .NE. 0) GO TO 106	00670
	X(N)=XS	00671
	Y(N)=YS	00672
	ST(N,1)=1.0E+20	00673
	IF(NPT .LT. N) NPT=N	00674
	IF(NP .EQ. 0) GO TO 108	00675
	IF(INCR .EQ. 0) INCR=1	00676
	NS=N	00677
	IF(D .LT. .01 .OR. D .GT. 100.) D = 1.0	00678
	NM=(NP-NS)/INCR	00679
	NMIS = IABS (NM)	00680
	IF (NMIS .GT. 1) GO TO 1080	00681
	INCR = NP- NS	00682
	NM = 1	00683
	NMIS = 1	00684
	GOTO 1081	00685
1080	CONTINUE	00686
	NPS= (NP - NS)	00687
	NPS2 = IABS(NPS)	00688
	INCR2 = IABS (INCR)	00689
	NCHK = NMIS * INCR2- NPS2	00690
	IF (NCHK .EQ. 0) GOTO 1081	00691
	NP = N + NPS/NPS2 *INCR2 * NMIS	00692
1081	CONTINUE	00693
	INCR=INCR*NM/NMIS	00694
	DU2=NMIS	00695
	DU1=1.0/DU2	00696
	IF(D.EQ.1.0) GO TO 109	00697
	DU1=(1.0-D)/(1.0-D**NMIS)	00698
109	DX=(XP -XS)*DU1	00699
	DY=(YP -YS)*DU1	00700
	DO 110 I=1,NMIS	00701
	NS=NS+INCR	00702
	XS=XS+DX	00703
	YS=YS+DY	00704
	ST(NS,1)=1.0E+20	00705
	X(NS)=XS	00706
	Y(NS)=YS	00707
	DX=DX*D	00708
110	DY=DY*D	00709
	IF(NPT .LT. NS) NPT=NS	00710
	GO TO 108	00711
C		00712
C	ELEMENT INFORMATION	00713

		00714
112	MS=1	00715
	N=1	00716
	MNORS=1	00717
5	FORMAT (5(2H (,I3,1H),2F10.1))	00718
	IF (INOUT .GT.0)	00719
	1WRITE (3,25)((I, X(I), Y(I)), I= 1,NPT)	00720
113	READ(5,802) NSEC,(NOD(N,I),I=1,4),MNOR,M,NMIS,INCR,NMISP,INCRP	00721
	1 ,IPRNT	00722
	READ (99,805) IMAGE	00723
	WRITE (3,803) IMAGE	00724
	IF(NSEC .NE. 0) GO TO 132	00725
	M = M+INCL	00726
	IF (M .LT. 0) M=0	00727
	IF(NOD(N,3) .EQ. 0)NOD(N,3)=NOD(N,2)	00728
	IF(NOD(N,4) .EQ. 0)NOD(N,4)=NOD(N,3)	00729
	NS=N	00730
	INCRS=0	00731
	INCRZ=INCR	00732
	NMISZ=NMISP	00733
	IF(MNOR.EQ.0) MNOR=MNORS	00734
	MNORS=MNOR	00735
	IF(M.EQ.0) M=MS	00736
	MS=M	00737
	MNO(N)=MNOR*1000+M*10+IPRNT	00738
114	DO 115 M=1,4	00739
115	NOD(N,M)=NOD(NS ,M)+INCRS	00740
	MNO(N)=MNO(NS)	00741
	N=N+1	00742
	INCRS=INCRS+INCRP	00743
	NMISP=NMISP-1	00744
	IF(NMISP .GE. 0)GO TO 114	00745
	NMISP=NMISZ	00746
	INCRS=INCRZ	00747
	INCRZ=INCRZ+INCR	00748
	NMIS=NMIS-1	00749
	IF(NMIS .GE. 0)GO TO 114	00750
	GO TO 113	00751
		00752
C	GENERATE COORDINATES FOR UNSPECIFIED INTERIOR NODES	00753
C		00754
132	NELEM =N-1	00755
28	FORMAT (5 (3H (,I3,1H),4I4))	00756
	IF (INOUT .GT.0)	00757
	1WRITE (3,28) ((I, (NOD(I,K),K=1,4)),I=1,NELEM)	00758
	NMIS=0	00759
	DO 135 K=3,NPT	00760
	IF(ST(K,1) .GT. .9E+20)GO TO 135	00761

	X(K)=0.5*(X(K-2)+X(K-1))	00762
	Y(K)=0.5*(Y(K-2)+Y(K-1))	00763
	NMIS=NMIS+6	00764
135	CONTINUE	00765
	IF(NMIS .EQ. 0)GO TO 163	00766
	DO 155 NV=1,NMIS	00767
	IOT=0	00768
	DO 137 K=1,NPT	00769
	ST(K,2)=0.0	00770
	ST(K,3)=0.0	00771
137	ST(K,4)=0.0	00772
	DO 141 IE=1,NELEM	00773
	MN=MNO(IE)/1000	00774
	ITYP=MOD(NON(MN),10)+1	00775
	IF(ITYP.EQ.5) GO TO 141	00776
	DO 140 JJ=1,4	00777
	J=NOD(IE,JJ)	00778
	I=JJ-1	00779
	IF(I .EQ. 0)I=4	00780
	I=NOD(IE,I)	00781
	K=JJ+1	00782
	IF(K .EQ. 5)K=1	00783
	K=NOD(IE,K)	00784
	ST(J,2)=ST(J,2)+X(I)+X(K)	00785
	ST(J,3)=ST(J,3)+Y(I)+Y(K)	00786
140	ST(J,4)=ST(J,4)+2.0	00787
141	CONTINUE	00788
	DO 150 K=1,NPT	00789
	IF(ST(K,1) .GT. 0.9E+20 .OR. ST(K,4) .EQ. 0.0)GO TO 150	00790
	D1=X(K)	00791
	D2=Y(K)	00792
	X(K)=ST(K,2)/ST(K,4)	00793
	Y(K)=ST(K,3)/ST(K,4)	00794
	D1=ABS((X(K)-D1)/(ABS(D1)+1.0E-20))	00795
	D2=ABS((Y(K)-D2)/(ABS(D2)+1.0E-20))	00796
	IF(D1+D2 .GT. .0001)IOT=1	00797
150	CONTINUE	00798
	IF(IOT .EQ. 0)GO TO 163	00799
155	CONTINUE	00800
C		00801
C	PRINT NODE AND ELEMENT DATA	00802
C		00803
163	CONTINUE	00804
	CALL RESOUT(1)	00805
	WRITE (6,908)	00806
	DO 168 N=1,NELEM	00807
	MS=MOD(MNO(N),1000)/10	00808
	MNORS=MNO(N)/1000	00809

C		00810
C	CHECK FOR NEGATIVE ELEMENT AREA	00811
C		00812
	N1=NOD(N,1)	00813
	N2=NOD(N,2)	00814
	N3=NOD(N,3)	00815
	N4=NOD(N,4)	00816
	IF (N4 .NE. N3)GO TO 164	00817
	N4=0	00818
	IF(N3.EQ.N2)N3=0	00819
	GO TO 166	00820
164	A1=X(N1)*(Y(N2)-Y(N4))+X(N2)*(Y(N4)-Y(N1))+X(N4)*(Y(N1)-Y(N2))	00821
	A2=X(N2)*(Y(N3)-Y(N4))+X(N3)*(Y(N4)-Y(N2))+X(N4)*(Y(N2)-Y(N3))	00822
	B1=X(N1)*(Y(N2)-Y(N3))+X(N2)*(Y(N3)-Y(N1))+X(N3)*(Y(N1)-Y(N2))	00823
	B2=X(N1)*(Y(N3)-Y(N4))+X(N3)*(Y(N4)-Y(N1))+X(N4)*(Y(N1)-Y(N3))	00824
	IF(A1+A2 .GT. 0.0) GO TO 165	00825
	IXP=0	00826
	WRITE(6,920) N	00827
165	A1=A1*A2	00828
	A2=B1*B2	00829
	IF(A1 .GE. A2) GO TO 166	00830
	NOD(N,1)=N2	00831
	NOD(N,2)=N3	00832
	NOD(N,3)=N4	00833
	NOD(N,4)=N1	00834
166	CONTINUE	00835
168	CONTINUE	00836
	CALL RESOUT(2)	00837
	GO TO 126	00838
C		00839
C	BOUNDARY CONDITIONS	00840
C		00841
175	WRITE (6,915)	00842
	I=1	00843
180	READ (5,806)NSEC, KK, (IIFLG(N),BIVD(N),N=1,2), TH, IA ,KKP, INCR, PJ, PK	00844
	READ (99,805) IMAGE	00845
	WRITE (3,803) IMAGE	00846
	IF(NSEC .NE. 0) GO TO 106	00847
	NMIS=0	00848
	IF(KKP .EQ. 0)GO TO 182	00849
	IF(INCR .EQ. 0) INCR=1	00850
	NM=(KKP-KK)/INCR	00851
	NMIS=JABS(NM)	00852
	INCR=INCR*NM/NMIS	00853
182	IF(IA .EQ. 0) IA=1	00854
	NM=1+NMIS	00855
	DP=PK-PJ	00856
	IF(NMIS .EQ. 0) GO TO 185	00857

	M=KK	0085
	XL=0.0	0085
	DO 183 L=1,NMIS	0086
	MP=M	0086
	M=M+INCR	0086
183	XL=SQRT((X(M)-X(MP))**2+(Y(M)-Y(MP))**2)+XL	0086
	DP=DP/XL	0086
185	DXB=0.0	0086
	DYB=0.0	0086
	IADD=0	0086
	IF (TH.NE.0.0) IADD=4	0086
	DO 190 L=1,NM	0086
	DXF=0.0	0087
	DYF=0.0	0087
	IF (L .EQ. NM) GO TO 186	0087
	DXF=X(KK+INCR)-X(KK)	0087
	DYF=Y(KK+INCR)-Y(KK)	0087
	PK=PJ+DP*(SQRT(DXF*DXF+DYF*DYF))	0087
186	BIV(I,1)=BIVD(1)-(2.0*(DYF+DYB)*PJ+DYB*PI+DYF*PK)/6.0	0087
	BIV(I,2)=BIVD(2)+(2.0*(DXF+DXB)*PJ+DXB*PI+DXF*PK)/6.0	0087
	DXB=DXF	0087
	DYB=DYF	0087
	PI=PJ	0088
	PJ=PK	0088
	BIV(I,3)=TH	0088
	NODE(I)=KK*10000+IIFLG(1)*10+IIFLG(2) +IA*100	0088
	DO 187 J=1,2	0088
	K=2*J-1+IADD	0088
	AN(J) =ANI(K+1)	0088
	IF (IIFLG(J) .EQ. 0) GO TO 187	0088
	AN(J)=ANI(K)	0088
187	CONTINUE	0089
	WRITE (6,906) KK , (AN(J),BIV(I,J),J=1,3),IA	0089
	KK=KK+INCR	0089
	BIV(I,3)=TH*0.0174533	0089
190	I=I+1	0089
	GO TO 180	0089
195	NBPTC=I-1	0089
C		0089
C	THE SIZE OF THE PROBLEM IS CHECKED TO SEE IF IT IS TOO LARGE	0089
C	AND DATA ERRORS ARE SOUGHT	0089
C		0089
	IF (NELEM .LT. 600) GO TO 206	0090
	WRITE (6,912)	0090
	IX=0	0090
206	IF (NPT .LT. 701)GO TO 207	0090
	WRITE (6,913)	0090
	IX=0	0090

207	IF(NBPTC.LT.200) GO TO 208	00906
	WRITE (6,914)	00907
	IX=0	00908
208	IF (NMAT.LT.11) GO TO 210	00909
	WRITE (6,911)	00910
	IX=0	00911
210	IF(IXP .EQ. 0)IX=0	00912
	CALL FINEL(WIDTH)	00913
	RETURN	00914
700	STOP	00915
	END	00916
	SUBROUTINE RESOUT(ITYP)	00917
	COMMON/BLK1/ X(700),Y(700),NOD(600,4),IXXX	00918
	COMMON/BLK2/MNO(600),NODB(200),BIV(200,3),IIFLG(3),BIVD(3)	00919
	I, NELEM, NPT, NUMPC, NINC	00920
	COMMON/BLK3/ C1(17,17),ZY(17),RT(3),ZT(3),RQ(4),ZQ(4),	00921
	1 NQ(700),U(700),V(700),ITOQ(2,3),ATOQ(2,3),EST(4,3)	00922
902	FORMAT (1H1,3(' ELEM',7X,'ELEMENT',7X,'MAT CONST',5X,1H) /	00923
	* 3(' NO.',4X,'NODAL POINTS NO. INCR. ') /1H)	00924
908	FORMAT(1H1,3(1X,'NODAL',8X,'X',13X,'Y',11X,1H) / 1X,	00925
	* 3(1X,'POINT',3X,'COORDINATE',4X,'COORDINATE',7X,1H) /1H)	00926
909	FORMAT(3(1X,I4,2(1X,F13.2) , 7X,1H))	00927
917	FORMAT(2X,3(I3,3X,I3,3(1X,I3),2(4X,I2),9X,1H))	00928
922	FORMAT(1H1,3(1X,'NODAL',8X,'X',13X,'Y',11X,1H) / 1X,	00929
	* 3(1X,'POINT',3X,'DISPLCEMNT',4X,'DISPLCEMNT',7X,1H) /1H)	00930
1001	FORMAT(83X,I4, 2F14.2)	00931
1002	FORMAT(83X,I4, 2(1X,1PE13.2))	00932
1006	FORMAT(3(1X,I4,2(1X,1PE13.2),7X,1H))	00933
1010	FORMAT(88X, I3,3X,I3,3(1X,I3),2(4X,I2))	00934
	IF(ITYP .EQ. 2) GOTO 166	00935
163	CONTINUE	00936
	LLINE = NPT / 3	00937
	NPG = LLINE / 37	00938
	LINES = NPG *37	00939
	LINS = 1	00940
	N1 = 1	00941
	IF (LLINE .LT. 37) GO TO 550	00942
	INC = 37	00943
	KSHIFT = 3*INC	00944
502	CONTINUE	00945
	IF(LINS .GT. LINES) GOTO 550	00946
	N3 = N1+2*INC	00947
	LINE = 1	00948
	IF(ITYP .EQ. 4) GOTO 504	00949
	WRITE (6,908)	00950
	GOTO 505	00951
504	WRITE (6,922)	00952
		00953

505	CONTINUE	00954
	IF(LINS .GT. LINES) GOTO 550	00955
	IF(ITYP .EQ. 4) GOTO 520	00956
	WRITE (6,909) (N, X(N), Y(N) ,N=N1,N3,INC)	00957
	GOTO 523	00958
520	CONTINUE	00959
	WRITE(6,1006)(N, U(N), V(N), N=N1,N3,INC)	00960
523	CONTINUE	00961
	LINS = LINS + 1	00962
	LINE = LINE + 1	00963
	N1 = N1 + 1	00964
	N3 = N3 + 1	00965
	IF (LINE .LE. 37) GO TO 505	00966
	N1 = N1 + 2*INC	00967
	GO TO 522	00968
550	CONTINUE	00969
	IF (LINES .EQ. LLINE) GOTO 552	00970
	INC = LLINE -LINES	00971
	LINES = LLINE	00972
	GOTO 502	00973
552	CONTINUE	00974
	N3=LINES*3+1	00975
	IF (N3 .GT. NPT) GOTO 555	00976
	IF(ITYP .EQ. 4) GOTO 554	00977
	WRITE(6,1001) (N,X(N),Y(N),N=N3,NPT)	00978
	GOTO 555	00979
554	CONTINUE	00980
	WRITE(6,1001) (N,U(N),V(N),N=N3,NPT)	00981
555	CONTINUE	00982
	IF(ITYP .EQ. 1) GOTO 730	00983
	IF(ITYP .EQ. 4) GOTO 730	00984
166	CONTINUE	00985
	LLINE = NELEM/3	00986
	NPG = LLINE / 37	00987
	LINES = NPG *37	00988
	LINS = 1	00989
	N1 = 1	00990
	IF (LLINE .LT. 37) GO TO 700	00991
	INC = 37	00992
	KSHIFT = 3*INC	00993
600	CONTINUE	00994
	IF(LINS .GT. LINES) GOTO 700	00995
	N2 = N1 + INC	00996
	N3 = N1+2*INC	00997
	WRITE(6,902)	00998
	LINE = 1	00999
610	CONTINUE	01000
	IF(LINS .GT. LINES) GOTO 700	01001

MN1	= MNO(N1)/1000	01002
MN2	= MNO(N2)/1000	01003
MN3	= MNO(N3)/1000	01004
INC1	= MOD(MNO(N1),1000)/10	01005
INC2	= MOD(MNO(N2),1000)/10	01006
INC3	= MOD(MNO(N3),1000)/10	01007
	WRITE(6,917) N1,(NOD(N1,K),K=1,4),MN1,INC1, N2,(NOD(N2,K),K=1,4)	01008
*	,MN2, INC2, N3,(NOD(N3,K),K=1,4), MN3, INC3	01009
	LINE = LINE + 1	01010
	LINES = LINES + 1	01011
	N1 = N1 + 1	01012
	N2=N2+1	01013
	N3 = N3 + 1	01014
	IF (LINE .LE. 37) GO TO 610	01015
	N1 = N1 + 2*INC	01016
	GO TO 600	01017
700	CONTINUE	01018
	IF (LINES .EQ. LLINE) GOTO 707	01019
	INC = LLINE -LINES	01020
	LINES = LLINE	01021
	GOTO 600	01022
707	CONTINUE	01023
	N3=LINES*3+1	01024
709	CONTINUE	01025
	IF (N3 .GT. NELEM) GOTO 730	01026
	MN3 = MNO(N3)/1000	01027
	INC3 = MOD(MNO(N3),1000)/10	01028
	WRITE(6,1010)N3,(NOD(N3,K),K=1,4),MN3,INC3	01029
	N3=N3+1	01030
	GOTO 709	01031
730	CONTINUE	01032
	RETURN	01033
	END	01034
C		01035
C		01036
C	INCREMENTAL PLAIN STRAIN ANALYSIS	01037
	COMMON /CNTRL/ WIDTH, INOUT, INCL	01038
	COMMON/BLK1/ X(700),Y(700),NOD(600,4),IX	01039
	COMMON/BLK2/MNO(600),NODB(200),BIV(200,3),IIFLG(3),BIVD(3)	01040
1	,NELEM, NPT, NBPTC, MINC	01041
	COMMON/BLK3/ C1(17,17),ZY(17),RT(3),ZT(3),RQ(4),ZQ(4),	01042
1	NQ(700),U(700),V(700),ITOQ(2,3),ATOQ(2,3),EST(4,3)	01043
2	, IS(5), BS(3), AS(3), RD, J1,	01044
3	AL(3,3), BT(3,3), GA(3,3) , Z5(12,12), Z4(12)	01045
4	,T(28,2), ITRW(28,2), NETCL(17,2), CTP(12,17), STORE(17)	01046
	COMMON/BLK4/ SL(112),S(112,56)	01047
	COMMON/BLK5/ DEN(10),NON(10),GNU(10,10),E(10,10),H(10,10),	01048
1	ST(600,9),CP(3,3)	01049

	COMMON/BLK6/AB(10),EB(10),XIB(10),BE(10),DE(10),TE(10),F(3)	0105
	1 ,TK(10)	0105
30	FORMAT(1H1,8X,28HINPUT DATA CARD IMAGE **** /2X,1H)	0105
	WRITE (3,30)	0105
C		0105
C		0105
C	THE SIZE OF THE EQUATION BLOCK IS SET	0105
C		0105
	CALL DHRERD	0105
	NEQ=56	0105
	NBW=NEC	0105
	CALL ESTAB	0106
C		0106
C	INPUT DATA IS READ	0106
C		0106
100	IX=NEQ	0106
	HTOP=-1.0E+09	0106
	CALL PREP	0106
	IF (INCUT .GT.0) GOTO 590	0106
	IF(IX .EQ. 0) GO TO 100	0106
C		0107
C	INITIALIZATION OF STORAGE ARRAYS	0107
C		0107
	DO 140 I=1,NPT	0107
	U(I)=0.0	0107
140	V(I)=0.0	0107
	DO 142 I=1,NELEM	0107
	DO 142 J=1,9	0107
142	ST(I,J)=0.0	0107
C		0107
C	INCREMENTAL ANALYSIS LOOP	0107
C		0108
	IA=0	0108
150	IA=IA+1	0108
C		0108
C	THE EQUATION POSITIONING MATRIX FOR THE SYSTEM MATRIX IS FORMED	0108
C	AND THE ELEVATION OF THE TOP OF THE CONSTRUCTION INCREMENT ESTABLISHED	0108
C		0108
	DO 160 I=1,NPT	0108
160	NQ(I+1)=0	0108
	HTOPP=HTOP	0108
	DO 198 M=1,NELEM	0109
	IAC=MOD(MNO(M),1000)/10	0109
	IF(IAC.GT.1A) GO TO 198	0109
	LS=200	0109
	MN=MNO(M)/1000	0109
	ITYP=MOD(NON(MN),10)+1	0109
	IF(ITYP.EQ.5)LS=300	0109

I=(300-LS)/100	01098
DU1=I	01099
DO 180 J=1,4	01100
I=NOD(M,J)+1	01101
DU=Y(I-1)*DU1	01102
IF(HTOP .LT. DU)HTOP=DU	01103
180 IF(NQ(I).LT.300)NQ(I)=LS	01104
198 CONTINUE	01105
NQ(1)=100	01106
DO 200 I=1,NPT	01107
200 NQ(I+1)=NQ(I)+NQ(I+1)	01108
C	01109
C THE BAND WIDTH-NPC- IS COMPUTED	01110
C	01111
NPC=0	01112
DO 218 I=1,NELEM	01113
MN=MNO(I)	01114
MN=MOD(MN ,1000)/10	01115
IF(MN.GT.1A) GO TO 218	01116
DO 202 J=1,4	01117
JJ=NOD(I,J)	01118
NQ(JJ)=NQ(JJ)+1	01119
DO 202 K=1,4	01120
KK=NOD(I,K)+1	01121
IV=NQ(KK)/100-NQ(JJ)/100	01122
IF (NPC .LT. IV) NPC=IV	01123
202 CONTINUE	01124
218 CONTINUE	01125
C	01126
C COMPUTE MATRIX SPECIFICATIONS	01127
C	01128
IF (NPC .LE. NEQ) GO TO 220	01129
WRITE (6,910)	01130
910 FORMAT (//, 1X 25HERROR-BAND WIDTH TO LARGE)	01131
GO TO 100	01132
220 NCOL = NPC	01133
NROW=NQ(NPT +1)/100-1	01134
C	01135
C INITIALIZE SYSTEM MATRIX	01136
C	01137
MN=2*NEQ	01138
DO 223 N=1,MN	01139
SL(N)=0.	01140
DO 223 J=1,NEQ	01141
223 S(N,J) = 0.	01142
C	01143
C THE STIFFNESS MATRIX IS GENERATED IN BLOCKS AND STORED ON TAPE	01144
C	01145

	REWIND 1	01146
	LB=C	01147
	LB1=C	01148
	NELEMT=0	01149
288	LB=LP+1	01150
	NB=(LB-1)*NEQ+1	01151
	MB=LB*NEQ	01152
C		01153
C	EACH ELEMENT IS EXAMINED TO DETERMINE IF IT CONTRIBUTES TO THE	01154
C	BLOCK	01155
C		01156
	DO 355 I=1,NELEM	01157
	IX=I	01158
	IF(NOD(I,1) .LT. 0) GO TO 355	01159
	IAC=MOD(MNO(I),1000)/10	01160
	MN=MNO(I)/1000	01161
	RO=DEN(MN)	01162
	IF(IAC-IA) 290,292,355	01163
290	RO=0.0	01164
292	DO 300 L=1,4	01165
	KK=NOD(I,L)	01166
	K1=NO(KK)/100	01167
	IF (K1 .LE. MB) GO TO 305	01168
300	CONTINUE	01169
	GO TO 355	01170
C		01171
C	CALCULATE THAT PORTION OF THE STIFFNESS MATRIX GIVEN BY A	01172
C	CONSIDERATION OF ELEMENT I	01173
C		01174
305	ITYP=MOD(NON(MN),10)+1	01175
	NP=NON(MN)/1000	01176
	ND=IAC-IA	01177
	GO TO (3(6,308,306,320,349),ITYP)	01178
306	L=0	01179
	IF(NP .GT. 1)GO TO 308	01180
	DO 307 J=1,3	01181
	DO 307 K=J,3	01182
	L=L+1	01183
	CP(J,K)= H(MN,L)	01184
307	CP(K,J)=CP(J,K)	01185
	GO TO 349	01186
308	CALL INTPI(EI,GNUI,MN,HTOP,ND,HTOPP,I,NP)	01187
	CALL CONV(T(EI,GNUI)	01188
	GO TO 349	01189
320	CALL REINF(MN,HTOP,ND,HTOPP,I,NP)	01190
349	CALL STIFNS(IA,LB1,NEQ,MN)	01191
	NELEMT=NELEMT+1	01192
	NOD(I,1)=-NOD(I,1)	01193

C	355 CONTINUE	01194
C	IF HAVE LESS THAN 1 BLOCK OF EQUATIONS LEFT NO ADDITIONAL TAPE	01195
C	STORAGE IS USED	01196
C	IF(NROW .LE. MB) GO TO 560	01197
C	LBI=LB1+1	01198
C	THE BLOCK OF EQUATIONS IS REDUCED AND PUT ON TAPE	01199
C	CALL REDUCI(NEQ,NCOL)	01200
C	WRITE (1) (SL(N),(S(N,M),M=1,NCOL), N=1,NEQ)	01201
C	THE NUMBER TWO BLOCK OF EQUATIONS IS SHIFTED INTO THE NUMBER ONE	01202
C	POSITION	01203
C	DO 555 L=1,NEQ	01204
C	LRH=L+NEQ	01205
C	SL(L)=SL(LRH)	01206
C	SL(LRH)=0.0	01207
C	DO 555 M=1,NCOL	01208
C	S(L,M)=S(LRH,M)	01209
C	555 S(LRH,M)=0.0	01210
C	GO TO 289	01211
C	560 NT=NROW-LBI*NEQ	01212
C	THE FINAL TWO BLOCKS OF EQUATIONS ARE REDUCED AND BACK-SUBSTITUED	01213
C	CALL REDUCI(NT,NCOL)	01214
C	NS=LBI	01215
C	CALL BAKSUB(NT,NCOL,LB,NEQ)	01216
C	IF (LBI .EQ. 0) GO TO 564	01217
C	DO 563 J=1,LBI	01218
C	DO 562 L=1, NEQ	01219
C	LL=L+NEQ	01220
C	562 SL(LL)=SL(L)	01221
C	L =LBI-J+1	01222
C	ANY BLOCKS ON TAPE ARE RECALLED AND BACK SUBSTITUED	01223
C	BACKSPACE 1	01224
C	READ (1) (SL(N),(S(N,M),M=1,NCOL),N=1,NEQ)	01225
C	BACKSPACE 1	01226
C	CALL BAKSUB(NEQ,NCOL,L,NEQ)	01227
C	563 CONTINUE	01228
C	564 L=0	01229
C	DO 566 N=1,LB	01230
C	K=NEQ	01231
C		01232
C		01233
C		01234
C		01235
C		01236
C		01237
C		01238
C		01239
C		01240
C		01241

	DO 566 KK=1,NEQ	0124
	K=K+1	0124
	L=L+1	0124
	566 SL(L)=S(K,N)	0124
C		0124
C	STRESSES AND STRAINS COMPUTED	0124
C		0124
	CALL STRESS(IA,NELEMT,HTOP,HTOPP)	0124
	IF (IA .LT. NINC) GO TO 150	0124
590	CONTINUE	0125
	GO TO 100	0125
	END	0125
	SUBROUTINE BEAMST(I,MN)	0125
C		0125
C	THIS SUBROUTINE CALCULATES BEAM FORCES, SHEARS AND MOMENTS	0125
C		0125
	COMMON/BLK1/ X(700),Y(700),NOD(600,4),IX	0125
	COMMON/BLK3/ C1(17,17),ZY(17),RT(3),ZT(3),RQ(4),ZQ(4),	0125
1	NQ(700),U(700),V(700),ITDQ(2,3),ATDQ(2,3),EST(4,3)	0125
2	, IS(5), BS(3), AS(3), RO, J1,	0126
3	AL(3,3), BT(3,3), GA(3,3), Z5(12,12), Z4(12)	0126
4	, T(28,2), ITRW(28,2), NETCL(17,2), CTP(12,17), STORE(17)	0126
	COMMON/BLK4/ SL(I12),S(I12,56)	0126
C		0126
C	STIFFNESS MATRIX TIMES DISPLACEMENT	0126
C		0126
	COST=STORE(1)	0126
	SINT=STORE(2)	0126
	ZY(5)=ZY(4)	0126
	ZY(4)=ZY(3)	0127
	N1=NOD(I,1)	0127
	ND=NG(N1)/100+2	0127
	ZY(3)=SL(ND)	0127
	DO 100 K=1,6	0127
	DU=0.0	0127
	DO 90 L=1,6	0127
90	DU=DU+C1(K,L)*ZY(L)	0127
100	STORE(K)=DU	0127
	RQ(1)=-STORE(1)*COST-STORE(2)*SINT	0128
	RQ(2)=STORE(1)*SINT-STORE(2)*COST	0128
	RO(3)=-STORE(3)	0128
	ZQ(1)=STORE(4)*COST+STORE(5)*SINT	0128
	ZQ(2)=-STORE(4)*SINT+STORE(5)*COST	0128
	ZQ(3)=STORE(6)	0128
	DO 200 K=1,3	0128
200	RQ(K)=0.5*(RQ(K)+ZQ(K))	0128
	RETURN	0128
	END	0128

	SUBROUTINE BEAMEL(I,MN)	01290
C		01291
C	THIS SUBROUTINE CALCULATES THE STIFFNESS MATRIX FOR A BENDING ELEMENT	01292
C		01293
	COMMON/BLK3/ C1(17,17),ZY(17),RT(3),ZT(3),RQ(4),ZQ(4),	01294
1	NQ(700),U(700),V(700),ITQ(2,3),ATOQ(2,3),EST(4,3)	01295
2	, IS(5), ES(3), AS(3), RO, J1,	01296
3	AL(3,3), BT(3,3), GA(3,3), Z5(12,12), Z4(12)	01297
4	, T(28,2), ITRW(28,2), NETCL(17,2), CTP(12,17), STORE(17)	01298
	COMMON/BLK5/ DEN(10),NON(10),GNU(10,10),E(10,10),H(10,10),	01299
1	ST(600,9),CP(3,3)	01300
	CA=RQ(2)-RQ(1)	01301
	SA=ZQ(2)-ZQ(1)	01302
	XL=SQRT(CA*CA+SA*SA)	01303
	CA=CA/XL	01304
	SA=-SA/XL	01305
	STORE(1)=CA	01306
	STORE(2)=-SA	01307
	GNUM=GNU(MN,1)	01308
	EB=E(MN,1)/(1.-GNUM*GNUM)	01309
	XIB=H(MN,2)	01310
	AB=H(MN,1)	01311
	DU=EB*AB/XL	01312
	C1(1,1)=DU	01313
	C1(4,1)=-DU	01314
	C1(1,4)=-DU	01315
	C1(4,4)=DU	01316
	XL=0.5*XL	01317
	RQ(1)=0.0	01318
	RQ(3)=0.0	01319
	D=.25/XL	01320
	RQ(2)=-D	01321
	RQ(4)=D	01322
	ZQ(2)=D	01323
	ZQ(4)=D	01324
	D=D/XL	01325
	ZQ(1)=D	01326
	ZQ(3)=-D	01327
	D=8.0*XL*EB*XIB	01328
	DO 120 L=1,4	01329
	LS=L+1+L/3	01330
	DO 120 J=1,4	01331
	JS=J+1+J/3	01332
C		01333
	120 C1(LS,JS)=D*(RQ(J)*RQ(L)+3.*ZQ(J)*ZQ(L))	01334
C		01335
C	LOCAL UNKNOWNNS TRANSFORMED TO GLOBAL UNKNOWNNS	01336
	DO 400 NR=1,4,3	01337

	DO 315 JJ=1,6	0133
	D2=C1(NR+1,JJ)	0133
	D1=C1(NR,JJ)	0134
	C1(NR,JJ)=D1*CA+D2*SA	0134
315	C1(NR+1,JJ)=-D1*SA+D2*CA	0134
	DO 318 II=1,6	0134
	D1=C1(II,NR)	0134
	D2=C1(II,NR+1)	0134
	C1(II,NR)=D1*CA+D2*SA	0134
318	C1(II,NR+1)=-D1*SA+D2*CA	0134
400	CONTINUE	0134
	RETURN	0134
	END	0135
	SUBROUTINE CONVT(D1,D2)	0135
C		0135
C	THIS SUBROUTINE EXPRESSES ISOTROPIC PROPERTIES IN ANISOTROPIC FORMS	0135
C		0135
	COMMON/BLK5/ DEN(10),NON(10),GNU(10,10),E(10,10),H(10,10),	0135
1	ST(600,9),CP(3,3)	0135
	IF(D2 .EQ. 0.5)D2=.495	0135
	CP(3,3)=D1*.5/(1.3+D2)	0135
	D1=D1/((1.0+D2)*(1.0-2.0*D2))	0135
	CP(1,2)=D2*D1	0136
	CP(2,1)=CP(1,2)	0136
	CP(1,3)=0.0	0136
	CP(2,3)=0.0	0136
	CP(3,1)=0.0	0136
	CP(3,2)=0.0	0136
	D1=D1*(1.0-D2)	0136
	CP(1,1)=D1	0136
	CP(2,2)=D1	0136
	RETURN	0137
	END	0137
	SUBROUTINE ANISP(C11, C12, C22, C33, PI)	0137
C		0137
C	THIS SUBROUTINE TRANSFORMS ORTHOTROPIC PROPERTIES FROM THEIR	0137
C	PREFERED DIRECTIONS TO GLOBAL COORDINATES	0137
C		0137
	COMMON/BLK5/ DEN(10),NON(10),GNU(10,10),E(10,10),H(10,10),	0137
1	ST(600,9),CP(3,3)	0137
	DIMENSION TH(3,3),RO(3,3)	0137
	CP(1,3)=0.0	0137
	CP(2,3)=0.0	0137
	CP(3,1)=0.0	0138
	CP(3,2)=0.0	0138
	CP(1,1)=C11	0138
	CP(1,2)=C12	0138
	CP(2,2)=C22	0138

CP(3,3)=C33	01386
CP(2,1)=C12	01387
IF(PI .EQ. 0.0)GO TO 80	01388
PI=PI*0.0174533	01389
SPH=SIN(PI)	01390
CPH=COS(PI)	01391
D1=CPH*CPH	01392
D2=SPH*SPH	01393
C1=SPH*CPH	01394
TH(1,1)=D1	01395
TH(1,2)=D2	01396
TH(1,3)=C1	01397
TH(2,1)=D2	01398
TH(2,2)=D1	01399
TH(2,3)=-C1	01400
TH(3,1)=-2.0*C1	01401
TH(3,2)=2.0*C1	01402
TH(3,3)=D1-D2	01403
DO 67 M=1,3	01404
DO 67 N=1,3	01405
DU=0.0	01406
DO 65 L=1,3	01407
65 DU=DU+TH(L,N)*CP(M,L)	01408
67 RO(M,N)=DU	01409
DO 75 M=1,3	01410
DO 75 N=1,3	01411
DUI=0.0	01412
DO 72 L=1,3	01413
72 DUI=DUI+TH(L,M)*RO(L,N)	01414
75 CP(M,N)=DUI	01415
80 RETURN	01416
END	01417
SUBROUTINE INTPI(EI,GNUI,MN,HTOP,ND,HTOPP,I,NP)	01418
C	01419
C THIS SUBROUTINE CALCULATES THE VALUES OF THE MATERIAL	01420
C PROPERTIES FOR A GIVEN OVERBURDEN	01421
C	01422
COMMON/BLK1/ X(700),Y(700),NOD(600,4),IX	01423
COMMON/BLK5/ DEN(10),NON(10),GNU(10,10),E(10,10),H(10,10),	01424
1 ST(600,9),CP(3,3)	01425
C	01426
IF(NP .LT. 2)GO TO 440	01427
C	01428
C TYPE A	01429
C	01430
GAM=DEN(MN)	01431
HAVG=C.0	01432
DO 300 J=1,4	01433

	N=NOD(I,J)	01434
300	HAVG=HAVG+0.25*Y(N)	01435
	HO=HTOPP-HAVG+0.5*(HTOP-HTOPP)	01436
	IF(ND .EQ. 0)HO=0.5*(HTOP-HAVG)	01437
	HC=HC*GAM	01438
	HO = -ST (I,5)	01439
	IF (HO .LT. 100.0) HO = 100.0	01440
	IF(NP .GT. 2)GO TO 390	01441
	A=E(MN,1)	01442
	B=H(MN,1)	01443
	PH=H(MN,2)	01444
	DU=(45.0+0.5*PH)*0.0174533	01445
	PH=PH*0.0174533	01446
	C=H(MN,3)	01447
	SINP=SIN(PH)	01448
	XNPH=(SIN(DU)/COS(DU))**2	01449
	DU1=(1.0-SINP)*HO	01450
	DU2=2.0*(C*COS(PH)+SINP*(HO/XNPH-2.0*C/SQRT(XNPH)))	01451
	DU3= (1.0-DU1*SINP/DU2)**2	01452
	EI=(A+B*DU1)*DU3	01453
	GO TO 445	01454
C		01455
C	TYPE B	01456
C		01457
390	IC=NP-1	01458
	IF(ND .NE. 0)HO=GAM*0.5*(HTOP-HTOPP)	01459
	P1=ABS(ST(I,5))+ABS(HO)	01460
	DO 400 J=1,IC	01461
	K=J	01462
	DU1=H(MN,K)	01463
	IF(P1.LE.DU1) GO TO 430	01464
400	CONTINUE	01465
	P1=DU1	01466
430	IF(K.EQ.1) GO TO 440	01467
	DU2=GNI(MN,K-1)	01468
	DU3=H(MN,K-1)	01469
	GNI=DU2+(GNI(MN,K)-DU2)*(P1-DU3)/(DU1-DU3)	01470
	DU2=E(MN,K-1)	01471
	EI=DU2+(E(MN,K)-DU2)*(P1-DU3)/(DU1-DU3)	01472
	GO TO 450	01473
440	EI=E(MN,1)	01474
445	GNI=GNI(MN,1)	01475
450	RETURN	01476
	END	01477
	SUBROUTINE STIFNS(IA,LB1,NEQ,MN)	01478
C		01479
C	THIS SUBROUTINE FORMS THE ELEMENT MATRIX FOR A QUADRILATERAL	01480
C	ELEMENT	01481

	COMMON/BLK1/ X(700),Y(700),NOD(600,4),I	01482
	COMMON/BLK2/MNO(600),NODR(200),BIV(200,3),JIFLG(3),BIVD(3)	01483
	1 ,NELEM, NPT, NBPTC, NINC	01484
	COMMON/BLK3/ C1(17,17),ZY(17),XT(3),YT(3),RQ(4),ZQ(4),	01485
	1 NO(700),U(700),V(700),ITDQ(2,3),ATOQ(2,3),EST(4,3)	01486
	2 , IS(5), BS(3), AS(3), RO, J1,	01487
	3 AL(3,3), RT(3,3), GA(3,3), CT(12,12), ZT(12)	01488
	4 ,T(28,2), ITRW(28,2), NETCL(17,2), CTP(12,17), STORE(17)	01489
	COMMON/BLK4/ SL(112),S(112,56)	01490
	COMMON/BLK5/ DEN(10),NON(10),GNU(10,10),E(10,10),H(10,10),	01491
	1 ST(600,9),CP(3,3)	01492
		01493
	IDENTIFICATION CODE FOR TRIANGULAR ELEMENTS SET	01494
		01495
	JTRY=2	01496
	IF(NOD(I,4).EQ.NOD(I,3)) JTRY=1	01497
	DO 60 J=1,17	01498
	DO 50 K=1,17	01499
	50 C1(J,K)=0.0	01500
	60 ZY(J)=0.0	01501
		01502
	THE CORNER POINT COORDINATES ARE FOUND	01503
		01504
	DO 90 J=1,4	01505
	K=NOD(I,J)	01506
	RQ(J)=X(K)	01507
	90 ZQ(J)=Y(K)	01508
	NU=2	01509
	IF(NOD(I,3).NE.NOD(I,2)) GO TO 97	01510
	CALL BEAMEL(I,MN)	01511
	NU=3	01512
	GO TO 313	01513
		01514
	THE SUB-ELEMENT MATRICES ARE FOUND AND ADDED INTO THE ELEMENT	01515
	MATRIX	01516
		01517
	97 DO 300 J=1,JTRY	01518
	JI=J	01519
		01520
	NODE COORDINATES OF SUB-ELEMENT ARE FOUND	01521
		01522
	DO 100 K=1,3	01523
	XT(K)=RQ(K)	01524
	100 YT(K)=ZQ(K)	01525
	IF(JTRY.EQ.1) GO TO 105	01526
	IF(J1 .EQ. 2) GO TO 103	01527
	XT(3)=RQ(4)	01528
		01529

	YT(3)=ZQ(4)	0150
	GO TO 105	0150
103	XT(1)=RQ(4)	0153
	YT(1)=ZQ(4)	0153
105	M=6*JI-7	0153
	DO 220 K=1,3	0153
	M=M+2	0153
	STORE(M)=XT(K)	0153
220	STORE(M+1)=YT(K)	0153
	CALL STFSUB	0153
300	CONTINUE	0153
C		0154
C	THE ELEMENT UNKNOWNNS ARE ELIMINATED	0154
C		0154
	IF(JTRY.EQ.1) GO TO 313	0154
	DO 312 K=1,9	0154
	LL=17-K	0154
	KK=18-K	0154
	DU3=C1(KK, KK)	0154
	DU2=ZY(KK)	0154
	DO 312 L=1,LL	0154
	DUI=C1(L, KK)/DU3	0155
	DO 310 M=1,LL	0155
310	C1(L, M)=C1(L, M)-C1(KK, M)*DUI	0155
312	ZY(L)=ZY(L)-DUI*DU2	0155
C		0155
C	STIFFNESS MATRIX STORED	0155
C		0155
313	STORE(17)=I	0155
	WRITE(2)(ZY(M), STORE(M), (C1(M, N), N=1, 17), M=1, 17), ((CP(J, K), K=1, 3),	0155
1	J=1, 3)	0155
C		0156
C	THE BOUNDARY CONDITIONS ARE CONSIDERED	0156
C		0156
	DO 334 J=1,4	0156
	NRQ=NOD(I, J)	0156
	DO 331 K=1, NBPTC	0156
	KK=IABS(NODB(K))	0156
	K1=KK/10000	0156
	IF (NRQ .NE. K1) GO TO 331	0156
	XX=1.0	0156
	IF (NODB(K) .LT. 0) XX=0.0	0157
	NODB(K)=-KK	0157
	NR=NU*(J-1)	0157
	IIFLG(1)=MOD(KK, 100)/10	0157
	IIFLC(2)=MOD(KK, 10)	0157
	IIFLG(3)=IIFLG(1)+IIFLG(2)	0157
	BIVD(1)=BIV(K, 1)	0157
		0157

	BIVD(2)=BIV(K,2)	01578
	BIVD(3)=0.0	01579
	IAN=MOD(KK,10000)/100	01580
	ANG=BIV(K,3)	01581
	IF(ANG .EQ. 0.0) GO TO 320	01582
C		01583
C	TRANSFORMATION TO N-S AXES	01584
C		01585
	CA=COS(ANG)	01586
	SA=SIN(ANG)	01587
	D1=ZY(NR+1)	01588
	D2=ZY(NR+2)	01589
	ZY(NR+1)=D1*CA+D2*SA	01590
	ZY(NR+2)=-D1*SA+D2*CA	01591
	DO 315 JJ=1,8	01592
	D1=C1(NR+1,JJ)	01593
	D2=C1(NR+2,JJ)	01594
	C1(NR+1,JJ)=D1*CA+D2*SA	01595
315	C1(NR+2,JJ)=-D1*SA+D2*CA	01596
	DO 318 II=1,8	01597
	D1=C1(II,NR+1)	01598
	D2=C1(II,NR+2)	01599
	C1(II,NR+1)=D1*CA+D2*SA	01600
318	C1(II,NR+2)=-D1*SA+D2*CA	01601
320	DO 330 M=1,NU	01602
	DUI=0.0	01603
	IF(IAN .EQ. IA) DUI=BIVD(N)	01604
	NR=NR+1	01605
C		01606
C	LOADS ADDED IN	01607
C		01608
	ZY(NR)=ZY(NR)+XX*DUI	01609
	IF(IIFLG(N) .EQ. 0) GO TO 330	01610
C		01611
C	DISPLACEMENTS SPECIFIED	01612
C		01613
	ZY(NR)=DUI*XX	01614
	C1(NR,NR)=0.0	01615
	DO 327 M=1,8	01616
	ZY(M)=ZY(M)-C1(M,NR)*DUI	01617
	C1(M,NR)=0.0	01618
327	C1(NR,M)=0.0	01619
330	CONTINUE	01620
331	CONTINUE	01621
334	CONTINUE	01622
C		01623
C	THE ELEMENT MATRIX IS NOW ADDED INTO THE SYSTEM MATRIX	01624
C		01625

NRCC=0	0162
IJU=LBI*NEQ	0162
DO 350 K=1,4	0162
KK=NOD(I,K)	0162
NR=NQ(KK)/100-I	0163
NRM=NR-IJU	0163
DO 350 M=1,NU	0163
NRCC=NRCC+1	0163
NRM=NRM+1	0163
NCCC=0	0163
DO 345 L=1,4	0163
JJ=NOD(I,L)	0163
NCN=NQ(JJ)/100-NR-M	0163
DO 345 N=1,NU	0163
NCCC=NCCC+1	0163
NCN=NCN+1	0164
IF (NCN.LT. 1) GO TO 344	0164
S(NRM,NCN) =S(NRM,NCN) +C1(NRCC,NCCC)	0164
344 CONTINUE	0164
345 CONTINUE	0164
350 SL(NRM) =SL(NRM) +ZY(NRCC)	0164
RETURN	0164
END	0164
SUBROUTINE GEOM(AA,D1,D2,D3)	0164
COMMON/BLK3/ C1(17,17),ZY(17),XT(3),YT(3),RQ(4),ZQ(4),	0165
1 NQ(700),U(700),V(700),ITQ(2,3),ATOQ(2,3),EST(4,3)	0165
2 , IS(5), BS(3), AS(3), RQ, J1,	0165
3 AL(3,3), BT(3,3), GA(3,3) , Z5(12,12), Z4(12)	0165
4 ,T(28,2), ITRW(28,2), NETCL(17,2), CTP(12,17), STORE(17)	0165
C	0165
C GEOMETRIC PROPERTIES OF ELEMENT CALCULATED	0165
C	0165
AA=0.0	0165
D1=0.0	0165
D2=0.0	0165
D3=0.0	0166
DO 110 I=1,3	0166
J=IS(I+1)	0166
K=IS(I+2)	0166
D4=YT(J)-YT(K)	0166
D5=XT(K)-XT(J)	0166
AA=AA+XT(I)*D4	0166
D1=D1+D4*D4	0166
D2=D2+D4*D5	0166
D3=D3+D5*D5	0166
BS(I)=D4	0167
110 AS(I)=D5	0167
C	0167

C	CONSTRAINT EQUATIONS NECESSARY FOR CONVERGENCE FORMED	01674
C	DU=1.0/AA	01675
	IF(J1 .EQ. 2) GO TO 117	01676
	DO 112 I=1,3	01677
	T(I+18,1)=YT(I)*DU	01678
	T(I+24,1)=YT(I)*DU	01679
112	T(I+21,1)=-XT(I)*DU	01680
	GO TO 140	01681
117	DO 121 I=1,3	01682
	T(I+19,2)=-XT(I)*DU	01683
	T(I+25,2)=-XT(I)*DU	01684
121	T(I+22,2)=YT(I)*DU	01685
140	RETURN	01686
	END	01687
	SUBROUTINE STFSUB	01688
C		01689
C	THIS SUBROUTINE FORMS THE ELEMENT MATRIX FOR A TRIANGULAR	01690
C	ELEMENT	01691
C		01692
	COMMON/BLK1/ X(700),Y(700),NOD(600,4),IX	01693
	COMMON/BLK3/ C1(17,17),ZY(17),XT(3),YT(3),RQ(4),ZQ(4),	01694
1	NQ(700),U(700),V(700),ITDQ(2,3),ATDQ(2,3),EST(4,3)	01695
2	, IS(5), BS(3), AS(3), RO, J1,	01696
3	AL(3,3), BT(3,3), GA(3,3), CT(12,12), ZT(12)	01697
4	, T(28,2), ITRW(28,2), NETCL(17,2), CTP(12,17), STORE(17)	01698
	COMMON/BLK5/ DEN(10),NON(10),GNU(10,10),E(10,10),H(10,10),	01699
1	ST(600,9),CP(3,3)	01700
	CALL GEOM(AA,D1,D2,D3)	01701
	DO 155 N=1,3	01702
	BN=BS(N)/12.0	01703
	AN=AS(N)/12.0	01704
	DO 150 I=1,3	01705
	AL(N,I)=2.0*BN *BS(I)	01706
	BT(N,I)=AN *BS(I)+AS(I)*BN	01707
150	GA(N,I)=2.0*AN *AS(I)	01708
	AL(N,N)=D1/12.0	01709
	BT(N,N)=D2/12.0	01710
155	GA(N,N)=D3/12.0	01711
	DU=0.5/AA	01712
	C11=CP(1,1)*DU	01713
	C12=CP(1,2)*DU	01714
	C13=CP(1,3)*DU	01715
	C22=CP(2,2)*DU	01716
	C23=CP(2,3)*DU	01717
	C33=CP(3,3)*DU	01718
	FY = -RO * AA / 8.0	01719
C		01720
		01721

C	CHECK FOR DATA ERROR	0172
C	IF(AA.LE.0.0) WRITE(6,911) IX	0172
	911 FORMAT (// 7X 21HDATA ERROR IN ELEMENT , I4//)	0172
C	FORM ELEMENT STIFFNESS MATRIX	0172
C	DO 250 N=1,3	0172
	DUI = 1.0	0172
	IF (N*J1 .LT. 2 .OR. N*J1 .GT. 4) DUI = 2.0	0173
	BN=BS(N)	0173
	AN=AS(N)	0173
	ZT(N)=0.0	0173
	ZT (N+3) = FY * DUI	0173
	ZT(N+6)=0.0	0173
	ZT (N+9) = 0.0	0173
	DO 250 I=1,3	0173
	D2=-1.0/3.0	0173
	D4=AL(I,N)	0174
	D5=BT(I,N)	0174
	D6=GA(I,N)	0174
	BI=BS(I)	0174
	AI=AS(I)	0174
	X1=BI*BN	0174
	X2=BI*AN	0174
	X3=AI*BN	0174
	X4=AI*AN	0174
	X5=X2+X3	0174
	CT(N,I)= C11*X1+C13* X5 +C33*X4	0175
	CT(N,I+3)= C12*X3+C13*X1+C23*X4+C33*X2	0175
	CT(N,I+6)=D2*CT(N,I)	0175
	CT(N,I+9)=D2*CT(N,I+3)	0175
	CT(N+3,I+3)= C22*X4+C23* X5 +C33*X1	0175
	CT(N+3,I+6)=D2*(C13*X1+C12*X2+ C33*X3+C23*X4)	0175
	CT(N+3,I+9)=D2*CT(N+3,I+3)	0175
	CT(N+6,I+6)=C11*D4+2.0*C13*D5+C33*D6	0175
	CT(N+6,I+9)=C13*D4 +(C12+C33)*D5+C23*D6	0175
250	CT(N+9,I+9)=C22*D6+2.0*C23*D5+C33*D4	0175
	DO 300 N=1,12	0176
	DO 300 I=N,12	0176
300	CT(I,N)=CT(N,I)	0176
C		0176
C	SUB-ELEMENT UNKNOWNNS TRANSFORMED TO ELEMENT UNKNOWNNS	0176
C		0176
	KP=1	0176
	MC=1	0176
	DO 400 K=1,17	0176
	KA=NETCL(K,J1)	0176

	DO 320 MM=1,KA	01770
	M=ITRW(KB,J1)	01771
	ZY(K)=ZY(K)+ZT(M)*T(KB,J1)	01772
320	KB=KB+1	01773
	DO 380 L=1,12	01774
	CTP(L,K)=0.0	01775
	MP=MC	01776
	DO 380 MM=1,KA	01777
	M=ITRW(MP,J1)	01778
	CTP(L,K)=CTP(L,K)+CT(L,M)*T(MP,J1)	01779
380	MP=MP+1	01780
400	MC=MC+KA	01781
	MC=1	01782
	DO 410 I=1,17	01783
	KA=NETCL(I,J1)	01784
	DO 405 K=1,17	01785
	MP=MC	01786
	DO 405 MM=1,KA	01787
	M=ITRW(MP,J1)	01788
	C1(I,K)=C1(I,K)+CTP(M,K)*T(MP,J1)	01789
405	MP=MP+1	01790
410	MC=MC+KA	01791
	RETURN	01792
	END	01793
	SUBROUTINE REDUCI(NN,NCOL)	01794
C		01795
C	THIS SUBROUTINE REDUCES A BLOCK OF EQUATIONS	01796
C		01797
	COMMON/BLK4/ B(112),A(112,56)	01798
	DO 300 N=1,NN	01799
	IF(A(N,1) .EQ. 0.0)GO TO 300	01800
	D =B(N)/A(N,1)	01801
	B(N)=D	01802
	I=N	01803
	DO 275 L=2,NCOL	01804
	C=A(N,L)/A(N,1)	01805
	I=I+1	01806
	IF (C .EQ. 0.0) GO TO 275	01807
	J=0	01808
	DO 250 K=L,NCOL	01809
	J=J+1	01810
250	A(I,J)=A(I,J)-C*A(N,K)	01811
	B(I)=B(I)-A(N,L)*D	01812
275	A(N,L)=C	01813
300	CONTINUE	01814
	RETURN	01815
	END	01816
	SUBROUTINE BAKSUB(NN,NCOL,LB,NEQ)	01817

C		0181
C	THIS SUBROUTINE BACK SUBSTITUTES A BLOCK OF EQUATIONS	0181
C		0182
	COMMON/BLK4/ B(112),A(112,56)	0182
	N=NN+1	0182
	DO 450 M=1,NN	0182
	N=N-1	0182
	DUI=R(N)	0182
	IF (A(N,1) .EQ. 0.0) GO TO 430	0182
	L=N	0182
	DO 425 K=2,NCOL	0182
	L=L+1	0182
425	DUI=DUI-A(N,K)*B(L)	0182
430	LL=N+NEQ	0182
	A(LL,LP)=DUI	0183
450	B(N)=DUI	0183
	RETURN	0183
	END	0183
	SUBROUTINE PRINC (XM, XML)	0183
C		0183
C	THIS SUBROUTINE FINDS THE PRINCIPAL COMPONENTS OF A SECOND RANK	0183
C	TENSOR IN TWO-DIMENSIONS	0183
C		0184
	DIMENSION XM(4), XML(4)	0184
	XML(3)=0.0	0184
	DUI=(XM(1)+XM(2))/2.0	0184
	DU2=SQRT(((XM(1)-XM(2))/2.0)**2+XM(3)**2)	0184
	XML(1)=DUI+DU2	0184
	XML(2)=DUI-DU2	0184
	IF (XM(1) .LE. XM(2)) GO TO 705	0184
	DU3=XML(1)-XM(2)	0184
	IF(DU3.EQ.0.0) GO TO 718	0184
	DU2=XM(3)/DU3	0184
	DUI=SQRT(1.0/(1.0+DU2**2))	0185
	DU2=DU2*DUI	0185
	GO TO 716	0185
705	DU3=XML(1)-XM(1)	0185
	IF(DU3.EQ.0.0) GO TO 718	0185
	DUI=XM(3)/DU3	0185
	DU2=SQRT(1.0/(1.0+DUI**2))	0185
	DUI=DUI*DU2	0185
716	XML(3)=ATAN2(DU2,DUI)/0.01745329	0185
718	RETURN	0185
	END	0186
	SUBROUTINE ESTAB	0186
C		0186
C	TRANSFORMATION RELATIONSHIPS BETWEEN ELEMENT AND SUB-ELEMENT	0186
C	UNKNOWN ESTABLISHED	0186
		0186

C	COMMON/BLK3/ C1(17,17),ZY(17),RT(3),ZT(3),RQ(4),ZQ(4),	01866
1	NQ(700),U(700),V(700),ITQQ(2,3),ATQQ(2,3),EST(4,3)	01867
2	, IS(5), BS(3), AS(3), RO, J1,	01868
3	AL(3,3), BT(3,3), GA(3,3), Z5(12,12), Z4(12)	01869
4	,T(28,2), ITRW(28,2), NETCL(17,2), CTP(12,17), STORE(17)	01870
	IS(1)=1	01871
	IS(2)=2	01872
	IS(3)=3	01873
	IS(4)=1	01874
	IS(5)=2	01875
	DO 55 I=1,2	01876
	DO 50 J=1,28	01877
	ITRW(J,I)=1	01878
50	T(J,I)=1.0	01879
	DO 55 J=1,17	01880
55	NETCL(J,I)=1	01881
	DO 57 I=1,3	01882
	ITRW(I+ 8,1)=I+6	01883
	ITRW(I+12,1)=I+9	01884
	ITRW(I+18,1)=I+6	01885
	ITRW(I+21,1)=I+9	01886
	ITRW(I+24,1)=I+6	01887
	ITRW(I+ 9,2)=I+6	01888
	ITRW(I+13,2)=I+9	01889
	ITRW(I+19,2)=I+9	01890
	ITRW(I+22,2)=I+6	01891
57	ITRW(I+25,2)=I+9	01892
	NETCL(9,1)=3	01893
	NETCL(11,1)=3	01894
	NETCL(15,1)=6	01895
	NETCL(16,1)=3	01896
	NETCL(10,2)=3	01897
	NETCL(12,2)=3	01898
	NETCL(16,2)=3	01899
	NETCL(17,2)=6	01900
	ITRW(2,1)=4	01901
	ITRW(3,1)=2	01902
	ITRW(4,1)=5	01903
	ITRW(7,1)=3	01904
	ITRW(8,1)=6	01905
	ITRW(17,1)=7	01906
	ITRW(18,1)=10	01907
	T(5,1)=0.0	01908
	T(6,1)=0.0	01909
	T(12,1)=0.0	01910
	T(16,1)=0.0	01911
	T(28,1)=0.0	01912
		01913

ITRW(3,2)=2	0191
ITRW(4,2)=5	0191
ITRW(5,2)=3	0191
ITRW(6,2)=6	0191
ITRW(8,2)=4	0191
ITRW(17,2)=9	0191
ITRW(18,2)=12	0191
T(1,2)=0.0	0192
T(2,2)=0.0	0192
T(9,2)=0.0	0192
T(13,2)=0.0	0192
T(19,2)=0.0	0192
DO 60 I=1,2	0192
DO 60 J=1,3	0192
ATDQ(I,J)=0.5	0192
60 ITOQ(I,J)=J	0192
ITOQ(1,3)=4	0192
ITOQ(2,1)=4	0192
ATCQ(1,1)=1.0	0193
ATOQ(2,3)=1.0	0193
RETURN	0193
END	0193
SUBROUTINE REINF(MN,HTOP,ND,HTOPP,I,NP)	0193
C	0193
C THIS SUBROUTINE FORMS THE STRESS STRAIN MATRIX FOR THE COMPOSITE	0193
C	0193
COMMON/BLK6/AB(10),EB(10),XIB(10),BE(10),DE(10),TE(10),F(3)	0193
1 ,TK(10)	0194
CALL INTPI(EI,GNUI,MN,HTOP,ND,HTOPP,I,NP)	0194
ALPH=AB(MN)*EB(MN)/(BE(MN)*DE(MN)*EI)	0194
A11=1./(EI*(1.+ALPH))	0194
A12=-A11*GNUI	0194
A13=A12	0194
A22=A11*(1.+ALPH*(1.-GNUI*GNUI))	0194
A23=-A11*GNUI*(1.+ALPH*(1.+GNUI))	0194
A33=A22	0194
D1=A22*A33-A23*A23	0194
D2=A13*A23-A12*A33	0195
D3=A12*A23-A13*A22	0195
DET=A11*D1+A12*D2+A13*D3	0195
D4=1.0/DET	0195
C11=D1*D4	0195
C12=D2*D4	0195
C22=(A11*A33 -A13*A13)*D4	0195
C33= EI/(2.*(1.+GNUI))	0195
C6=TE(MN)	0195
CALL ANISP(C11,C12,C22,C33,C6)	0195
RETURN	0196

```

END 01962
SUBROUTINE STREH(DUXX,DUXY,DUYX,DVXX,DVXY,D,MN,HTOP,ND,HTOPP,I,NP) 01963
C 01964
C THIS SUBROUTINE DETERMINES THE STRESSES IN THE SOIL AND THE STRIP 01965
C 01966
COMMON/BLK3/ C1(17,17),ZY(17),RT(3),ZT(3),RQ(4),ZQ(4), 01967
1 NQ(700),U(700),V(700),ITOQ(2,3),ATOQ(2,3),EST(4,3) 01968
2 , IS(5), PS(3), AS(3), RO, J1, 01969
3 AL(3,3), BT(3,3), GA(3,3), Z5(12,12), Z4( 12) 01970
4 ,T(28,2), ITRW(28,2), NETCL(17,2), CTP(12,17), STORE(17) 01971
COMMON/BLK6/AB(10),EB(10),XIB(10),BE(10),DE(10),TE(10),F(3) 01972
1 ,TK(10) 01973
DVYY=D 01974
THETA=TE(MN)*.0174533 01975
COST=COS(THETA) 01976
SINT=SIN(THETA) 01977
E1=RQ(1)*COST*COST+RQ(2)*SINT*SINT+RQ(3)*COST*SINT 01978
G12=2.*(RQ(2)-RQ(1))*SINT*COST+RQ(3)*(COST*COST-SINT*SINT) 01979
C 01980
C STRESSES IN COMPOSITE AXES ALIGNED WITH STRIP 01981
C 01982
S1=ZQ(1)*COST*COST+ZQ(2)*SINT*SINT+2.*ZQ(3)*SINT*COST 01983
S2=ZQ(1)*SINT*SINT+ZQ(2)*COST*COST-2.*ZQ(3)*SINT*COST 01984
T12=SINT*COST*(-ZQ(1)+ZQ(2))+ZQ(3)*(COST*COST-SINT*SINT) 01985
CALL INTPI( EI,GNUI,MN,HTOP,ND,HTOPP,I,NP) 01986
SS=EB(MN)*E1 01987
S1=S1-SS*AB(MN)/(BE(MN)*DE(MN)) 01988
C2=EI/(2.*(1.+GNUI)) 01989
TA12=C2*G12 01990
C 01991
C FORCES IN REINFORCING STRIP 01992
C 01993
F(1)=SS*AB(MN) 01994
DU1=COST*DVXX+SINT*(-DUXX+2.*DVXY) 01995
DU2=SINT*DUYY+COST*(2.*DUXY-DVYY) 01996
DU3=COST*COST*DU1-SINT*SINT*DU2 01997
F(2)=EB(MN)*XIB(MN)*DU3 01998
TH=-TE(MN)*.0174533 01999
COST=COS(TH) 02000
SINT=SIN(TH) 02001
ZQ(1)=S1*COST*COST+S2*SINT*SINT+2.*TA12*SINT*COST 02002
ZQ(2)=S1*SINT*SINT+S2*COST*COST-2.*TA12*SINT*COST 02003
ZQ(3)=COST*SINT*(-S1+S2)+TA12*(COST*COST-SINT*SINT) 02004
RETURN 02005
END 02006
***** ABOVE ACTION SATISFACTORILY COMPLETED *****

```

OUTPUT EXAMPLE

FOR

THE LAST CONSTRUCTION INCREMENT



CONSTRUCTION INCREMENT 12

ELEMENT NO.	X	Y	EPSILON-X	EPSILON-Y	ELEMENT ST GAMA-XY
1	1.67E 01	7.24E 01	-3.87E-04	-5.27E-03	-3.80E-04
2	1.31E 01	1.17E 02	-1.31E-03	-4.47E-03	-5.35E-04
3	4.82E 01	7.24E 01	-2.66E-04	-5.44E-03	-9.19E-04
4	4.12E 01	1.17E 02	-1.04E-03	-4.81E-03	-1.64E-03
5	7.97E 01	7.24E 01	-1.10E-04	-5.64E-03	-1.17E-03
6	6.92E 01	1.17E 02	-5.63E-04	-5.34E-03	-2.05E-03
7	1.11E 02	7.26E 01	3.07E-05	-5.75E-03	-1.11E-03
8	9.81E 01	1.18E 02	-2.42E-04	-5.68E-03	-2.07E-03
9	1.42E 02	7.33E 01	9.10E-05	-5.65E-03	-8.47E-04
10	1.23E 02	1.21E 02	1.61E-05	-5.83E-03	-2.02E-03
11	1.72E 02	7.43E 01	6.29E-05	-5.23E-03	-5.07E-04
12	1.48E 02	1.24E 02	1.67E-04	-5.87E-03	-1.70E-03
13	1.93E 02	8.13E 01	1.02E-04	-4.76E-03	8.05E-04
14	1.68E 02	1.27E 02	2.23E-04	-5.84E-03	-1.53E-03
15	2.10E 02	9.00E 01	2.77E-04	-5.07E-03	1.64E-03
16	1.87E 02	1.32E 02	2.84E-04	-5.69E-03	-9.02E-04
17	2.27E 02	9.75E 01	5.47E-04	-5.39E-03	1.91E-03
18	2.05E 02	1.38E 02	4.72E-04	-5.76E-03	-1.63E-04
19	2.42E 02	1.08E 02	7.61E-04	-5.65E-03	2.13E-03
20	2.21E 02	1.45E 02	6.57E-04	-5.95E-03	2.36E-04
21	2.58E 02	1.18E 02	9.47E-04	-5.87E-03	2.24E-03
22	2.37E 02	1.54E 02	8.85E-04	-6.14E-03	6.02E-04
23	2.73E 02	1.28E 02	1.12E-03	-6.04E-03	2.31E-03
24	2.53E 02	1.62E 02	1.10E-03	-6.30E-03	9.03E-04
25	2.88E 02	1.38E 02	1.27E-03	-6.17E-03	2.32E-03
26	2.69E 02	1.71E 02	1.30E-03	-6.41E-03	1.17E-03
27	3.04E 02	1.49E 02	1.41E-03	-6.27E-03	2.30E-03
28	2.85E 02	1.79E 02	1.47E-03	-6.48E-03	1.38E-03
29	3.19E 02	1.59E 02	1.54E-03	-6.37E-03	2.26E-03
30	3.01E 02	1.88E 02	1.63E-03	-6.53E-03	1.52E-03
31	3.34E 02	1.70E 02	1.67E-03	-6.44E-03	2.27E-03
32	3.16E 02	1.98E 02	1.76E-03	-6.64E-03	1.55E-03
33	3.49E 02	1.81E 02	1.76E-03	-6.47E-03	2.28E-03
34	3.31E 02	2.08E 02	1.91E-03	-6.71E-03	1.68E-03
35	3.64E 02	1.92E 02	1.83E-03	-6.46E-03	2.29E-03
36	3.46E 02	2.18E 02	2.06E-03	-6.76E-03	1.81E-03
37	3.79E 02	2.03E 02	1.87E-03	-6.39E-03	2.31E-03
38	3.61E 02	2.28E 02	2.20E-03	-6.76E-03	1.98E-03
39	3.94E 02	2.13E 02	1.88E-03	-6.26E-03	2.31E-03
40	3.76E 02	2.38E 02	2.30E-03	-6.69E-03	2.20E-03
41	4.09E 02	2.24E 02	1.88E-03	-6.08E-03	2.26E-03
42	3.91E 02	2.48E 02	2.33E-03	-6.51E-03	2.41E-03

ELEMENT
NO.

SIGMA-X

SIGMA-Y

TAU-XY

SIGMA-1

SIGMA-2

ANG

1	-3.56E 03	-7.32E 03	-1.46E 02	-3.56E 03	-7.32E 03	-2.23E 00
2	-4.34E 03	-6.77E 03	-2.06E 02	-4.32E 03	-6.78E 03	-4.80E 00
3	-3.50E 03	-7.48E 03	-3.53E 02	-3.47E 03	-7.51E 03	-5.04E 00
4	-4.17E 03	-7.07E 03	-6.30E 02	-4.04E 03	-7.20E 03	-1.18E 01
5	-3.40E 03	-7.66E 03	-4.51E 02	-3.35E 03	-7.70E 03	-5.99E 00
6	-3.84E 03	-7.51E 03	-7.89E 02	-3.67E 03	-7.67E 03	-1.16E 01
7	-3.27E 03	-7.72E 03	-4.27E 02	-3.23E 03	-7.76E 03	-5.44E 00
8	-3.60E 03	-7.79E 03	-7.97E 02	-3.46E 03	-7.93E 03	-1.04E 01
9	-3.13E 03	-7.55E 03	-3.26E 02	-3.11E 03	-7.57E 03	-4.20E 00
10	-3.34E 03	-7.84E 03	-7.77E 02	-3.21E 03	-7.97E 03	-9.54E 00
11	-2.93E 03	-7.01E 03	-1.95E 02	-2.93E 03	-7.02E 03	-2.74E 00
12	-3.16E 03	-7.81E 03	-6.54E 02	-3.07E 03	-7.90E 03	-7.86E 00
13	-2.61E 03	-6.35E 03	3.10E 02	-2.58E 03	-6.38E 03	4.70E 00
14	-3.07E 03	-7.73E 03	-5.87E 02	-2.99E 03	-7.80E 03	-7.07E 00
15	-2.55E 03	-6.67E 03	6.32E 02	-2.46E 03	-6.76E 03	8.54E 00
16	-2.90E 03	-7.50E 03	-3.47E 02	-2.87E 03	-7.52E 03	-4.29E 00
17	-2.37E 03	-6.94E 03	7.35E 02	-2.26E 03	-7.05E 03	8.92E 00
18	-2.69E 03	-7.48E 03	-6.28E 01	-2.69E 03	-7.48E 03	-7.50E-01
19	-2.24E 03	-7.17E 03	8.21E 02	-2.10E 03	-7.30E 03	9.20E 00
20	-2.55E 03	-7.64E 03	9.07E 01	-2.55E 03	-7.64E 03	1.02E 00
21	-2.11E 03	-7.36E 03	8.63E 02	-1.97E 03	-7.50E 03	9.11E 00
22	-2.35E 03	-7.75E 03	2.32E 02	-2.34E 03	-7.76E 03	2.45E 00
23	-1.98E 03	-7.49E 03	8.87E 02	-1.84E 03	-7.63E 03	8.93E 00
24	-2.16E 03	-7.84E 03	3.47E 02	-2.13E 03	-7.86E 03	3.48E 00
25	-1.85E 03	-7.57E 03	8.93E 02	-1.72E 03	-7.71E 03	8.67E 00
26	-1.95E 03	-7.88E 03	4.51E 02	-1.91E 03	-7.91E 03	4.32E 00
27	-1.72E 03	-7.63E 03	8.85E 02	-1.59E 03	-7.76E 03	8.34E 00
28	-1.76E 03	-7.87E 03	5.33E 02	-1.71E 03	-7.92E 03	4.94E 00
29	-1.60E 03	-7.69E 03	8.68E 02	-1.48E 03	-7.81E 03	7.96E 00
30	-1.57E 03	-7.85E 03	5.86E 02	-1.52E 03	-7.90E 03	5.29E 00
31	-1.46E 03	-7.71E 03	8.72E 02	-1.35E 03	-7.82E 03	7.80E 00
32	-1.46E 03	-7.92E 03	5.97E 02	-1.40E 03	-7.97E 03	5.23E 00
33	-1.36E 03	-7.70E 03	8.76E 02	-1.24E 03	-7.82E 03	7.73E 00
34	-1.30E 03	-7.93E 03	6.45E 02	-1.24E 03	-7.99E 03	5.50E 00
35	-1.27E 03	-7.64E 03	8.82E 02	-1.15E 03	-7.76E 03	7.73E 00
36	-1.12E 03	-7.90E 03	6.97E 02	-1.05E 03	-7.98E 03	5.81E 00
37	-1.17E 03	-7.53E 03	8.88E 02	-1.05E 03	-7.65E 03	7.80E 00
38	-9.40E 02	-7.83E 03	7.63E 02	-8.57E 02	-7.91E 03	6.24E 00
39	-1.08E 03	-7.34E 03	8.88E 02	-9.52E 02	-7.47E 03	7.91E 00
40	-7.70E 02	-7.69E 03	8.47E 02	-6.68E 02	-7.79E 03	6.88E 00
41	-9.84E 02	-7.11E 03	8.69E 02	-8.63E 02	-7.23E 03	7.93E 00
42	-6.23E 02	-7.43E 03	9.26E 02	-4.99E 02	-7.55E 03	7.62E 00

ELEMENT NO.	X	Y	EPSILON-X	EPSILON-Y	GAMA-XY
43	4.22E 02	2.34E 02	1.86E-03	-5.84E-03	2.22E-03
44	4.04E 02	2.58E 02	2.26E-03	-6.31E-03	2.43E-03
45	4.33E 02	2.42E 02	1.82E-03	-5.60E-03	2.07E-03
46	4.14E 02	2.66E 02	2.17E-03	-6.01E-03	2.41E-03
47	4.43E 02	2.50E 02	1.80E-03	-5.32E-03	1.80E-03
48	4.25E 02	2.74E 02	2.03E-03	-5.63E-03	2.23E-03
49	4.53E 02	2.58E 02	1.80E-03	-5.04E-03	1.39E-03
50	4.35E 02	2.82E 02	1.85E-03	-5.18E-03	1.83E-03
51	4.64E 02	2.66E 02	1.84E-03	-4.78E-03	8.01E-04
52	4.46E 02	2.90E 02	1.62E-03	-4.67E-03	1.22E-03
53	4.74E 02	2.74E 02	1.93E-03	-4.55E-03	3.21E-06
54	4.56E 02	2.98E 02	1.34E-03	-4.10E-03	4.40E-04
55	4.85E 02	2.81E 02	2.10E-03	-4.44E-03	-1.10E-03
56	4.66E 02	3.07E 02	9.11E-04	-3.40E-03	-4.63E-04
57	4.95E 02	2.90E 02	2.16E-03	-4.09E-03	-2.66E-03
58	4.77E 02	3.15E 02	2.21E-04	-2.78E-03	-8.05E-04
59	5.07E 02	2.98E 02	-2.41E-04	-4.15E-03	-6.98E-03
60	4.89E 02	3.24E 02	5.78E-04	-2.53E-03	-3.24E-04
61	5.20E 02	3.08E 02	-6.46E-04	-2.59E-03	-6.30E-03
62	5.02E 02	3.34E 02	6.85E-04	-2.67E-03	-1.71E-03
63	5.33E 02	3.18E 02	-8.07E-04	-1.90E-03	-5.17E-03
64	5.15E 02	3.43E 02	6.84E-04	-2.42E-03	-2.75E-03
65	5.46E 02	3.28E 02	-5.86E-04	-1.88E-03	-3.86E-03
66	5.28E 02	3.53E 02	8.19E-04	-2.50E-03	-3.01E-03
67	5.59E 02	3.37E 02	3.84E-04	-3.02E-03	-1.94E-03
68	5.42E 02	3.63E 02	1.16E-03	-2.67E-03	-3.46E-03
69	5.69E 02	3.50E 02	1.66E-03	-4.37E-03	-8.43E-04
70	5.66E 02	3.82E 02	2.64E-03	-6.12E-03	-1.54E-03
71	1.31E 01	1.45E 02	-2.34E-03	-7.39E-03	-1.55E-03
72	3.98E 01	1.45E 02	-1.53E-03	-8.32E-03	-4.06E-03
73	6.94E 01	1.44E 02	-1.36E-03	-9.66E-03	-5.44E-03
74	8.83E 01	1.51E 02	-5.40E-04	-1.00E-02	-5.27E-03
75	1.16E 02	1.48E 02	1.31E-04	-1.08E-02	-4.92E-03
76	1.08E 02	1.59E 02	-2.13E-04	-1.06E-02	-5.75E-03
77	1.35E 02	1.52E 02	3.13E-04	-1.09E-02	-4.74E-03
78	1.26E 02	1.69E 02	2.14E-04	-1.10E-02	-5.75E-03
79	1.53E 02	1.60E 02	6.69E-04	-1.11E-02	-4.24E-03
80	1.43E 02	1.78E 02	5.87E-04	-1.13E-02	-5.74E-03
81	1.70E 02	1.65E 02	9.09E-04	-1.13E-02	-3.95E-03
82	1.59E 02	1.85E 02	1.02E-03	-1.16E-02	-5.29E-03
83	1.88E 02	1.69E 02	1.09E-03	-1.12E-02	-3.12E-03
84	1.75E 02	1.92E 02	1.39E-03	-1.19E-02	-4.87E-03
85	2.04E 02	1.76E 02	1.54E-03	-1.13E-02	-1.85E-03
86	1.91E 02	2.00E 02	1.68E-03	-1.21E-02	-4.32E-03
87	2.20E 02	1.84E 02	1.92E-03	-1.17E-02	-1.09E-03
88	2.06E 02	2.07E 02	2.06E-03	-1.23E-02	-3.47E-03

ELEMENT
NO.

ELEMENT NO.	SIGMA-X	SIGMA-Y	TAU-XY	SIGMA-1	SIGMA-2	ANG
43	-8.62E 02	-6.79E 03	8.54E 02	-7.42E 02	-6.91E 03	8.03E 00
44	-5.94E 02	-7.19E 03	9.34E 02	-4.64E 02	-7.31E 03	7.92E 00
45	-7.76E 02	-6.48E 03	7.96E 02	-6.66E 02	-6.59E 03	7.80E 00
46	-5.44E 02	-6.83E 03	9.28E 02	-4.09E 02	-6.97E 03	8.22E 00
47	-6.52E 02	-6.13E 03	6.92E 02	-5.65E 02	-6.22E 03	7.09E 00
48	-5.14E 02	-6.40E 03	8.56E 02	-3.92E 02	-6.53E 03	8.10E 00
49	-4.89E 02	-5.75E 03	5.34E 02	-4.36E 02	-5.80E 03	5.74E 00
50	-4.97E 02	-5.91E 03	7.03E 02	-4.07E 02	-6.00E 03	7.28E 00
51	-2.81E 02	-5.37E 03	3.08E 02	-2.63E 02	-5.39E 03	3.45E 00
52	-5.05E 02	-5.34E 03	4.70E 02	-4.60E 02	-5.39E 03	5.49E 00
53	-2.69E 01	-5.01E 03	1.24E 00	-2.69E 01	-5.01E 03	1.42E-02
54	-5.68E 02	-4.75E 03	1.69E 02	-5.61E 02	-4.76E 03	2.31E 00
55	2.67E 02	-4.76E 03	-4.22E 02	3.02E 02	-4.80E 03	-4.77E 00
56	-7.36E 02	-4.05E 03	-1.78E 02	-7.27E 02	-4.06E 03	-3.06E 00
57	5.46E 02	-4.26E 03	-1.02E 03	7.56E 02	-4.46E 03	-1.15E 01
58	-1.31E 03	-3.61E 03	-3.10E 02	-1.26E 03	-3.65E 03	-7.52E 00
59	-2.72E 03	-5.73E 03	-2.69E 03	-1.14E 03	-7.30E 03	-3.04E 01
60	-6.84E 02	-3.08E 03	-1.24E 02	-6.77E 02	-3.08E 03	-2.97E 00
61	-2.37E 03	-3.86E 03	-2.42E 03	-5.81E 02	-5.65E 03	-3.64E 01
62	-6.22E 02	-3.21E 03	-6.60E 02	-4.63E 02	-3.36E 03	-1.35E 01
63	-2.18E 03	-3.03E 03	-1.99E 03	-5.75E 02	-4.64E 03	-3.90E 01
64	-4.76E 02	-2.86E 03	-1.06E 03	-7.39E 01	-3.27E 03	-2.08E 01
65	-1.87E 03	-2.87E 03	-1.49E 03	-8.02E 02	-3.94E 03	-3.58E 01
66	-3.38E 02	-2.89E 03	-1.16E 03	1.09E 02	-3.33E 03	-2.11E 01
67	-1.22E 03	-3.84E 03	-7.47E 02	-1.03E 03	-4.04E 03	-1.49E 01
68	1.59E 01	-2.93E 03	-1.33E 03	5.29E 02	-3.44E 03	-2.11E 01
69	-2.91E 02	-4.93E 03	-3.24E 02	-2.69E 02	-4.95E 03	-3.98E 00
70	2.79E 01	-6.71E 03	-5.93E 02	7.97E 01	-6.77E 03	-4.99E 00
71	-4.11E 03	-6.27E 03	-3.30E 02	-4.06E 03	-6.32E 03	-8.51E 00
72	-3.80E 03	-6.70E 03	-8.67E 02	-3.56E 03	-6.94E 03	-1.54E 01
73	-4.11E 03	-7.66E 03	-1.16E 03	-3.77E 03	-8.00E 03	-1.66E 01
74	-3.61E 03	-7.65E 03	-1.12E 03	-3.31E 03	-7.94E 03	-1.45E 01
75	-3.35E 03	-8.01E 03	-1.05E 03	-3.13E 03	-8.23E 03	-1.21E 01
76	-3.56E 03	-8.00E 03	-1.23E 03	-3.24E 03	-8.32E 03	-1.45E 01
77	-3.26E 03	-8.04E 03	-1.01E 03	-3.05E 03	-8.25E 03	-1.15E 01
78	-3.36E 03	-8.14E 03	-1.23E 03	-3.06E 03	-8.43E 03	-1.36E 01
79	-3.04E 03	-8.06E 03	-9.06E 02	-2.89E 03	-8.21E 03	-9.94E 00
80	-3.17E 03	-8.24E 03	-1.23E 03	-2.89E 03	-8.52E 03	-1.29E 01
81	-2.94E 03	-8.14E 03	-8.43E 02	-2.80E 03	-8.28E 03	-8.97E 00
82	-2.95E 03	-8.33E 03	-1.13E 03	-2.72E 03	-8.55E 03	-1.14E 01
83	-2.78E 03	-8.04E 03	-6.66E 02	-2.70E 03	-8.12E 03	-7.10E 00
84	-2.76E 03	-8.42E 03	-1.04E 03	-2.58E 03	-8.61E 03	-1.01E 01
85	-2.47E 03	-7.97E 03	-3.95E 02	-2.44E 03	-8.00E 03	-4.09E 00
86	-2.61E 03	-8.47E 03	-9.21E 02	-2.47E 03	-8.61E 03	-8.72E 00
87	-2.31E 03	-8.14E 03	-2.32E 02	-2.30E 03	-8.15E 03	-2.28E 00
88	-2.40E 03	-8.54E 03	-7.41E 02	-2.31E 03	-8.63E 03	-6.79E 00

ELEMENT NO.	X	Y	EPSILON-X	EPSILON-Y	GAMA-XY
89	2.36E 02	1.91E 02	2.24E-03	-1.19E-02	-5.18E-04
90	2.22E 02	2.15E 02	2.47E-03	-1.26E-02	-2.53E-03
91	2.52E 02	1.99E 02	2.52E-03	-1.21E-02	-1.28E-04
92	2.37E 02	2.23E 02	2.83E-03	-1.26E-02	-1.70E-03
93	2.68E 02	2.07E 02	2.81E-03	-1.23E-02	3.70E-04
94	2.53E 02	2.31E 02	3.16E-03	-1.29E-02	-1.38E-03
95	2.85E 02	2.12E 02	3.07E-03	-1.23E-02	8.61E-04
96	2.71E 02	2.35E 02	3.36E-03	-1.29E-02	-5.78E-04
97	2.64E 02	2.51E 02	3.33E-03	-1.32E-02	-1.56E-03
98	3.01E 02	2.21E 02	3.35E-03	-1.23E-02	1.49E-03
99	2.88E 02	2.41E 02	3.56E-03	-1.28E-02	1.29E-05
100	2.77E 02	2.57E 02	3.71E-03	-1.32E-02	-1.12E-03
101	3.16E 02	2.31E 02	3.69E-03	-1.25E-02	1.67E-03
102	3.03E 02	2.50E 02	3.86E-03	-1.29E-02	2.53E-04
103	2.92E 02	2.66E 02	4.07E-03	-1.33E-02	-8.84E-04
104	3.31E 02	2.41E 02	4.02E-03	-1.27E-02	1.82E-03
105	3.17E 02	2.60E 02	4.23E-03	-1.31E-02	4.34E-04
106	3.06E 02	2.76E 02	4.42E-03	-1.34E-02	-7.18E-04
107	3.46E 02	2.51E 02	4.33E-03	-1.29E-02	2.08E-03
108	3.32E 02	2.70E 02	4.67E-03	-1.34E-02	6.64E-04
109	3.21E 02	2.85E 02	4.83E-03	-1.36E-02	-6.72E-04
110	3.60E 02	2.60E 02	4.60E-03	-1.29E-02	2.49E-03
111	3.47E 02	2.80E 02	5.13E-03	-1.36E-02	1.11E-03
112	3.35E 02	2.95E 02	5.37E-03	-1.41E-02	-5.19E-04
113	3.75E 02	2.70E 02	4.76E-03	-1.28E-02	3.14E-03
114	3.61E 02	2.89E 02	5.59E-03	-1.39E-02	1.72E-03
115	3.50E 02	3.05E 02	5.87E-03	-1.43E-02	-1.11E-04
116	3.88E 02	2.79E 02	4.81E-03	-1.24E-02	4.03E-03
117	3.74E 02	2.98E 02	6.01E-03	-1.41E-02	2.78E-03
118	3.62E 02	3.14E 02	6.74E-03	-1.54E-02	8.48E-05
119	3.98E 02	2.87E 02	4.69E-03	-1.20E-02	4.67E-03
120	3.84E 02	3.06E 02	6.08E-03	-1.38E-02	4.21E-03
121	3.73E 02	3.21E 02	7.38E-03	-1.59E-02	2.30E-03
122	4.09E 02	2.95E 02	4.35E-03	-1.11E-02	5.02E-03
123	3.95E 02	3.14E 02	5.85E-03	-1.31E-02	5.71E-03
124	3.84E 02	3.29E 02	7.30E-03	-1.54E-02	4.51E-03
125	4.19E 02	3.04E 02	3.89E-03	-1.00E-02	4.89E-03
126	4.06E 02	3.22E 02	5.32E-03	-1.17E-02	6.61E-03
127	3.95E 02	3.37E 02	7.09E-03	-1.43E-02	6.01E-03
128	4.30E 02	3.12E 02	3.45E-03	-8.91E-03	4.39E-03
129	4.16E 02	3.30E 02	4.89E-03	-1.01E-02	6.27E-03
130	4.06E 02	3.45E 02	7.40E-03	-1.23E-02	7.13E-03
131	4.40E 02	3.20E 02	3.02E-03	-7.71E-03	3.80E-03
132	4.27E 02	3.38E 02	5.02E-03	-9.20E-03	5.83E-03
133	4.17E 02	3.52E 02	8.52E-03	-1.13E-02	8.44E-03
134	4.51E 02	3.28E 02	2.67E-03	-6.67E-03	3.44E-03
135	4.38E 02	3.46E 02	5.08E-03	-8.23E-03	6.36E-03
136	4.28E 02	3.60E 02	6.82E-03	-9.65E-03	9.71E-03

ELEMENT NO.	SIGMA-X	SIGMA-Y	TAU-XY	SIGMA-1	SIGMA-2	ANG
80	-2.15E 03	-8.19E 03	-1.11E 02	-2.15E 03	-8.19E 03	-1.05E 00
90	-2.19E 03	-8.63E 03	-5.41E 02	-2.15E 03	-8.68E 03	-4.77E 00
91	-2.01E 03	-8.27E 03	-2.73E 01	-2.01E 03	-8.27E 03	-2.50E-01
92	-1.93E 03	-8.54E 03	-3.64E 02	-1.91E 03	-8.56E 03	-3.14E 00
93	-1.83E 03	-8.27E 03	7.90E 01	-1.83E 03	-8.27E 03	7.02E-01
94	-1.78E 03	-8.64E 03	-2.94E 02	-1.77E 03	-8.66E 03	-2.45E 00
95	-1.65E 03	-8.22E 03	1.84E 02	-1.64E 03	-8.22E 03	1.60E 00
96	-1.62E 03	-8.56E 03	-1.23E 02	-1.62E 03	-8.56E 03	-1.02E 00
97	-1.74E 03	-8.79E 03	-3.34E 02	-1.72E 03	-8.81E 03	-2.70E 00
98	-1.44E 03	-8.12E 03	3.18E 02	-1.42E 03	-8.13E 03	2.72E 00
99	-1.44E 03	-8.43E 03	2.76E 00	-1.44E 03	-8.43E 03	2.26E-02
100	-1.44E 03	-8.65E 03	-2.40E 02	-1.44E 03	-8.66E 03	-1.91E 00
101	-1.25E 03	-8.17E 03	3.56E 02	-1.23E 03	-8.19E 03	2.94E 00
102	-1.25E 03	-8.40E 03	5.39E 01	-1.25E 03	-8.40E 03	4.32E-01
103	-1.21E 03	-8.62E 03	-1.89E 02	-1.21E 03	-8.62E 03	-1.46E 00
104	-1.06E 03	-8.21E 03	3.89E 02	-1.04E 03	-8.23E 03	3.11E 00
105	-1.03E 03	-8.42E 03	9.27E 01	-1.03E 03	-8.42E 03	7.18E-01
106	-9.90E 02	-8.60E 03	-1.53E 02	-9.87E 02	-8.61E 03	-1.15E 00
107	-8.78E 02	-8.21E 03	4.45E 02	-8.51E 02	-8.24E 03	3.46E 00
108	-7.91E 02	-8.49E 03	1.42E 02	-7.88E 02	-8.49E 03	1.05E 00
109	-7.55E 02	-8.63E 03	-1.44E 02	-7.53E 02	-8.64E 03	-1.04E 00
110	-7.03E 02	-8.19E 03	5.32E 02	-6.65E 02	-8.23E 03	4.04E 00
111	-5.29E 02	-8.53E 03	2.37E 02	-5.22E 02	-8.54E 03	1.69E 00
112	-5.21E 02	-8.85E 03	-1.11E 02	-5.20E 02	-8.85E 03	-7.62E-01
113	-5.47E 02	-8.05E 03	6.71E 02	-4.87E 02	-8.11E 03	5.07E 00
114	-2.74E 02	-8.60E 03	3.67E 02	-2.58E 02	-8.61E 03	2.52E 00
115	-2.06E 02	-8.84E 03	-2.37E 01	-2.06E 02	-8.84E 03	-1.58E-01
116	-3.89E 02	-7.76E 03	8.61E 02	-2.90E 02	-7.85E 03	6.58E 00
117	-1.23E 01	-8.58E 03	5.93E 02	2.85E 01	-8.62E 03	3.94E 00
118	1.13E 02	-9.33E 03	1.81E 01	1.13E 02	-9.33E 03	1.10E-01
119	-3.29E 02	-7.44E 03	9.96E 02	-1.92E 02	-7.58E 03	7.82E 00
120	1.15E 02	-8.39E 03	8.99E 02	2.09E 02	-8.48E 03	5.97E 00
121	4.37E 02	-9.48E 03	4.91E 02	4.62E 02	-9.51E 03	2.83E 00
122	-3.10E 02	-6.92E 03	1.07E 03	-1.41E 02	-7.09E 03	8.99E 00
123	1.83E 02	-7.90E 03	1.22E 03	3.63E 02	-8.08E 03	8.39E 00
124	5.10E 02	-9.19E 03	9.62E 02	6.05E 02	-9.29E 03	5.61E 00
125	-3.06E 02	-6.26E 03	1.04E 03	-1.28E 02	-6.43E 03	9.67E 00
126	2.40E 02	-7.00E 03	1.41E 03	5.05E 02	-7.27E 03	1.06E 01
127	7.07E 02	-8.44E 03	1.28E 03	8.84E 02	-8.62E 03	7.83E 00
128	-2.76E 02	-5.55E 03	9.36E 02	-1.15E 02	-5.71E 03	9.77E 00
129	4.13E 02	-6.00E 03	1.34E 03	6.81E 02	-6.26E 03	1.13E 01
130	1.60E 03	-6.79E 03	1.52E 03	1.87E 03	-7.06E 03	9.97E 00
131	-2.10E 02	-4.79E 03	8.10E 02	-7.11E 01	-4.93E 03	9.74E 00
132	8.07E 02	-5.27E 03	1.24E 03	1.05E 03	-5.51E 03	1.11E 01
133	2.75E 03	-5.72E 03	1.80E 03	3.11E 03	-6.09E 03	1.15E 01
134	-1.44E 02	-4.13E 03	7.35E 02	-1.32E 01	-4.26E 03	1.01E 01
135	1.16E 03	-4.52E 03	1.36E 03	1.46E 03	-4.83E 03	1.28E 01
136	2.00E 03	-5.03E 03	2.07E 03	2.57E 03	-5.59E 03	1.53E 01

ELEMENT NO.	X	Y	EPSILON-X	EPSILON-Y	GAMA-XY
137	4.61E 02	3.36E 02	2.78E-03	-5.87E-03	3.13E-03
138	4.48E 02	3.54E 02	4.44E-03	-6.88E-03	6.41E-03
139	4.39E 02	3.68E 02	6.04E-03	-7.84E-03	9.48E-03
140	4.73E 02	3.45E 02	2.33E-03	-4.82E-03	1.98E-03
141	4.60E 02	3.63E 02	3.94E-03	-5.42E-03	5.78E-03
142	4.50E 02	3.76E 02	5.66E-03	-6.40E-03	8.96E-03
143	4.86E 02	3.55E 02	2.24E-03	-3.88E-03	9.56E-04
144	4.73E 02	3.72E 02	3.50E-03	-3.99E-03	4.48E-03
145	4.62E 02	3.85E 02	5.11E-03	-4.49E-03	8.38E-03
146	4.99E 02	3.64E 02	2.52E-03	-3.70E-03	-5.41E-04
147	4.85E 02	3.82E 02	3.44E-03	-3.11E-03	2.67E-03
148	4.74E 02	3.94E 02	4.62E-03	-2.74E-03	7.28E-03
149	5.12E 02	3.74E 02	2.98E-03	-3.79E-03	-1.88E-03
150	4.98E 02	3.91E 02	3.61E-03	-2.97E-03	8.92E-04
151	4.86E 02	4.03E 02	3.60E-03	-1.30E-03	3.90E-03
152	5.26E 02	3.85E 02	3.11E-03	-4.28E-03	-1.87E-03
153	5.11E 02	4.02E 02	4.44E-03	-3.72E-03	7.02E-04
154	5.01E 02	4.08E 02	5.09E-03	-3.50E-03	1.06E-03
155	5.43E 02	3.95E 02	4.32E-03	-6.22E-03	-2.76E-03
156	5.31E 02	4.06E 02	5.69E-03	-5.60E-03	-1.50E-03
157	1.77E 01	1.54E 02	-2.79E-03	-1.28E-02	-4.65E-03
158	1.24E 01	1.68E 02	-5.56E-03	-4.85E-03	-4.70E-03
159	4.30E 01	1.56E 02	-2.21E-03	-1.35E-02	-7.87E-03
160	3.98E 01	1.81E 02	-4.28E-03	-3.80E-03	-7.80E-03
161	6.51E 01	1.65E 02	-1.00E-03	-1.40E-02	-7.18E-03
162	5.97E 01	1.87E 02	-4.82E-03	-3.34E-03	-6.37E-03
163	8.22E 01	1.72E 02	-3.61E-04	-1.53E-02	-8.30E-03
164	7.58E 01	1.93E 02	-4.87E-03	-4.19E-03	-8.61E-03
165	9.92E 01	1.80E 02	4.78E-04	-1.61E-02	-7.99E-03
166	9.17E 01	2.02E 02	-3.61E-03	-5.19E-03	-1.03E-02
167	1.17E 02	1.90E 02	1.35E-03	-1.70E-02	-7.99E-03
168	1.08E 02	2.10E 02	-2.82E-03	-5.57E-03	-9.35E-03
169	1.33E 02	1.98E 02	2.25E-03	-1.79E-02	-8.13E-03
170	1.23E 02	2.18E 02	-2.28E-03	-6.08E-03	-9.15E-03
171	1.48E 02	2.06E 02	2.85E-03	-1.87E-02	-7.83E-03
172	1.37E 02	2.27E 02	-1.87E-03	-6.35E-03	-8.72E-03
173	1.63E 02	2.14E 02	3.40E-03	-1.95E-02	-7.40E-03
174	1.52E 02	2.35E 02	-1.51E-03	-6.62E-03	-8.18E-03
175	1.78E 02	2.22E 02	3.90E-03	-2.02E-02	-6.87E-03
176	1.66E 02	2.43E 02	-1.18E-03	-6.84E-03	-7.58E-03
177	1.93E 02	2.30E 02	4.35E-03	-2.08E-02	-6.31E-03
178	1.81E 02	2.52E 02	-8.37E-04	-7.07E-03	-6.80E-03
179	2.08E 02	2.38E 02	4.95E-03	-2.18E-02	-5.66E-03
180	1.95E 02	2.60E 02	-5.60E-04	-7.00E-03	-6.22E-03
181	2.25E 02	2.42E 02	5.46E-03	-2.30E-02	-4.63E-03

ELEMENT						
NO.	SIGMA-X	SIGMA-Y	TAU-XY	SIGMA-1	SIGMA-2	ANG
137	1.98E 02	-3.50E 03	6.68E 02	3.15E 02	-3.61E 03	9.94E 00
138	1.11E 03	-3.72E 03	1.37E 03	1.47E 03	-4.08E 03	1.48E 01
139	2.01E 03	-3.92E 03	2.02E 03	2.63E 03	-4.54E 03	1.72E 01
140	2.01E 02	-2.85E 03	4.24E 02	2.59E 02	-2.91E 03	7.75E 00
141	1.21E 03	-2.79E 03	1.23E 03	1.56E 03	-3.14E 03	1.58E 01
142	2.17E 03	-2.97E 03	1.91E 03	2.81E 03	-3.61E 03	1.83E 01
143	4.33E 02	-2.18E 03	2.04E 02	4.49E 02	-2.20E 03	4.44E 00
144	1.34E 03	-1.86E 03	9.56E 02	1.60E 03	-2.12E 03	1.54E 01
145	2.38E 03	-1.72E 03	1.79E 03	3.05E 03	-2.39E 03	2.05E 01
146	6.93E 02	-1.96E 03	-1.16E 02	6.98E 02	-1.97E 03	-2.49E 00
147	1.57E 03	-1.22E 03	5.71E 02	1.69E 03	-1.33E 03	1.11E 01
148	2.58E 03	-5.63E 02	1.55E 03	3.22E 03	-1.20E 03	2.23E 01
149	1.01E 03	-1.88E 03	-4.02E 02	1.06E 03	-1.94E 03	-7.77E 00
150	1.74E 03	-1.07E 03	1.90E 02	1.76E 03	-1.08E 03	3.86E 00
151	2.27E 03	1.83E 02	8.32E 02	2.56E 03	-1.08E 02	1.92E 01
152	9.54E 02	-2.20E 03	-4.00E 02	1.00E 03	-2.25E 03	-7.11E 00
153	2.13E 03	-1.36E 03	1.50E 02	2.14E 03	-1.36E 03	2.46E 00
154	2.68E 03	-9.82E 02	2.26E 02	2.70E 03	-9.96E 02	3.51E 00
155	1.24E 03	-3.27E 03	-5.88E 02	1.31E 03	-3.34E 03	-7.32E 00
156	2.45E 03	-2.37E 03	-3.20E 02	2.48E 03	-2.39E 03	-3.78E 00
157	-3.31E 03	-5.51E 03	-5.26E 02	-3.19E 03	-5.63E 03	-1.27E 01
158	-3.00E 03	-2.79E 03	-5.24E 02	-2.36E 03	-3.43E 03	1.29E 02
159	-3.18E 03	-5.65E 03	-8.94E 02	-2.89E 03	-5.94E 03	-1.80E 01
160	-2.27E 03	-2.12E 03	-8.57E 02	-1.34E 03	-3.06E 03	1.32E 02
161	-2.75E 03	-5.57E 03	-8.20E 02	-2.53E 03	-5.79E 03	-1.51E 01
162	-2.38E 03	-2.01E 03	-6.98E 02	-1.47E 03	-2.92E 03	1.28E 02
163	-2.69E 03	-5.90E 03	-9.35E 02	-2.44E 03	-6.16E 03	-1.51E 01
164	-2.52E 03	-2.33E 03	-9.36E 02	-1.48E 03	-3.36E 03	1.32E 02
165	-2.47E 03	-5.98E 03	-8.93E 02	-2.25E 03	-6.19E 03	-1.35E 01
166	-2.18E 03	-2.46E 03	-1.10E 03	-1.20E 03	-3.43E 03	-4.13E 01
167	-2.25E 03	-6.08E 03	-8.84E 02	-2.05E 03	-6.27E 03	-1.24E 01
168	-1.92E 03	-2.44E 03	-9.90E 02	-1.15E 03	-3.20E 03	-3.76E 01
169	-2.04E 03	-6.21E 03	-8.90E 02	-1.86E 03	-6.39E 03	-1.16E 01
170	-1.78E 03	-2.50E 03	-9.58E 02	-1.12E 03	-3.16E 03	-3.46E 01
171	-1.92E 03	-6.32E 03	-8.51E 02	-1.76E 03	-6.48E 03	-1.06E 01
172	-1.65E 03	-2.50E 03	-9.04E 02	-1.08E 03	-3.08E 03	-3.24E 01
173	-1.81E 03	-6.41E 03	-8.00E 02	-1.68E 03	-6.55E 03	-9.59E 00
174	-1.55E 03	-2.51E 03	-8.40E 02	-1.06E 03	-3.00E 03	-3.01E 01
175	-1.72E 03	-6.50E 03	-7.40E 02	-1.61E 03	-6.61E 03	-8.60E 00
176	-1.45E 03	-2.51E 03	-7.74E 02	-1.04E 03	-2.91E 03	-2.79E 01
177	-1.64E 03	-6.57E 03	-6.79E 02	-1.55E 03	-6.67E 03	-7.70E 00
178	-1.35E 03	-2.50E 03	-6.90E 02	-1.03E 03	-2.83E 03	-2.51E 01
179	-1.57E 03	-6.74E 03	-6.11E 02	-1.49E 03	-6.82E 03	-6.64E 00
180	-1.24E 03	-2.41E 03	-6.29E 02	-9.66E 02	-2.69E 03	-2.35E 01
181	-1.56E 03	-7.02E 03	-5.12E 02	-1.51E 03	-7.07E 03	-5.31E 00

ELEMENT
NO.

ELEMENT NO.	X	Y	EPSILON-X	EPSILON-Y	GAMA-XY
182	2.14E 02	2.61E 02	8.73E-04	-1.08E-02	-5.98E-03
183	2.08E 02	2.76E 02	-9.88E-04	-4.04E-03	-6.59E-03
184	2.40E 02	2.51E 02	6.75E-03	-2.44E-02	-2.13E-03
185	2.31E 02	2.66E 02	-8.95E-04	-1.57E-02	-4.08E-03
186	2.21E 02	2.81E 02	7.43E-03	-4.68E-03	-5.57E-03
187	2.54E 02	2.60E 02	3.51E-03	-2.49E-02	-1.01E-03
188	2.45E 02	2.75E 02	-4.62E-04	-1.51E-02	-3.42E-03
189	2.36E 02	2.90E 02	8.16E-03	-5.15E-03	-4.36E-03
190	2.69E 02	2.70E 02	3.95E-03	-2.54E-02	-6.75E-04
191	2.59E 02	2.84E 02	-8.72E-05	-1.53E-02	-2.42E-03
92	2.50E 02	2.99E 02	8.70E-03	-2.56E-02	-3.84E-03
93	2.83E 02	2.79E 02	4.44E-03	-1.55E-02	-3.24E-04
94	2.73E 02	2.93E 02	2.84E-04	-5.09E-03	-1.98E-03
95	2.64E 02	3.07E 02	4.88E-03	-2.60E-02	-3.12E-03
96	2.97E 02	2.89E 02	9.27E-03	-1.56E-02	-2.24E-04
97	2.88E 02	3.02E 02	6.14E-04	-5.12E-03	-1.74E-03
98	2.78E 02	3.16E 02	5.84E-03	-2.63E-02	-2.71E-03
99	3.12E 02	2.98E 02	8.30E-04	-1.58E-02	-3.97E-04
100	3.02E 02	3.11E 02	1.05E-02	-5.13E-03	-1.85E-03
101	2.93E 02	3.25E 02	5.52E-03	-2.69E-02	-2.56E-03
102	3.26E 02	3.07E 02	8.74E-04	-1.59E-02	-1.15E-03
103	3.16E 02	3.21E 02	1.29E-02	-5.08E-03	-2.50E-03
104	3.07E 02	3.34E 02	8.74E-04	-2.99E-02	-2.62E-03
105	3.45E 02	3.15E 02	1.29E-02	-2.44E-02	-1.23E-04
106	3.38E 02	3.20E 02	9.48E-03	-1.37E-02	-4.21E-03
107	3.29E 02	3.31E 02	4.20E-03	-4.50E-03	-4.17E-03
108	3.21E 02	3.43E 02	6.18E-04	-3.06E-02	-2.93E-03
109	3.54E 02	3.21E 02	1.34E-02	-2.00E-02	-6.11E-04
110	3.42E 02	3.31E 02	7.21E-03	-2.93E-02	-7.46E-03
111	3.55E 02	3.30E 02	1.24E-02	-3.42E-02	-4.63E-03
112	3.67E 02	3.30E 02	1.51E-02	-3.66E-02	-1.09E-03
113	3.77E 02	3.35E 02	1.58E-02	-1.00E-02	4.91E-03
114	3.35E 02	3.41E 02	1.96E-03	-1.26E-02	-4.89E-03
115	3.42E 02	3.41E 02	2.52E-03	-2.17E-02	-6.92E-03
116	3.52E 02	3.40E 02	8.29E-03	-3.08E-02	-1.08E-02
117	3.64E 02	3.41E 02	1.32E-02	-3.32E-02	-3.71E-03
118	3.75E 02	3.42E 02	1.44E-02	-3.45E-02	3.85E-03
119	3.88E 02	3.43E 02	1.52E-02	-5.02E-03	6.81E-03
120	3.30E 02	3.49E 02	1.18E-03	-6.35E-03	-3.26E-03
121	3.41E 02	3.49E 02	2.05E-03	-1.51E-02	-1.05E-03
122	3.52E 02	3.49E 02	2.14E-03	-2.82E-02	-1.50E-02
123	3.64E 02	3.49E 02	1.01E-02	-3.08E-02	-7.88E-03
124	3.76E 02	3.49E 02	1.25E-02	-3.16E-02	2.88E-03
125	3.88E 02	3.50E 02	1.45E-02	-3.38E-02	3.54E-03
126	4.01E 02	3.50E 02	1.72E-02		2.16E-03

ELEMENT NO.	SIGMA-X	SIGMA-Y	TAU-XY	SIGMA-1	SIGMA-2	
182	-1.31E 03	-3.47E 03	-6.10E 02	-1.15E 03	-3.63E 03	-1
183	-9.39E 02	-1.47E 03	-6.48E 02	-5.03E 02	-1.90E 03	-2
184	-1.31E 03	-7.23E 03	-2.73E 02	-1.30E 03	-7.24E 03	-7
185	-1.22E 03	-4.73E 03	-4.37E 02	-1.17E 03	-4.79E 03	-
186	-9.95E 02	-1.65E 03	-5.52E 02	-6.81E 02	-1.97E 03	-
187	-1.15E 03	-7.22E 03	-1.67E 02	-1.14E 03	-7.23E 03	-
188	-1.04E 03	-4.46E 03	-3.74E 02	-9.95E 02	-4.50E 03	-
189	-9.11E 02	-1.73E 03	-4.37E 02	-7.22E 02	-1.92E 03	-
190	-9.60E 02	-7.20E 03	-1.39E 02	-9.57E 02	-7.20E 03	-
191	-9.09E 02	-4.41E 03	-2.80E 02	-8.87E 02	-4.44E 03	-
192	-7.68E 02	-1.63E 03	-3.86E 02	-6.21E 02	-1.78E 03	-
193	-8.12E 02	-7.15E 03	-1.10E 02	-8.10E 02	-7.15E 03	-
194	-7.66E 02	-4.37E 03	-2.40E 02	-7.50E 02	-4.39E 03	-
195	-6.53E 02	-1.60E 03	-3.17E 02	-5.56E 02	-1.69E 03	-
196	-6.63E 02	-7.14E 03	-1.07E 02	-6.62E 02	-7.14E 03	-
197	-6.42E 02	-4.34E 03	-2.76E 02	-4.76E 02	-4.36E 03	-
198	-5.46E 02	-1.56E 03	-1.31E 02	-5.20E 02	-1.63E 03	-
199	-5.22E 02	-7.16E 03	-2.29E 02	-5.19E 02	-7.16E 03	-
200	-5.33E 02	-4.34E 03	-2.56E 02	-4.12E 02	-4.35E 03	-
201	-4.70E 02	-1.54E 03	-2.06E 02	-3.58E 02	-1.60E 03	-
202	-3.64E 02	-7.25E 03	-2.86E 02	-4.44E 02	-7.26E 03	-
203	-4.65E 02	-4.35E 03	-2.51E 02	-3.81E 02	-4.37E 03	-
204	-4.36E 02	-1.53E 03	-8.04E 01	1.54E 01	-1.58E 03	-
205	1.46E 01	-7.98E 03	-4.72E 02	-3.37E 02	-7.98E 03	-
206	-3.73E 02	-6.64E 03	-4.13E 02	-5.22E 02	-6.67E 03	-
207	-5.73E 02	-3.88E 03	-2.64E 02	-3.49E 02	-3.93E 03	-
208	-4.15E 02	-1.39E 03	-1.21E 02	7.85E 01	-1.46E 03	-
209	7.67E 01	-8.15E 03	-7.24E 02	-3.73E 02	-8.15E 03	-
210	-4.74E 02	-5.54E 03	-4.74E 02	-4.93E 01	-5.64E 03	-
211	-7.79E 01	-7.89E 03	-1.25E 02	1.21E 02	-7.92E 03	-
212	1.19E 02	-9.11E 03	4.56E 02	4.32E 01	-9.12E 03	-
213	2.21E 01	-9.78E 03	-4.51E 02	-6.70E 02	-9.80E 03	-
214	-7.57E 02	-3.01E 03	-6.36E 02	-7.91E 02	-3.10E 03	-
215	-9.26E 02	-3.77E 03	-9.99E 02	-1.48E 02	-3.91E 03	-
216	-3.21E 02	-5.93E 03	-3.38E 02	2.44E 01	-6.11E 03	-
217	1.05E 01	-8.19E 03	3.63E 02	1.01E 02	-8.21E 03	-
218	8.60E 01	-8.80E 03	6.35E 02	2.13E 02	-8.81E 03	-
219	1.69E 02	-9.10E 03	-2.90E 02	-2.22E 02	-9.14E 03	-
220	-2.89E 02	-1.47E 03	-8.12E 01	-1.63E 02	-1.54E 03	-
221	-1.67E 02	-1.79E 03	-1.35E 03	-8.16E 02	-1.80E 03	-
222	-1.30E 03	-4.57E 03	-7.06E 02	-4.45E 02	-5.06E 03	-
223	-5.14E 02	-7.68E 03	2.74E 02	-8.56E 01	-7.74E 03	-
224	-9.49E 01	-8.17E 03	3.31E 02	5.01E 02	-8.18E 03	-
225	4.88E 02	-8.14E 03	1.97E 02	1.11E 03	-8.18E 03	-
226	1.11E 03	-8.46E 03				-

ELEMENT NO.	X	Y	EPSILON-X	EPSILON-Y	GAMA-XY
227	3.65E 02	3.56E 02	1.70E-04	-3.37E-02	-2.00E-02
	STRIP AXIAL FORCE=		1.351E 03	MOMENT= 7.010E-02	
	SKIN MEMRRANE STRESS= 0.166E 06				
228	3.76E 02	3.56E 02	2.34E-04	-2.50E-02	-5.80E-03
	STRIP AXIAL FORCE=		1.862E 03	MOMENT= -1.548E-03	
229	3.88E 02	3.57E 02	5.17E-04	-2.62E-02	-1.38E-03
	STRIP AXIAL FORCE=		4.113E 03	MOMENT= 1.109E-02	
230	4.00E 02	3.57E 02	6.67E-04	-2.61E-02	1.02E-03
	STRIP AXIAL FORCE=		5.299E 03	MOMENT= 1.619E-02	
231	4.12E 02	3.58E 02	9.74E-03	-2.67E-02	4.01E-03
232	3.65E 02	3.61E 02	4.46E-04	-2.86E-02	-1.15E-02
	STRIP AXIAL FORCE=		3.543E 03	MOMENT= 3.475E-03	
	SKIN MEMBRANE STRESS= 0.142E 06				
233	3.77E 02	3.61E 02	2.31E-04	-2.30E-02	-8.40E-03
	STRIP AXIAL FORCE=		1.837E 03	MOMENT= 2.002E-03	
234	3.89E 02	3.61E 02	2.38E-04	-2.31E-02	-3.74E-03
	STRIP AXIAL FORCE=		1.888E 03	MOMENT= 2.176E-03	
235	4.00E 02	3.61E 02	2.62E-04	-2.33E-02	1.70E-04
	STRIP AXIAL FORCE=		2.081E 03	MOMENT= 1.594E-04	
236	4.09E 02	3.61E 02	7.79E-03	-2.42E-02	3.69E-03
237	3.65E 02	3.66E 02	4.23E-04	-2.29E-02	-6.94E-03
	STRIP AXIAL FORCE=		3.364E 03	MOMENT= -9.450E-04	
	SKIN MEMBRANE STRESS= 0.117E 06				
238	3.77E 02	3.66E 02	3.15E-04	-2.06E-02	-7.28E-03
	STRIP AXIAL FORCE=		2.504E 03	MOMENT= -7.034E-04	
239	3.89E 02	3.66E 02	2.83E-04	-2.01E-02	-3.63E-03
	STRIP AXIAL FORCE=		2.253E 03	MOMENT= 5.728E-04	
240	4.00E 02	3.66E 02	2.99E-04	-2.07E-02	-6.08E-04
	STRIP AXIAL FORCE=		2.380E 03	MOMENT= 5.682E-04	
241	4.09E 02	3.66E 02	6.44E-03	-2.10E-02	2.50E-03
242	4.19E 02	3.65E 02	7.48E-03	-2.27E-02	3.57E-03
243	3.65E 02	3.70E 02	6.18E-04	-1.94E-02	-4.75E-03
	STRIP AXIAL FORCE=		4.915E 03	MOMENT= -5.001E-03	
	SKIN MEMBRANE STRESS= 0.995E 05				

ELEMENT NO.	SIGMA-X	SIGMA-Y	TAU-XY	SIGMA-1	SIGMA-2	ANG
227	-3.98E 03	-9.38E 03	-1.62E 03	-3.53E 03	-9.83E 03	-1.55E 01
228	-2.93E 03	-6.96E 03	-4.59E 02	-2.88E 03	-7.01E 03	-6.42E 00
229	-3.01E 03	-7.29E 03	-9.75E 01	-3.01E 03	-7.29E 03	-1.30E 00
230	-2.95E 03	-7.22E 03	8.88E 01	-2.94E 03	-7.22E 03	1.19E 00
231	-5.31E 02	-7.16E 03	3.74E 02	-5.10E 02	-7.18E 03	3.22E 00
232	-3.41E 03	-8.19E 03	-9.69E 02	-3.22E 03	-8.38E 03	-1.10E 01
233	-2.78E 03	-6.59E 03	-6.97E 02	-2.65E 03	-6.72E 03	-1.00E 01
234	-2.79E 03	-6.64E 03	-2.98E 02	-2.77E 03	-6.66E 03	-4.41E 00
235	-2.81E 03	-6.70E 03	3.62E 01	-2.81E 03	-6.70E 03	5.33E-01
236	-8.28E 02	-6.64E 03	3.45E 02	-8.07E 02	-6.66E 03	3.39E 00
237	-2.82E 03	-6.81E 03	-6.08E 02	-2.73E 03	-6.90E 03	-8.46E 00
238	-2.56E 03	-6.14E 03	-6.30E 02	-2.45E 03	-6.24E 03	-9.70E 00
239	-2.50E 03	-5.99E 03	-3.04E 02	-2.48E 03	-6.02E 03	-4.94E 00
240	-2.58E 03	-6.18E 03	-3.59E 01	-2.58E 03	-6.18E 03	-5.71E-01
241	-8.27E 02	-5.83E 03	2.36E 02	-8.16E 02	-5.84E 03	2.69E 00
242	-7.19E 02	-6.27E 03	3.31E 02	-6.99E 02	-6.29E 03	3.40E 00
243	-2.39E 03	-5.94E 03	-4.22E 02	-2.34E 03	-5.99E 03	-6.68E 00

NO.	X	Y	EPSILON-X	EPSILON-Y	GAMA-XY
244	3.77E 02	3.70E 02	4.66E-04	-1.84E-02	-5.51E-03
	STRIP AXIAL FORCE=		3.707E 03	MOMENT= -1.461E-03	
245	3.89E 02	3.70E 02	3.84E-04	-1.79E-02	-2.94E-03
	STRIP AXIAL FORCE=		3.055E 03	MOMENT= -1.398E-03	
246	4.00E 02	3.70E 02	3.88E-04	-1.82E-02	-3.62E-04
	STRIP AXIAL FORCE=		3.085E 03	MOMENT= -2.208E-03	
247	4.12E 02	3.70E 02	5.93E-03	-2.00E-02	1.54E-03
248	4.23E 02	3.70E 02	6.33E-03	-1.98E-02	2.69E-03
249	3.65E 02	3.74E 02	6.73E-04	-1.59E-02	-2.52E-03
	STRIP AXIAL FORCE=		5.346E 03	MOMENT= 1.840E-03	
	SKIN MEMBRANE STRESS=		0.864E 05		
250	3.65E 02	3.78E 02	5.86E-04	-1.35E-02	-1.56E-03
	STRIP AXIAL FORCE=		4.656E 03	MOMENT= 1.313E-03	
	SKIN MEMBRANE STRESS=		0.747E 05		
251	3.77E 02	3.74E 02	5.52E-04	-1.55E-02	-3.88E-03
	STRIP AXIAL FORCE=		4.386E 03	MOMENT= 4.839E-05	
252	3.77E 02	3.78E 02	5.03E-04	-1.35E-02	-2.63E-03
	STRIP AXIAL FORCE=		4.000E 03	MOMENT= 1.581E-03	
253	3.89E 02	3.74E 02	4.64E-04	-1.51E-02	-2.31E-03
	STRIP AXIAL FORCE=		3.684E 03	MOMENT= -2.195E-05	
254	3.89E 02	3.78E 02	4.08E-04	-1.33E-02	-1.62E-03
	STRIP AXIAL FORCE=		3.246E 03	MOMENT= 1.266E-03	
255	4.00E 02	3.74E 02	4.57E-04	-1.56E-02	-4.24E-04
	STRIP AXIAL FORCE=		3.634E 03	MOMENT= 1.153E-03	
256	4.00E 02	3.78E 02	4.11E-04	-1.37E-02	-1.21E-04
	STRIP AXIAL FORCE=		3.263E 03	MOMENT= 8.697E-04	
257	4.11E 02	3.74E 02	5.12E-03	-1.69E-02	6.73E-04
258	4.11E 02	3.78E 02	4.12E-03	-1.45E-02	3.44E-04
259	4.24E 02	3.74E 02	5.35E-03	-1.67E-02	2.13E-03
260	4.24E 02	3.78E 02	4.95E-03	-1.60E-02	1.84E-03
261	4.34E 02	3.74E 02	6.15E-03	-1.81E-02	3.52E-03
262	4.35E 02	3.78E 02	5.47E-03	-1.53E-02	1.55E-03
263	3.65E 02	3.82E 02	5.04E-04	-1.03E-02	-8.53E-04
	STRIP AXIAL FORCE=		4.003E 03	MOMENT= 6.026E-04	
	SKIN MEMBRANE STRESS=		0.633E 05		

ELEMENT NO.	SIGMA-X	SIGMA-Y	TAU-XY	SIGMA-1	SIGMA-2	ANG
244	-2.30E 03	-5.64E 03	-4.89E 02	-2.23E 03	-5.71E 03	-8.16E 00
245	-2.27E 03	-5.51E 03	-2.56E 02	-2.25E 03	-5.53E 03	-4.49E 00
246	-2.31E 03	-5.61E 03	-2.94E 01	-2.31E 03	-5.61E 03	-5.10E-01
247	-8.69E 02	-5.66E 03	1.43E 02	-8.65E 02	-5.67E 03	1.70E 00
248	-6.93E 02	-5.52E 03	2.52E 02	-6.80E 02	-5.53E 03	2.98E 00
249	-2.07E 03	-5.28E 03	-2.47E 02	-2.06E 03	-5.30E 03	-4.38E 00
250	-1.79E 03	-4.58E 03	-1.56E 02	-1.79E 03	-4.58E 03	-3.20E 00
251	-2.06E 03	-5.16E 03	-3.79E 02	-2.02E 03	-5.21E 03	-6.86E 00
252	-1.83E 03	-4.60E 03	-2.68E 02	-1.81E 03	-4.62E 03	-5.49E 00
253	-2.04E 03	-5.04E 03	-2.16E 02	-2.02E 03	-5.06E 03	-4.08E 00
254	-1.83E 03	-4.52E 03	-1.56E 02	-1.82E 03	-4.53E 03	-3.31E 00
255	-2.10E 03	-5.20E 03	-3.04E 01	-2.10E 03	-5.20E 03	-5.63E-01
256	-1.89E 03	-4.68E 03	-3.19E 00	-1.89E 03	-4.68E 03	-6.57E-02
257	-7.29E 02	-4.96E 03	6.86E 01	-7.28E 02	-4.96E 03	9.29E-01
258	-7.24E 02	-4.30E 03	2.89E 01	-7.23E 02	-4.30E 03	4.64E-01
259	-6.13E 02	-4.83E 03	2.12E 02	-6.02E 02	-4.85E 03	2.87E 00
260	-6.38E 02	-4.68E 03	1.88E 02	-6.29E 02	-4.69E 03	2.66E 00
261	-5.18E 02	-5.18E 03	3.50E 02	-4.92E 02	-5.21E 03	4.27E 00
262	-3.19E 02	-4.36E 03	1.40E 02	-3.14E 02	-4.37E 03	1.98E 00
263	-1.52E 03	-3.92E 03	-9.20E 01	-1.52E 03	-3.93E 03	-2.19E 00

ELEMENT NO.	X	Y	EPSILON-X	EPSILON-Y	GAMA-XY
264	3.65E 02	3.85E 02	4.72E-04	-8.63E-03	-6.92E-04
	STRIP AXIAL FORCE=		3.755E 03	MOMENT= -3.072E-04	
	SKIN MEMBRANE STRESS=		0.537E 05		
265	3.77E 02	3.82E 02	4.79E-04	-1.06E-02	-1.48E-03
	STRIP AXIAL FORCE=		3.806E 03	MOMENT= 5.489E-04	
266	3.77E 02	3.85E 02	4.47E-04	-8.91E-03	-9.33E-04
	STRIP AXIAL FORCE=		3.550E 03	MOMENT= 5.122E-04	
267	3.89E 02	3.82E 02	4.26E-04	-1.05E-02	-9.80E-04
	STRIP AXIAL FORCE=		3.387E 03	MOMENT= 6.216E-04	
268	3.89E 02	3.86E 02	3.94E-04	-8.87E-03	-5.23E-04
	STRIP AXIAL FORCE=		3.129E 03	MOMENT= 6.467E-04	
269	4.00E 02	3.82E 02	4.16E-04	-1.09E-02	-2.24E-05
	STRIP AXIAL FORCE=		3.307E 03	MOMENT= 1.833E-05	
270	4.00E 02	3.86E 02	4.11E-04	-9.33E-03	2.02E-04
	STRIP AXIAL FORCE=		3.269E 03	MOMENT= -8.010E-05	
271	4.11E 02	3.82E 02	3.70E-03	-1.18E-02	7.49E-04
272	4.11E 02	3.86E 02	3.34E-03	-1.03E-02	1.09E-03
273	4.23E 02	3.82E 02	4.11E-03	-1.29E-02	8.96E-04
274	4.23E 02	3.86E 02	3.32E-03	-1.08E-02	6.88E-04
275	4.34E 02	3.82E 02	4.03E-03	-1.22E-02	1.59E-03
276	4.37E 02	3.86E 02	3.66E-03	-1.10E-02	1.44E-03
277	4.44E 02	3.80E 02	4.69E-03	-1.36E-02	2.28E-03
278	4.47E 02	3.86E 02	4.39E-03	-1.08E-02	3.64E-04
279	3.65E 02	3.90E 02	4.35E-04	-5.43E-03	-2.70E-04
	STRIP AXIAL FORCE=		3.461E 03	MOMENT= 2.317E-04	
	SKIN MEMBRANE STRESS=		0.408E 05		
280	3.65E 02	3.95E 02	3.54E-04	-3.46E-03	-7.45E-05
	STRIP AXIAL FORCE=		2.815E 03	MOMENT= 1.251E-03	
	SKIN MEMBRANE STRESS=		0.268E 05		
281	3.77E 02	3.90E 02	4.16E-04	-5.73E-03	-3.03E-04
	STRIP AXIAL FORCE=		3.304E 03	MOMENT= 1.868E-04	

ELEMENT NO.	SIGMA-X	SIGMA-Y	TAU-XY	SIGMA-1	SIGMA-2	ANG
264	-1.29E 03	-3.37E 03	-7.57E 01	-1.29E 03	-3.38E 03	-2.08E 00
265	-1.56E 03	-4.01E 03	-1.65E 02	-1.55E 03	-4.02E 03	-3.84E 00
266	-1.35E 03	-3.48E 03	-1.10E 02	-1.34E 03	-3.49E 03	-2.94E 00
267	-1.57E 03	-3.97E 03	-1.04E 02	-1.56E 03	-3.97E 03	-2.47E 00
268	-1.36E 03	-3.48E 03	-5.75E 01	-1.36E 03	-3.48E 03	-1.56E 00
269	-1.65E 03	-4.15E 03	5.11E 00	-1.65E 03	-4.15E 03	1.17E-01
270	-1.44E 03	-3.66E 03	2.44E 01	-1.44E 03	-3.66E 03	6.26E-01
271	-5.11E 02	-3.69E 03	7.82E 01	-5.09E 02	-3.69E 03	1.41E 00
272	-3.79E 02	-3.23E 03	1.23E 02	-3.74E 02	-3.23E 03	2.47E 00
273	-5.15E 02	-4.03E 03	8.84E 01	-5.13E 02	-4.04E 03	1.44E 00
274	-4.81E 02	-3.45E 03	6.52E 01	-4.80E 02	-3.45E 03	1.26E 00
275	-4.34E 02	-3.78E 03	1.69E 02	-4.25E 02	-3.79E 03	2.88E 00
276	-3.83E 02	-3.51E 03	1.63E 02	-3.74E 02	-3.52E 03	2.97E 00
277	-3.98E 02	-4.18E 03	2.52E 02	-3.81E 02	-4.19E 03	3.80E 00
278	-2.28E 01	-3.30E 03	2.71E 01	-2.26E 01	-3.30E 03	4.74E-01
279	-9.79E 02	-2.73E 03	-3.67E 01	-9.78E 02	-2.73E 03	-1.20E 00
280	-6.45E 02	-1.92E 03	-8.38E 00	-6.45E 02	-1.92E 03	-3.77E-01
281	-1.05E 03	-2.86E 03	-4.92E 01	-1.05E 03	-2.87E 03	-1.55E 00

ELEMENT NO.	X	Y	EPSILON-X	EPSILON-Y	GAMA-XY
282	3.77E 02	3.95E 02	3.68E-04	-3.73E-03	3.28E-05
STRIP AXIAL FORCE= 2.925E 03 MOMENT= 6.475E-04					
283	3.89E 02	3.90E 02	3.74E-04	-5.73E-03	-1.48E-04
STRIP AXIAL FORCE= 2.972E 03 MOMENT= 3.542E-04					
284	3.89E 02	3.96E 02	3.30E-04	-3.73E-03	1.33E-04
STRIP AXIAL FORCE= 2.623E 03 MOMENT= 5.815E-04					
285	4.00E 02	3.90E 02	4.06E-04	-6.15E-03	2.03E-05
STRIP AXIAL FORCE= 3.229E 03 MOMENT= 7.174E-05					
286	4.00E 02	3.96E 02	3.49E-04	-4.03E-03	-1.43E-04
STRIP AXIAL FORCE= 2.774E 03 MOMENT= 1.056E-03					
287	4.11E 02	3.90E 02	2.56E-03	-7.09E-03	2.99E-04
288	4.11E 02	3.96E 02	1.84E-03	-4.78E-03	-3.99E-05
289	4.23E 02	3.91E 02	2.73E-03	-7.55E-03	6.33E-04
290	4.23E 02	3.96E 02	2.24E-03	-5.32E-03	5.79E-04
291	4.35E 02	3.91E 02	2.88E-03	-7.77E-03	6.05E-04
292	4.35E 02	3.96E 02	2.31E-03	-5.35E-03	3.09E-04
293	4.45E 02	3.91E 02	2.84E-03	-7.20E-03	1.92E-04
294	4.48E 02	3.96E 02	2.48E-03	-5.61E-03	1.64E-04
295	4.58E 02	3.91E 02	3.64E-03	-8.49E-03	1.45E-03
296	4.60E 02	3.96E 02	2.80E-03	-5.51E-03	-1.31E-04
297	3.65E 02	4.01E 02	2.07E-04	-1.40E-03	-3.04E-04
STRIP AXIAL FORCE= 1.645E 03 MOMENT= 4.480E-04					
SKIN MEMBRANE STRESS= 0.134E 05					
298	3.77E 02	4.01E 02	2.74E-04	-1.67E-03	9.56E-05
STRIP AXIAL FORCE= 2.174E 03 MOMENT= 2.991E-04					
299	3.89E 02	4.01E 02	2.87E-04	-1.63E-03	1.89E-04
STRIP AXIAL FORCE= 2.282E 03 MOMENT= -6.098E-04					
300	4.00E 02	4.01E 02	3.19E-04	-1.82E-03	-1.02E-04
STRIP AXIAL FORCE= 2.534E 03 MOMENT= -1.305E-03					

ELEMENT NO.	SIGMA-X	SIGMA-Y	TAU-XY	SIGMA-1	SIGMA-2	ANG
282	-7.02E 02	-2.06E 03	8.71E-01	-7.02E 02	-2.06E 03	3.67E-02
283	-1.07E 03	-2.86E 03	-2.44E 01	-1.07E 03	-2.86E 03	-7.81E-01
284	-7.24E 02	-2.07E 03	2.11E 01	-7.24E 02	-2.07E 03	8.99E-01
285	-1.15E 03	-3.08E 03	1.62E 00	-1.15E 03	-3.08E 03	4.79E-02
286	-7.90E 02	-2.24E 03	-2.76E 01	-7.90E 02	-2.24E 03	-1.09E 00
287	-2.16E 02	-2.60E 03	4.18E 01	-2.15E 02	-2.60E 03	1.01E 00
288	-9.62E 01	-1.87E 03	-5.69E 00	-9.62E 01	-1.87E 03	-1.84E-01
289	-2.20E 02	-2.78E 03	9.06E 01	-2.17E 02	-2.78E 03	2.02E 00
290	7.59E 00	-2.05E 03	8.81E 01	1.14E 01	-2.05E 03	2.45E 00
291	-1.85E 02	-2.87E 03	8.06E 01	-1.82E 02	-2.87E 03	1.72E 00
292	6.76E 01	-2.04E 03	3.78E 01	6.83E 01	-2.04E 03	1.02E 00
293	-8.29E 01	-2.58E 03	1.73E 01	-8.28E 01	-2.58E 03	3.96E-01
294	9.63E 01	-2.14E 03	2.50E 01	9.66E 01	-2.14E 03	6.42E-01
295	4.87E 01	-2.98E 03	2.02E 02	6.21E 01	-2.99E 03	3.80E 00
296	2.86E 02	-2.03E 03	-3.47E 01	2.86E 02	-2.03E 03	-8.58E-01
297	-3.22E 02	-1.09E 03	-6.06E 01	-3.17E 02	-1.10E 03	-4.48E 00
298	-3.57E 02	-1.27E 03	2.16E 01	-3.56E 02	-1.27E 03	1.35E 00
299	-3.33E 02	-1.24E 03	4.16E 01	-3.31E 02	-1.24E 03	2.63E 00
300	-3.76E 02	-1.39E 03	-2.72E 01	-3.76E 02	-1.39E 03	-1.54E 00

ELEMENT NO.	X	Y	EPSILON-X	EPSILON-Y	GAMA-XY
301	4.11E 02	4.01E 02	1.35E-03	-2.35E-03	-8.60E-05
302	4.23E 02	4.01E 02	1.43E-03	-2.65E-03	2.85E-04
303	4.35E 02	4.01E 02	1.44E-03	-2.59E-03	3.35E-04
304	4.48E 02	4.01E 02	1.42E-03	-2.66E-03	-5.86E-05
305	4.62E 02	4.02E 02	1.32E-03	-2.43E-03	6.89E-05
306	4.71E 02	4.00E 02	1.90E-03	-3.44E-03	7.76E-04
307	3.34E 02	3.57E 02	-1.04E-03	-1.68E-03	-4.08E-03
308	3.42E 02	3.57E 02	8.72E-05	-3.35E-03	-3.06E-03
309	3.53E 02	3.57E 02	5.62E-04	-4.24E-03	1.02E-03
310	3.37E 02	3.62E 02	-1.42E-03	-2.45E-04	-4.80E-03
311	3.45E 02	3.62E 02	-8.57E-04	-1.69E-03	-2.53E-03
312	3.46E 02	3.67E 02	-1.85E-03	3.24E-04	-2.35E-03
313	3.55E 02	3.62E 02	-1.44E-04	-2.58E-03	6.45E-04
314	3.55E 02	3.67E 02	-9.80E-04	-6.95E-04	3.42E-04
315	3.65E 02	4.07E 02	5.60E-05	-3.30E-04	-2.15E-04
316	3.77E 02	4.07E 02	3.31E-05	-4.32E-04	3.53E-05
317	3.89E 02	4.07E 02	4.10E-05	-4.03E-04	2.45E-05
318	4.00E 02	4.07E 02	4.78E-05	-4.13E-04	-1.99E-05
319	4.11E 02	4.07E 02	5.46E-05	-4.03E-04	-3.82E-06
320	4.23E 02	4.07E 02	1.06E-04	-4.30E-04	1.02E-04
321	4.35E 02	4.07E 02	1.86E-04	-4.61E-04	5.66E-05
322	4.48E 02	4.07E 02	2.68E-04	-4.97E-04	1.03E-04
323	4.62E 02	4.07E 02	2.83E-04	-5.17E-04	-2.16E-04
324	4.80E 02	4.07E 02	4.65E-04	-5.30E-04	4.19E-04

FLEMENT NO.	SIGMA-X	SIGMA-Y	TAU-XY	SIGMA-1	SIGMA-2	ANG
301	2.01E 02	-1.10E 03	-1.73E 01	2.01E 02	-1.10E 03	-7.62E-01
302	1.85E 02	-1.26E 03	5.08E 01	1.86E 02	-1.26E 03	2.02E 00
303	2.16E 02	-1.22E 03	5.93E 01	2.18E 02	-1.22E 03	2.36E 00
304	1.92E 02	-1.28E 03	-1.59E 01	1.93E 02	-1.28E 03	-6.18E-01
305	1.88E 02	-1.12E 03	1.55E 01	1.88E 02	-1.12E 03	6.79E-01
306	2.83E 02	-1.48E 03	1.43E 02	2.95E 02	-1.49E 03	4.63E 00
307	-6.03E 02	-7.36E 02	-3.99E 02	-2.65E 02	-1.07E 03	-4.03E 01
308	-4.53E 02	-1.14E 03	-2.90E 02	-3.47E 02	-1.25E 03	-2.01E 01
309	-4.25E 02	-1.36E 03	1.23E 02	-4.09E 02	-1.37E 03	7.40E 00
310	-5.36E 02	-2.97E 02	-4.86E 02	8.40E 01	-9.16E 02	1.28E 02
311	-5.42E 02	-7.42E 02	-2.43E 02	-3.79E 02	-9.04E 02	-3.38E 01
312	-6.23E 02	-1.85E 02	-2.54E 02	-6.91E 01	-7.40E 02	1.15E 02
313	-4.17E 02	-8.95E 02	1.10E 02	-3.93E 02	-9.19E 02	1.23E 01
314	-3.89E 02	-3.48E 02	8.56E 01	-2.81E 02	-4.57E 02	5.17E 01
315	-9.10E 01	-3.26E 02	-6.54E 01	-7.40E 01	-3.43E 02	-1.46E 01
316	-1.62E 02	-4.45E 02	1.07E 01	-1.61E 02	-4.45E 02	2.17E 00
317	-1.40E 02	-4.10E 02	7.46E 00	-1.40E 02	-4.11E 02	1.58E 00
318	-1.38E 02	-4.19E 02	-6.06E 00	-1.38E 02	-4.19E 02	-1.23E 00
319	-1.26E 02	-4.06E 02	-1.16E 00	-1.26E 02	-4.06E 02	-2.39E-01
320	-8.31E 01	-4.11E 02	3.11E 01	-8.02E 01	-4.14E 02	5.38E 00
321	-1.21E 01	-4.07E 02	1.73E 01	-1.13E 01	-4.08E 02	2.50E 00
322	5.84E 01	-4.10E 02	3.14E 01	6.05E 01	-4.12E 02	3.82E 00
323	6.60E 01	-4.25E 02	-6.62E 01	7.48E 01	-4.33E 02	-7.55E 00
324	2.41E 02	-3.35E 02	1.21E 02	2.65E 02	-3.59E 02	1.14E 01

NODAL POINT	X DISPLCEMNT	Y DISPLCEMNT	NODAL POINT	X DISPLCEMNT	Y DISPLCEMNT
1	0.0	0.0	38	-1.51E-01	-5.60E-01
2	0.0	-2.34E-01	39	-1.97E-01	-6.51E-01
3	0.0	-4.33E-01	40	-3.25E-01	-8.82E-01
4	0.0	-5.08E-01	41	-5.44E-01	-1.25E 00
5	0.0	-6.59E-01	42	-6.22E-01	-1.32E 00
6	0.0	0.0	43	0.0	0.0
7	0.0	0.0	44	-4.24E-02	-2.70E-01
8	0.0	0.0	45	-1.60E-01	-5.73E-01
9	-2.48E-02	-2.39E-01	46	-2.66E-01	-7.74E-01
10	-4.88E-02	-4.41E-01	47	-3.86E-01	-9.75E-01
11	-7.56E-02	-5.15E-01	48	-6.30E-01	-1.36E 00
12	-1.29E-01	-6.78E-01	49	-7.00E-01	-1.44E 00
13	-1.88E-01	-7.77E-01	50	0.0	0.0
14	0.0	0.0	51	0.0	0.0
15	0.0	0.0	52	0.0	0.0
16	-4.20E-02	-2.49E-01	53	-5.11E-02	-2.92E-01
17	-8.98E-02	-4.72E-01	54	-1.67E-01	-5.77E-01
18	-1.30E-01	-5.74E-01	55	-2.92E-01	-8.17E-01
19	-2.93E-01	-9.06E-01	56	-4.33E-01	-1.05E 00
20	-2.97E-01	-9.62E-01	57	-7.00E-01	-1.47E 00
21	0.0	0.0	58	-7.75E-01	-1.56E 00
22	0.0	0.0	59	0.0	0.0
23	-4.97E-02	-2.59E-01	60	0.0	0.0
24	-1.14E-01	-5.02E-01	61	0.0	0.0
25	-2.04E-01	-6.92E-01	62	-6.19E-02	-2.94E-01
26	-3.70E-01	-9.99E-01	63	-1.72E-01	-5.81E-01
27	-3.76E-01	-1.04E 00	64	-3.12E-01	-8.52E-01
28	0.0	0.0	65	-4.76E-01	-1.13E 00
29	0.0	0.0	66	-7.64E-01	-1.58E 00
30	-4.94E-02	-2.70E-01	67	-8.44E-01	-1.68E 00
31	-1.36E-01	-5.35E-01	68	0.0	0.0
32	-2.50E-01	-7.60E-01	69	0.0	0.0
33	-4.44E-01	-1.11E 00	70	0.0	0.0
34	-5.03E-01	-1.16E 00	71	-7.02E-02	-2.93E-01
35	0.0	0.0	72	-1.75E-01	-5.68E-01
36	0.0	0.0	73	-3.29E-01	-8.82E-01
37	-4.51E-02	-2.75E-01	74	-5.15E-01	-1.19E 00

NODAL POINT	X DISPLCEMNT	Y DISPLCEMNT	NODAL POINT	X DISPLCEMNT	Y DISPLCEMNT
75	-8.23E-01	-1.68E 00	112	-1.06E 00	-2.12E 00
76	-9.08E-01	-1.79E 00	113	-1.11E 00	-2.16E 00
77	0.0	0.0	114	0.0	0.0
78	0.0	0.0	115	0.0	0.0
79	0.0	0.0	116	-9.50E-02	-2.73E-01
80	-7.78E-02	-2.93E-01	117	-2.10E-01	-5.47E-01
81	-1.88E-01	-5.78E-01	118	-4.12E-01	-9.63E-01
82	-3.53E-01	-9.16E-01	119	-6.52E-01	-1.39E 00
83	-5.50E-01	-1.25E 00	120	-9.24E-01	-1.88E 00
84	-8.77E-01	-1.78E 00	121	-1.11E 00	-2.16E 00
85	-9.67E-01	-1.90E 00	122	-1.16E 00	-2.24E 00
86	0.0	0.0	123	0.0	0.0
87	0.0	0.0	124	0.0	0.0
88	0.0	0.0	125	-9.67E-02	-2.65E-01
89	-8.40E-02	-2.92E-01	126	-2.08E-01	-5.26E-01
90	-1.98E-01	-5.80E-01	127	-3.66E-01	-8.61E-01
91	-3.72E-01	-9.38E-01	128	-5.53E-01	-1.20E 00
92	-5.81E-01	-1.30E 00	129	-6.83E-01	-1.42E 00
93	-9.27E-01	-1.86E 00	130	-9.65E-01	-1.92E 00
94	-1.02E 00	-2.00E 00	131	-1.15E 00	-2.21E 00
95	0.0	0.0	132	-1.21E 00	-2.29E 00
96	0.0	0.0	133	0.0	0.0
97	0.0	0.0	134	-9.83E-02	-2.62E-01
98	-8.88E-02	-2.88E-01	135	-2.13E-01	-5.27E-01
99	-2.06E-01	-5.75E-01	136	-3.82E-01	-8.74E-01
100	-3.88E-01	-9.49E-01	137	-5.77E-01	-1.22E 00
101	-6.05E-01	-1.33E 00	138	-7.13E-01	-1.45E 00
102	-9.71E-01	-1.95E 00	139	-9.97E-01	-1.95E 00
103	-1.06E 00	-2.08E 00	140	-1.18E 00	-2.25E 00
104	0.0	0.0	141	-1.25E 00	-2.33E 00
105	0.0	0.0	142	0.0	0.0
106	0.0	0.0	143	-9.91E-02	-2.59E-01
107	-9.25E-02	-2.81E-01	144	-2.17E-01	-5.24E-01
108	-2.09E-01	-5.64E-01	145	-3.95E-01	-8.81E-01
109	-4.01E-01	-9.57E-01	146	-5.98E-01	-1.24E 00
110	-6.22E-01	-1.35E 00	147	-7.39E-01	-1.47E 00
111	-8.78E-01	-1.81E 00	148	-1.03E 00	-1.97E 00

NODAL POINT	X DISPLCEMNT	Y DISPLCEMNT	NODAL POINT	X DISPLCEMNT	Y DISPLCEMNT
149	-1.22E 00	-2.27E 00	186	-1.04E 00	-1.94E 00
150	-1.28E 00	-2.36E 00	187	-1.25E 00	-2.21E 00
151	0.0	0.0	188	-1.36E 00	-2.35E 00
152	-9.89E-02	-2.54E-01	189	-1.42E 00	-2.40E 00
153	-2.18E-01	-5.19E-01	190	-1.41E 00	-2.39E 00
154	-4.04E-01	-8.84E-01	191	-7.09E-02	-2.84E-01
155	-6.16E-01	-1.25E 00	192	-6.02E-02	-2.40E-01
156	-7.61E-01	-1.49E 00	193	-6.83E-02	-3.15E-01
157	-1.05E 00	-1.99E 00	194	-6.50E-02	-3.12E-01
158	-1.25E 00	-2.29E 00	195	-1.23E 00	-2.18E 00
159	-1.32E 00	-2.38E 00	196	-1.34E 00	-2.30E 00
160	0.0	0.0	197	-1.37E 00	-2.35E 00
161	-9.76E-02	-2.47E-01	198	-7.37E-02	-3.20E-01
162	-2.16E-01	-5.11E-01	199	-7.87E-02	-3.27E-01
163	-4.08E-01	-8.84E-01	200	-8.36E-02	-3.27E-01
164	-6.28E-01	-1.26E 00	201	0.0	0.0
165	-7.80E-01	-1.50E 00	202	-9.33E-02	-2.23E-01
166	-1.07E 00	-2.00E 00	203	-2.09E-01	-4.72E-01
167	-1.27E 00	-2.30E 00	204	-3.98E-01	-8.58E-01
168	-1.35E 00	-2.39E 00	205	-6.33E-01	-1.28E 00
169	0.0	0.0	206	-8.07E-01	-1.55E 00
170	-9.55E-02	-2.39E-01	207	-1.11E 00	-2.06E 00
171	-2.12E-01	-4.98E-01	208	-1.25E 00	-2.28E 00
172	-4.07E-01	-8.79E-01	209	-1.40E 00	-2.51E 00
173	-6.34E-01	-1.27E 00	210	-4.16E-01	-1.47E 00
174	-1.29E 00	-2.25E 00	211	-4.58E-01	-1.55E 00
175	-1.34E 00	-2.32E 00	212	-4.93E-01	-1.56E 00
176	-7.94E-01	-1.52E 00	213	-4.94E-01	-1.49E 00
177	-1.09E 00	-2.02E 00	214	-5.04E-01	-1.46E 00
178	-1.31E 00	-2.31E 00	215	-5.34E-01	-1.52E 00
179	-1.38E 00	-2.40E 00	216	-4.77E-01	-1.29E 00
180	0.0	0.0	217	-4.94E-01	-1.31E 00
181	-9.35E-02	-2.30E-01	218	-4.28E-01	-1.07E 00
182	-2.06E-01	-4.79E-01	219	-4.50E-01	-1.09E 00
183	-4.00E-01	-8.68E-01	220	-2.85E-01	-6.26E-01
184	-6.34E-01	-1.28E 00	221	-9.27E-02	-2.31E-01
185	-8.05E-01	-1.53E 00	222	0.0	0.0

NODAL POINT	X DISPLCEMNT	Y DISPLCEMNT	NODAL POINT	X DISPLCEMNT	Y DISPLCEMNT
223	-9.52E-02	-2.15E-01	260	-4.18E-01	-9.72E-01
224	-2.14E-01	-4.59E-01	261	-4.42E-01	-9.92E-01
225	-3.96E-01	-8.34E-01	262	-2.80E-01	-5.67E-01
226	-6.28E-01	-1.27E 00	263	-9.33E-02	-2.33E-01
227	-7.97E-01	-1.55E 00	264	0.0	0.0
228	-9.51E-01	-1.87E 00	265	-1.08E-01	-1.97E-01
229	-1.11E 00	-2.14E 00	266	-2.37E-01	-4.20E-01
230	-1.31E 00	-2.43E 00	267	-4.05E-01	-7.41E-01
231	-4.10E-01	-1.51E 00	268	-6.32E-01	-1.15E 00
232	-4.54E-01	-1.51E 00	269	-8.11E-01	-1.43E 00
233	-4.87E-01	-1.50E 00	270	0.0	0.0
234	-4.86E-01	-1.42E 00	271	0.0	0.0
235	-4.97E-01	-1.39E 00	272	-1.02E 00	-1.79E 00
236	-5.28E-01	-1.45E 00	273	-4.07E-01	-1.33E 00
237	-4.72E-01	-1.23E 00	274	-4.51E-01	-1.36E 00
238	-4.89E-01	-1.26E 00	275	-4.81E-01	-1.35E 00
239	-4.23E-01	-1.02E 00	276	-4.76E-01	-1.28E 00
240	-4.46E-01	-1.04E 00	277	-4.86E-01	-1.25E 00
241	-2.83E-01	-6.01E-01	278	-5.19E-01	-1.31E 00
242	-9.27E-02	-2.35E-01	279	-4.62E-01	-1.11E 00
243	0.0	0.0	280	-4.80E-01	-1.13E 00
244	-9.98E-02	-2.07E-01	281	-4.14E-01	-9.17E-01
245	-2.23E-01	-4.42E-01	282	-4.39E-01	-9.37E-01
246	-3.97E-01	-7.94E-01	283	-2.76E-01	-5.31E-01
247	-6.26E-01	-1.23E 00	284	-9.30E-02	-2.29E-01
248	-7.97E-01	-1.51E 00	285	0.0	0.0
249	-8.67E-01	-1.74E 00	286	-1.21E-01	-1.88E-01
250	-9.49E-01	-1.84E 00	287	-2.58E-01	-3.93E-01
251	-1.18E 00	-2.13E 00	288	-4.19E-01	-6.82E-01
252	-4.08E-01	-1.45E 00	289	-6.49E-01	-1.06E 00
253	-4.52E-01	-1.47E 00	290	-8.20E-01	-1.30E 00
254	-4.84E-01	-1.45E 00	291	-8.81E-01	-1.44E 00
255	-4.81E-01	-1.36E 00	292	0.0	0.0
256	-4.91E-01	-1.33E 00	293	0.0	0.0
257	-5.23E-01	-1.39E 00	294	-4.07E-01	-1.17E 00
258	-4.66E-01	-1.17E 00	295	-4.49E-01	-1.21E 00
259	-4.84E-01	-1.20E 00	296	-4.78E-01	-1.23E 00

NODAL POINT	X DISPLCEMNT	Y DISPLCEMNT	NODAL POINT	X DISPLCEMNT	Y DISPLCEMNT
297	-4.72E-01	-1.18E 00	334	0.0	0.0
298	-4.81E-01	-1.16E 00	335	0.0	0.0
299	-5.15E-01	-1.22E 00	336	0.0	0.0
300	-4.57E-01	-1.04E 00	337	0.0	0.0
301	-4.75E-01	-1.07E 00	338	0.0	0.0
302	-4.10E-01	-8.66E-01	339	-3.56E-01	-8.85E-01
303	-4.36E-01	-8.90E-01	340	-3.54E-01	-8.31E-01
304	-2.72E-01	-5.05E-01	341	-4.22E-01	-9.40E-01
305	-9.26E-02	-2.26E-01	342	-3.74E-01	-8.37E-01
306	0.0	0.0	343	-4.15E-01	-8.80E-01
307	-1.42E-01	-1.80E-01	344	-3.56E-01	-7.17E-01
308	-2.84E-01	-3.64E-01	345	-3.96E-01	-7.46E-01
309	-4.37E-01	-6.18E-01	346	-2.44E-01	-4.33E-01
310	-6.52E-01	-9.70E-01	347	-9.36E-02	-2.04E-01
311	-7.69E-01	-1.18E 00	348	0.0	0.0
312	0.0	0.0	349	-2.27E-01	-1.64E-01
313	0.0	0.0	350	-3.36E-01	-3.01E-01
314	0.0	0.0	351	-4.64E-01	-4.94E-01
315	0.0	0.0	352	-6.33E-01	-7.76E-01
316	-4.04E-01	-1.09E 00	353	-7.24E-01	-9.26E-01
317	-3.88E-01	-1.02E 00	354	-3.72E-01	-7.57E-01
318	-4.13E-01	-1.04E 00	355	-3.09E-01	-6.24E-01
319	-4.30E-01	-1.05E 00	356	-3.76E-01	-7.31E-01
320	-4.77E-01	-1.11E 00	357	-3.24E-01	-6.16E-01
321	-4.19E-01	-9.51E-01	358	-3.73E-01	-6.45E-01
322	-4.40E-01	-9.83E-01	359	-2.27E-01	-3.83E-01
323	-3.86E-01	-8.05E-01			
324	-4.20E-01	-8.34E-01			
325	-2.58E-01	-4.77E-01			
326	-9.35E-02	-2.19E-01			
327	0.0	0.0			
328	-1.72E-01	-1.75E-01			
329	-3.16E-01	-3.30E-01			
330	-4.51E-01	-5.55E-01			
331	-6.41E-01	-8.78E-01			
332	-7.43E-01	-1.06E 00			
333	0.0	0.0			

NODAL POINT	X DISPLCEMNT	Y DISPLCEMNT	NODAL POINT	X DISPLCEMNT	Y DISPLCEMNT
360	-9.26E-02	-1.85E-01	386	0.0	0.0
361	-1.17E-01	-8.82E-02	387	-2.59E-01	-1.96E-01
362	-2.57E-01	-1.49E-01	388	-3.19E-01	-2.10E-01
363	-3.66E-01	-2.74E-01	389	-3.96E-01	-2.60E-01
364	-4.76E-01	-4.23E-01	390	-4.87E-01	-3.48E-01
365	-6.28E-01	-6.66E-01	391	-6.03E-01	-4.83E-01
366	-7.01E-01	-7.89E-01	392	-6.28E-01	-5.36E-01
367	-3.45E-01	-6.13E-01	393	0.0	0.0
368	-2.87E-01	-4.82E-01	394	0.0	0.0
369	-3.41E-01	-5.15E-01	395	0.0	0.0
370	-2.09E-01	-3.24E-01	396	0.0	0.0
371	-8.82E-02	-1.60E-01	397	0.0	0.0
372	0.0	0.0	398	0.0	0.0
373	0.0	0.0	399	0.0	0.0
374	-1.99E-01	-1.51E-01	400	-3.00E-01	-2.27E-01
375	-2.89E-01	-1.73E-01	401	-3.39E-01	-2.55E-01
376	-3.87E-01	-2.54E-01	402	-3.91E-01	-2.92E-01
377	-4.87E-01	-3.72E-01	403	-4.73E-01	-3.57E-01
378	-6.21E-01	-5.60E-01	404	-5.70E-01	-4.47E-01
379	-6.76E-01	-6.50E-01	405	-5.97E-01	-4.66E-01
380	-3.26E-01	-3.94E-01	406	-3.11E-01	-2.35E-01
381	-1.93E-01	-2.41E-01	407	-3.37E-01	-3.29E-01
382	-8.78E-02	-1.30E-01	408	-3.79E-01	-3.39E-01
383	0.0	0.0	409	-4.28E-01	-4.12E-01
384	0.0	0.0	410	-4.44E-01	-4.40E-01
385	0.0	0.0	411	-2.86E-01	-5.55E-01
			412	-0.21	-0.71
			413	-0.31	-0.40